Contents

Related Methodology Review Article

Annual Review

Contributors

Numbers in parentheses indicate the pages on which the authors' contributions begin.

Abdullah A. Al-Badr (3, 153), Department of Pharmaceutical Chemistry, College of Pharmacy, King Saud University, P.O. Box 2457, Riyadh-11451, Kingdom of Saudi Arabia

Badraddin M. H. Al-Hadiya (67), Department of Clinical Pharmacy, College of Pharmacy, King Saud University, P.O. Box 2457 Riyadh 11451, Kingdom of Saudi Arabia

Abdulrahman Al-Majed (119, 131, 149), Department of Pharmaceutical Chemistry, College of Pharmacy, King Saud University, P.O. Box 2457, Riyadh 11451, Saudi Arabia

M. Al-Omar (209), Department of Pharmaceutical Chemistry, College of Pharmacy, King Saud University, P.O. Box 2457, Riyadh 11451, Kingdom of Saudi Arabia

Ibrahim A. Alsarra (209), Department of Pharmaceutics, College of Pharmacy, King Saud University, P.O. Box 2457, Riyadh 11451, Kingdom of Saudi Arabia

Fathallah Belal (119, 131, 149, 209), Department of Pharmaceutical Chemistry, College of Pharmacy, King Saud University, P.O. Box 2457, Riyadh 11451, Saudi Arabia

Harry G. Brittain (263), Center for Pharmaceutical Physics, 10 Charles Road, Milford, New Jersey 08848

Hussein El-Subbagh (119), Department of Pharmaceutical Chemistry, College of Pharmacy, King Saud University, P.O. Box 2457, Riyadh 11451, Saudi Arabia

Gunawan Indrayanto (97, 243), Assessment Service Unit, Faculty of Pharmacy, Airlangga University, Surabaya 60283, Indonesia

Saeed Julkhuf (119, 131, 149), Department of Pharmaceutical Chemistry, College of Pharmacy, King Saud University, P.O. Box 2457, Riyadh 11451, Saudi Arabia

Mochammad Yuwono (97, 243), Assessment Service Unit, Faculty of Pharmacy, Airlangga University, Surabaya 60283, Indonesia

Preface

The comprehensive profiling of drug substances and pharmaceutical excipients as to their physical and analytical characteristics remains at the core of pharmaceutical development. As a result, the compilation and publication of comprehensive summaries of physical and chemical data, analytical methods, routes of compound preparation, degradation pathways, uses and applications, *etc.*, has always been a vital function to both academia and industry.

As the science of pharmaceutics grows and matures, the need for information similarly expands along new fronts and causes equivalent growth in the vehicles where investigators find the information they need. The content of the ***Profiles*** series has expanded to meet this need, with chapters falling into one or more of the following main categories:

1. Comprehensive profiles of a drug substance or excipient
2. Physical characterization of a drug substance or excipient
3. Analytical methods for a drug substance or excipient
4. Detailed discussions of the clinical uses, pharmacology, pharmacokinetics, safety, or toxicity of a drug substance or excipient
5. Reviews of methodology useful for the characterization of drug substances or excipients
6. Annual reviews of areas of importance to pharmaceutical scientists

Several of the chapters in the current volume are comprehensive in nature, but others are more specialized. Volume 32 also contains a methodology review article on the validation of chromatographic methods of analysis. New to the series are annual reviews, and volume 32 contains a summary of the publications appearing during 2004 that dealt with polymorphism and solvatomorphism. It is anticipated that future volumes in the ***Profiles*** series will contain similar methodology reviews, as well as other types of review articles that summarize the current state in a particular field of pharmaceutics. As always, I welcome communications from anyone in the pharmaceutical community who might want to provide an opinion or a contribution.

Harry G. Brittain
Editor

Miconazole Nitrate: Comprehensive Profile

Abdullah A. Al-Badr

Department of Pharmaceutical Chemistry, College of Pharmacy, King Saud University, P.O. Box 2457, Riyadh-11451, Kingdom of Saudi Arabia

Contents

PROFILES OF DRUG SUBSTANCES, EXCIPIENTS, AND RELATED METHODOLOGY, VOLUME 32
ISSN: 0099-5428

DOI: 10.1016/S0099-5428(05)32001-6

1. DESCRIPTION

1.1. Nomenclature

1.1.1. Systematic chemical names

2-(2,4-Dichlorophenyl)-2-(2,4-dichlorobenzyloxy)-1-(1*H*-imidazol-1-yl)-ethane.
1-[2-(2,4-Dichlorophenyl)-2-[(2,4-dichlorophenyl)-methoxy]-ethyl]-1*H*-imidazole.
1-[2,4-Dichloro-2-(2,4-dichlorobenzyloxy)-phenethyl]-1*H*-imidazole.
1*H*-Imidazole, 1-[2-(2,4-dichlorophenyl)-2-[(2,4-dichlorophenyl)-methoxy]-ethyl].
1-[2-(2,4-Dichlorophenyl)-2-(2,4-dichlorobenzyloxy)-ethyl]-1*H*-imidazole.
1-[2,4-Dichloro-*β*-(2,4-dichlorobenzyloxy)-phenethyl]-1*H*-imidazole.
1-[2,4-Dichloro-*β*-(2,4-dichlorobenzyloxy)phenyl ethyl]-1*H*-imidazole [1–4].

1.1.2. Nonproprietary names

Miconazole, Miconazolum, Miconazol [1–4].

1.1.3. Proprietary names

1. Miconazole: 18134, Andergin, Brenospor, Brentan, Castillani Neu, Daktanol, Daktar, Daktarin, Dumicoat, Fungisidin, Fungo solution, Fungucit, Gin Daktanol, Infectosoor, Itrizole, Leuko Gungex Antifungal, Micofim, Miconal, Micotar, Micotef, Miderm, Monistat, Nizakol, Rojazol [1–4].

2. Miconazole nitrate: 14889, Aflorix, Albistat, Aloid, Andergen, Andergin, Brinazol, Brenospor, Brentan, Britane, Conoderm, Curex, Daktar, Daktarin, Daktozin, Deralbine, Derma Mykotral, Dermacure, Dermifun, Dermonistat, Desenex, Epi-Monistat, Femeron, Femizol-M, Florid, Fungiderm, Fungisidin, Fungo Powder, Fungoid, Fungur, Gindak, Gyno-Daktar, Gyno-Daktarin, Gyno Femidazol,

Gyno-Monistat, Gyno-Mykotral, Lotrimin AF, M-Zole, Medizole, Micane, Micatin, Micoderm, Micogel, Micogyn, Miconal Ecoba, Miconazol, Miconazole, Micotar, Micotef, Miderm, Mikonazol CCS, Monistat, Monistat-Derm, Micoderm, Mikotin mono, Neomicol, Nizacol, Prilagin, Rojazol, Ting, Vodol, Zeasorb, Zole [1–4].

3. Pivoxil hydrochloride (miconazole pivaloyloxymethyl chloride): Micomax, Pivaanazolo [4].

1.2. Formulae

1.2.1. Empirical formula, molecular weight, and CAS number

1.2.1.1. Miconazole

$C_{18}H_{14}Cl_4N_2O$ 416.13 [22916−47−8]

1.2.1.2. Miconazole nitrate

$C_{18}H_{14}Cl_4N_2O{\cdot}HNO_3$ 479.14 [22832−87−7]

1.2.2. Structural formula

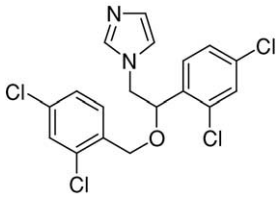

1.3. Elemental analysis

Miconazole
C 51.96%, H 3.39%, Cl 34.08%, N 6.73%, O 3.84%.
Miconazole nitrate
C 45.12%, H 3.16%, Cl 29.59%, N 8.77%, O 13.36%.

1.4. Appearance

Miconazole base is a white or almost white powder. Miconazole nitrate is a white or almost white powder [1–3].

1.5. Uses and applications

Miconazole is an imidazole antifungal agent used as miconazole base or miconazole nitrate for the treatment of superficial candidiasis and of skin infections dermatophytosis and pityriasis versicolor. The drug has also been given intravenously by infusion for the treatment of disseminated fungal infections. Miconazole can be given by mouth in a dose of 120–240 mg, as oral gel four times daily after food, for

the treatment of oropharyngeal and intestinal candidiasis. Children aged 6 years may be given 120 mg four times daily, aged 2–6 years, 120 mg twice daily; under 2 years, 60 mg twice daily. The drug as an oral gel may be applied directly for the treatment of oral lesions. A sustained release lacquer is available for dentures [3].

Miconazole nitrate is usually applied twice daily as a 2% cream, lotion, or powder in the treatment of fungal infections of skin including candidiasis, dermatophytosis, and pityriasis versicolor. The drug is also used for treatment of vaginal candidiasis, 5 g of a 2% intravaginal cream is inserted into the vagina once daily for 10–14 days or twice daily for 7 days. Miconazole nitrate pessaries may be inserted in dosage regimens of 100 mg once daily for 7–14 days, 100 mg twice daily for 7 days, 200 or 400 mg daily for 3 days, or in a single dose of 1200 mg [3].

Intravenous doses of miconazole have ranged from 0.2 g daily to 1.2 g three times daily, depending on the sensitivity and severity of the infection. It should be diluted in sodium chloride 0.9% or glucose 5% and given by slow infusion; the manufacturers recommend that daily dose up to 2.4 g should be diluted to a concentration of 1 mg/mL and infused at a rate of 100 mg/h, in order to reduce toxicity. Children over 1 year of age may be given 20–40 mg/kg body weight daily but not more than 15 mg/kg of miconazole should be given at each infusion [3].

2. METHODS OF PREPARATION

1. Miconazole nitrate was prepared by Godefori and co-workers [5–7]. Imidazole **1** was coupled with brominated 2,4-dichloroacetophenone **2** and the resulting ketonic product **3** was reduced with sodium borohydride to its corresponding alcohol **4**. The latter compound **4** was then coupled with 2,4-dichlorotoluene by sodium borohydride in hexamethylphosphoramide (an aprotic solvent), which was then extracted with nitric acid to give miconazole nitrate.

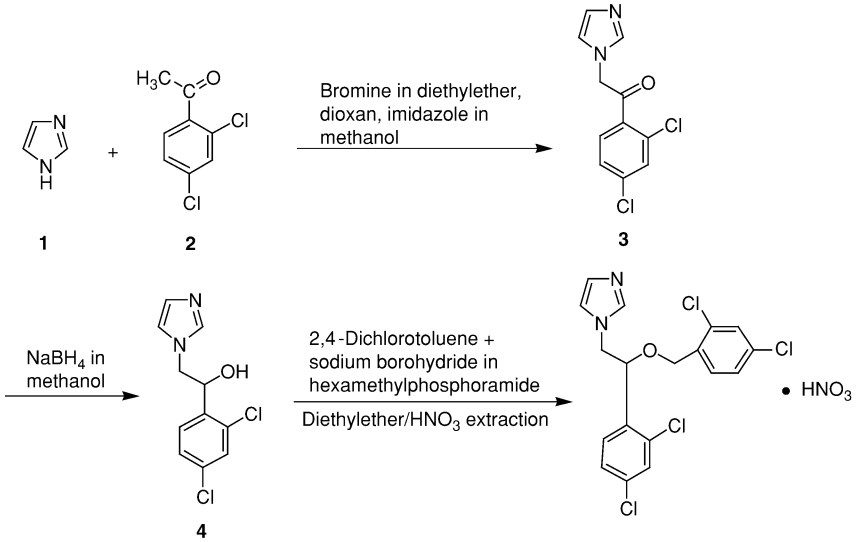

2. Miconazole was also prepared by Molina Caprile [8] as follows:
Phenyl methyl ketone **1** was brominated to give 1-phenyl-2-bromoethanone **2**. Compound **2** was treated with methylsulfonic acid to yield the corresponding methylsulfonate **3**. Etherification of **3** gave the α-benzyloxy derivative **4** and compound **4** was then chlorinated to give the 2,4-dichlorinated derivatives in both aromatic ring systems **5**. Compound **5** reacted with imidazole in dimethylformamide to give miconazole **6** [7], which is converted to miconazole nitrate.

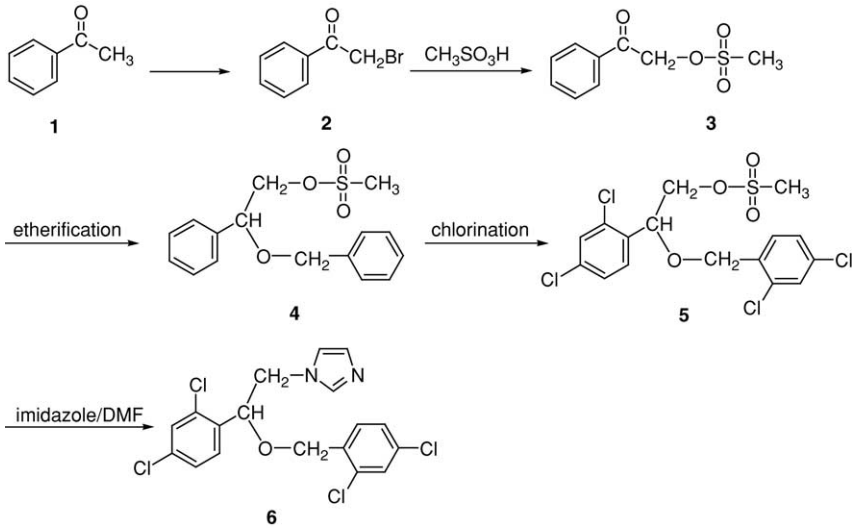

3. Ye *et al.* reported that the reduction of 2,4-dichlorophenyl-2-chloroethanone **1** with potassium borohydride in dimethylformamide to give 90% α-chloromethyl-2,4-dichlorobenzyl alcohol **2**. Alkylation of imidazole with compound **2** in dimethyl formamide in the presence of sodium hydroxide and triethylbenzyl ammonium chloride, gave 1-(2,4-dichlorophenyl-2-imidazolyl)ethanol **3** and etherification of **3** with 2,4-dichlorobenzyl chloride under the same condition, 62% yield of miconazole [9].

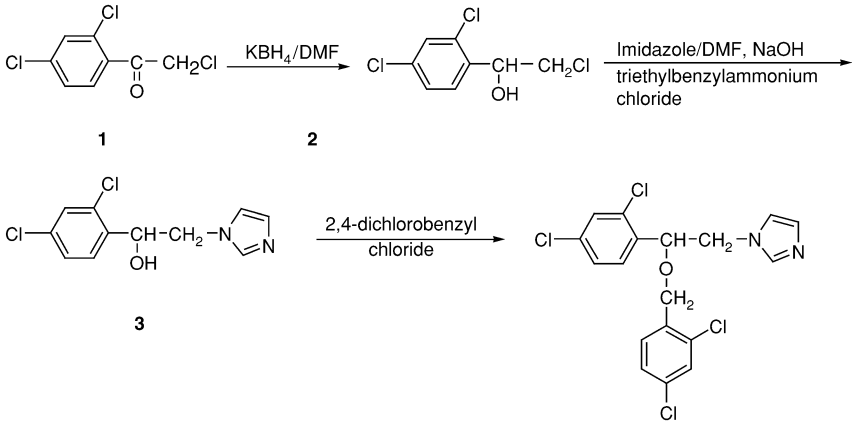

4. Liao and Li enantioselectively synthesized and studied the antifungal activity of optically active miconazole and econazole. The key step was the enantioselective reduction of 2-chloro-1-(2,4-dichlorophenyl)ethanone catalyzed by chiral oxazaborolidine [10].

5. Yanez *et al.* reported the synthesis of miconazole and analogs through a carbenoid intermediate. The process involves the intermolecular insertion of carbenoid species to imidazole from α-diazoketones with copper acetylacetonate as the key reaction of the synthetic route [11].

3. PHYSICAL CHARACTERISTICS

3.1. Ionization constant

$pK_a = 6.7$ [2].

3.2. Solubility characteristics

3.2.1. Miconazole

Slightly soluble in water, soluble 1 in 9.5 of ethanol, 1 in 2 of chloroform, 1 in 15 of ether, 1 in 4 of isopropanol, 1 in 5.3 of methanol and 1 in 9 of propylene glycol. Freely soluble in acetone and in dimethylformamide, protect from light [1–3].

3.2.2. Miconazole nitrate

Soluble 1 in 6250 of water, 1 in 312 of alcohol, 1 in 75 in methanol, 1 in 525 of chloroform, 1 in 1408 of isopropanol, 1 in 119 of propylene glycol, freely soluble in dimethylsulfoxide, protect from light [1–3].

3.3. Optical activity

(+) Form nitrate $[\alpha]_D^{20} + 59^\circ$ (methanol) [2].
(−) Form nitrate $[\alpha]_D^{20} - 58^\circ$ (methanol) [2].

3.4. X-ray powder diffraction pattern

The X-ray powder diffraction pattern of miconazole was performed using a Simmons XRD-5000 diffractometer. Figure 1 shows the X-ray powder diffraction pattern of miconazole nitrate, which was obtained on a pure sample of the drug substance. Table 1 shows the values for the scattering angles (2θ (°)), the interplanar *d*-spacing (Å), and the relative intensities (%) observed for the major diffraction peaks of miconazole.

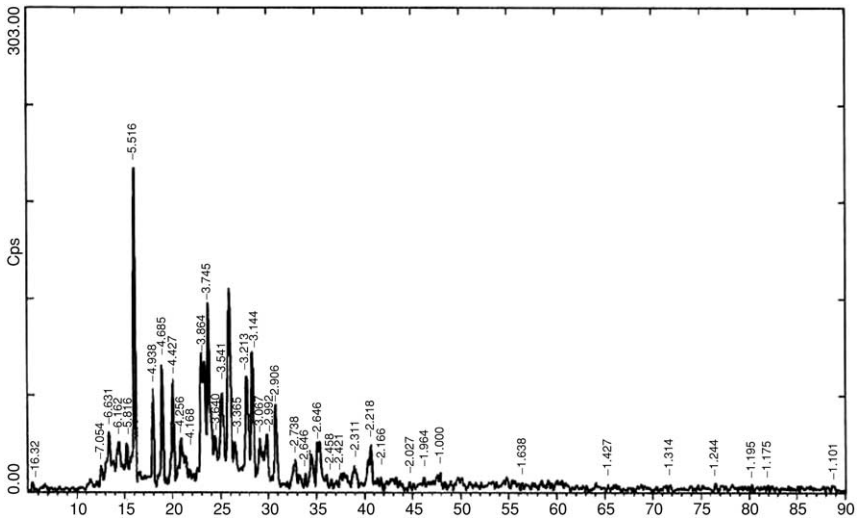

Fig. 1. X-ray powder diffraction pattern of miconazole nitrate.

Table 1. The X-ray powder diffraction pattern of miconazole nitrate

Scattering angle 2θ	*d*-spacing (Å)	Relative intensity (%)	Scattering angle 2θ	*d*-spacing (Å)	Relative intensity (%)
5.411	16.3187	2.77	12.538	7.0542	8.07
13.341	6.63155	18.39	14.361	6.1623	15.41
15.222	5.8156	15.00	16.054	5.5164	100.00
16.423	5.3931	6.06	17.948	4.9382	31.77
18.927	4.6847	39.22	20.042	4.4266	34.69
20.857	4.2555	16.62	21.300	4.1680	11.03
23.000	3.8636	42.86	23.296	3.8151	40.31
23.740	3.7449	58.38	24.434	3.6400	17.41
25.127	3.5412	30.43	25.930	3.4333	62.78
26.465	3.3651	15.24	27.745	3.2127	35.64
28.359	3.1445	43.24	29.094	3.0667	16.49
29.834	2.9923	17.86	30.740	2.9062	26.93
32.783	2.7296	9.91	33.849	2.6460	5.73
34.455	2.6008	11.51	35.088	2.5553	15.32
35.336	2.5380	15.60	36.529	2.4578	3.97
37.104	2.4210	3.52	38.948	2.3105	8.15
40.634	2.2185	14.62	41.663	2.1660	4.57
44.663	2.0272	3.11	46.175	1.9643	4.60
47.859	1.8991	5.93	56.401	1.6300	2.87
65.335	1.4271	2.28	71.779	1.3140	2.20
76.487	1.2444	2.82	80.271	1.1950	2.37
81.923	1.1750	2.15	88.743	1.1015	2.15

3.5. Thermal methods of analysis

3.5.1. Melting behavior

Miconazole base melts at 83–87 °C. Miconazole nitrate melts at 170.5 °C, 184–185 °C. The (+)-form of miconazole nitrate melts at 135.3 °C and the (–)-form melts at 135 °C [1].'

3.5.2. Differential scanning calorimetry

The differential scanning calorimetry (DSC) thermogram of miconazole was obtained using a DuPont 2100 thermal analyzer system. The thermogram shown in Fig. 2 was obtained at a heating rate of 10 °C/min and was run over the range 50–300 °C. Miconazole was found to melt at 186.55 °C.

3.6. Spectroscopy

3.6.1. Ultraviolet spectroscopy

The ultraviolet absorption spectrum of miconazole nitrate in methanol (0.0104%) shown in Fig. 3 was recorded using a Shimadzu Ultraviolet-visible spectrophotometer 1601 PC. The compound exhibited three maxima at 264, 272, and 280 nm. Clarke reported the following: Methanol 264 and 272 nm ($A^{1\%}_{1\ cm} = 17$a), 282 nm [2].

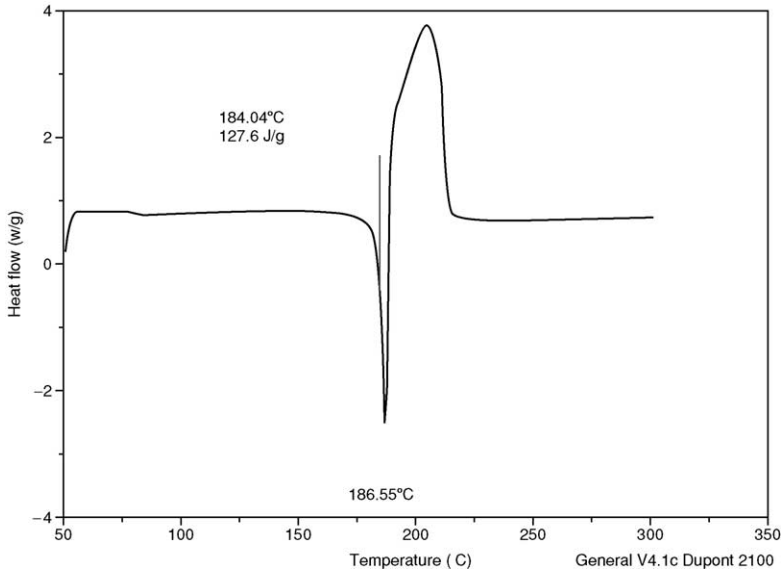

Fig. 2. Differential scanning calorimetry thermogram of miconazole nitrate.

3.6.2. Vibrational spectroscopy

The infrared absorption spectrum of miconazole nitrate was obtained in a KBr pellet using a Perkin-Elmer infrared spectrophotometer. The IR spectrum is shown in Fig. 4, where the principal peaks were observed at 3140, 3070, 2995, 2920, 1566, 1525, 1445, 1385, 1310, 1070, and 710 cm^{-1}. Assignments for the major infrared absorption band are provided in Table 2. Clarke reported principal peaks at 1085, 1319, 827, 1302, 1038, and 812 cm^{-1} (miconazole nitrate, KBr disc) [2].

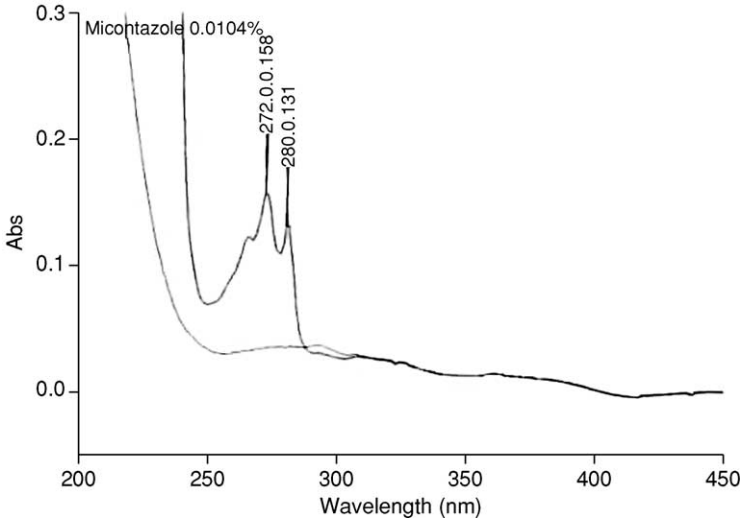

Fig. 3. Ultraviolet absorption spectrum of miconazole nitrate.

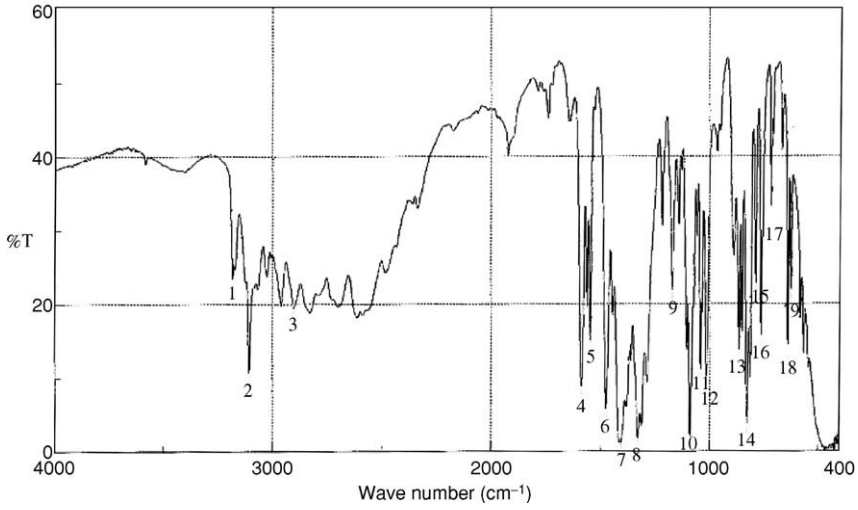

Fig. 4. Infrared absorption spectrum of miconazole nitrate (KBr pellet).

Table 2. Vibrational assignments for miconazole nitrate infrared absorption bands

Frequency (cm^{-1})	Assignment
3140	Imidazole C—N stretch
3070	Aromatic CH stretch
2995	Aliphatic CH_2 stretch
2920	Aliphatic CH stretch
1566	C=C aromatic
1525	C=C aromatic
1445	—CH_2– bending
1385	C—H bending (aliphatic)
1310	C—N stretch
1070	C—C stretch
710	C—H bending (aromatic)

3.6.3. Nuclear magnetic resonance spectrometry

3.6.3.1. ^1H NMR spectrum

The proton NMR spectrum of miconazole nitrate was obtained using a Bruker Instrument operating at 300, 400, or 500 MHz. Standard Bruker Software was used to execute the recording of DEPT, COSY, and HETCOR spectra. The sample was dissolved in DMSO-d_6 and all resonance bands were referenced to the tetramethylsilane (TMS) internal standard. The ^{1}H NMR spectra of miconazole nitrate are shown in Figs. 5–7 and the COSY ^{1}H NMR spectrum is shown in Fig. 8. The ^{1}H NMR assignments for miconazole nitrate are provided in Table 3.

3.6.3.2. ^{13}C NMR spectrum

The carbon-13 NMR spectra of miconazole nitrate were obtained using a Bruker Instrument operating at 75, 100, or 125 MHz. The sample was dissolved in DMSO-d_6 and tetramethylsilane (TMS) was added to function as the internal standard. The ^{13}C NMR spectra are shown in Figs. 9 and 10 and the HSQC and HMBC NMR spectra are shown in Figs. 11 and 12, respectively. The DEPT 90 and DEPT 135 are shown in Figs. 13 and 14, respectively. The assignments for the observed resonance bands associated with the various carbons are listed in Table 4.

3.7. Mass spectrometry

The mass spectrum of miconazole nitrate was obtained using a Shimadzu PQ-5000 mass spectrometer. The parent ion was collided with helium as the carrier gas. Figure 15 shows the detailed mass fragmentation pattern and Table 5 shows the mass fragmentation pattern of the drug substance. Clarke reported the presence of the following principal peaks at m/z = 159, 161, 81, 335, 333, 163, 337, and 205 [2].

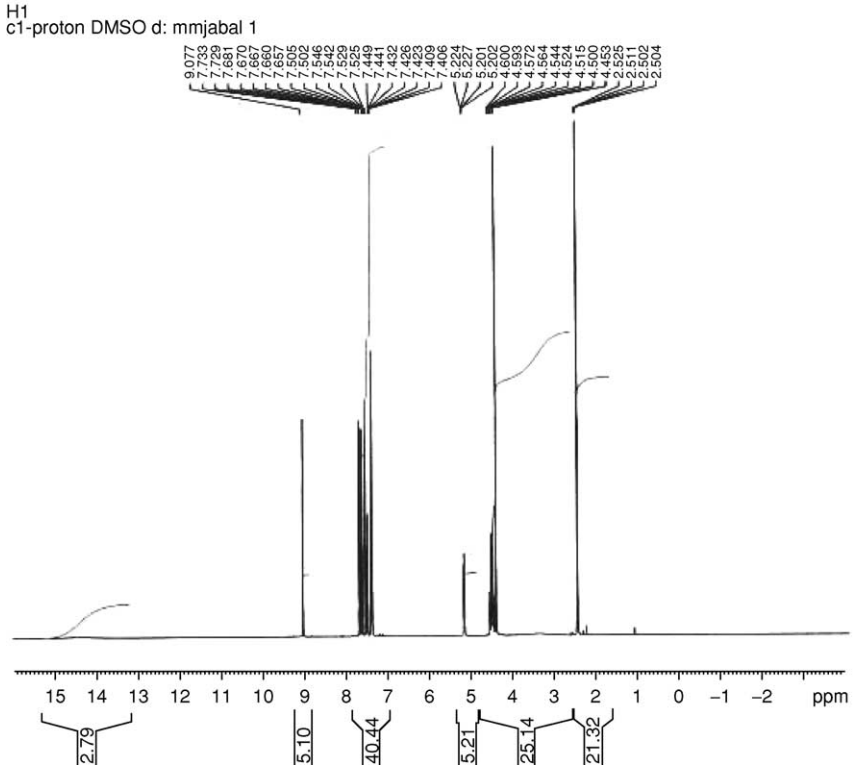

Fig. 5. The ^{1}H NMR spectrum of miconazole nitrate in DMSO-d_6.

4. METHODS OF ANALYSIS

4.1. Compendial methods

4.1.1. British pharmacopoeia methods [12]

4.1.1.1. Miconazole

Miconazole contains not less than 99% and not more than the equivalent of 101% of (*RS*)-1-[2-(2,4-dichlorobenzyloxy)-2-(2,4-dichlorophenyl)ethyl]-1*H*-imidazole, calculated with reference to the dried substance.

Identification

Test 1. When miconazole is tested according to the general method (2.2.14), the melting point of miconazole is in the range 83–87 °C.

Test 2. According to the general method (2.2.24), examine miconazole by infrared absorption spectrophotometry, comparing with the spectrum obtained with *miconazole CRS*. Examine the substance as discs prepared using *potassium bromide R*.

Test 3. According to the general method (2.2.27), examine by thin-layer chromatography using a suitable octadecylsilyl silica gel as the coating substance.

Test solution. Dissolve 30 mg of miconazole in the mobile phase and dilute to 5 mL with the mobile phase.

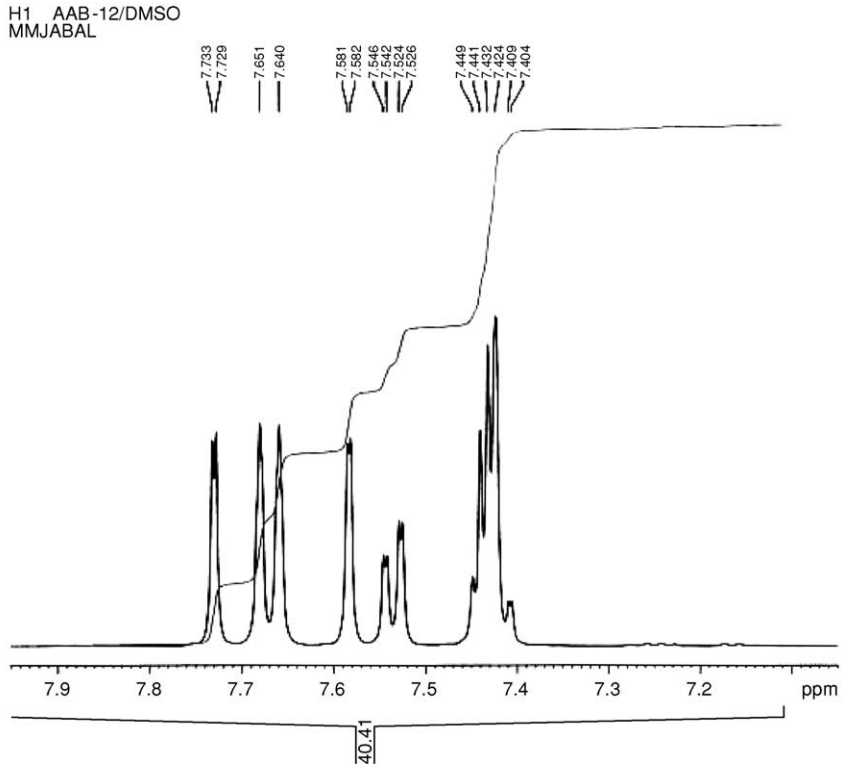

Fig. 6. Expanded ^{1}H NMR of miconazole nitrate in DMSO-d_6.

Reference solution (a). Dissolve 30 mg of *miconazole CRS* in the mobile phase and dilute to 5 mL with the mobile phase.

Reference solution (b). Dissolve 30 mg of *miconazole CRS* and 30 mg of *econazole nitrate CRS* in the mobile phase and dilute to 5 mL with the mobile phase.

Apply separately to the plate 5 μL of each solution. Develop over a path of 15 cm using a mixture of 20 volumes of *ammonium acetate solution R*, 40 volumes of *dioxan R* and 40 volumes of *methanol R*. Dry the plate in a current of warm air for 15 min and expose it to iodine vapor until the spots appear. Examine in daylight. The principal spot in the chromatogram obtained with the test solution is similar in position, color, and size to the principal spot in the chromatogram obtained with reference solution (a). The test is not valid unless the chromatogram obtained with reference solution (b) shows two clearly separated spots.

Test 4. To 30 mg of miconazole in a porcelain crucible add 0.3 g of *anhydrous sodium carbonate R*. Heat over an open flame for 10 min. Allow to cool. Take up the residue with 5 mL of *dilute nitric acid R* and filter. To 1 mL of the filtrate add 1 mL of *water R*. The solution gives reaction (a) of chloride (general test (2.3.1)).

Tests

Solution S. Dissolve 0.1 g of miconazole in *methanol R* and dilute to 10 mL with the same solvent.

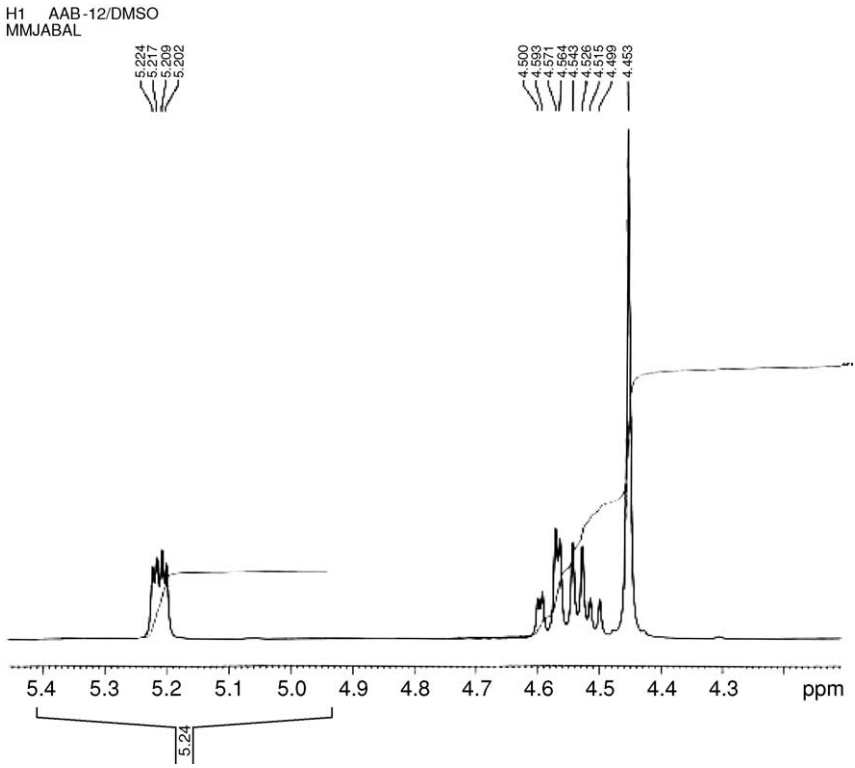

Fig. 7. Expanded ^{1}H NMR spectrum of miconazole nitrate in DMSO-d_6.

Appearance of solution. When the test is carried out as directed in general method (2.2.1), solution S is clear and is not more intensely colored than reference solution Y_6, as directed in general method (method II, 2.2.2).

Optical rotation. When test is carried out as directed in general method (2.2.7), the angle of optical rotation of solution S is $-0.10°$ to $+0.10°$.

Related substances. Examine by liquid chromatography, as directed in general method (2.2.29).

Test solution. Dissolve 0.1 g of miconazole in the mobile phase and dilute to 10 mL with the mobile phase.

Reference solution (a). Dissolve 2.5 mg of *miconazole CRS* and 2.5 mg of *econazole nitrate CRS* in the mobile phase and dilute to 100 mL with the mobile phase.

Reference solution (b). Dilute 1 mL of the test solution to 100 mL with the mobile phase. Dilute 5 mL of this solution to 20 mL with the mobile phase.

The chromatographic procedure may be carried out using:

– a stainless steel column 0.1 m long and 4.6 mm in internal diameter packed with *octadecylsilyl silica gel for chromatography R* (3 μm).
– as mobile phase at a flow rate of 2 mL/min a solution of 6 g of *ammonium acetate R* in a mixture of 300 mL of *acetonitrile R*, 320 mL of *methanol R* and 380 mL of *water R*.
– as detector, a spectrophotometer set at 235 nm.

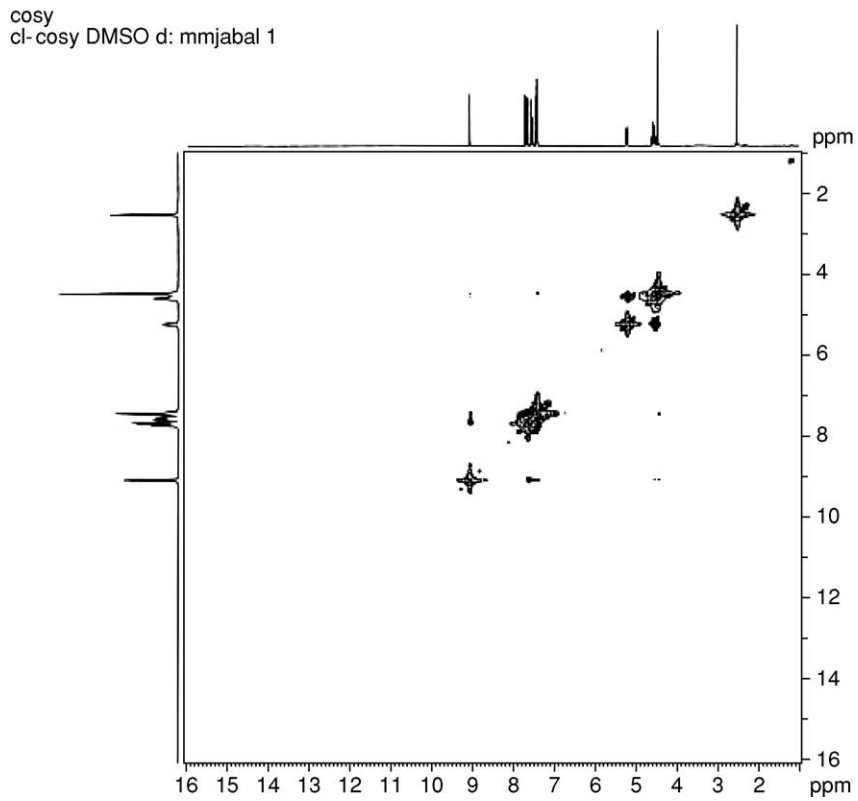

Fig. 8. COSY ^{1}H NMR spectrum of miconazole nitrate in DMSO-d_6.

Equilibrate the column with the mobile phase at a flow rate of 2 mL/min for about 30 min.

Adjust the sensitivity of the system so that the height of the principal peak in the chromatogram obtained with 10 μL of reference solution (b) is not less than 50% of the full scale of the recorder.

Inject 10 μL of reference solution (a). When the chromatograms are recorded in the prescribed conditions, the retention times are: econazole nitrate, about 10 min; miconazole, about 20 min. The test is not valid unless the resolution between the peaks corresponding to econazole nitrate and miconazole is not less than 10; if necessary, adjust the composition of the mobile phase.

Inject separately 10 μL of the test solution and 10 μL of reference solution (b). Continue the chromatography for 1.2 times the retention time of the principal peak. In the chromatogram obtained with the test solution, the area of any peak, apart from the principal peak, is not greater than the area of the principal peak in the chromatogram obtained with reference solution (b) (0.25%); the sum of the areas of all peaks, apart from the principal peak, is not greater than twice that of the principal peak in the chromatogram obtained with reference solution (b) (0.5%). Disregard any peak due to the solvent and any peak with an area less than 0.2 times the area of the principal peak in the chromatogram obtained with reference solution (b).

Table 3. Assignments of the resonance bands in the ^{1}H NMR spectrum of miconazole nitrate

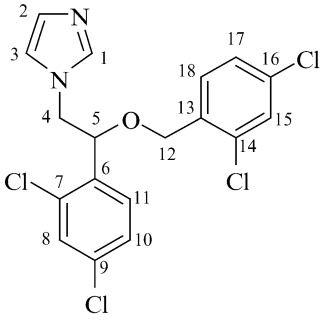

Chemical shift (ppm, relative to TMS)	Number of protons	Multiplicity*	Assignment (proton at carbon number)
9.09	1	s	1
7.66, 7.72	1	dd	3 or 2
7.58, 7.68	1	dd	2 or 3
7.42–7.52	2	m	8 and 15
7.43–7.45	4	m	10, 11 and 17, 18
5.21–5.23	1	m	5
4.51–4.61	2	m	4
4.45	2	s	12

*s, singlet; dd, double doublet; m, multiplet.

Loss on drying. When miconazole is tested according to the general method (2.2.32), not more than 5%, determined on 1 g by drying in vacuo at 60 °C for 4 h.

Sulfated ash. When miconazole is tested according to the general method (2.4.14), not more than 0.1%, determined on 1 g.

Assay

Dissolve 0.3 g of miconazole in 50 mL of a mixture of 1 volume of *glacial acetic acid R* and 7 volumes of *methyl ethyl ketone R*. Using 0.2 mL of *naphthalbenzein solution R* as indicator, titrate with 0.1 M *perchloric acid* until the color changes from orange-yellow to green. One milliliter of 0.1 M perchloric acid is equivalent to 41.61 mg of $C_{18}H_{14}Cl_4N_2O$.

Storage

Store in a well-closed container, protected from light.

Impurities

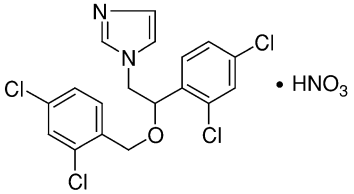

1. Miconazole nitrate

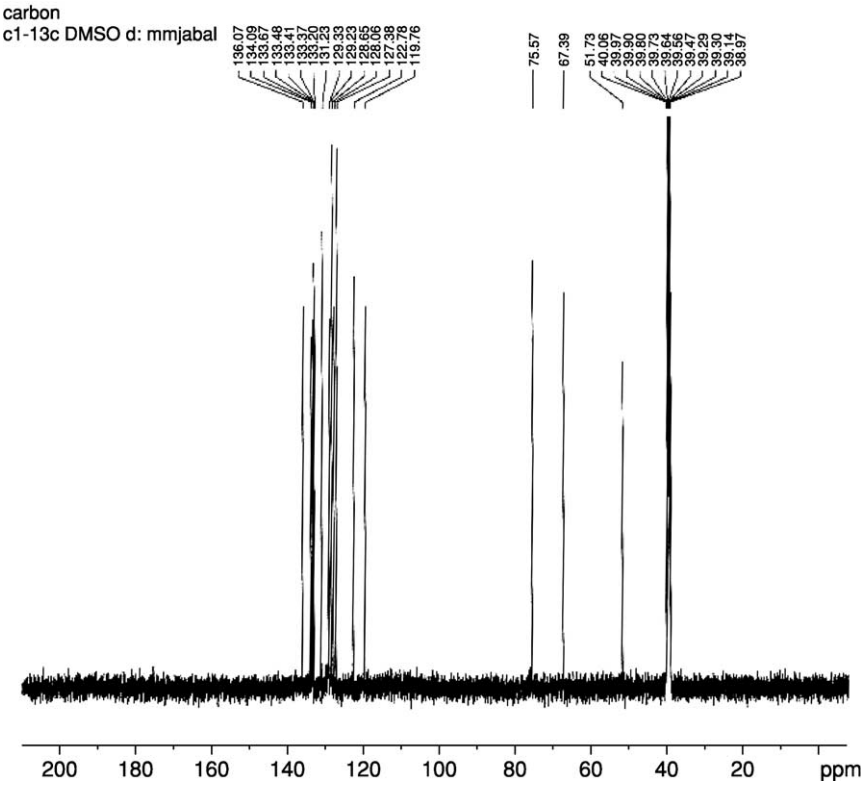

Fig. 9. ^{13}C NMR spectrum of miconazole nitrate in DMSO-d_6.

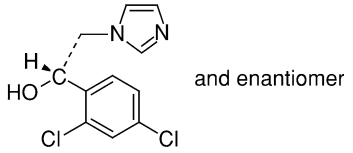

2. (*RS*)-1-(2,4-dichlorophenyl)-2-imidazol-1-ylethanol

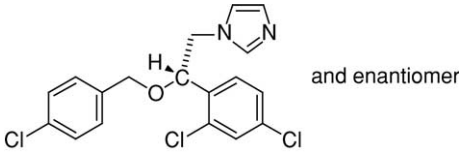

3. (*RS*)-1-[2-(4-chlorobenzyloxy)-2-(2,4-dichlorophenyl)ethyl)]imidazole

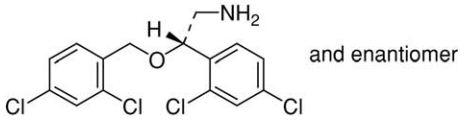

4. (*RS*)-2-(2,4-dichlorobenzyloxy)-2-(2,4-dichlorophenyl)ethylamine

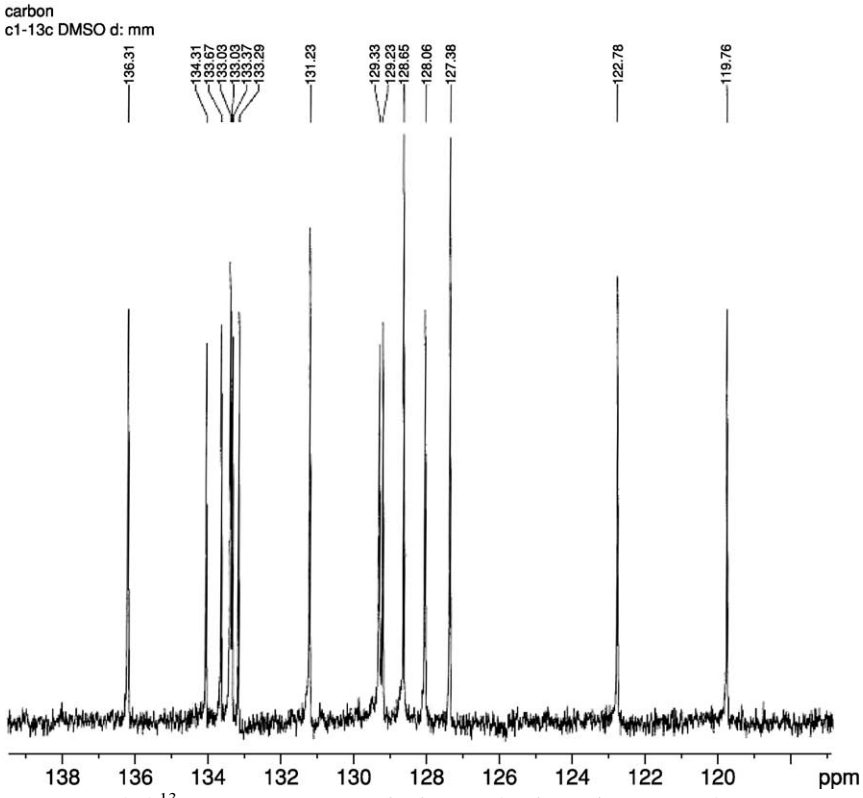

Fig. 10. Expanded ^{13}C NMR spectrum of miconazole nitrate in DMSO-d_6.

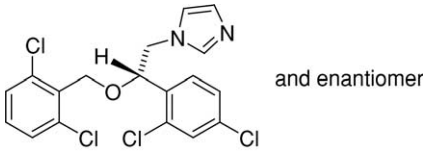

5. (*RS*)-1-[2-(2,6-dichlorobenzyloxy)-2-(2,4-dichlorophenyl)ethyl]imidazole

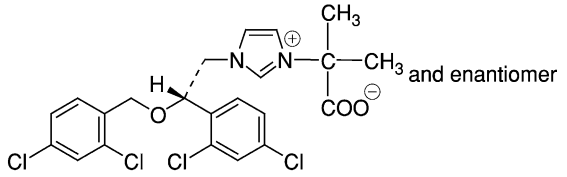

6. (*RS*)-1-(1-carboxylato-1-methylethyl)-3-[2-(2,4-dichlorobenzyloxy)-2-(2,4-dichlorophenyl) ethyl]imidazolium

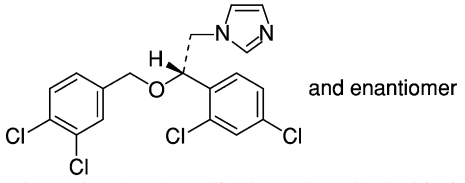

7. (*RS*)-1-[2-(3,4-dichlorobenzyloxy)-2-(2,4-dichlorophenyl)ethyl]imidazole

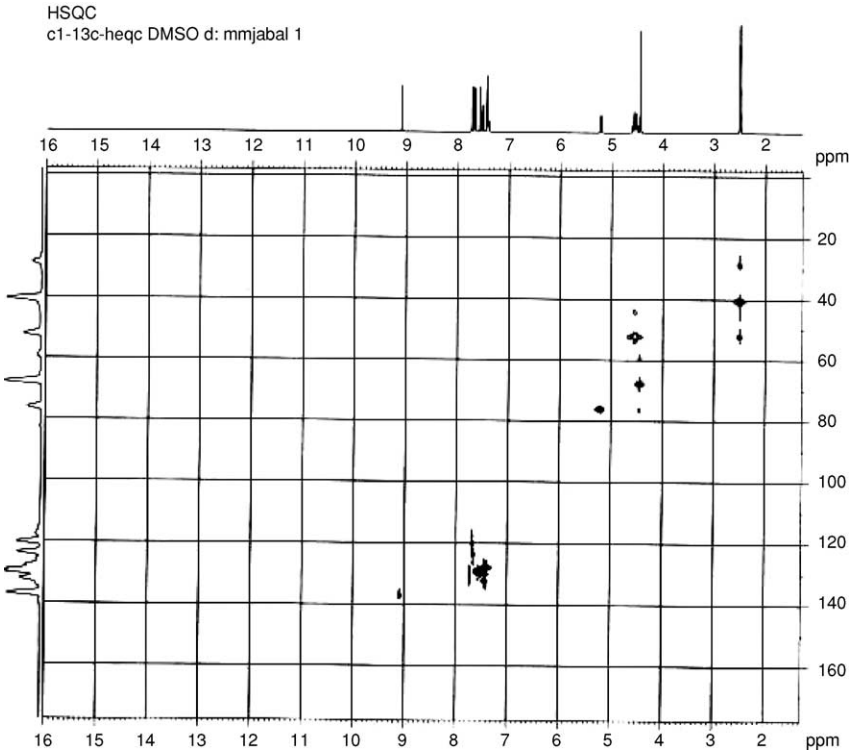

Fig. 11. The HSQC NMR spectrum of miconazole nitrate in DMSO-d_6.

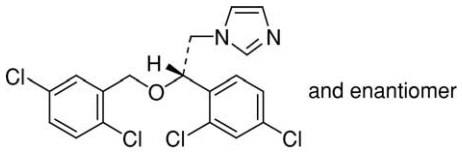

8. (*RS*)-1-[2-(2,5-dichlorobenzyloxy)-2-(2,4-dichlorophenyl)ethyl]imidazole

4.1.1.2. Miconazole in pharmaceutical formulation

4.1.1.2.1. Miconazole oromucosal gel. Miconazole oromucosal gel is a suspension of miconazole, *in very fine powder*, in a suitable water-miscible basis, it may be flavored. The gel contains not less than 95% and not more than 105% of the prescribed or the stated amount of $C_{18}H_{14}Cl_4N_2O$.

Identification

Test 1. Shake a quantity of the gel containing 20 mg of miconazole with sufficient *methanol* to produce a 0.05% (w/v) solution. The *light absorption* of this solution, Appendix II B, in the range 250–350 nm exhibits two maxima at 272 and 280 nm and a broad shoulder at about 263 nm.

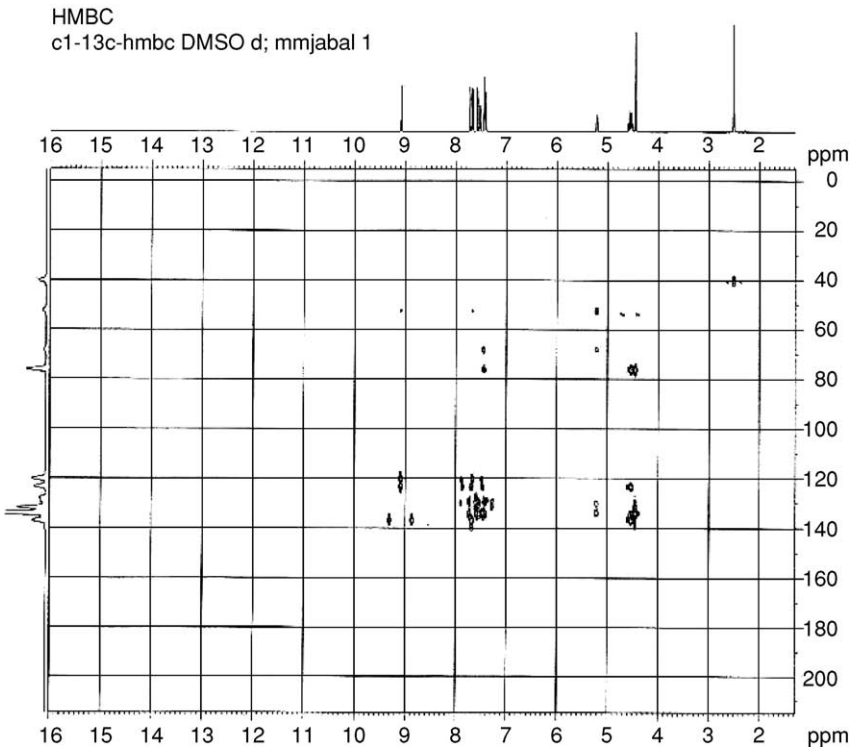

Fig. 12. The HMBC NMR spectrum of miconazole in DMSO-d_6.

Test 2. In the Assay, the principal peak in the chromatogram obtained with solution (1) has the same retention time as the principal peak in the chromatogram obtained with solution (2).

Acidity or alkalinity. pH, 5.5–7.5, Appendix VL.

Related substances. Carry out the method for *liquid chromatography*, Appendix III D, using the following solutions. For solution (1) shake a quantity of the gel containing 50 mg of miconazole with 25 mL of *methanol* for 30 min, add sufficient *methanol* to produce 50 mL and filter through a glass microfibre (Whatman GF/C is suitable). For solution (2) dilute 1 volume of solution (1) to 100 volumes with *methanol* and dilute 5 volumes of the resulting solution to 20 volumes with *methanol.* Solution (3) contains 0.0025% (w/v) of *miconazole nitrate BPCRS* and *econazole nitrate BPCRS* in *methanol.*

The chromatographic procedure may be carried out using (a) a stainless steel column (10 cm × 4.6 mm) packed with *stationary phase C* (3 μm) (Hypersil ODS in suitable), (b) as the mobile phase with a flow rate of 2 mL/min a 0.6% (w/v) solution of *ammonium acetate* in a mixture of 300 volumes of *acetonitrile*, 320 volumes of *methanol* and 380 volumes of *water*, and (c) a detection wavelength of 235 nm.

Inject 10 μL of solution (3). The test is not valid unless the *resolution factor* between the peaks due to miconazole and econazole is at least 10.

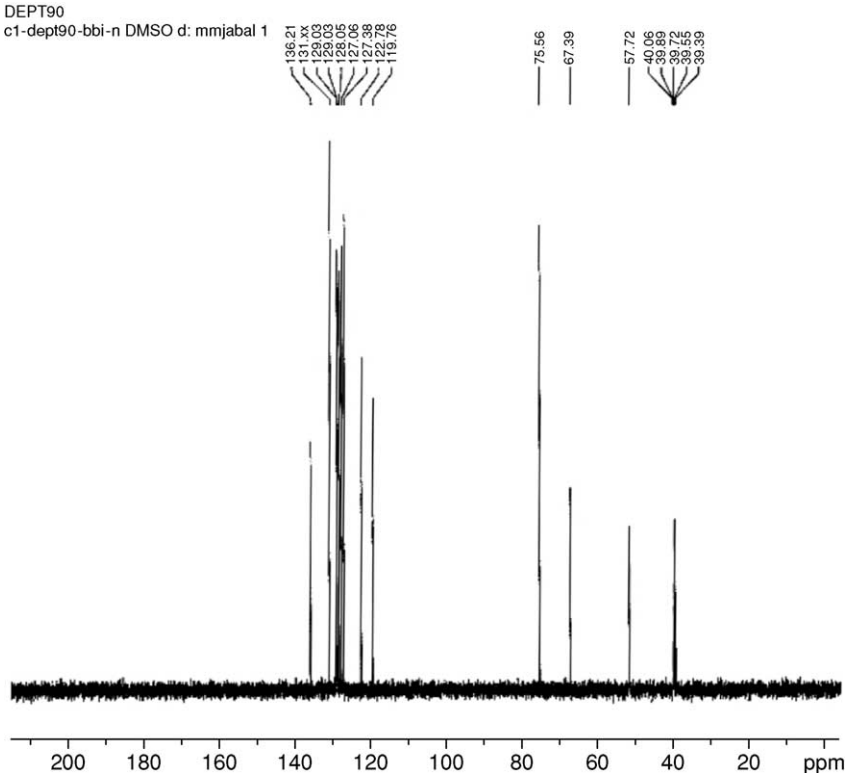

Fig. 13. The DEPT 90 ^{13}C NMR of miconazole nitrate in DMSO-d_6.

Inject separately 10 μL of each solution (1) and solution (2). For solution (1), continue the chromatography for twice the retention time of the principal peak. In the chromatogram obtained with solution (1), the area of any *secondary peak* is not greater than the area of the principal peak in the chromatogram obtained with solution (2) (0.25%), and the sum of the areas of any *secondary peak* is not greater than twice the area of the principal peak in the chromatogram obtained with solution (2) (0.5%). Disregard any peak with an area less than 0.2 times the area of the principal peak in the chromatogram obtained with solution (2) (0.05%).

Assay

Carry out the method for *liquid chromatography*, Appendix III D, using the following solutions. For solution (1) shake a quantity of the gel containing 50 mg of miconazole with 25 mL of *miconazole* for 30 min, add sufficient *methanol* to produce 50 mL and filter through a glass microfibre filter (Whatman GF/C is suitable). Solution (2) contains 0.12% (w/v) of *miconazole nitrate BPCRS* in *methanol*. Solution (3) contains 0.0025% (w/v) of each *miconazole BPCRS* and *econazole nitrate BPCRS* in *methanol*.

The chromatographic conditions described under Related substances may be used.

The test is not valid unless, in the chromatogram obtained with solution (3), the *resolution factor* between the peak due to miconazole and econazole is at least 10.

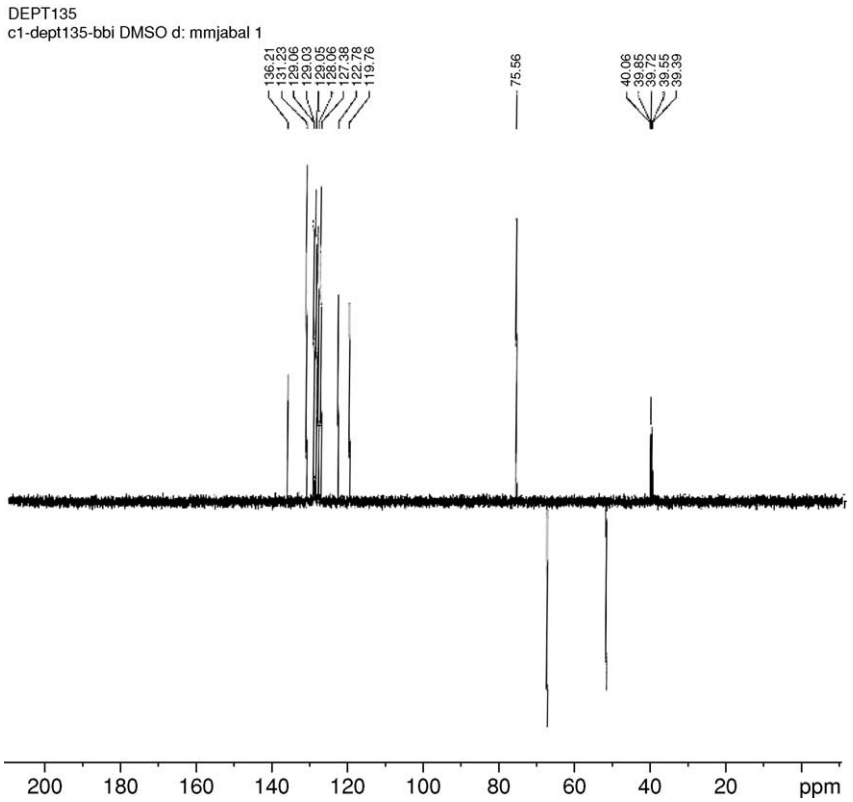

Fig. 14. The DEPT 135 ^{13}C NMR spectrum of miconazole nitrate in DMSO-d_6.

Calculate the content of $C_{18}H_{14}Cl_4N_2O$ in the gel using the declared content of $C_{18}H_{14}Cl_4N_2O$ in *miconazole nitrate BPCRS*.

Storage

Miconazole Ormucosul Gel should be kept in a well-closed container and protected from light.

Labeling

The label states (1) the date after which the gel is not intended to be used; (2) the conditions under which the gel should be stored; (3) the directions for use.

4.1.1.3. Miconazole nitrate

Miconazole nitrate contains not less than 99% and not more than the equivalent of 101% of (*RS*)-1-[2-(2,4-dichlorobenzyloxy)-2-(2,4-dichlorophenyl)ethyl]-1*H*-imidazole nitrate.

Identification

Test 1. When miconazole nitrate is tested according to the general method (2.2.14), the drug substance melts in the range 178–184 °C.

Table 4. Assignments for the resonance bands in the ^{13}C NMR spectrum

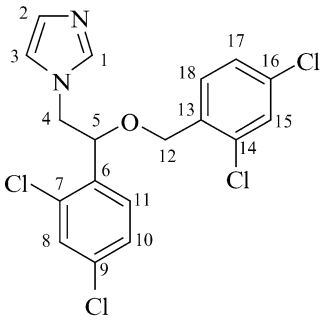

Chemical shift (ppm relative to TMS)	Assignment (carbon number)	Chemical shift (ppm relative to TMS)	Assignment (carbon number)
136.1	1	122.76	3
134.08, 133.67	Six, quaternary	122.78	2
133.43, 133.41	carbon atoms at:		
133.37, 133.20	6, 7, 9, 13, 14, 16		
131.23, 129.33	8 and 15	75.56	5
129.23, 128.65	10 and 17	67.39	12
128.23, 127.38	11 and 18	51.72	4

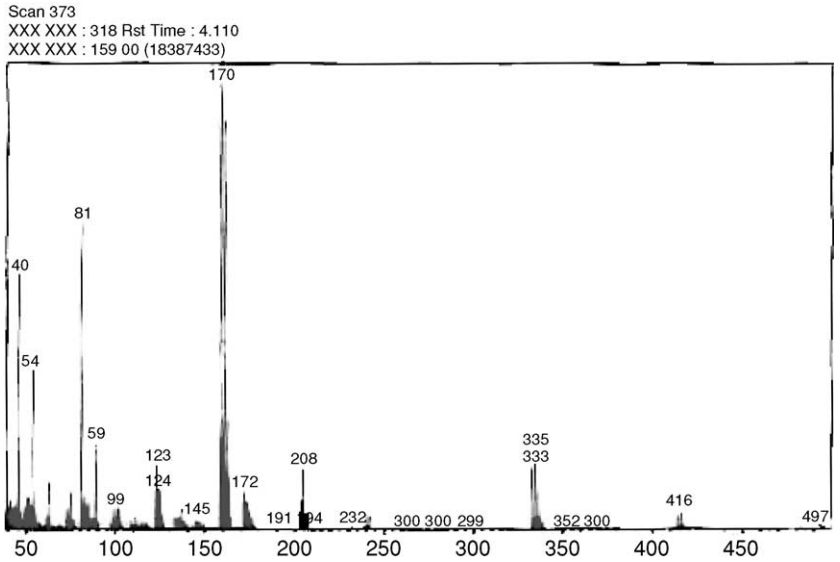

Fig. 15. Mass spectrum of miconazole nitrate.

Test 2. Examine miconazole nitrate by infrared absorption spectrophotometry according to the general method (2.2.24), comparing with the spectrum obtained with *miconazole nitrate CRS*. Examine the drug substance prepared as disc using *potassium bromide R*.

Table 5. Mass spectral fragmentation pattern of miconazole

m/z	Relative intensity (%)	Fragment	
		Formula	Structure
414	5	$C_{18}H_{14}Cl_4N_2O$	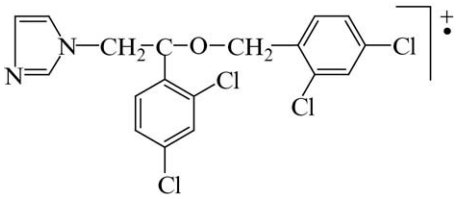
333	15	$C_{14}H_9Cl_4O$	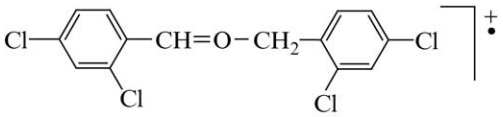
205	15	$C_{11}H_{10}ClN_2$	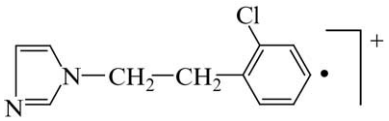
172	10	$C_8H_6Cl_2$	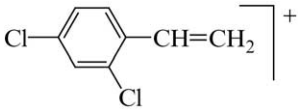
159	100	$C_7H_5Cl_2$	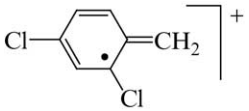
145	3	$C_6H_3Cl_2$	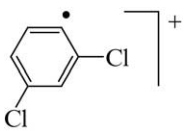
124	10	$C_6H_8N_2O$	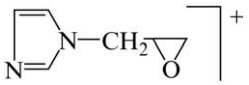
123	16	$C_6H_7N_2O$	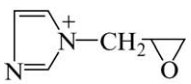
99	8	C_5H_4Cl	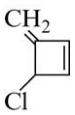

(*Continues*)

Table 5. (*Continued*)

m/z	Relative intensity (%)	Fragment	
		Formula	Structure
89	12	C_3H_2ClO	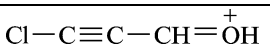
81	60	$C_4H_5N_2$	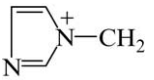
54	32	C_3H_4N	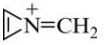
46	50	C_2H_6O	

Test 3. Examine miconazole nitrate by thin-layer chromatography according to the general method (2.2.27), using a suitable octadecylsilyl silica gel as the coating substance.

Test solution. Dissolve 30 mg of miconazole nitrate in the mobile phase and dilute to 5 mL with the mobile phase.

Reference solution (a). Dissolve 30 mg of *miconazole nitrate CRS* in the mobile phase and dilute to 5 mL with the mobile phase.

Reference solution (b). Dissolve 30 mg of *miconazole nitrate CRS* and 30 mg of *econazole nitrate CRS* in the mobile phase and dilute to 5 mL with the mobile phase.

Apply separately to the plate 5 µL of each solution. Develop over a path of 15 cm using a mixture of 20 volumes of *ammonium acetate solution R*, 40 volumes of *dioxan R* and 40 volumes of *methanol R*. Dry the plate in a current of warm air for 15 min and expose it to iodine vapor until the spots appear. Examine in daylight. The principal spot in the chromatogram obtained with the test solution is similar in position, color, and size to the principal spot in the chromatogram obtained with reference solution (a). The test is not valid unless the chromatogram obtained with reference solution (b) shows two clearly separated spots.

Test 4. When miconazole nitrate is tested according to the general procedure (2.3.1), it gives the reaction of nitrates.

Tests

Solution S. Dissolve 0.1 g in *methanol R* and dilute to 10 mL with the same solvent.

Appearance of solution. When the test is carried out according to the general method (2.2.1), solution S is clear and is not more intensely colored than reference solution Y_7 (Method II, 2.2.2).

Optical rotation. When miconazole nitrate is tested according to the general method (2.2.7). The angle of optical rotation of solution S is $-0.10°$ to $+0.10°$.

Related substances. Examine by liquid chromatography according to the general procedure (2.2.29).

Test solution. Dissolve 0.1 g of miconazole nitrate in the mobile phase and dilute to 10 mL with the mobile phase.

Reference solution (a). Dissolve 2.5 mg of *miconazole nitrate CRS* and 2.5 mg of *econazole nitrate CRS* in the mobile phase and dilute to 100 mL with the mobile phase.

Reference solution (b). Dilute 1 mL of the test solution to 100 mL with the mobile phase. Dilute 5 mL of this solution to 20 mL with the mobile phase.

The chromatographic procedure may be carried out using:

– a stainless steel column 0.1 m long and 4.6 mm in internal diameter packed with *octadecylsilyl silica gel for chromatography R* (3 μm).
– a mobile phase at a flow rate of 2 mL/min a solution of 6.0 g of *ammonium acetate R* in a mixture of 300 mL of *acetonitrile R*, 320 mL of *methanol R* and 380 mL of *water R*.
– as detector, a spectrophotometer set at 235 nm.

Equilibrate the column with the mobile phase at a flow rate of 2 mL/min for about 30 min.

Adjust the sensitivity of the system so that the height of the principal peak in the chromatogram obtained with 10 μL of reference solution (b) is not less than 50% of the full scale of the recorder.

Inject 10 μL of reference solution (a). When the chromatogram is recorded in the prescribed conditions, the retention times are: econazole nitrate, about 10 min; miconazole nitrate, about 20 min. The test is not valid unless the resolution between the peaks corresponding to econazole nitrate and miconazole nitrate is at least 10; if necessary, adjust the composition of the mobile phase.

Inject separately, 10 μL of the test solution and 10 μL of the reference solution (b). Continue the chromatography for 1.2 times the retention time of the principal peak. In the chromatogram obtained with the test solution, the area of any peak apart from the principal peak is not greater than the area of the principal peak in the chromatogram obtained with reference solution (b) (0.25%); the sum of the areas of the peaks apart from the principal peak is not greater than twice the area of the principal peak in the chromatogram obtained with reference solution (b) (0.5%). Disregard any peak due to the nitrate ion and any peak with an area less than 0.2 times the area of the principal peak in the chromatogram obtained with reference solution (b).

Loss on drying. When miconazole nitrate is tested according to the general method (2.2.32), not more than 0.5%, determined on 1 g by drying in an oven at 100–105 °C for 2 h.

Sulfated ash. When miconazole nitrate is tested according to the general method (2.4.14); not more than 0.1%, determined on 1 g.

Assay

Dissolve 0.35 g of miconazole nitrate in 75 mL of *anhydrous acetic acid* R, with slight heating, if necessary. Titrate with 0.1 M *perchloric acid* determining the end point potentiometrically, according the general method (2.2.20). Carry out a blank titration. One milliliter of 0.1 M *perchloric acid* is equivalent to 47.91 mg of $C_{18}H_{15}Cl_4N_3O_4$.

Storage

Store in a well-closed container, protected from light.

Impurities

A solution of 6 g of *ammonium acetate R* in a mixture of 300 mL of *acetonitrile R*, 320 mL of *methanol R* and 380 mL of *water R*.

– as detector, a spectrophotometer set at 235 nm.

Equilibrate the column with the mobile phase at a flow rate of 2 mL/min for about 30 min.

Adjust the sensitivity of the system so that the height of the principal peak in the chromatogram obtained with 10 μL of reference solution (b) is not less than 50% of the full scale of the recorder.

Inject 10 μL of reference solution (a). When the chromatograms are recorded in the prescribed conditions, the retention times are: econazole nitrate, about 10 min; miconazole, about 20 min. The test is not valid unless the resolution between the peaks corresponding to econazole nitrate and miconazole is not less than 10; if necessary, adjust the composition of the mobile phase.

Inject separately 10 μL of the test solution and 10 μL of reference solution (b). Continue the chromatography for 1.2 times the retention time of the principal peak. In the chromatogram obtained with the test solution, the area of any peak, apart from the principal peak, is not greater than the area of the principal peak in the chromatogram obtained with reference solution (b) (0.25%); the sum of the areas of all peaks, apart from the principal peak is not greater than twice that of the principal peak in the chromatogram obtained with reference solution (b) (0.5%). Disregard any peak due to solvent and any peak with an area less than 0.2 times the area of the principal peak in the chromatogram obtained with reference solution (b).

Loss on drying. When miconazole nitrate is tested according to the general method (2.2.32); not more than 0.5%, determined on 1.000 g by drying in vacuo at 60 °C for 4 h.

Sulfated ash. When miconazole nitrate is tested according to the general method (2.2.14); not more than 0.1%, determined on 1.0 g.

Assay

Dissolve 0.3 g of miconazole nitrate in 50 mL of a mixture of 1 volume of *glacial acetic acid R* and 7 volumes of *methyl ethyl ketone R*. Using 0.2 mL of *naphtholbenzein solution R* as indicator, titrate with 0.1 M *perchloric acid* until the color changes from orange-yellow to green. One milliliter of 0.1 M *perchloric acid* is equivalent to 41.61 mg of $C_{18}H_{14}Cl_4N_2O$.

Storage

Store miconazole nitrate in a well-closed container, protected from light.

Impurities

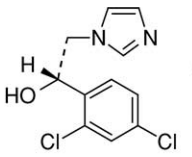

and enantiomer

1. (*RS*)-1-(2,4-dichlorophenyl)-2-imidazol-1-ylethanol

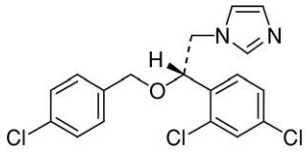
and enantiomer

2. (*RS*)-1-[2-(4-chlorobenzyloxy)-2-(2,4-dichlorophenyl)ethyl]imidazole

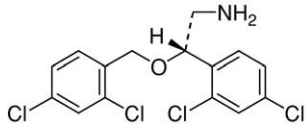
and enantiomer

3. (*RS*)-2-(2,4-dichlorobenzyloxy)-2-(2,4-dichlorophenyl)ethylamine

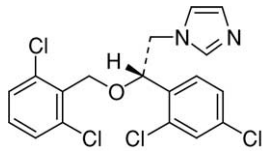
and enantiomer

4. (*RS*)-1-[2-(2,6-dichlorobenzyloxy)-2-(2,4-dichlorophenyl)ethyl]imidazole

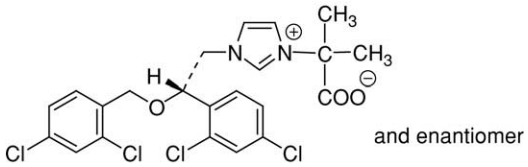
and enantiomer

5. (*RS*)-1-(1-carboxylato-1-methylethyl)-3-[2-(2,4-dichlorobenzyloxy)-2-(2,4-dichlorophenyl) ethyl]imidazolium

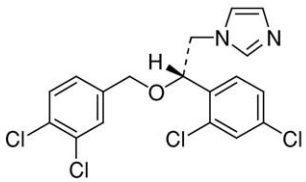
and enantiomer

6. (*RS*)-1-[2-(3,4-dichlorobenzyloxy)-2-(2,4-dichlorophenyl)ethyl]imidazole

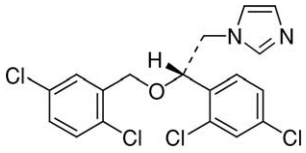
and enantiomer

7. (*RS*)-1-[2-(2,5-dichlorobenzyloxy)-2-(2,4-dichlorophenyl)ethyl]imidazole

4.1.1.4. Miconazole nitrate in pharmaceutical formulation

4.1.1.4.1. Miconazole cream. Miconazole cream contains miconazole nitrate $C_{18}H_{14}Cl_4N_2O{\cdot}HNO_3$ 90–110% of prescribed or stated amount in a suitable basis.

Identification

Test 1. Mix a quantity containing 40 mg of miconazole nitrate with 20 mL of a mixture of 1 volume of 1 M *sulfuric acid* and 4 volumes of *methanol* and shake with two 50 mL quantities of *hexane*, discarding the organic layers. Make the aqueous phase alkaline with 2 M *ammonia* and extract with two 40 mL quantities of *chloroform*. Combine the chloroform extracts, shake with 5 g of *anhydrous sodium sulfate*, filter, and dilute the filtrate to 100 mL with *chloroform*. Evaporate 50 mL to dryness and dissolve the residue in 50 mL of a mixture of 1 volume of 0.1 M *hydrochloric acid* and 9 volumes of *methanol*. The *light absorption* of the resulting solution, Appendix II B, in the range 230–350 nm exhibits maxima at 264, 272, and 282 nm.

Test 2. In the assay, the principal peak in the chromatogram obtained with solution (2) has the same retention time as the peak due to miconazole in the chromatogram obtained with solution (1).

Assay

Carry out the method for *gas chromatography*, Appendix III B, using the following solutions. For solution (1) shake 40 mg of *miconazole nitrate BPCRS* with 10 mL of a 0.3% (w/v) solution of *1,2,3,4-tetraphenylcyclopenta-1,3-dienone* (internal standard) in *chloroform* and 0.2 mL of 13.5 M *ammonia*, and 1 g of *anhydrous sodium sulfate*, shake again and filter. Prepare solution (2) in the same manner as solution (3) but omitting the addition of the internal standard solution. For solution (3) mix a quantity of the cream containing 40 mg of miconazole nitrate with 20 mL of a mixture of 1 volume of 0.5 M *sulfuric acid* and 4 volumes of *methanol* and shake with two 50 mL quantities of *carbon tetrachloride*. Wash each organic layer in turn with the same 10 mL quantity of a mixture of 1 volume of 0.5 M *sulfuric acid* and 4 volumes of *methanol*. Combine the aqueous phase and the washings, make alkaline with 2 M *ammonia* and extract with two 50 mL quantities of *chloroform*. To the combined extracts add 10 mL of a 0.3% (w/v) solution of the internal standard in *chloroform* and 5 g of *anhydrous sodium sulfate*, shake, filter, evaporate the filtrate to a low volume and add sufficient *chloroform* to produce 10 mL.

The chromatographic procedure may be carried out using a glass column (1.5 m × 2 mm) packed with *acid-washed*, *silanized diatomaceous support* (80–100 mesh) coated with 3% (w/w) of phenyl methyl silicone fluid (50% phenyl) (OV-17 is suitable) and maintained at 270 °C.

Calculate the content of $C_{18}H_{14}Cl_4N_2O$, HNO_3 using the declared content of $C_{18}H_{14}Cl_4N_2O$, HNO_3 in *miconazole nitrate BPCRS*.

Storage

If miconazole cream is kept in aluminium tubes, their inner surfaces should be coated with a suitable lacquer.

4.1.2. United States Pharmacopoeia (1995) [13]

Miconazole

Miconazole contains not less than 98% and not more than 102% of $C_{18}H_{14}Cl_4N_2O$, calculated on the dried basis.

4.1.2.1. Identification

Test 1. Carry out the infrared test according to the general procedure <197 K>. The infrared absorption spectrum of a potassium bromide dispersion of it, previously dried, exhibits maxima only at the same wavelength as that of a similar preparation of *USP miconazole RS*.

Test 2. Transfer 40 mg to a 100 mL volumetric flask, dissolve in 50 mL of isopropyl alcohol, add 10 mL of 0.1 N hydrochloric acid, dilute with isopropyl alcohol to volume, and mix: the ultraviolet absorption spectrum of this solution exhibits maxima and minima at the same wavelength as that of a similar solution of *USP Miconazole RS*, concomitantly measured.

Loss on drying. Dry miconazole in vacuum at 60 °C for 4 h, according to the general method <731>, miconazole loses not more than 0.5% of its weight.

Residue on ignition. When the test is carried out according to the general method <281>, the residue of miconazole is not 0.2%.

Chromatographic purity. Dissolve 30 mg in 3 mL of chloroform to obtain the *Test preparation*. Dissolve a suitable quantity of *USP Miconazole RS* in chloroform to obtain a *Standard solution* having a concentration of 10 mg/mL. Dilute a portion of this solution quantitatively with chloroform to obtain *Diluted standard solution* having a concentration of 100 μg/mL. Apply separate 5 μL portions of the three solutions to the starting line of a suitable thin-layer chromatographic plate according to the general procedure <621>, coated with a 0.25 mm layer of chromatographic silica gel mixture. Develop the chromatogram in a suitable chamber with a freshly prepared solvent system consisting of a mixture of *n*-hexane, chloroform, methanol and ammonium hydroxide (60:30:10:1) until the solvent front has moved about three-fourths of the length of the plate. Remove the plate from the chamber and allow to the solvent to evaporate. Expose the plate to iodine vapors in a closed chamber for about 30 min, and locate the spots: the R_f value of the principal spot obtained from the *Test solution* corresponds to that obtained from the *Standard solution* and any other spot obtained from the *Test solution* does not exceed, in size or intensity, the principal spot obtained from the *Diluted standard solution* (1%).

Assay

Dissolve about 300 mg of Miconazole, accurately weighed, in 40 mL of glacial acetic acid, add 4 drops of *p*-naphtholbenzein TS, and titrate with 0.1 N perchloric acid VS to a green endpoint. Perform a blank determination, and make any necessary correction. Each mL of 0.1 N perchloric acid is equivalent to 41.61 mg of $C_{18}H_{14}Cl_4N_2O$.

4.1.2.2. Miconazole injection

Miconazole injection is a sterile solution of miconazole in water for injection. It contains not less than 90% and not more than 110% of the labeled amount of $C_{18}H_{14}Cl_4N_2O$.

Identification

Dragendorff's reagent: Dissolve 0.85 g of bismuth subnitrate in a mixture of 40 mL of water and 10 mL of glacial acetic acid (*Solution A*). Dissolve 8 g of potassium iodide in 20 mL of water (*Solution B*). Transfer 5 mL of *Solution A*, 5 mL of *Solution B*, and 20 mL of glacial acetic acid to a 100 mL volumetric flask, dilute with water to volume, and mix.

Procedure: Transfer a volume of injection, equivalent to about 50 mg of miconazole, to a 10 mL volumetric flask, dilute with methanol to volume, and mix. Dissolve a suitable quantity of *USP Miconazole RS* in methanol to obtain a Standard solution having a known concentration of about 5 mg/mL. Apply separate 5 µL portions of the two solutions to the starting line of a suitable thin-layer chromatographic plate, according to the general method, *Chromatography* <621>, coated with a 0.25 mm layer of chromatographic silica gel mixture. Develop the chromatogram in a suitable chamber with a freshly prepared solvent system consisting of a mixture of *n*-hexane, chloroform, methanol and ammonium hydroxide (60:30:10:1) until the solvent front has moved about three-fourths of the length of the plate. Remove the plate from the chamber, and allow the solvent to evaporate. Locate the spots on the plate by spraying with *Dragendorff's reagent*. The R_f value of one of the principal spots obtained from the test solution corresponds to that obtained from the Standard solution.

Bacterial endotoxins. When tested according to the general test <85>, miconazole injection contains not more than 0.1 USP Endotoxin Unit per mg of miconazole.

pH. The pH, when determined according to the general procedure <791>, is between 3.7 and 5.7.

Particulate matter. When tested according to the general procedure <788>, meets the requirements under *small volume injection*.

Other requirements. When tested according to the general procedure <1> it meets the requirements under injection.

Assay

Mobile phase: Dissolve 5 g of ammonium acetate in 200 mL of water, add 300 mL of acetonitrile and 500 mL of methanol, mix, filter, and degas. Make adjustments, if necessary (*see system suitability under Chromatography* <621>).

Standard preparation: Dissolve an accurately weighed quantity of *USP Miconazole RS* in *Mobile phase* and dilute quantitatively, and stepwise if necessary, with *Mobile phase* to obtain a solution having a known concentration of about 0.5 mg/mL. Transfer 10 mL of this solution to 100 mL volumetric flask, dilute with *Mobile phase* to volume, and mix to obtain a *Standard preparation* having a known concentration of about 50 µg/mL.

Resolution solution: Dissolve suitable quantities of *USP Miconazole RS* and dibutyl phthalate in *Mobile phase* to obtain a solution containing about 50 microgram of each per mL.

Assay preparation: Transfer an accurately measured volume of injection, equivalent to about 50 mg of miconazole, to a 100 mL volumetric flask, dilute with *Mobile phase* to volume, and mix. Transfer 10 mL of this solution to a 100-mL volumetric flask, dilute with *Mobile phase* to volume, and mix.

Chromatographic system: (See *Chromatography* <621>.) The liquid chromatograph is equipped with a 230 nm detector and a 4.6 mm × 30 cm column that contains packing L7. The flow rate is about 2 mL/min. Chromatograph the *Resolution solution* and the *Standard preparation*, and record the peak responses as directed under *Procedure*: the resolution, *R*, between the dibutyl phthalate and miconazole peaks is not less than 5, the tailing factor for the miconazole peak is not more than 1.3, and the relative standard deviation for replicate injections of the *Standard preparation* is not more than 2%. The relative retention times are about 0.7 for dibutyl phthalate and 1 for miconazole.

Procedure: (NOTE – Allow the chromatograph to run for at least 16–18 min between injections to allow for elution of all components associated with the injection vehicle.) Separately inject equal volumes (about 20 µL) of the *Standard preparation* and the *Assay preparation* into the chromatograph, record the chromatograms, and measure the responses for the major peaks. Calculate the quantity, in mg, of $C_{18}H_{14}CL_4N_2O$ in each milliliter of the injection given by the formula:

$$\frac{C}{V} \times \frac{r_U}{r_s}$$

in which *C* is the concentration, in µg/mL, of *USP Miconazole RS* in the *Standard preparation*, *V* is the volume, in mL, of injection taken and r_U and r_s are the peak responses obtained from the *Assay preparation* and the *Standard preparation*, respectively.

4.1.2.3. Miconazole nitrate

Miconazole nitrate contains not less than 98% and not more than 102% of $C_{18}H_{14}Cl_4N_2O{\cdot}HNO_3$ calculated on the dried basis.

Identification

Test 1. When the test is carried out according to the general procedure <197 K>, the infrared absorption spectrum of a potassium bromide dispersion of miconazole nitrate, previously dried, exhibits maxima only at the same wavelength as that of a similar preparation of *USP Miconazole nitrate RS*.

Test 2. When the test is carried out according to the general procedure <197 U>, the ultraviolet absorption spectrum of a 1 in 2500 solution of miconazole nitrate in a 1 in 10 solution of 0.1 N hydrochloric acid in isopropyl alcohol exhibits maxima and minima at the same wavelengths as that of a similar preparation of *USP Miconazole Nitrate RS*, concomitantly measured.

Loss on drying. Carry out the test according to the general procedure <731>: dry miconazole nitrate at 105 °C for 2 h; it loses not more than 0.5% of its weight.

Residue on ignition. When the test is performed according to the general procedure <281>, the residue is not more than 0.2%.

Chromatographic purity

Dragendorff's reagent: Dissolve 850 mg of bismuth subnitrate in a mixture of 40 mL of water and 10 mL of glacial acetic acid (*Solution A*). Dissolve 8 g of potassium iodide in 20 mL of water (*Solution B*). Transfer 5 mL of *Solution A*, 5 mL of *Solution B*, and 20 mL of glacial acetic acid to a 100-mL volumetric flask,

dilute with water to volume, and mix. Dissolve 100 mg in a solvent consisting of a mixture of chloroform and methanol (1:1), and dilute with the same solvent to 10 mL to obtain the test solution. Prepare a Standard solution of *USP Miconazole Nitrate RS* in a solvent consisting of a mixture of chloroform and methanol (1:1) to contain 10 mg/mL. Dilute a portion of this solution quantitatively and stepwise with the same solvent to obtain a diluted Standard solution having a concentration of 25 μg/mL. Apply separate 50-μL portions of the three solutions to the starting line of a suitable thin-layer chromatographic plate (see *Chromatography* <621> coated with a 0.25-mm layer of chromatographic silica gel. Develop the chromatogram in a suitable chamber with a freshly prepared solvent system consisting of a mixture of *n*-hexane, chloroform, methanol, and ammonium hydroxide (60:30:10:1) until the solvent front has moved about three-fourths of the length of the plate. Remove the plate from the chamber, air-dry, spray first with *Dragendorff's reagent* and then with hydrogen peroxide TS, and examine the chromatogram: the R_f value of the principal spot from the test solution corresponds to that of the Standard solution, and any other spot obtained from the test solution does not exceed, in size or intensity, the principal spot obtained from the diluted Standard solution (0.25%).

Ordinary impurities. Carry out the test according to the general method <466>.

Test solution: Methanol.

Standard solution: Methanol.

Eluent: A mixture of toluene, isopropyl alcohol, and ammonium hydroxide (70:29:1), in a nonequilibrated chamber.

Visualization: 3, followed by overspraying with hydrogen peroxide TS (NOTE – Cover the TLC plate with a glass plate to slow fading to the spots).

Assay

Dissolve about 350 mg of miconazole nitrate, accurately weighed, in 50 mL of glacial acetic acid, and titrate with 0.1 N perchloric acid VS, determining the endpoint potentiometrically using a glass calomel-electrode system. Perform a blank determination, and make any necessary correction. Each milliliter of 0.1 N perchloric acid is equivalent to 47.92 mg of $C_{18}H_{14}Cl_4N_2O{\cdot}HNO_3$.

4.1.2.4. Miconazole nitrate cream

Miconazole nitrate cream contains not less than 90% and not more than 110% of the labeled amount of miconazole nitrate ($C_{18}H_{14}Cl_4N_2O{\cdot}HNO_3$).

Identification

Place about 25 mL of the stock solution, prepared as directed in the *Assay*, in a 50 mL beaker, and evaporate on a steam bath with the aid of a current of filtered air to dryness. Dry the residue at 105 °C for 10 min: the infrared absorption spectrum of a potassium bromide dispersion of it so obtained exhibits maxima only at the same wavelengths as that of similar preparations of *USP Miconazole Nitrate RS*.

Minimum fill. When the test is carried out according to the general procedure <755>: meets the requirements.

Assay

Internal standard solution: Dissolve a suitable quantity of cholestane in a mixture of chloroform and methanol (1:1) to obtain a solution having a concentration of about 1 mg/mL.

Standard preparation: Dissolve an accurately weighed quantity of *USP Miconazole Nitrate RS* in methanol to obtain a solution having a known concentration of about 500 μg/mL. Transfer 10 mL of this solution to a test tube, and evaporate on a steam bath with the aid of a current of filtered air to dryness. Dissolve the residue in 2 mL of the *Internal standard solution*. This *Standard preparation* has a concentration of about 2500 μg/mL.

Assay preparation: Transfer an accurately weighed portion of cream, equivalent to about 100 mg of miconazole nitrate, to a 100 mL volumetric flask. Dissolve in a mixture of isopropyl alcohol and chloroform (1:1), dilute with the same solvent mixture to volume, and mix. Pipete 25 mL of this solution into a 150-mL beaker and evaporate on a steam bath with the aid of a stream of nitrogen to dryness. Add 10 mL of chloroform to the residue, and heat on a steam bath just to boiling. Remove the beaker from the steam bath, and stir to dissolve. (NOTE – Avoid excessive evaporation of chloroform.) Add 50 mL of pentane in small portions with continuous stirring. Allow to crystallize for 10–15 min. Filter through a medium porosity sintered-glass filter funnel with the aid of a current of air applied to the surface through a one-hole stopper fitted onto the funnel. Wash the beaker with four 5 mL portions of pentane and add the washings to the filter funnel. Wash the funnel and precipitate with four 5-mL portions of pentane. Dry the precipitate on the filter by allowing filtered air to pass through the funnel for several minutes. Dissolve the precipitate by washing the beaker and the funnel with small portions of methanol, and collect the filtrate in a 50-mL volumetric flask using filtered air applied to the top of the funnel to aid in filtration. Dilute with methanol to volume, and mix. Transfer 10 mL of this stock solution to a test tube, and evaporate on a steam bath with the aid of a current of filtered air to dryness. Dissolve the residue in 2 mL of *Internal standard solution*.

Chromatographic system. (Follow the method described in the general procedure <621>.) The gas chromatograph is equipped with a flame ionization detector and a 1.2 m × 2 mm column packed with 3% phase G32 on support S1A. The injection port, detector, and column temperatures are maintained at about 250, 300, and 250 °C, respectively, and helium is used as the carrier gas, flowing at rate of about 50 mL/min. The relative retention times for cholestane and miconazole nitrate are about 0.44 and 1, respectively. Chromatograph the *Standard preparation*, and record the peak responses as directed for *procedure*: The resolution, *R*, between cholestane and miconazole nitrate is not less than 2 and the relative standard deviation of replicate injections is not more than 3%.

Procedure: Separately inject equal volumes (about 1 μL) of the *Assay preparation* and the *Standard preparation* into the chromatograph, record the chromatograms, and measure the peak responses. Calculate the quantity, in mg, of miconazole nitrate ($C_{18}H_{14}Cl_4N_2O{\cdot}HNO_3$) in the portion of cream given by the formula:

$$0.04C \times \frac{R_U}{R_s}$$

in which C is the concentration, in μg/mL of *USP Miconazole Nitrate RS* in the *Standard preparation*, and R_U and R_s are the peak response ratios of miconazole nitrate to cholestane obtained from the *Assay preparation* and the *Standard preparation*, respectively.

4.1.2.5. Miconazole nitrate topical powder

Miconazole nitrate topical powder contains not less than 90% and not more than 110% of the labeled amount of $C_{18}H_{14}Cl_4N_2O \cdot HNO_3$.

USP Reference standards <11> USP Miconazole Nitrate *RS*.

Identification

Transfer a portion of topical powder, equivalent to about 100 mg of miconazole nitrate to a 50 mL beaker, disperse in 40 mL of methanol, and mix for a minimum of 5 min. Allow to settle for 5–10 min, and filter into 100-mL beaker. Evaporate on a steam bath to dryness. Dry the residue at 105 °C for 10 minutes: the infrared absorption spectrum of a potassium bromide dispersion of the residue so obtained exhibits maxima only at the same wavelengths as that of a similar preparation of *USP Miconazole Nitrate RS*.

Microbial limits. Carry out the test according to the general procedure <61>. The total count does not exceed 100 microorganisms per gram, and tests for *Staphylococcus aureus*, and *Pseudomonas aeruginosa*, are negative.

Minimum fill. When the test is carried out according to the general procedure <755>: meets the requirements.

Assay

Internal standard solution: Dissolve cholestane in chloroform to obtain a solution having a concentration of about 0.5 mg/mL.

Standard preparation: Dissolve an accurately weighed quantity of *USP Miconazole Nitrate RS* in a mixture of chloroform and methanol (1:1) to obtain a solution having a known concentration of about 0.8 mg/mL. Transfer 5 mL of this solution to a test tube, add 2 mL of *Internal standard solution*, and evaporate at a temperature not higher than 40 °C with the aid of a current of nitrogen to dryness. Dissolve the residue in 2 mL of a mixture of chloroform and methanol (1:1), and mix to obtain a *Standard preparation* having a known miconazole nitrate concentration of about 2 mg/mL.

Assay preparation: Transfer an accurately weighed portion of topical powder, equivalent to about 20 mg of miconazole nitrate, to a stoppered 50-mL centrifuge tube. Add 25 mL of methanol, and shake by mechanical means for 30 min to dissolve the miconazole nitrate. Centrifuge to obtain a clear supernatant liquid. Transfer 5 mL of this solution to a test tube, add 2 mL of *Internal standard solution* and evaporate at a temperature not higher than 40 °C with the aid of a current of nitrogen to dryness. Dissolve the residue in 2 mL of a mixture of chloroform and methanol (1:1).

Chromatographic system: (Follow the method described in the general procedure <621>.) The gas chromatograph is equipped with a flame ionization detector and a 1.2 m × 2 mm glass column containing 3% phase G32 on support S1A. The injection port, detector, and column are maintained at temperatures of about 250, 300, and 250 °C, respectively. Helium is used as the carrier gas, at a flow rate of about 50 mL/min. Chromatograph the *Standard preparation* and record the peak responses as directed under *Procedure*: the resolution, *R*, between the cholestane and miconazole nitrate peaks is not less than 2, and the relative standard deviation for replicate injections is not more than 3%.

Procedure: Separately inject equal volumes (about 5 μL) of the *Standard preparation* and the *Assay preparation* into the chromatograph, record the chromatograms, and measure the responses for the major peaks. The relative retention times for cholestane and miconazole nitrate are about 0.5 and 1, respectively. Calculate the quantity, in mg, of $C_{18}H_{14}Cl_4N_2O{\cdot}HNO_3$ in the portion of topical powder given by the formula:

$$10C \times \frac{R_U}{R_S}$$

in which C is the concentration, in mg/mL, of *USP Miconazole Nitrate RS* in the *Standard preparation*, and R_U and R_S are the peak response ratios of the miconazole nitrate peak to the cholestane peak obtained from the *Assay preparation* and the *Standard preparation*, respectively.

4.1.2.6. Miconazole nitrate vaginal suppositories

Miconazole nitrate vaginal suppositories contain not less than 90% and not more than 110% of the labeled amount of $C_{18}H_{14}Cl_4N_2O{\cdot}HNO_3$.

Reference standard: *USP Miconazole Nitrate Reference Standard*. Dry at 105 °C for 2 h before using.

Identification

Place a portion of the stock solution, prepared as directed in the *Assay*, containing about 25 mg of miconazole nitrate, in a 50-mL beaker, and evaporate on a steam bath with the aid of a current of filtered air to dryness. Dry the residue at 105 °C for 10 minutes: the infrared absorption spectrum of a potassium bromide dispersion of it so obtained exhibits maxima only at the same wavelength as that of a similar preparation of *USP Miconazole Nitrate RS*.

Assay

Internal standard solution, Standard preparation, and Chromatographic system: Prepare as directed in the Assay under Miconazole nitrate cream.

Assay preparation: Transfer one miconazole nitrate vaginal suppository to a stoppered, 50-mL centrifuge tube. Add 30 mL of pentane, and shake by mechanical means for 20 min to dissolve the suppository base and to disperse the miconazole nitrate. Centrifuge to obtain a clear supernatant liquid. Aspirate and discard the clear liquid. Wash the residue with three 20-mL portions of pentane, shaking, centrifuging, and aspirating in the same manner. Discard the pentane washings. Evaporate the residual pentane from the residue with the aid of a current of filtered air. Using small portions of methanol, transfer the residue to 100-mL volumetric flask. Dissolve in methanol, dilute with methanol to volume, and mix. Transfer an accurately measured volume of this stock solution, equivalent to about 5 mg of miconazole nitrate, to a suitable container, and evaporate on a steam bath with the aid of a current of filtered air to dryness. Dissolve the residue in 2 mL of *Internal standard solution*.

Procedure: Proceed as directed for *Procedure* in the *Assay* under *Miconazole nitrate cream*. Calculate the quantity, in mg, of $C_{18}H_{14}Cl_4N_2O{\cdot}HNO_3$ in the suppository given by the formula:

$$\frac{0.2C}{V} \times \frac{R_U}{R_s}$$

in which V is the volume, in mL, of stock solution used to prepare the *Assay preparation* and the other terms are as defined therein.

4.2. Reported methods of analysis

4.2.1. Titrimetric method

Massaccesi reported the development of a two-phase titration method for the analysis of miconazole and other imidazole derivatives in pure form and in pharmaceutical formulation [14]. To the sample (10 mg) are added 10 mL of water, 10 mL of 1 M-sulfuric acid, 25 mL of dichloromethane and 1 mL of 0.05% indophenol blue (C.I. No. 49700) in dichloromethane solution and the solution is titrated with 10 mM sodium dodecyl sulfate until the color of the organic phase changes from blue to pale yellow. Results obtained for the drug in pure form, tablets, suppositories, cream and lotion agreed with the expected values and the coefficient of variation ($n = 6$) were 0.3–0.35%. Imidazole and the other constituents of the pharmaceutical preparations did not interfere.

Szabolcs determined the active principle in preparations based on miconazole and clotrimazole [15]. The two drugs were determined in ointments by extraction with chloroform, evaporation of the solvent, dissolution of the residue in acetic acid, and titration with 0.1 N perchloric acid in the presence of Gentian Violet.

Mapsi *et al.* [16] reported the use of a potentiometric method for the determination of the stability constants of miconazole complexes with iron(II), iron(III), cobalt(II), nickel(II), copper(II), and zinc(II) ions. The interaction of miconazole with the ions was determined potentiometrically in methanol–water (90:10) at an ionic force of 0.16 and at 20 °C. The coordination number of iron, cobalt, and nickel was 6; copper and zinc show a coordination number of 4. The values of the respected log βn of these complexes were calculated by an improved Scatchard (1949) method and they are in agreement with the Irving–Williams (1953) series of $Fe^{2+} < Co^{2+} < Ni^{2} < Cu^{2+} < Zn^{2+}$.

Shamsipur and Jalali described a simple and accurate pH metric method for the determination of two sparingly soluble (in water) antifungal agents; miconazole and ketoconazole in micellar media [17]. Cetyltrimethylammonium bromide and sodium dodecyl sulfate micelles were used to solubilize these compounds. The application of this method to the analysis of pharmaceutical preparation of the related species gave satisfactory results. Simplicity and the absence of harmful organic solvents in this method make it possible to be used in the routine analyses.

4.2.2. Spectrophotometric methods

4.2.2.1. Ultraviolet spectrometry

Bonazzi *et al.* [18] reported the determination of miconazole and other imidazole antimycotics in creams by supercritical fluid extraction and derivative ultraviolet spectroscopic method. Cream based pharmaceuticals were mixed with celite and anhydrous sodium sulfate and extracted by supercritical fluid extractor (SFE) with

four static (1 min) and one dynamic extraction step (4 min) with pure supercritical CO_2 and 10% methanol-modified CO_2. Miconazole and the other drugs were trapped on a ODS SPE column and were eluted with methanol. Extraction conditions for each analyte are tabulated. Derivative ultraviolet spectra were recorded. Calibration graphs were linear from 0.12−0.32 mg/mL for miconazole.

Goger and Gokcen [19] developed a quantitative method for the determination of miconazole in cream formulations that contain benzoic acid as preservative by second order derivative spectrophotometry. The procedure was based on the linear relationship in the range 100−500 μg/mL between the drug concentration and the second-derivative amplitudes at 276 nm. Results of the recovery experiments performed on various amounts of benzoic acid and the determination of miconazole in cream confirmed the applicability of the method to complex formulations.

Erk [20] described a spectrophotometric method for the simultaneous determination of metronidazole and miconazole nitrate in ovules. Five capsules were melted together in a steam bath, the product was cooled and weighed, and the equivalent of one capsule was dissolved to 100 mL in methanol; this solution was then diluted 500-fold with methanol. In the first method, the two drugs were determined from their measure $dA/d\lambda$ values at 328.6 and 230.8 nm, respectively, in the first derivative spectrum. The calibration graphs were linear for 6.2−17.5 μg/mL of metronidazole and 0.7−13.5 μg/mL of miconazole nitrate. In the second (absorbance ratio) method, the absorbance was measured at 310.4 nm for metronidazole, at 272 nm for miconazole nitrate and at 280.6 nm (isoabsorptive point). The calibration graphs were linear over the same ranges as in the first method.

El-Shabouri *et al.* [21] used a charge-transfer complexation method for the spectrophotometric assay of miconazole nitrate and other imidazole antifungal drugs. A 1 mL portion of a solution containing miconazole nitrate and the other azole antifungal agent was mixed with 1 mL of 0.01 M iodine solution and the volume was made up to 10 mL with 1,2-dichloroethane and allowed to stand at 25 °C for 50 min. The absorbance was measured at 290 nm. Beer's law was obeyed from 5-22 μg/mL for miconazole nitrate. The method was applied to the analysis of tablets and other pharmaceutical preparations. Results are tabulated and discussed. The composition, association constants, and free energy changes of the complexes were determined.

Chen used a second-derivative spectrophotometric method for the determination of miconazole nitrate in Pikangshuang [22]. Sample of miconazole nitrate was dissolved in anhydrous ethanol and the second-derivative spectrum of the resulting solution was recorded from 200–300 nm; miconazole nitrate was determined by measuring the amplitude value between the peak at 233 nm and the trough at 228 nm. The recovery was 99.8% with a relative standard deviation ($n = 6$) of 0.2%.

Liu *et al.* [23] used a third-derivative spectrophotometric method for the determination of miconazole nitrate in Pikangshuang (cream). The detection range was 60–300 μg/mL and recovery was 100.1%.

Erk and Altun [24] used a ratio spectra derivative spectrophotometric method and a high performance liquid chromatographic method for the analysis of miconazole nitrate and metronidazole in ovules. The spectral method depends on ratio spectra first derivative spectrophotometry, by utilizing the linear relationship between substances concentration and ratio spectra first derivative peak amplitude. The ratio

first derivative amplitude at 242.6, 274.2, 261.8, 273.5, and 281.5 nm were selected for the assay of metronidazole and miconazole.

He *et al.* [25] described an ultraviolet spectrophotometric method for the quantitative determination of miconazole in liniments. The drug was analyzed at 272 nm, the average recovery was 99.76% and the relative standard deviation was 0.3%.

Hewala *et al.* [26] described a derivative ratios spectrophotometric method for the identification and differentiation between miconazole and other benzenoid ultraviolet absorbing drugs. This approach is based on calculation of the ratios of derivative optima (2D, 3D, 4D) of the ultraviolet absorption spectra, named in this study, derivative spectrophotometric indexes, are described for this analysis. These include three-element indexes and six-element indexes. The three-element indexes are calculated by using either the ratios of peak maximum to minimum of the same derivative order, the derivative ratios of peaks maxima of mixed derivative order and the derivative ratios of peaks minima of mixed derivative order. The six-element indexes are based on calculating the derivative ratios at selected wavelength ranges of the derivative (2D, 3D, 4D) spectra of the ultraviolet absorption spectrum. These approaches were applied to differentiate between 10 benzenoid ultraviolet absorbing drugs. These approaches are suitable and furnish general derivative spectrophotometric indexes for the identification and differentiation between miconazole and nine other benzenoid ultraviolet absorbing drugs.

El-Shabouri *et al.* [27] described a charge-transfer complexation method for the spectrophotometric assay of miconazole and other imidazole antifungal drugs. The method is based on the formation of a charge-transfer complex between the drug as *n*-electron donor and iodine as σ acceptor. The product exhibited two absorption maxima at 290 and 377 nm, measurements are made at 290 nm. Beer's law is obeyed in a concentration range of 1–40 μg/mL. The method is rapid, simple, and sensitive and can be applied to the analysis of some commercial dosage forms without interference. A more detailed investigation of the formed complex was made with respect to its composition, association constant, and free energy change.

Korany *et al.* [28] used Fourier descriptors for the spectrophotometric identification of miconazole and 11 different benzenoid compounds. Fourier descriptor values computed from spectrophotometric measurements were used to compute a purity index. The Fourier descriptors calculated for a set of absorbencies are independent of concentration and is sensitive to the presence of interferents. Such condition was proven by calculating the Fourier descriptor for pure and degraded benzylpenicillin. Absorbance data were measured and recorded for miconazole and for all the 11 compounds. The calculated Fourier descriptor value for these compounds showed significant discrimination between them. Moreover, the reproducibility of the Fourier descriptors was tested by measurement over several successive days and the relative standard deviation obtained was less than 2%.

Wrobel *et al.* [29] described a simple method for the determination miconazole in pharmaceutical creams, based on extraction and second-derivative spectrophotometry. In the presence of sodium lauryl sulfate (0.5%) and sulfuric acid (0.4 mol/L), the miconazole and internal standard (methylene blue) were extracted to 100 μL of methylene chloride. The organic phase was evaporated in the nitrogen stream and the dry residue was dissolved in methanol (1.5 mL). The analytical signal was obtained as the ratio between second-derivative absorbances measured at 236.9 nm

(miconazole) and at 663.2 nm (internal standard). The use of internal standard in such multistage procedure enabled quite good analytical performance in calibration range 50–400 mg/L: linear correlation coefficient 0.9995, precision at 50 and at 400 mg/L of miconazole was 1.5 and 0.5, respectively. Four commercial pharmaceutical creams were analyzed and the results obtained were in good agreement with the results obtained by reversed phase high performance liquid chromatography.

Xue *et al.* [30] prepared a vaginal suppository formulation containing miconazole nitrate and determined its content by P-matrix ultraviolet spectrophotometry. The production of the suppository was finished with melting by the excipient of glyceryl esters fatty acid of artificial synthesis. Quantitative assay was conducted with a P-matrix ultraviolet spectrophotometer. The suppository was smooth and met the clinical requirement of vaginal disease treatment. The method of assay was accurate.

4.2.2.2. Colorimetry

Thomas *et al.* [31] used a colorimetric method for the estimation of miconazole nitrate in creams. The method is based on the ion-pair extraction with bromocresol purple solution and measurement of the solution at 410 nm.

Cavrini *et al.* [32] reported the development of a colorimetric method for the determination of miconazole nitrate in pharmaceutical preparation. The method is based on the formation of a yellow complex between the drug and bromocresol green. The absorption peak of this complex, extracted by chloroform over the pH 2−4 range, was at 424 nm, and linear response was obtained from 3−13 μg/mL. The molar absorptivity of the complex in chloroform was 1.845×10^4. This procedure is suitable for the analysis of miconazole nitrate in commercial dosage forms.

Lemli and Knockaert [33] described a spectrophotometric method for the determination of miconazole nitrate suspensions and other organic bases in pharmaceutical preparations by the use of cobalt thiocyanate. The drug and the amines (as their anhydrous hydrochlorides in dichloromethane) react with solid cobalt thiocyanate to form an ion-pair complex that contains two molecules of base to one $[Co(SCN)_4]^{2-}$. The complex is determined quantitatively by spectrophotometry versus dichloromethane at 625 nm with rectilinear response for up to 400 μg/mL of the base. This method was applied to miconazole nitrate suspensions and the coefficient of variations were generally $\leq 2\%$.

4.2.2.3. Spectrofluorimetric method

Khashaba *et al.* [34] suggested the use of sample spectrophotometric and spectrofluorimetric methods for the determination of miconazole and other antifungal drugs in different pharmaceutical formulations. The spectrophotometric method depend on the interaction between imidazole antifungal drugs as *n*-electron donor with the pi-acceptor; 2,3-dichloro-5,6-dicyano-1,4-benzoquinone, in methanol or with *p*-chloranilic acid in acetonitrile. The produced chromogens obey Beer's law at λ_{max} 460 and 520 nm in the concentration range 22.5–200 and 7.9–280 μg/mL for 2,3-dichloro-5,6-dicyano-1,4-benzoquinone and *p*-chloranilic acid, respectively. Spectrofluorimetric method is based on the measurement of the native fluorescence of ketoconazole at 375 nm with excitation at 288 nm and/or fluorescence intensity versus concentration is linear for ketoconazole at 49.7–800 ng/mL. The methods

were applied successfully for the determination of miconazole and the other antifungal drug in their pharmaceutical formulation.

4.2.2.4. Calorimetry

Weuts *et al.* [35] compared and evaluated different calorimetric methods used to determine the glass transition temperature and molecular mobility below the glass transition temperature for miconazole and other amorphous drugs. The purpose of this study was to compare the different calorimetric methods used to determine the glass transition temperature and to evaluate the relaxation behavior and hence the stability of the amorphous drugs below their glass transition temperature. Data showed that the values of the activation energy for the transition of a glass to its supercooled liquid state qualitatively correlate with the values of the mean molecular relaxation time constant of miconazole.

4.3. Electrochemical method

4.3.1. Voltammetric method

Pereira *et al.* [36] studied the voltammetric characteristics of miconazole and its cathodic stripping voltammetric determination. Miconazole was reduced at mercury electrode above pH 6 involving organometallic compound formation, responsible for an anomalous polarographic behavior. The electronic process presents a large contribution of the absorption effects. The drug can be determined by cathodic stripping voltammetry from 8×10^{-8} to 1.5×10^{-6} mol/L in Britton–Robenson buffer, pH 8, when pre-accumulated for 30 s at an accumulation potential of 0 V. A relative standard deviation of 3.8% was obtained for 10 measurements of 1×10^{-7} mol/L miconazole in Britton–Robenson buffer pH 8 and a limit of detection of 1.7×10^{-8} mol/L was determined using 60 s of deposition time and scan rate of 100 mV/s. The method is simple, precise and was applied successfully for the determination of miconazole in pure form and in commercial formulations, showing mean recoveries of 99.7–98.4%.

4.3.2. Polarographic method

Willems *et al.* [37] used a polarographic method to study the miconazole complexes of some trace elements. Manganese, iron, cobalt, and zinc element formed miconazole complexes with different stability constants. Polarography was used for detecting stability constants. The evolution of the respective formation constants followed the natural (Irving–Williams) order. The stepwise constant of the complexes formed increased from manganese to cobalt and decreased for zinc. The results are discussed with respect to the possible mechanism of action of miconazole.

4.4. X-ray powder diffraction

Arndt and Ahlers [38] used X-ray powder diffraction method for studying the influence of cations on the mode of action of miconazole on yeast cells. The influence of miconazole nitrate on yeast plasma membranes was studied in a concentration range of 0–100 μM. The reaction of 100 μM miconazole with the

plasma membranes led to a rapid breakdown of the transmembrane pH gradient and to an efflux of metabolites from the cytoplasm of the cells. This effect of miconazole could be reversed by monovalent, divalent, and most effectively by trivalent cations due to the formation of miconazole cation complexes. At a ratio of trivalent cation/miconazole (1:3), the effect was completely reversed. X-ray diffraction studies indicated a crystal structure of the aluminium–miconazole complex.

Salole and Pearson reported the X-ray powder diffraction data for miconazole and econazole [39]. The X-ray powder diffraction patterns and data for the unsolvated samples of miconazole and econazole are reported.

4.5. Chromatography

4.5.1. Thin-layer chromatography

Clarke (2) recommended the following three thin-layer chromatographic systems:

System 1

Plates: Silica gel G, 250 μm thick, dipped in, or sprayed with, 0.1 M potassium hydroxide in methanol and dried.

Mobile phase: Methanol:strong ammonia solution (100:1.5).

Reference compounds: Diazepam R_f 75, chlorprothixene $R_f = 56$, codeine $R_f = 33$ and atropine $R_f = 18$.

$R_f = 73$ [40].

System 2

Plates: Use the same plates as system 1 with which it may be used because of the low correlation of R_f values.

Mobile phase: Cyclohexane:toluene:diethylamine (75:15:10).

Reference compounds: Dipipanone $R_f = 66$, Pethidine $R_f = 37$, disipramine $R_f = 20$, codeine $R_f = 06$.

$R_f = 11$ [40].

System 3

Plates: This system uses the same plates as systems 1 and 2 with which it may be used because of the low correlation of R_f values.

Mobile phase: Chloroform:methanol (90:10).

Reference compounds: Meclocine $R_f = 79$, caffeine $R_f = 58$, dipipanone $R_f = 33$, disipramine $R_f = 11$.

$R_f = 67$ (Dragendorff spray) [40].

Roychowdhury and Das [41] reported the use of a rapid method for the identification of and quantitation of miconazole and other antifungal drugs in pharmaceutical creams and ointments by thin-layer chromatography-densitometry. The drug was extracted with chloroform–isopropanol (1:1). The samples were applied to precoated silica gel F_{254} plates (10 cm × 10 cm) and developed to 9 cm with hexane–chloroform–methanol–diethylamine (50:40:10:1). Visualization of the spots was possible under ultraviolet light and scanning densitometry at 220 nm allowed quantitation. The drug was well separated from other antifungal drugs and was determined by

comparison with standards. Calibration graphs were linear from 2.5−10 mg/mL of the drug. Recoveries ranged from 97−104% with a mean of 100.2 ± 2.9%. The method was compared with the official liquid chromatographic methods.

Indrayanto *et al.* [42] described and validated a simultaneous densitometric method for the determination of miconazole nitrate and betamethasone valerate in cream. Sample (1 g) was extracted by ultrasonic agitation for 15 min with 8 mL of 96% ethanol and centrifuged. The supernatant was filtered, diluted to 10 mL with ethanol and 4 μL portions were applied by a Nanomat III applicator (Camag) to silica gel 60 F_{254} plates, which were developed for 8 cm with anhydrous acetic acid–acetone–chloroform (3:4:34). The plates were scanned densitometrically at 233 nm, the isobestic point for the two drugs. Linear calibration graphs were obtained from 320−960 ng/spot and 5.3−16 μg/spot, respectively for betamethasone valerate and miconazole nitrate, both corresponding to 66−200% of the expected values, with detection limits of 50.9 ng and 0.68 μg/spot, respectively. Recovery of 6.4−9.6 μg of miconazole per spot averaged 100.49% with relative standard deviation of 1.36%.

Musumarra *et al.* [43] identified miconazole and other drugs by principal components analysis of standardized thin-layer chromatographic data in four eluent systems. The eluents, ethylacetate–methanol–30% ammonium hydroxide (85:10:15), cyclohexane–toluene–diethylamine (65:25:10), ethylacetate–chloroform (50:50), and acetone with the plates dipped in potassium hydroxide solution, provided a two-component model that accounts for 73% of the total variance. The scores plot allowed the restriction of the range of inquiry to a few candidates. This result is of great practical significance in analytical toxicology, especially when account is taken of the cost, the time, the analytical instrumentation and the simplicity of the calculations required by the method.

Musumarra *et al.* [44] also identified miconazole and other drugs by principal components analysis of standardized thin-layer chromatographic data in four eluent systems and of retention indexes on SE 30. The principal component analysis of standardized R_f values in four eluents systems: ethylacetate–methanol–30% ammonia (85:10:15), cyclohexane–toluene–diethylamine (65:25:10), ethylacetate–chloroform (50:50), and acetone with plates dipped in potassium hydroxide solution, and of gas chromatographic retention indexes in SE 30 for 277 compounds provided a two principal components model that explains 82% of the total variance. The scores plot allowed identification of unknowns or restriction of the range of inquiry to very few candidates. Comparison of these candidates with those selected from another principal components model derived from thin-layer chromatographic data only allowed identification of the drug in all the examined cases.

Van de Vaart *et al.* [45] used a thin-layer chromatographic method for the analysis of miconazole and other compounds in pharmaceutical creams. The drugs in creams were analyzed by thin-layer chromatography on silica gel plates with ether in pentane-saturated chamber or with butanol–water–acetic acid (20:5:2). Both active ingredients and vehicle components were detected and R_f values of 67 active ingredients are tabulated. Additional eluents may be needed to separate certain combinations of ingredients.

Qian *et al.* [46] determined miconazole nitrate and benzoic acid in paint by a thin-layer chromatographic densitometric method. The drug was spotted on a GF_{254} silica gel plate, developed with a 42:21:13:5 *n*-hexane–chloroform–methanol–

diethylamine mixture and analyzed by densitometry at 220 nm. The peaks area and sample concentration showed a linear relation in 2−6 μg for benzoic acid and in 12−36 μg for miconazole nitrate.

Aleksic *et al.* [47] estimated the hydrophobicity of miconazole and other antimycotic drugs by a planar chromatographic method. The retention behavior of the drugs have been determined by TLC by using the binary mobile phases acetone–*n*-hexane, methanol–toluene, and methyl ethyl ketone–toluene containing different amounts of organic modifier. Hydrophobicity was established from the linear relationships between the solute RM values and the concentration of organic modifier. Calculated values of RMO and CO were considered for application in quantitative structure–activity relationship studies of the antimycotics.

4.5.2. Gas chromatography

Clarke recommended the following gas chromatographic system for the separation of miconazole [2].

Column: 2.5% SE-30 on 80–100 mesh Chromosorb G (acid-washed and dimethyldichlorosilane-treated), 2 m × 4 mm internal diameter glass column. It is essential that the support is fully deactivated.

Carrier gas: Nitrogen at 45 mL/min.

Reference compounds: *n*-Alkanes with an even number of carbon atoms.

Retention indices: RI 2980 [48, 49].

Szathmary and Luhmann [50] described a sensitive and automated gas chromatographic method for the determination of miconazole in plasma samples. Plasma was mixed with internal standard; 1-[2,4-dichloro-2-(2,3,4-trichlorobenzyloxy) phenethyl]imidazole and 0.1 M sodium hydroxide and extracted with heptane-isoamyl alcohol (197:3) and the drug was back-extracted with 0.05 M sulfuric acid. The aqueous phase was adjusted to pH 10 and extracted with an identical organic phase, which was evaporated to dryness. The residue was dissolved in isopropanol and subjected to gas chromatography on a column (12 m × 0.2 mm) of OV-1 (0.1 μm) at 265 °C, with nitrogen–phosphorous detection. Recovery of miconazole was 85% and the calibration graph was rectilinear for 0.25–250 ng/mL.

Ros and Van der Meer [51] determined miconazole in its oral gel formulation by a gas chromatographic method. Gel (1 gm) was homogenized with 10 mL of water and then 1 mL of aqueous 6 N-ammonia and 1 mL of flurazepam solution (60 mg/mL; internal standard) were added and the mixture was extracted with 25 mL of dichloromethane. A 2-μL portion of the extract was analyzed by gas chromatography on a column (11 m × 0.22 mm) of CP Sil 5CB (0.12 mm) at 270 °C with nitrogen as carrier gas (1 mL/min) and nitrogen phosphorous detection.

Kublin and Kaniewska [52] used a gas chromatographic method for the determination of miconazole and other imidazole antimycotic substances. The conditions have been established for the quantitative determination of miconazole and the other drugs, which are present in pharmaceuticals such as ointments and creams. The column, packed with UCW-98 on Chromosorb WAW, and flame-ionization detector were used. The statistical data indicate satisfactory precision of the method, both in the determination of imidazole derivatives in substances and in preparation.

Guo *et al.* [53] developed a gas chromatographic method for the analysis of miconazole nitrate in creams and injections. The conditions were: flame ionization detector, stationary phase of 5% SE 30; support of Chromosorb W (AS-DMCS, 80−100 mesh); packed column 3 m × 3 mm; column temperature 275 °C; injection temperature 290 °C; and diisooctyl sebacate and internal standard. The average recoveries for creams and injections were 97.7 and 101.4%, respectively. The relative standard deviations were 2.2 and 1.3%, respectively.

4.5.3. Gas chromatography–mass spectrometric method

Neill *et al.* [54] described an automated screening procedure using gas chromatography–mass spectrometry for identification miconazole and other drugs after their extraction from biological sample. This novel analytical procedure has been developed, using computer-controlled gas chromatography–mass spectrometry (GC–MS) to detect 120 drugs of interest to read safety. This method is suitable for use on extracts of biological origin. The method was devised to identify drugs in extracts of blood samples, as part of an investigation into the involvement of drugs, other than alcohol, in road accidents. The method could be adopted to screen for other substances. The method depends on a 'macro' program, which was written to automate the search of gas chromatographic–mass spectrometric data for target drugs. The strategy used was to initially search for drug in the database by monitoring for a single characteristic ion at the expected retention time. If a peak is found in this first mass chromatogram, a peak for a second characteristic ion is sought within 0.02 min of the first and, if found, the ratio of peak areas calculated. Probable drug identification is based on the simultaneous appearance of peaks for both characteristic ions at the expected retention time and in the correct ratio. If the ratio is outside acceptable limits, a suspected drug (requiring further investigation) is reported. The search macro can use either full mass spectra or, for enhanced sensitivity, data from selected ion monitoring (which requires switching between groups of ions during data acquisition). Quantitative data can be obtained in the usual way by the addition of internal standards.

4.5.4. High performance liquid chromatographic methods

Wallace *et al.* [55] described an electron capture gas chromatographic assay method for the analysis of miconazole and clotrimazole in skin samples. Gas chromatographic assay procedures using an electron capture detector were developed for the quantitation of the antifungal agents, clotrimazole, and miconazole. The chromatographic column was packed with 3% OV-17 on Gas Chrom Q (100−120 mesh) with argon–methane as the carrier gas and column temperature of approximately 250 °C. The procedures were specifically developed for the analysis of the drugs in superficial samples of human skin. The compounds were extracted with ether. The analytical methods were sensitive to 5 ng of miconazole and 10 ng of clotrimazole per tissue samples (2 mg).

Turner and Warnock [56] determined miconazole in human saliva using high performance liquid chromatography. Deproteinated human saliva samples containing miconazole was chromatographed on a C_8 reversed-phase radial compression column using 77% methanol in 0.01 M EDTA with 0.005 M *n*-nonylamine at a flow

rate of 1.5 mL/min as mobile phase and ultraviolet detection. The method was applied to the determination of miconazole in saliva of human subjects after single doses of 5 or 10 mL miconazole oral gel. Peak concentration observed at 15 min following treatment varied considerably from subject to subject (3.5−40 mg/L after lower and 5.3−51.6 mg/L after higher dose). Most subjects reached the limit of detection (0.5 mg/L) at 3 h following dosing.

Cavrini *et al.* [57] used a high performance liquid chromatography method for the analysis of miconazole and other imidazole antifungal agents in commercial dosage forms. The drugs were determined in tablets, creams, lotions, and powders by extracting with methanol and chromatographing the extract on octadecylsilanized silica gel column with methanol–0.05 M ammonium dihydrogen phosphate (85:15) at 2 mL/min, monitoring the eluate at 230 nm. The separation took less than 10 min. and the relative standard deviation was 0.5−1.32%, better than that of the United States Pharmacopoeia method. Common excipients did not interfere.

Sternson *et al.* [58] used a high performance liquid chromatographic method for the analysis of miconazole in plasma. Miconazole was extracted from alkalinized plasma with *n*-heptane-isamyl alcohol (98.5:1.5) and separated by high performance performance liquid chromatography on μ-Bondapak C_{18} with ultraviolet detection at 254 nm. The mobile phase was methanol–tetrahydrofuran–acetate buffer (pH 5) (62.5:5:32.5) containing 5 mmol octanesulfonate per liter. The flow rate was 2 mL/min. Recovery was 100%. The relative standard deviation for injection-to-injection reproducibility was 0.4% and that for sample-to-sample variation was 5% at high miconazole concentrations (30 μg/mL) and 1% at low (1 μg/mL) concentrations. The limit of detection was 250 ng/mL.

Fan used a high performance liquid chromatographic method for the qualitative and quantitative analysis of miconazole [59]. Miconazole sample was dissolved in methanol and determined by high performance liquid chromatography using methanol–water (75:25) as the mobile phase and ultraviolet detection at 214 nm, the recovery was more than 99.4% and the accuracy was satisfactory for the qualitative and quantitative analysis.

Sellinger *et al.* [60] used a high performance liquid chromatographic method for the determination of miconazole in vaginal fluid. Miconazole and the internal standard (hydrocortisone 21-caprylate) were extracted with chloroform from human vaginal fluid (made pH 2.5 by addition of sodium octanesulfonate). The residue after solvent evaporation was dissolved in the mobile phase, and miconazole was determined by high performance liquid chromatography on Spherisorb C_8, with methlcyanide−1 M sodium phosphate buffer (pH 2.5)−water (600:10:390) as mobile phase and ultraviolet detection at 205 nm. The calibration plot was linear over the range 0.20−200 μg/mL. The method allows the drug concentration in vaginal fluid to be monitored 72 h after a dose of 400 mg miconazole nitrate.

Di Pietra *et al.* [61] used a reversed phase high performance liquid chromatography on different column packing materials (Hypersil C_{18}, Spherisorb–CN, Chromspher–B) to obtain selective separations of miconazole and other imidazole antimycotic drugs. The use of a post-column online photochemical reactor was useful for the enhancement of the sensitivity of the high performance liquid chromatography analysis with ultraviolet detection. This high performance liquid chromatographic method was applied to the analysis of commercial dosage forms

(creams) with a solid-phase extraction procedure, using a diol sorbent, this being a convenient sample preparation technique giving quantitative drug recovery.

Alhaique *et al.* [62] used a reversed phase high performance liquid chromatography method for the determination of miconazole in bulk or pharmaceuticals using bezafibrate as internal standard.

Kobylinska *et al.* [62] described a high performance liquid chromatographic analytical method for the determination of miconazole in human plasma using solid-phase extraction. The method uses a solid-phase extraction as the sample preparation step. The assay procedure is sensitive enough to measure concentrations of miconazole for 8 h in a pharmacokinetic study of Mikonazol tablets and Daktarin tablets in human volunteers. The pharmacokinetics of the two formulations was equivalent.

Chankvetadze *et al.* [64] used a high performance liquid chromatographic method for the enantioseparation of miconazole and other chiral pharmaceutical using *tris*–(chloromethylphenylcarbamate(s)) of cellulose. The chiral recognition abilities of this recently developed new type of cellulose phenyl carbamates were studied. These chiral stationary phases simultaneously contain both electron-withdrawing chlorine atom and electron donating methyl substituents on the phenyl moiety. Chiral pharmaceuticals belonging to the various pharmaceutical groups including miconazole were resolved to enantiomers. These new chiral stationary phases sometimes exhibit alternative chiral recognition ability to that most successful commercially available cellulose chiral stationary phases chiralcel-OD and can be used as a good complement to it in analytical and preparative scale enantioseparation.

Ng *et al.* [65] used a rapid high performance liquid chromatographic assay method for the analysis of miconazole and other antifungal agents in human sera. Serum concentrations of the drugs were assayed using a single-step sample preparation and an isocratic high performance liquid chromatography procedure based on three mobile phases of similar components. This method is simple, flexible, and rapid, the assays being completed within 0.5 h. The method showed high reproducibility, good sensitivity with detection limits of 0.078–0.625 mg/L except for miconazole and econazole, and high recovery rates of 86−105%. High performance liquid chromatography assay should be useful in the clinical laboratory for monitoring patients on antifungal therapy.

Yuan *et al.* [66] determined miconazole and beclomethasone in compound mikangzuoshuang by a high performance liquid chromatographic method. Chromatographic conditions included Nova-Pak C_{18} column and the mobile phase consisting of methanol and water (containing 0.05% diethylamine). Econazole was used as internal standard. The method was simple and sensitive, and the peak shape was good. The average recoveries of miconazole and beclomethasone were 98.3% (relative standard deviation = 1.1%) and 97.6% (relative standard deviation = 1.1%), respectively.

Puranajoti *et al.* [67] described stability-indicating assay methods for the analysis of miconazole in skin, serum, and phase-solubility studies. A reversed phase high performance liquid chromatographic assay and a bioassay using *Saccharomyces cerevisiae*-seeded agar were developed. The high performance liquid chromatography and the bioassay were linear in the range of 0.5−100 and 0.64−1.56 μg/mL, respectively. The sensitivity of the high performance liquid chromatography and the bioassay methods were 0.5 and 0.64 μg/mL, respectively. The bioassay was less cumbersome and much faster than the high performance liquid chromatography

assay by obviating the need for extraction from serum. Miconazole content in the phase solubility studies and in the serum samples was comparatively evaluated by both assay methods. There was good correlation between the two methods (r^2 more than 0.99). The drug extraction efficiency from the serum and the skin were 97.7 and 90.2%, respectively. Where necessary, the bioassay can be an alternative for the high performance liquid chromatography analysis. The within and between day variations of high performance liquid chromatography assay were 3.6 and 4.9%, respectively.

Tyler and Genzale [68] determined miconazole nitrate in creams and in suppositories using a high performance liquid chromatographic method. A sample containing 8 mg of miconazole nitrate was dissolved with worming in ethanol (80 mL) and the solution was diluted to 100 mL with ethanol and further diluted 1:20 with aqueous 50% acetonitrile. The solution was filtered and 20 μL of the filtrate was analyzed by high performance liquid chromatography on a column (15 cm × 4.6 mm) of μ-Bondapak C_{18} with a mobile phase (2 mL/min) prepared by dissolving sodium octane-1-sulfonate in water and adding triethylamine–85% phosphoric acid buffer and acetonitrile. Detection was at 214 nm. The calibration graph was rectilinear for 0.4–6 mg/L of miconazole nitrate. Recoveries of miconazole nitrate from placebo and cream samples were 99.4% and 98.8%, respectively.

Wrobel *et al.* [29] determined miconazole in pharmaceutical creams using internal standard and second-derivative spectrophotometry. Pharmaceutical cream formulation (800 mg) was dissolved in 40 mL of ethanol (60 °C, 40 min), filtered and diluted to 50 mL. A 2-mL portion was mixed with 2 mL 1 M sulfuric acid, 0.5 mL of 5% sodium lauryl sulfate and 0.5 mL internal standard (1 g/L methylene blue) then 100 μL extracted with 100 μL dichloromethane. After centrifugation, 50 μL was evaporated under nitrogen, dichloromethane traces removed with methanol, the residue reconstituted in 1.5 mL methanol and the absorbance was measured from 200−800 nm. Second derivative spectra were calculated ($\Delta\lambda = 12$ nm) using the Savitsky–Golay procedure; the analytical signal was obtained as the ratio between absorbances for miconazole and methylene blue measured at 236.9 and 663.2 nm, respectively. Samples were also analyzed by ion-pair high performance liquid chromatography using a method based on Tyler and Genzale [68]. Beer's law was obeyed from 50 to 400 mg/L with relative standard deviation ($n = 10$) < 2%. The presence of other cream components did not interfere. Results obtained for miconazole in four commercial pharmaceutical creams were in good agreement with those obtained by high performance liquid chromatography procedures.

Guillaume *et al.* [69] presented a high performance liquid chromatographic method for an association study of miconazole and other imidazole derivatives in surfactant micellar using a hydrophilic reagent, Montanox DF 80. The thermodynamic results obtained showed that imidazole association in the surfactant micelles was effective over a concentration of surfactant equal to 0.4 μM. In addition, an enthalpy–entropy compensation study revealed that the type of interaction between the solute and the RP-18 stationary phase was independent of the molecular structure. The thermodynamic variations observed were considered the result of equilibrium displacement between the solute and free ethanol (respectively free surfactant) and its clusters (respective to micelles) created in the mobile phase.

Guillaume *et al.* [70] described a novel approach to study the inclusion mechanism of miconazole and other imidazole derivatives in Micellar Chromatography. The chromatographic approach was proposed to describe the existence of surfactant micelles in a surfactant/hydroorganic phosphate buffer mobile phase. Using this mixture as a mobile phase, a novel mathematical theory is presented to describe the inclusion mechanism of imidazole derivative in surfactant micelles. Using this model, enthalpy, entropy and the Gibbs free energy were determined for two chromatographic chemical processes: the transfer of the imidazole derivative from the mobile phase to the stationary phase, and the imidazole derivative inclusion in surfactant micelles. The thermodynamic data indicate that the main parameter determining chromatographic retention is distribution of the imidazole derivatives to micelles of surfactant while the interaction with the stationary phase plays a minor role.

Erk and Altun [24] used a ratio spectra derivative spectrophotometric method and high performance liquid chromatographic methods for the determination of miconazole nitrate and metronidazole in ovules. The first method depends on ratio spectra first derivative spectrophotometry, by utilizing the linear relationship between substances concentration and ratio spectra first derivative peak amplitude. The ratio first derivative amplitudes at 242.6, 274.2, 261.8, 273.5, and 281.5 nm were selected for the assay of metronidazole and miconazole nitrate, respectively. The second method was based on high performance liquid chromatography on a reversed-phase column using a mobile phase of pH 2.8 methanol–water–phosphoric acid (30:70:0.20) with programmable detection at 220 nm. The minimum concentration detectable by high performance liquid chromatography was 0.9 μg/mL for metranidazole and 0.3 μg/mL for miconazole nitrate and by ratio derivative spectrophotometry 4 μg/mL for metronidazole and 0.5 μg/mL for miconazole nitrate. This procedure was successfully applied to the simultaneous determination of mitronidazole and miconazole nitrate in ovules with a high percentage of recovery, good accuracy, and precision.

Akay *et al.* [71] described a reversed phase high performance liquid chromatography method, with ultraviolet detection, for the simultaneous determination of miconazole and metronidazole in pharmaceutical dosage form. Chromatography was carried out on a C_{18} reversed-phase column, using a mixture of methanol–water (40:60, v/v) as mobile phase, at a flow rate of 1 mL/min. Sulphamethoxazole was used as an internal standard and detection was performed using a diode array detector of a 254 nm. The method produced linear responses in the concentration ranges 10−70 and 1−20 μg/mL with detection limits 0.33 and 0.27 μg/mL for metronidazole and miconazole, respectively. This procedure was found to be convenient and reproducible for the analysis of these drugs in ovule dosage forms.

Gagliardi *et al.* [72] developed a simple high performance liquid chromatographic method for the determination of miconazole and other antimycotics in cosmetic antidandruff formulations. This high performance liquid chromatographic method was carried out on a Discovery RP Amide C_{16} column and spectrophotometric detection was performed at 220 nm. The initial mobile phase was a mixture of acetonitrile and aqueous 0.001 M sodium perchlorate (pH 3) in the ratio of 15:85 (v/v); then a linear gradient less than 46% acetonitrile in 70 min, and less than 50% in 80 min. The extraction procedure was validated by analyzing samples of shampoo

and lotion spiked with 1% of the active principles. The recoveries were more than 95% and the reproducibility was within 3%.

Lee [73] studied the stability of miconazole on dry heating in vegetable oils. Miconazole was stable when subjected to dry heat (160 °C for 90 min) in either peanut or castor oil as determined by high performance liquid chromatography analysis. Thus, ophthalmic preparations of miconazole can be prepared in peanut or castor oil with dry heat sterilization without the loss of the drug due to degradation. The procedure also facilitates quick and easy dissolution of the drug in the oil base.

Holmes and Aldous [74] determined the stability of miconazole in peritoneal dialysis fluid. The stability of the drug when mixed with peritoneal dialysis fluid and stored in plastic bags or glass ampules was studied. Admixture of miconazole and peritoneal dialysis fluid were prepared in 2L polyvinyl chloride bags and in 1 mL glass ampules to give a nominal initial concentration of 20 mg/mL. Duplicate samples of each solution were assayed in duplicate by high performance liquid chromatography immediately after preparation and at various intervals up to 9 days. All admixtures were stored in ambient light at 20 ± 2 °C. A substantial loss of miconazole (greater than 10% of the initial concentration) occurred within 4 h for admixtures stored in polyvinyl chloride bags, whereas similar solution retained more than 90% of their initial miconazole concentration for at least 3 days, when stored in glass ampules under the same conditions. This suggests that the observed loss of miconazole from the polyvinyl chloride bags was largely due to an interaction with the container, rather than due to chemical degradation in solution. About 28% of the miconazole lost from the solution during storage in polyvinyl chloride bags was recovered from the plastic by methanolic extraction. The rapid loss of the drug when mixed with peritoneal dialysis fluid and stored in polyvinyl chloride bags indicates that such admixtures should be prepared immediately before administration.

Zhang and Deng [75] described a high performance liquid chromatographic method for the analysis of miconazole in plasma. Miconazole was extracted with acetonitrile from rabbit plasma and determined by high performance liquid chromatography, using methanol–0.05 M ammonium dihydrogen phosphate (84:16) as the mobile phase and detection at 230 nm. The detection limit was 0.5 μg/mL and the average recovery was 96.5%. The pharmacokinetics of miconazole from vaginal suppositories was studied in rabbit by this method.

Hasegawa *et al.* [76] measured miconazole serum concentration by a high performance liquid chromatographic method. The authors assessed whether the internal standard method produced an intra-assay error and found that the method gave more precise and more reproducible results compared to the absorption calibration curve method. With 0.5 μg/mL of miconazole, the coefficient of variation produced by that method was 3.41%, whereas that of the absorption calibration curve method was 5.20%. The concentration of absorptions calibration curve method showed higher values than the internal standard method. This indicated that the internal standard method was far more precise in measuring the miconazole serum concentrations than the absorption calibration curve method.

El-Abbes Faouzi *et al.* [77] studied the stability, compatibility and plasticizer extraction of miconazole injection added to infusion solutions and stored in polyvinyl chloride containers. The stability of miconazole in various diluents and in

polyvinyl chloride containers was determined and the release of diethyl hexyl phthalate from polyvinyl chloride bags into the intravenous infusions of miconazole was measured. An injection formulation (80 mL) containing a 1% solution of miconazole with 11.5% of Cremophor EL was added to 250 mL polyvinyl chloride bags containing 5% glucose injection or 0.9% sodium chloride injection, to give an initial nominal miconazole concentration of 2.42 mg/mL, the mean concentration commonly used in clinical practice. Samples were assayed by stability-indicating high performance liquid chromatography and the clarity was determined visually. Experiments were conducted to determine whether the stability and compatibility of miconazole would be compromised, and whether diethyl hexyl phthalate would be leached from the polyvinyl chloride bags and polyvinyl chloride administration sets during storage and simulated infusion. There was no substantial loss of miconazole over 2 h simulated infusion irrespective of the diluents, and over a 24 h storage irrespective of temperature (2–6 and 22–26 °C). All the solutions initially appeared slightly hazy. Leaching of diethyl hexyl phthalate was also detected during simulated delivery using polyvinyl chloride bags and polyvinyl chloride administration sets. There was a substantial difference between the amounts of diethyl hexyl phthalate release from polyvinyl chloride bags and from administration sets, and also between the amounts released in solutions stored in polyvinyl chloride bags at 2–6 °C and 22–26 °C over 24 h. At the dilution studied, miconazole was visually and chemically stable for up to 24 h. The storage of miconazole solutions in polyvinyl chloride bags seems to be limited by the leaching of diethyl hexyl phthalate rather than by degradation. To minimize patient exposure to diethyl hexyl phthalate, miconazole solutions should be infused immediately after their preparation in polyvinyl chloride bags.

Aboul-Enein and Ali [78] compared the chiral resolution of miconazole and two other azole compounds by high performance liquid chromatography using normal-phase amylose chiral stationary phases. The resolution of the enantiomers of (±)-econazole, (±)-miconazole, and (±)-sulconazole was achieved on different normal-phase chiral amylose columns, Chiralpak AD, AS, and AR. The mobile phase used was hexane–isopropanol–diethylamine (400:99:1). The flow rates of the mobile phase used were 0.50 and 1 mL/min. The separation factor (α) values for the resolved enantiomers of econazole, miconazole, and sulconazole in the chiral phases were in the range 1.63–1.04; the resolution factors R_s values varied from 5.68 to 0.32.

In another study, the authors reported a comparative study of the enantiomeric resolution of miconazole and the other two chiral drugs by high performance liquid chromatography on various cellulose chiral columns in the normal phase mode [79]. The chiral resolution of the three drugs on the columns containing different cellulose derivatives namely Chiralcel OD, OJ, OB, OK, OC, and OF in normal phase mode was described. The mobile phase used was hexane–isopropanol–diethylamine (425:74:1). The flow rates of the mobile phase used were 0.5, 1, and 1.5 mL/min. The values of the separation factor (α) of the resolved enantiomers of econazole, miconazole, and sulconazole on chiral phases were ranged from 1.07 to 2.5 while the values of resolution factors (R_s) varied from 0.17 to 3.9. The chiral recognition mechanisms between the analytes and the chiral selectors are discussed.

In this study, Ali and Aboul-Enein [80] used cellulose *tris*–(3,5-dichlorophenyl carbamate) chiral stationary phase for the enantioseparation of miconazole and other clinically used drugs by high performance liquid chromatography. The mobile

phase used was isopropanol at 0.5 mL/min with detection at 220 nm. The separation factor (α) of these drugs ranged from 1.24 to 3.9 while the resolution factors R_s were 1.05–5. The chiral recognition mechanisms between the racemates and the chiral selector are discussed.

The authors also reported that the enantiomeric resolution of the three enantiomeric compounds was achieved by using a Chiralpak WH chiral stationary phase with the help of high performance liquid chromatography [81]. The mobile phase used was hexane–isopropanol–diethylamine (400:99:1). The flow rates of the mobile phase used were 0.5 and 1 mL/min. The values of separation factors (α) of the resolved enantiomers of econazole, miconazole, and sulconazole were in the range of 1.68–1.23 while the values of resolution factors (R_s) varied from 2.42 to 1.1. The resolution of these antifungal agents on Chiralpak WH column is governed by ligand-exchange mechanism. Hydrophobic interactions also play an important role for the enantiomeric resolution of the antifungal agent on the reported chiral stationary phase.

Pan *et al.* [82] used a reversed phase high performance liquid chromatographic method for the determination of miconazole nitrate and its related substances.

Table 6 summarizes the conditions of the other high performance liquid chromatographic methods, which are reported in the literature for the separation and analysis of miconazole in bulk, pharmaceutical formulation, and biological fluids [60, 83–91].

4.5.5. High performance liquid chromatography–mass spectrometry

Zhang and Nunes [92] used a high performance liquid chromatographic-coupled with electrospray ionization mass spectrometry (HPLC–ESI–MS) method to study the structure and generation mechanism of a novel degradation product formed by oxidatively induced coupling of miconazole nitrate with butylated hydroxytoluene in a topical ointment. In a petrolatum-based topical ointment formulation containing miconazole nitrate as the active ingredient and 2,6-di-tert-butyl-4-methylphenol (BHT) as a vehicle antioxidant, an oxidatively induced coupling reaction between miconazole nitrate and BHT occurred to form a novel adduct: 1-(3,5-di-tert-butyl-4-hydroxybenzyl)-3-[2-(2,4-dichlorobenzyloxy)-2-(2,4-dichlorophenyl)-ethyl]-3H-imidazol-1-ium nitrate. The structure of the latter compound was established using HPLC–ESI–MS and was confirmed by comparing with a synthesized reference compound. The reaction proceeded through a quinone methide intermediate from BHT. Two synthetic methods were established from preparing this novel adduct.

4.5.6. Capillary electrophoresis

van-Eeckhaut *et al.* [93] reported the development and evaluation of a linear regression method for the prediction of maximal chiral separation of miconazole and other antifungal imidazole drug racemates by cyclodextrin-mediated capillary zone electrophoresis. An important step, in method development of chiral separations with neutral cyclodextrins as chiral selectors, is the estimation of the cyclodextrin concentration that gives the highest degree of separation. From the equation $[S]_{opt} = 1/(K_1K_2)^{1/2}$, this optimal cyclodextrin concentration can be calculated if any knowledge is available about the binding constant, K_1 and K_2 of both enantiomer complexes. These values can be obtained by measuring the effective velocities of

Table 6. High performance liquid chromatography conditions of the methods used for the determination of miconazole nitrate

Column	Mobile phase and [flow rate]	Detection	Remarks	Reference
5 cm × 4.6 mm of Spherisorb C_8 (5 μm)	Acetonitrile–1M sodium phosphate buffer (adjusted to pH 2.5 with 85% H_3PO_4–water (60:1:39) [1.5 mL/min]	205 nm	Recovery was 90–103.6%. Analysis in vaginal fluids	[60]
15 cm × 6 mm of AM-312 ODS (5 μm)	0.05M sodium acetate buffer (pH 7.4)–acetonitrile (1:4) [1.5 mL/min]	220 nm	Applied in pharmacokinetic studies. Recovery was 93–98% in human serum	[83]
15 cm × 3.9 mm of Novapak RP-18 (5 μm)	Methanol–tetrahydrofuran–0.1M triethylammonium acetate (pH 7) (35:6:9) [0.8 mL/min]	230 m	Analysis of miconazole in pharmaceutical formulation by derivative UV and HPLC	[84]
25 cm × 4.5 mm (5 μm) of Ultrasphere C_{18}	Methanol–20 mM NaH_2PO_4 (97:3) [1 mL/min]	235 nm	Analysis in suppository and ointment preparations	[85]
25 cm × 4 mm Nucleosil 120–5 C_{18} with a Nucleosil 120–5 C_{18} guard column (3 cm × 4mm)	Methanol–acetonitrile–0.01M phosphate buffer of pH 7 (9:9:7) [2.1 mL/min]	230 nm	Analysis in human plasma using solid-phase extraction. Recovery was 85.82%	[86]
15 cm × 3.2 mm (5 μm) of Hypersil ODS or (5 μm) Spherisorb-CN (15 cm × 4.6 mm) under reversed phase condition with post-column UV irradiation at 254 nm	Not given	230–240 nm	On line post-column photochemical derivatization in liquid chromatographic diode-array detection analysis of binary drug mixtures	[87]
15 cm × 5 mm (5 μm) Sherisorb C_8 at 35 °C	33:17 mixture of methanol and a buffer solution containing 4 g/L KH_2PO_4, 2.5 mL/L triethylamine and 1 g/L sodium-1-octanesulfonate adjusted to pH 2.5 with H_3PO_4 [1.5 mL/min]	235, 260, 320 nm	Determination in Kangtaizuo washing solution by HPLC. Recoveries were 100.9−101.2% with R.S.D. of <0.34%	[88]
12.5 cm × 4 mm (5 μm) C_{18} Silica Li Chro CART column operated at eleven temperatures from 8 to 70 °C	Methanol–aqueous 1% phosphate buffer of pH 3 containing 0−3 mM β-cyclodextrin and containing 5 mM-nonylamine [1 mL/min]	230 nm	A simple model for reversed-phase LC retention and selectivity of imidazole enantiomers using β-cyclodextrin as chiral selector	[89]
12.5 cm × 4 mm (5 μm) Li Chro CART RP_{18} operated at 10, 15, 20, 25, 30, 40, 45, and 50 °C	73% methanol in 30 mM ammonium phosphate buffer of pH 3 containing 5 mM *n*-nonylamine and 0–30 mM hydroxypropyl-β-cyclodextrin [1 mL/min]	230 nm	Peculiarities of the mechanism of retention of miconazole and five imidazole derivatives when usng hydroxy propyl-β-cyclodextrin as mobile phase additive	[90]
15 cm × 6 mm (10 μm) Shim-pak-CLC-phenyl column	7:3 mixture of methanol and aqueous triethylamine (2 mL triethylamine per 300 mL solution; adjusted to pH 7 with H_3PO_4) [1 mL/min]	230 nm	Determination of three component of compound Jianliao by HPLC. Recoveries were 100.4−100.6%. R.S.D. of 0.6−1.02%	[91]

each enantiomer as a function of the selector concentration and fitting these profiles by nonlinear least-squares regression. Another alternative approach makes it possible to predict the optimal cyclodextrin concentration from few experiments performed at low cyclodextrin concentrations. The model is developed using miconazole, econazole, and isoconazole as test substances and hydroxypropyl-β-cyclodextrin as chiral selector. The results obtained by this method are in good agreement with those from nonlinear least-squares regression.

Guillaume and Peyrin [94] designed a chemometric method to optimize the chiral separation of miconazole and other imidazole derivatives by capillary electrophoresis. Factorial design resulting in 18 experiments was used to generate data sufficient to fit a quadratic model, which was optimized by a simplex process to give a capillary electrophoretic method for the separation of the drug as one of a series of imidazole derivatives dissolved in the background electrolyte. Capillary electrophoresis was effected with 2 s pressure injection on fused-silica capillaries (57 cm $\times$ 75 μm, i.d; 50 cm to detector) operated at 35 °C with an applied voltage of +30 kV and ultraviolet detection at 230 nm. Optimum separation was achieved in 15 min with acetonitrile–phosphate buffer of pH 4.7 (5.2:94.8) containing 5.8 μM β-cyclodextrin as background electrolyte.

Lin *et al.* [95] used capillary electrophoresis with dual cyclodextrin systems for the enantiomer separation of miconazole. A cyclodextrin-modified micellar capillary electrophoretic method was developed using mixture of β-cyclodextrins and mono-3-*O*-phenylcarbamoyl-β-cyclodextrin as chiral additives for the chiral separation of miconazole with the dual cyclodextrins systems. The enantiomers were resolved using a running buffer of 50 mmol/L borate pH 9.5 containing 15 mmol/L β-cyclodextrin and 15 mmol/L mono-3-*O*-phenylcarbamoyl-β-cyclodextrin containing 50 mmol/L sodium dodecyl sulfate and 1 mol/L urea. A study of the respective influence of the β-cyclodextrin and the mono-3-*O*-phenylcarbamoyl-β-cyclodextrin concentration was performed to determine the optical conditions with respect to the resolution. Good repeatability of the method was obtained.

4.6. Biological methods

Grendahl and Sung [96] tested a simple, reliable, and inexpensive assay method for the quantitation of serum levels of miconazole and other imidazole drugs. This assay, which is similar to Kirby–Bauer test, was sensitive to 0.2 μg of drug/mL and linear from $\leq$0.2 to 10 μg/mL. Concentration of inoculum and agar depth in test plates was not as critical as the type of medium, amount of inoculum or type of drug used.

Puranajoti *et al.* [67] developed a reversed phase high performance liquid chromatographic assay and a bioassay using *Saccharomyces cerevisiae*-seeded agar. The high performance liquid chromatography and the bioassay methods were linear in the range 0.5−100 and 0.64−1.56 μg/mL, respectively. The sensitivities of the two methods were 0.5 and 0.64 μg/mL, respectively. The bioassay was less cumbersome and much faster than the high performance liquid chromatography method by obviating the need for extraction from serum.

Espinel-Ingroff *et al.* [97] described a radial diffusion bioassay method for miconazole, which employs *Candida stellatoidea* as the indicator organism. Results from

three patients treated with miconazole are presented. These include a case of aricular sporotrichosis treated for 30 days; a case of disseminated aspergillosis treated for 4 weeks, and a case of cryptococcosis in a renal transplant recipient treated for 5 weeks. The first two patients were treated intravenously with 10 mg of miconazole/kg every 8 h, the third patient received both recipients treated for 5 weeks. The first two patients were treated intravenous and intraventricular drug. All specimens were stored at −20 °C prior to bioassay; sera have been removed from blood specimen prior to storage. Excellent linearity and correlation were demonstrated between the concentrations of the drug and the corresponding diameters of the resulting zone of inhibition. In four bioassays, *r*, or the coefficient of correlation was 0.995 or better, the lowest value for *r* was 0.989. All three fungal isolates from the patients were found to be susceptible to miconazole, being inhibited by 1.56 μg or less of the drug per milliliter *in vitro*, yet all patients failed to respond favorably to the drug.

Egawa *et al.* [98] used quantitative bioassay methods for miconazole with *Candida albicans* as the indicator organism. Several reliable methods for the bioassay of miconazole in serum or other clinical specimens employing *Candida albicans* as the indicator organism are described. The well agar plate method with yeast morphological agar was sensitive to 1 μg/mL, and linear from 1 to ≥16 μg/mL. The disk agar plate method was much more sensitive, by which 0.06 μg miconazole per disk was quantitatively measurable. The bioautography method was the most sensitive; the lower limit of the assay was as low as 0.002 μg drug per sample applied. In the latter two methods, yeast morphological agar was used as the assay medium and serum specimens were extracted with cyclohexane or ether.

Temeyer tested the toxicity of miconazole and six other antifungal agents and solvents for use in horn fly larval rearing or bioassays. Each of which appeared to be potentially useful in bovine fecal medium [99].

5. STABILITY

Marciniec *et al.* [100] evaluated the radiochemical stability of miconazole and other antifungal drug by thermal analysis. Miconazole and the other drugs in solid phase were exposed to beta irradiations at the dose of 20−200 kGy and then alterations in the physicochemical properties of miconazole and the other drugs were studied using the following methods: scanning electron microscopy, differential scanning calorimetry, and X-ray powder diffraction analysis. It was found that the compound irradiated with sterilizing dose (20−50 kGy) showed no significant alterations in their physicochemical properties, while application of doses more than 50 kGy resulted in small changes in the X-ray diffraction patterns and in the course of differential scanning calorimetry curves, including a decrease in the melting points and enthalpy of the process. For miconazole and fluconazole, a linear and relatively strong correlation was found (from $r = 0.9782$ to $r = 0.9003$) between the size of the dose of irradiation and the decrease in the melting point and enthalpy value.

Lee [73] reported that miconazole was stable when subjected to dry heat (160 °C for 90 min) in either peanut or castor oil as determined by high performance liquid

chromatography analysis. Thus, ophthalmic preparations of miconazole can be prepared in peanut or castor oil with dry heat sterilization without the loss of the drug due to degradation. This procedure also facilitates quick and easy dissolution of the drug in the oil base.

Holmes and Aldous [74] determined the stability of the drug when mixed with peritoneal dialysis fluid and stored in plastic bags or glass ampules.

Nishikawa and Fujii [101] studied the effect of autooxidation of hydrogenated castor oil containing 60 oxyethylene groups on degradation of miconazole. When 30 mg/mL aqueous hydrogenated castor oil consisting of 60 oxyethylene groups solutions were shaken under fluorescent light at about 500 lux in a water bath at 30 or 60 °C, hydroperoxide, formaldehyde and formic acid were formed. An aqueous solution containing 10 mg/mL miconazole, 100 mg/mL hydrogenated castor oil consisting of 60 oxyethylene groups and 1 mg/mL lactic acid was sealed in ampules and stored at various temperature for 8 days. At 40 °C or above, the concentration of miconazole decreased accompanied by a decrease in pH and formaldehyde formation. However, in the presence of nitrogen, no degradation was observed. The degradation of miconazole was also observed in the presence of iron(II) ion and hydrogen peroxide. The degradation of miconazole and hydrogenated castor oil consisting of 60 oxyethylene groups was prevented by the addition of hydroxyl radical scavengers, especially potassium iodide and thiourea. These results indicate the hydroxyl radicals generated by autooxidation of hydrogenated castor oil consisting of 60 oxyethylene groups degraded miconazole.

El-Abbes Faouzi *et al.* [77] determined the stability of miconazole in various diluents and polyvinyl chloride containers, and the release of diethyl hexyl phthalate from the polyvinyl chloride bags into the intravenous infusion of miconazole.

Zhang and Nunes [92] studied the structure and the generation mechanism of a novel degradation product formed by oxidatively induced coupling of miconazole nitrate with butylated hydroxy toluene in a topical ointment studied by high performance liquid chromatography–electrospray ionization mass spectrometry and organic synthesis.

6. PHARMACOKINETICS, METABOLISM, AND EXCRETION

6.1. Pharmacokinetics

Foster and Stefanyszyn [102] reported that miconazole nitrate may penetrate the ocular compartments better than either natamycin or amphotericin B after intravenous subconjunctival, or topical administration in rabbits. The concentration of the drugs in cornea and in aqueous humor after either topical or subconjunctival administration were high, and a further threefold increase in the level was seen if the corneal epithelium had been removed prior to drug therapy. Miconazole nitrate was found in the vitreous in some animals after subconjunctival injections of the drug. Intravenous administration produced high concentrations of the drug in the aqueous humor, which rapidly decreased over 8 h. No signs of toxicity or adverse reactions were found in these short-term experiments. Miconazole nitrate may be useful in treatment of keratomycosis and oculomycosis.

Egawa *et al.* [103] by using a microbial assay method reported that miconazole was not detected in the blood after human subjects were given 100 mg tablets of miconazole intravaginally for 14 days. Six species of 12 strains of human vaginal *Lactobacillus* were insensitive to miconazole.

Daneshmend [104] measured the serum concentration of miconazole in 11 healthy adult females for 72 h following a single 1200 mg vaginal pessary. The mean peak serum miconazole concentration was 10.4 μg/L and the mean elimination half-life was 56.8 h. The mean area under the serum concentration–time curve was 967 μg/L/h. The calculated mean systemic bioavailability of the vaginal pessary was 1.4%. There was large intersubject variation in serum miconazole pharmacokinetics. This formulation may provide effective single dose treatment for vaginal candidiasis.

Pershing *et al.* [105] investigated a direct study, evaluating whether differential drug uptake of topical 2% miconazole and 2% ketoconazole from cream formulations into human stratum corneum correlated with differential pharmacological activity against *Candida albicans* in healthy human subjects. A single 24 h topical dose of 2% miconazole cream was applied unoccluded, at the same dose (2.6 mg of formulation per cubic centimeter of surface area), at four skin sites on both ventral forearms of six human subjects. At the end of the treatment, residual drug was removed with a tissue from all sites and the treated sites were tape striped 11 times, either 1, 4, 8, or 24 h later. The first tape disk was discarded. The remaining tape disks, 2–11, were combined and extracted for the drug quantification by high performance liquid chromatography and bioactivity against *Candida albicans* growth *in vitro*.

Garbe *et al.* [106] studied the dermal absorption of miconazole from a new topical preparation in pigs. The dermal absorption of the drug was studied in pigs after application of 0.5 g cream/kg body weight under occlusive dressing for 5 h. ^{14}C-labeled miconazole nitrate was introduced into the base cream as single component. The three resulting creams were tested in groups of three pigs each. To obtain a basis for the assessment of the data after dermal application of the two labeled drugs were also examined after intravenous injection.

Mikamo *et al.* [107] investigated the pharmacokinetics of miconazole in serum and exudates of pelvic retroperitoneal space after radical hysterectomy and pelvic lymphadenectomy. This study was designed to investigate the pharmacokinetics of miconazole in the excudate of the retroperitoneal space that is formed after radical hysterectomy and pelvic lymphadenectomy. A total of 600 mg miconazole was administered to patients for exactly 60 min using an automatic drip infusion pump. The parameters of the formulas analyzed by the two-compartment model were determined using the least squares method, and a simulation curve was made. The maximum drug concentration of miconazole in serum was 6.26 mg/L 1 h after drip infusion commencement and the $t_{½}$ in serum was 8.86 h.

Piel *et al.* compared the intravenous pharmacokinetics of miconazole in sheep after its administration in a polyoxyl-35 castor oil/lactic acid mixture, a 100 μM hydroxylpropyl-β-cyclodextrin–50 μM lactic acid solution, and a 50 μM sulfobutyl ether (SBE7)-β-cyclodextrin–50 μM lactic acid solution. Intravenous administration of 4 mg/kg of miconazole was completed within 5 min [108]. There were no differences of the miconazole blood plasma concentration versus time for the three dosage forms. The half-life of distribution was <2.4 min. Both hydroxylpropyl-β-

cyclodextrin and sulfobutyl ether (SBE7)-β-cyclodextrin do not interfere with the release of miconazole compared to polyoxyl-35 castor oil. Hydroxylpropyl-β-cyclodextrin and sulfobutyl ether (SBE7)-β-cyclodextrin are proposed as safe vehicles instead of surfactants for the parenteral delivery of miconazole.

Piel *et al.* [109] studied the pharmacokinetics of miconazole after intravenous administration to six sheep (4 mg/kg) of three aqueous solutions – a marketed micellar solution containing polyoxyl-35 castor oil was compared with two solutions both containing 50 μM lactic acid and a cyclodextrin derivative (100 μM hydroxylpropyl-β-cyclodextrin or 50 μM sulfobutyl ether (SBE7)-β-cyclodextrin. This work demonstrated that these cyclodextrin derivatives have no effect on the pharmacokinetics of miconazole by comparison with the micellar solution. The plasma concentration–time curves have shown that there is no significant difference between the three solutions.

Cardot *et al.* [110] compared the pharmacokinetics of miconazole after administration, via a bioadhesive slow release tablet and an oral gel, to healthy male and female subjects. This study aims to compare salivary miconazole pharmacokinetics following once daily application of bioadhesive tablets (50 or 100 mg) versus the current treatment with a gel (three times a day, 375 mg/day). A three-way crossover study was carried out in 18 healthy subjects (9 males and 9 females) with a 1-week washout period between each treatment. Plasma and salivary pharmacokinetics of miconazole were assessed over a 24-h period. Results in all subjects; the tablets gave higher and more prolonged salivary miconazole concentrations than the gel. Thus, salivary miconazole area under the curve (0, 24 h) was 37.2 times greater than the 100 mg tablet and 18.9 times greater for the 50 mg tablets compared with the gel. The data supports the further development of miconazole bioadhesive tablets as a sustained release formulation leading to improved antifungal exposure in the buccal cavity.

6.2. Metabolism

Ohzawa *et al.* [111] studied the metabolism of miconazole after a single oral or intravenous administration of ^{14}C miconazole at a dose of 10 mg/kg. After 1 h oral or intravenous administration to male rats, the four known metabolites besides the unchanged form were observed in the plasma, and the five unknown metabolites were observed in the plasma. At 24 h, metabolites were not detected in plasma except one of the known metabolites. After oral administration to female rats, the unchanged form and four of the known metabolite along with one of the unknown metabolites were observed in the plasma, but one of the known metabolites and three of the unknown metabolites were not detected. After oral or intravenous administration to male rats, two of the known metabolites and five of the unknown metabolites were observed in the urine collected until 24 h. After oral or intravenous administration to male rats, four of the known metabolites and five of the unknown metabolites and one of the known metabolites besides the unchanged form were observed in the feces collected until 24 h. The fecal excretion of the major known metabolite, within 24 h after oral or intravenous administration was 19.4% or 13.3% of the administered radioactivity, respectively. One of the unknown metabolite was isolated from plasma after oral administration to female rats.

Mass spectrometry indicated this metabolite has undergone oxidative cleavage of the imidazole ring.

Ohzawa *et al.* [112] studied the absorption, distribution, and excretion of ^{14}C miconazole in rats after a single administration. After the intravenous administration of ^{14}C miconazole at a dose of 10 mg/kg to the male rats, the plasma concentration of radioactivity declined biophysically with half-lives of 0.76 h (α phase) and 10.32 h (β phase). After oral administration of ^{14}C miconazole at a dose of 1, 3, or 10 mg/kg to male rats, the plasma concentration of radioactivity reached the maximum level within 1.25 h, after dosing and the decline of radioactivity after the maximum level was similar to that after intravenous administration. At a dose of 30 mg/kg, the pharmacokinetic profile of radioactivity in the plasma was different from that at the lower doses. In the female rats, the plasma concentration of radioactivity declined more slowly than that in male rats. The tests were conducted on pregnant rats, lactating rats, bile-duct cumulated male rats. Enterohepatic circulation was observed. In the *in situ* experiment, ^{14}C miconazole injected was observed from the duodenum, jejunum, and/or ileum, but not from the stomach.

Ohzawa *et al.* [113] studied the absorption, excretion, and metabolism of miconazole after a single oral administration of ^{14}C miconazole at a dose of 10 mg/kg to male dogs. After administration of ^{14}C miconazole, the blood concentration of radioactivity reached the maximum level at 4 h, and then declined slowly with a half-life of about 26 h. The plasma concentration reached the maximum level at 5 h and then declined slowly with a half-life of 30 h. After the administration of miconazole, the plasma concentration of the unchanged form reached the maximum level at 3 h; and then rapidly declined with half-life of about 4.3 h. Within 168 h after administration of ^{14}C miconazole, urinary and fecal excretion amounted to about 6% and 66% of the administration radioactivity, respectively. After administration of ^{14}C miconazole, the plasma concentration of the unchanged form rapidly declined, but the plasma level of two major metabolites reached maximum at 5 and 12 h, respectively and then declined.

Ohzawa *et al.* [114] studied the absorption, distribution, and excretion of ^{14}C miconazole in male rats during and after consecutive oral administration at a dose of 10 mg/kg once a day for 15 days. During consecutive administration, the plasma concentration of radioactivity reached the steady state on day 4 and was 0.48 approximately 0.52 μg eq./mL at 24 h after each dose. After the final dose, the plasma concentration of radioactivity reached the maximum level of 1.67 μg eq./mL at 7.5 h and declined with a half-life of about 18.68 h. The area under the curve 24 h was 28.3 μg h/mL, which is close to the area under the curve $0–\infty$ of a single oral dose.

Ohzawa *et al.* [115] studied the plasma concentration, distribution, and metabolism of ^{14}C miconazole, after application of ^{14}C miconazole gel (10 mg/kg of miconazole) to oral mucosa of male rats. After application, the plasma radioactivity reached the maximum level of 1.82 μg eq./mL at 2 h, and then declined in a similar manner as after oral administration of ^{14}C miconazole. At 1 h after application, high levels of radioactivity were observed in the epidermis of lip, palatum, tongue, and buccal mucosa on the enlarged autoradiograms, and the radioactivity was high in the epidermis of buccal mucosa, while low in the buccal muscle.

6.3. Excretion

From 10 to 20% of an oral dose of miconazole is excreted in the urine, mainly as metabolites, within 6 days. About 50% of an oral dose may be excreted mainly unchanged in the feces. The elimination pharmacokinetics of miconazole have been described as triphasic, with a biological half-life of about 24 h. With an initial half-life of about 0.4 h, and intermediate half-life of about 2.5 h and elimination half-life of 24 h. Very little miconazole is removed by haemodialysis [3].

7. PHARMACOLOGY

Vlassis *et al.* [116] investigated the stability of the obtained cures after treatment with 2% miconazole nitrate vaginal cream and evaluated the therapeutic effects and its tolerance. Fifty-three females suffering from vaginal candidiasis were included in this study. Those without positive cultures or those who did not return for reexamination or were treated with other antimycotic agents were excluded from this study. All patients entered in this trial were treated during a first period for their vaginal candidiasis with miconazole nitrate. Those who were cured later after two courses of therapy were followed up at monthly intervals until 8 months. Evaluating criteria were the cultures, the microscopic examination, the subjective symptoms, and the objective findings of the investigators. Fifty-one patients (96.3%) were cured after one course of treatment (14 days) with miconazole nitrate and the remaining two, after a second course. The effect of the treatment on the subjective complaints as well as the objective findings of the investigators was very satisfactory and statistically highly significant. Three patients – two on the fifth, one on the sixth month – relapsed during the follow-up period. Of the relapse cases, two had been treated with oral contraceptives for 4 months and the third with trichomonacides for a month. It is concluded that miconazole nitrate is an effective and safe anticandidal agent ensuring high cure stability rates in vaginal candidiasis patients.

Hoeprich and Huston [117] assessed the stability of miconazole and three other antifungal agents under conditions encountered in bioassay and susceptibility testing *in vitro*. Although the amphotericins were labile as compared with other drugs, tests should be reliable with all four drugs in view of the rapid action of the polyenes and the relatively slow action of miconazole and 5-fluorocytosines.

Eloy [118] studied the stability of cure in 72 cases of vulvo-vaginal candidiasis treated locally with miconazole.

Hildick-Smith [119] discussed the pharmacology, mode of action, therapeutic uses and toxicology of miconazole and other antifungal agents.

Sawyer *et al.* [120] presented a review on the antifungal activity and therapeutic efficacy of miconazole. The drug is active against *Candida* spp., *Trichophyton* spp. *Epidermophyton* spp., *Microsporum* spp, and *Pityrosporon orbiculare* (*Malassesia furfur*). The drugs possess some activity against Gram-positive bacteria. In vaginal candidiasis, miconazole vaginal cream has produced higher cure rate than conventional nystatin vaginal tablets or amphotericin B vaginal cream.

Stevens *et al.* [121] discussed the therapeutic and pharmacologic action of miconazole in man for the treatment of coccidioidomycosis. Up to 3.6 g/day of miconazole

was given for up to 3 months. Minimal inhibitory concentrations of mycelial and endospore phases of all clinical isolate of *Candida immitis* were less than 2 μg/mL. Peak concentrations in the blood of up to 7.5 μg/mL (by assay against *Candida immitis in vitro*) were achieved. Doses above 9 mg/kg or 350 mg/m^2 were more efficacious in producing blood level over 1 μg/mL. Serum protein binding, determined by several methods, was approximately 90%.

Ito *et al.* [122] reported that the administration of miconazole to laboratory animals (mice, rats, and rabbits) decreased body temperature, blood pressure, and heart rate, increased intestinal motility, prolonged hexobarbital sleeping time, induced drug-metabolizing enzymes in the liver, inhibited carrageenin-induced edema, but had no effect on spontaneous movement, breathing, blood vessels, and urine volume. The drug had no local anesthetic, stimulating, or muscle-relaxing effects.

Raab [123] presented a discussion on the topical clinical pharmacology of miconazole and two other azole antifungal agents.

Cartwright [124] reported that miconazole was slightly absorbed from epithelial and mucosal surface. The drug is well absorbed from the gastrointestinal tract, but caused nausea and vomiting in some patients. The drug may be given intravenously but was associated phlebitis. Up to 90% of the active compound was bound to plasma protein. Distribution into other body compartments was poor. Metabolism was primarily in the liver, and only metabolites were excreted in the urine. At therapeutic levels, they were relatively nontoxic both locally and systematically, but occasionally produced disturbances on the central nervous system.

8. REVIEWS

Fukushiro [125] discussed the activity of the antifungal agent with a special emphasis on miconazole and econazole. Janssen *et al.* and Van Bever [126] presented a review on the pharmacology of miconazole. Heel *et al.* [127] also presented a preliminary review on the therapeutic efficacy of miconazole in systemic fungal infections. Stranz [128] reviewed the antifungal and pharmacology of miconazole. Zhang [129] discussed the antimicrobial spectra, action mechanism, adverse side effects, and clinical application of miconazole and other antifungal agents. Watanabe [130] reviewed the treatment of systemic mycoses in humans with miconazole and other antifungal drugs. Watanabe [131] reviewed the *in vivo* and *in vitro* actins of miconazole and other antifungal agents. Benson and Nahata [132] discussed the chemistry, pharmacology, pharmacokinetics, clinical uses, adverse effects, and drug interactions of miconazole and three other antifungal drugs. McGeary [133] presented a review on miconazole and drugs that are currently available for use against systemic fungal infections.

ACKNOWLEDGEMENT

The author wishes to thank Mr Tanvir A. Butt, Pharmaceutical Chemistry Department, College of Pharmacy, King Saud University for his secretarial assistance in preparing this profile.

REFERENCES

[1] S. Budavari (ed.), *The Merck Index*, 12th edn., Merck and Co, NJ, 1996, p. 894.
[2] A. C. Moffat (ed.), *Clarke's Isolation and Identification of Drugs*, 2nd edn., The Pharmaceutical Press, London, 1989, p. 784.
[3] Sean C. Sweetman (ed.), *Martindale, The Complete Drug Reference*, 32nd edn., Pharmaceutical Press, London, 2002, p. 384.
[4] Swiss Pharmaceutical Society (ed.), *Index Nominum 2000, International Drug Directory*, 17th edn., Medpharm. GmbH-Scientific Publishers, Stuttgart, 2000, p. 690.
[5] E. F. Godefori and J. Heeres, *German Patent 1,940,388* (1970).
[6] E. F. Godefori and J. Heeres, *U.S. Patent 3,717,655* (1973).
[7] E. F. Godefori, J. Heeres, J. van Cutsem and P. A. J. Janssen, *J. Med. Chem.*, 1969, **12**, 784.
[8] F. Molina Caprile, *Spanish Patent ES 510870 A1* (1983).
[9] B. Ye, K. Yu and Q. Huang, *Zhongguo Yiyao Gongye Zazhi*, 1990, **21**, 56.
[10] Y. W. Liao and H. X. Li, *Yaoxue Xuebao*, 1993, **28**, 22.
[11] E. C. Yanez, A. C. Sanchez, J. M. S. Becerra, J. M. Muchowski and C. R. Almanza, *Revista de la Sociedad Quimica de Mexico*, 2004, **48**, 49.
[12] *The British Pharmacopoeia 1998*, Her Majesty's Stationary Office, London, British Pharmacopoeia CD-ROM, Vol.1, 2000.
[13] *United States Pharmacopoeia*, United States Pharmaceutical Convention, Inc., Rockville, MD, 2003, p. 1112.
[14] M. Massaccesi, *Analyst*, 1986, **111**, 987.
[15] L. Szabolcs, *Acta Pharmaceutica Hungarica*, 1976, **46**, 43.
[16] N. Mapsi, C. J. De Ranter and W. Jottier, *J. Pharm. Belg.*, 1987, **42**, 29.
[17] M. Shamsipur and F. Jalali, *Chemia Analityczna*, 2002, **47**, 905.
[18] D. Bonazzi, V. Cavrini, R. Gatti, E. Boselli and M. Caboni, *J. Pharm. Biomed. Anal.*, 1998, **18**, 235.
[19] N. G. Goger and L. Gokcen, *Anal. Lett.*, 1999, **32**, 2595.
[20] N. Erk, *STP-Pharma Sci.*, 1996, **6**, 312.
[21] S. R. El-Shabouri, K. M. Emara, P. Y. Khashaba and A. M. Mohamed, *Anal. Lett.*, 1998, **31**, 1367.
[22] B. Chen, *Zhongguo Yiyao Gongye Zazhi*, 1993, **24**, 318.
[23] S. Liu, Y. Cui and X. Tan, *Zhongguo Yiyuan Yaoxue Zazhi*, 1993, **13**, 458.
[24] N. Erk and M. L. Altun, *J. Pharm. Biomed. Anal.*, 2001, **25**, 115.
[25] Y. He, Y. Ju and Z. Li, *Zhonggue Yaoxue Zazhi*, 1994, **29**, 488.
[26] I. I. Hewala, A. M. Wahbi, E. H. Hassan and Y. H. Hussein, *Alexandria J. Pharm. Sci.*, 1996, **10**, 59.
[27] S. R. El-Shabouri, K. M. Emara, P. Y. Khashaba and A. M. Mohamed, *Bollettino Chimico Farmaceutico*, 1998, **137**, 103.
[28] E. A. Korany, M. A. Korany, M. A. Bedair and I. I. Hewala, *Anal. Lett.*, 1998, **31**, 1387.
[29] K. Wrobel, K. Wrobel, I. M. De La Garza Rodriguez, P. L. Lopez De Alba and L. Lopez Martinez, *J. Pharm. Biomed. Anal.*, 1999, **20**, 99.
[30] D. Xue, Y. Xie and J. Zong, *Zhongguo Yiyuan Yaoxue Zazhi*, 2002, **22**, 463.
[31] K. M. Thomas, D. A. Dabholkar and C. L. Jain, *Indian J. Hosp. Pharm.*, 1993, **30**, 153.
[32] V. Cavrini, A. M. Di Pietra and M. A. Raggi, *Pharm. Acta Helv.*, 1981, **56**, 163.
[33] J. Lemli and I. Knockaert, *Pharm. Weekblad*, 1983, **5**, 142.
[34] P. Y. Khashaba, S. R. El-Shabouri, K. M. Emara and A. M. Mohamed, *J. Pharm. Biomed. Anal.*, 2000, **22**, 363.
[35] I. Weuts, D. Kempen, K. Six, J. Peeters, G. Verreck, M. Brewster and G. Van den Mooter, *Belg. Int. J. Pharm.*, 2003, **259**, 17.
[36] F. C. Pereira, N. R. Stradiotto and M. V. B. Zanoni, *Anais da Academia Brasileira de Ciencias*, 2002, **74**, 425.
[37] G. J. Willems, I. W. Jottier and C. J. De Ranter, *Analusis*, 1981, **9**, 327.
[38] R. Arndt and J. Ahlers, *Chem. Biol. Interact.*, 1984, **50**, 213.
[39] E. G. Salole and A. Pearson, *Acta Pharmaceutica Nordica*, 1991, **3**, 183.
[40] A. H. Stead, *Analyst*, 1982, **107**, 1106.
[41] U. Roychowdhury and S. K. Das, *J. AOAC Int.*, 1996, **79**, 656.
[42] G. Indrayanto, S. Widjaja and S. Sutiono, *J. Liq. Chromatogr. Relat. Technol.*, 1999, **22**, 143.

[43] G. Musumarra, G. Scarlata, G. Cirma, G. Romano, S. Palazzo, S. Clementi and G. Giulietti, *J. Chromatogr.*, 1985, **350**, 151.
[44] G. Musumarra, G. Scarlata, G. Romano G. Cappello, S. Clementi and G. Giulietti, *J. Anal. Toxicol.*, 1987, **11**, 154.
[45] F. J. Van de Vaart, A. Hulshoff and A. M. W. Indemans, *Pharm. Weekblad*, 1983, **5**, 113.
[46] Z. Qian, W. Yan, Y. He and G. Lu, *Zhongguo Yiyuan Yaoxue Zazhi*, 1991, **11**, 435.
[47] M. Aleksic, S. Eric, D. Agbaba, J. Odovic, D. Milojkovic-Opesnica and Z. Tesic, *J. Planar Chromatogr. Modern TLC*, 2002, **15**, 414.
[48] R. E. Ardry and A. C. Moffat, *J. Chromatogr.*, 1981, **220**, 195.
[49] P. T. Mannisto, R. Mantyla, S. Nykanen, U. Lamminsivo and P. Ottoila, *Antimicrob. Agents Chemother.*, 1982, **21**, 730.
[50] S. C. Szathmary and I. Luhmann, *J. Chromatogr. Biomed. Appl.*, 1988, **69**, 193.
[51] J. J. W. Ros and Y. G. Van der Meer, *Pharm. Weekblad*, 1990, **125**, 70.
[52] E. Kublin and T. Kaniewska, *Chemia Analityczna*, 1996, **41**, 19.
[53] Q. Guo, A. Zhang, L. Zhang, Y. Yang and B. Li, *Zhongguo Yiyaho Gongye Zazhi*, 1997, **28**, 454.
[54] G. P. Neill, N. W. Davies and S. McLean, *J. Chromatogr.*, 1991, **565**, 207.
[55] S. M. Wallace, V. P. Shah, S. Riegelman and W. L. Epstein, *Anal. Lett.*, 1978, **B11**, 461.
[56] A. Turner and D. W. Warnock, *J. Chromatogr. Biomed. Appl.*, 1982, **227**, 229.
[57] V. Cavrini, A. M. Di Pretra and A. M. Raggi, *Int. J. Pharm.*, 1982, **10**, 119.
[58] L. A. Sternson, T. F. Patton and T. B. King, *J. Chromatogr.*, 1982, **227**, 223.
[59] X. Fan, *Fenxi Ceshi Tongbao*, 1986, **5**, 20.
[60] K. Sellinger, D. Matheou and H. M. Hill, *J. Chromatogr.*, 1988, **434**, 259.
[61] A. M. Di Pietra, V. Cavrini, V. Andrisano and R. Gatti, *J. Pharm. Biomed. Anal.*, 1992, **10**, 873.
[62] F. Alhaique, C. Anchisi, A. M. Fadda, A. M. Maccioni and V. Travagli, *Acta Technologiae et Legis Medicamenti*, 1993, **4**, 169.
[64] B. Chankvetadze, L. Chankvetadze, Sh. Sidamonidze, E. Yashima and Y. Okamoto, *J. Pharm. Biomed. Anal.*, 1996, **14**, 1295.
[65] T. K. Ng, R. C. Chan, F. A. Adeyemi-Doro, S. W. Cheung and A. F. Cheng, *J. Antimicrob. Chemother.*, 1996, **37**, 465.
[66] Y. Yuan, J. Yuan, Q. Shu and A. Yan, *Zhonggou Yiyuan Yaoxue Zazhi*, 1997, **17**, 503.
[67] P. Puranajoti, R. Kasina and S. Tenjarla, *J. Clin. Pharm. Ther.*, 1999, **24**, 445.
[68] T. I. Tyler and J. A. Genzale, *J. Assoc. Off. Anal. Chem.*, 1989, **72**, 442.
[69] Y. C. Guillaume, F. Darrouzain, L. Hoang-Opperman, J. Millet and C. Guinchard, *J. Chrmatogr. Biomed. Appl.*, 2000, **749**, 225.
[70] Y. C. Guillaume, E. Peyrin, A. Ravel, A. Villet, C. Grosset and J. Millet, *Talanta*, 2000, **52**, 233.
[71] C. Akay, S. A. Ozkan, Z. Senturk and S. Cevheroglu, *Farmaco*, 2002, **57**, 953.
[72] L. Gagliardi, D. De Orsi, P. Chimenti, R. Porra and D. Tonelli, *Anal. Sci.*, 2003, **19**, 1195.
[73] R. L. H. Lee, *Aust. J. Hosp. Pharm.*, 1985, **15**, 233.
[74] S. E. Holmes and S. Aldous, *Am. J. Hosp. Pharm.*, 1991, **48**, 286.
[75] H. Zhang and S. Deng, *Zhongguo Kangshengsu Zazhi*, 1992, **17**, 236.
[76] Y. Hasegawa, T. Noro, M. Misuno, E. Kondo, M. Hattori, Y. Nakahara, K. Tsushita, M. Utsumi and M. Tanaka, *Byoin Yakugaku*, 1995, **21**, 365.
[77] M. El-Abbes Faouzi, T. Dine, M. Luyckx, C. Brunet, M. L. Mallevais, F. Goudaliez, B. Gressier, M. Cazin, J. Kablan and J. C. Cazin, *J. Pharm. Biomed. Anal.*, 1995, **13**, 1363.
[78] H. Y. Aboul-Enein and I. Ali, *Fresenius' J. Anal. Chem.*, 2001, **370**, 951.
[79] H. Y. Aboul-Enein and I. Ali, *J. Pharm. Biomed. Anal.*, 2002, **27**, 441.
[80] I. Ali and H. Y. Aboul-Enein, *Biomed. Chromatogr.*, 2003, **113**, 113.
[81] H. Y. Aboul-Enein and I. Ali, *Chromatographia*, 2001, **54**, 200.
[82] F. Pan, H. Liang, M. Hu and X. Chen, *Fenxi Kexue Xuebao*, 2004, **20**, 667.
[83] H. Hosotsubo, *Chromatographia*, 1988, **25**, 717.
[84] V. Cavrini, A. M. Di Pietra and R. Gatti, *J. Pharm. Biomed. Anal.*, 1989, **7**, 1535.
[85] S. Zhang, S. Luo, F. Zhang, H. Cai and W. Yin, *Yaowu Fenxi Zazhi*, 1993, **13**, 198.
[86] M. Kobylinska, K. Kobylinska and B. Sobik, *J. Chromatogr. Biomed. Appl.*, 1996, **685**, 191.
[87] A. M. Di Pietra, V. Andrisano, R. Gotti and V. Cavrini, *J. Pharm. Biomed. Anal.*, 1996, **14**, 1191.
[88] J. Han, H. J. Zeng and H. F. Tang, *Yaowu Fenxi Zazhi*, 1997, **17**, 9.
[89] N. Morin, Y. C. Guillaume and J. C. Rouland, *Chromatographia*, 1998, **48**, 388.

[90] E. Peyrin and Y. C. Guillaume, *Chromatographia*, 1999, **49**, 691.
[91] L. H. Fei and X. C. Nie, *Yaowu Fenxi Zazhi*, 1999, **19**, 165.
[92] F. Zhang and M. Nunes, *J. Pharm. Sci.*, 2004, **93**, 300.
[93] A. van-Eeckhaut, S. Boonkerd, M. R. Detaevernier and Y. Michotte, *J. Chromatogr.*, 2000, **903**, 245.
[94] Y. C Guillaume and E. Peyrin, *Talanta*, 1999, **50**, 533.
[95] X. Lin, W. Hou and C. Zhu, *Anal. Sci.*, 2003, **19**, 1509.
[96] J. G. Grendahl and J. P. Sung, *Antimicrob. Agents Chemother.*, 1978, **14**, 509.
[97] A. Espinel-Ingroff, S. Shadomy and J. F. Fisher, *Antimicrob. Agents Chemother.*, 1977, **11**, 365.
[98] A. Egawa, H. Yamaguchi and K. Itawa, *Shinkin Shinkinsho*, 1981, **22**, 251.
[99] K. B. Temeyer, *Southwestern Entomologist*, 1998, **23**, 237.
[100] B. Marciniec, M. Kozak and K. Dettlaff, *J. Therm. Anal. Calorim.*, 2004, **77**, 305.
[101] M. Nishikawa and K. Fujii, *Chem. Pharm. Bull.*, 1991, **39**, 2408.
[102] C. S. Foster and M. Stefanyszyn, *Arch. Ophthalmol.*, 1979, **97**, 1703.
[103] A. Egawa, H. Yamaguchi and K. Itawa, *Shinkin Shinkinsho*, 1981, **22**, 258.
[104] T. K. Daneshmend, *J. Antimicrob. Chemother.*, 1988, **18**, 507.
[105] L. K. Pershing, J. Corlett and C. Jorgensen, *Antimicrob. Agents Chemother.*, 1994, **38**, 90.
[106] A. Garbe, K. Rogalla, H. P. Faro and R. Kunert, *Arzneimittel Forschung*, 1994, **44**, 1271.
[107] H. Mikamo, K. Kawazoe, Y. Sato, K. Ito and T. Tamaya, *Int. J. Antimicrob. Agents*, 1997, **9**, 207.
[108] G. Piel, T. Van Hees, B. Evrard and L. Delattre, *Proceedings of the 9th International Symposium on Cyclodextrins*, Santiago de Comostela, Spain, 1999, p. 215.
[109] G. Piel, B. Evrard, T. Van Hees and L. Delattre, *Int. J. Pharm.*, 1999, **180**, 41.
[110] J. M. Cardot, C. Chaumont, C. Dubray, D. Costantini and J. M. Aiache, *Br. J. Clin. Pharmacol.*, 2004, **58**, 345.
[111] N. Ohzawa, M. Imai, K. Nagasawa, H. Tanaka, H. Nakajima, Y. Nakai and T. Ogihara, *Iyakuhin Kenyu*, 1993, **24**, 173.
[112] N. Ohzawa, T. Tsuchiya, N. Sato, M. Imai, S. Egawa, T. Ogihara, H. Tanaka and K. Ida, *Iyakuhin Kenkyu*, 1993, **24**, 151.
[113] N. Ohzawa, H. Nakajima, Y. Nakai, H. Tanaka and T. Ogihara, *Iyakuhin Kenkyu*, 1993, **24**, 433.
[114] N. Ohzawa, S. Egawa, T. Tsuchiya, T. Ogihara and K. Ida, *Iyakuhin Kenkyu*, 1993, **24**, 443.
[115] N. Ohzawa, T. Tsuchiya, S. Egawa, T. Ogihara, H. Tanaka and K. Ida, *Yakubutso DFai*, 1993, **8**, 323.
[116] G. Vlassis, N. P. Zissis, A. Kyrou and A. Papaloukas, *Acta Clinica Belgica*, 1977, **32**, 291.
[117] P. D. Hoeprich and A. C. Huston, *J. Infect. Dis.*, 1978, **137**, 87.
[118] R. Eloy, *Journal de Gynecologi, Obstetrique et biologie de la reproduction*, 1972, **1**, 372.
[119] G. Hildick-Smith, *Adv. Biol. Skin*, 1972, **12**, 303.
[120] P. R. Sawyer, R. N. Bogden, R. M. Pinder, T. M. Speight and G. S. Avery, *Drugs*, 1975, **9**, 406.
[121] D. A. Stevens, H. B. Levine and S. C. Deresinski, *Am. J. Med.*, 1976, **60**, 191.
[122] C. Ito, S. Tsukuda, J. Ishiguro, K. Yamaguchi, K. Naguchi and H. Ohnishi, *Iyakuhin Kenkyu*, 1976, **7**, 340.
[123] W. Raab, *Curr. Therapeutic Res.*, 1977, **22**, 65.
[124] P. Y. Cartwright, *Mykosen, Suppl.*, 1978, **1**(Mid Micol), 298.
[125] R. Fukushiro, *Farumashia*, 1979, **15**, 491.
[126] P. A. J. Janssen and W. F. M. Van Bever, *Pharmacol. Biochem. Properties Drug Substances*, 1979, **2**, 333.
[127] R. C. Heel, N. R. Brogden, G. E. Pakes, T. M. Speight and G. S. Avery, *Drugs*, 1980, **19**, 7.
[128] M. H. Stranz, *Drug Intelligence Clin. Pharmacy*, 1980, **14**, 86.
[129] X. Zhang, *Yaoxue Tongbao*, 1985, **20**, 167.
[130] K. Watanabe, *Shinkin Shinkinsho*, 1985, **26**, 159.
[131] K. Watanabe, *Sogo, Rinsho*, 1988, **37**, 2242.
[132] J. M. Benson and M. C. Nahata, *Clin. Pharmacy*, 1988, **7**, 424.
[133] R. P. McGeary, *Pathomechanisms. New Trends Drug Res.*, 2003, 281.

FURTHER READING

[63] M. Kobylinska, K. Kobylinska and B. Sobik, *World Meeting on Pharmaceutics, Biopharmaceutics and Pharmaceutical Technology,* 1st Budapest, May 9–11, 1995, p. 921.

Niclosamide: Comprehensive Profile

Badraddin M. H. Al-Hadiya

Department of Clinical Pharmacy, College of Pharmacy, King Saud University, P.O. Box 2457 Riyadh 11451, Kingdom of Saudi Arabia

Contents

PROFILES OF DRUG SUBSTANCES, EXCIPIENTS, AND RELATED METHODOLOGY, VOLUME 32
ISSN: 0099-5428

DOI: 10.1016/S0099-5428(05)32002-8

1. DESCRIPTION

1.1. Nomenclature [1]

1.1.1. Systematic chemical names [1–5]

2-Chloro-4-nitrophenylamide-6-chlorosalicylic acid.
2′,5-Dichloro-4′-nitrosalicylanilide.
2-Hydroxy-5-chloro-*N*-(2-chloro-4-nitrophenyl) benzamide.
5-Chloro-*N*-(2′-chloro-4′-nitrophenyl)-2-hydroxybenzamide.
5-Chloro-2′-chloro-4′-nitrosalicylanilide.
5-Chloro-*N*-(2′-chloro-4′-nitrophenyl) salicylamide.
N-(2-chloro-4-nitrophenyl)-5-chlorosalicylamide.
5-Chlorosalicyloyl-(*o*-chloro-*p*-nitranilide).
N-(2′-chloro 4′-nitrophenyl)-5-chlorosalicylamide.
Benzamide, 5-chloro-*N*-(2-chloro-4-nitrophenyl)-2-hydroxy.

1.1.2. Nonproprietary names

Generic: Niclosamide BAN, USAN, INN [3], DCF [5].

Synonyms: Bay-2353; Bayer 2353, Niclosamida Anidra; Niclosamidum Anhydricum; Phenasal; Bayluscide [1–4]. Niclosamidum; Niclosamid; Niclosamida;

Niclosamide anhydrous; Niclosmide, anhydre; Niclosamid, Wassefereies. HL 2447, NSC 178296, WR 46234 [5].

1.1.3. Proprietary names

Yomesan, Yomesane, Tredemine, Niclocide, Cestocid, Fenasal, Mansonil, Nasemo, Sulqui, Vermitid, Vermitin [1–3]. Anti-Tina, Defaten, Devermin, Kontal, Niclosan, Radeverm, Ruby, Teniarene, Taniaslop, Tenicure, Tenisid, Tenyagat, Tenylaizin. Cestocide, Devermine, Fedal-Telmin, Helmiantin, Lomesan, Linetex, Mato, Sagimid, Sulqui, Utosamide, Zestocarp [5].

1.2. Formulae [1–3]

1.2.1. Empirical formula, molecular weight, and CAS number

$C_{13}H_8Cl_2N_2O_4$	327.13	50-65-7

1.2.2. Structural formula

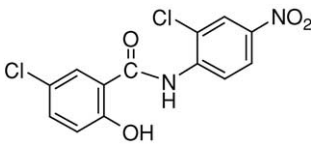

1.3. Elemental analysis

The theoretical elemental composition of niclosamide is as follows [2]:

Carbon: 47.73%
Hydrogen: 2.46%
Chlorine: 21.68%
Nitrogen: 8.57%
Oxygen: 19.56%

1.4. Appearance [1,6]

Pale yellow, yellowish-white to yellowish, fine crystals. Protect from light.

2. METHODS OF PREPARATION OF NICLOSAMIDE

Niclosamide was synthesized industrially by first chlorinating salicylic acid in chlorobenzene to yield 5-chlorosalicylic acid (I). Control of the amount of chlorine introduced is essential at this step, because an excess halogen leads to the formation of 3,5-dichlorosalicylic acid in addition to (I). When (I) is heated with 2-chloro-4-nitroaniline (II) in chlorobenzene (102−104°C) in the presence of phosphorus oxychloride, niclosamide (III) is obtained [7].

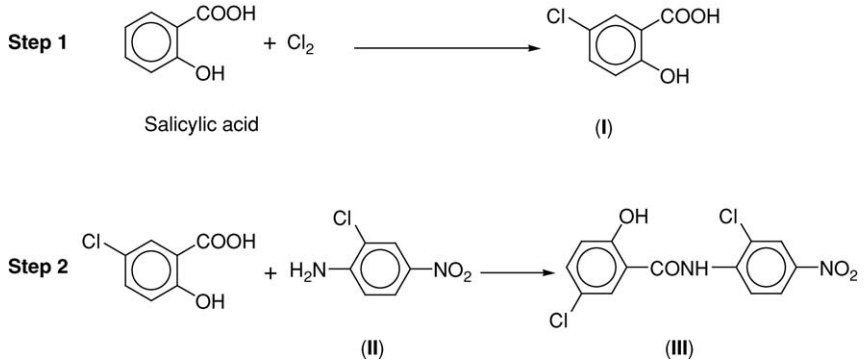

Another alternate synthetic method for the manufacturing of niclosamide is reported [1]. Phosphorus trichloride (PCl_3) is slowly introduced into a boiling xylene solution containing 5-chlorosalicylic acid and 2-chloro-4-nitroaniline in equimolar ratio and the heating continued for 3 h. Crystals of niclosamide separate on cooling and are recrystallized from ethanol [7,8].

van Tonder *et al.* [9] prepared and characterized three crystal forms of niclosamide namely the anhydrate and the two monohydrates.

3. PHYSICAL CHARACTERISTICS

3.1. Ionization constant

$pK_a = 7.45 \pm 0.43$ [17].

3.2. Solubility characteristics

Niclosamide is practically insoluble in water; soluble 1 in 150 of ethanol, 1 in 400 of chloroform, and 1 in 350 of ether; sparingly soluble in acetone [4].

3.3. Partition coefficient

Monkiedje *et al.* [10] investigated the fate of niclosamide in aquatic system both under laboratory and field conditions. The octanol/water partition coefficient (K_{ow}) of niclosamide was 5.880×10^{-4}. Adsorption isotherm studies indicated that the Freundlich parameters (K, n) for niclosamide were 0.02 and 4.93, respectively, for powder activated carbon (PAC), and 9.85×10^{-5} and 2.81, respectively, for silt loam soil. The adsorption coefficient (K_{oc}) for the drug was 0.02 for PAC, and 4.34×10^{-3} for the same soil. Hydrolysis of niclosamide occurred in distilled water buffer at pH above 7. No photolysis of the drug was observed in water after exposure to long-wave UV light for 4 h. Similarly, neither chemically volatilized from water following 5 h of sample aeration. Under field conditions, niclosamide persisted in ponds for over 14 days. The half-life of niclosamide was 3.40 days.

3.4. Particle morphology

Westesen and Siekmann [11] used suspensions of colloidal solid lipid particles as well as lyophilizates as delivery systems for the parenteral administration of the drug for its particle morphology determination.

3.5. Crystallographic properties

3.5.1. Single-crystal structure

Single-crystal X-ray structures of solvated forms of niclosamide revealed distinctly different modes of inclusion for different solvents. These modes were, respectively, cavity occupation by water molecules in 1:1 niclosamide:tetrahydrofuran, and intercalation by tetraethylene glycol molecules in 2:1 niclosamide:tetraethylene glycol. Crystallographic data and atmospheric coordinates were given. In all three compounds, the host drug molecule adopted the same, nearly planar conformation, which was maintained by an intramolecular N–H···O–H bond. Host–guest recognition invariably involved hydrogen bonding between the drug hydroxyl group and an O acceptor atom of the solvent molecule. The observed modes of solvent inclusion could be reconciled with the behavior of the crystals on heating [12].

3.5.2. X-ray powder diffraction pattern

The X-ray powder diffraction pattern of niclosamide has been measured using a Philips PW–1050 diffractometer, equipped with a single-channel analyzer and using a copper K_α radiation. The pattern obtained is shown in Fig. 1, and the data of scattering angle (degrees 2θ) and the relative intensities (I/I_{max}) are found in Table 1.

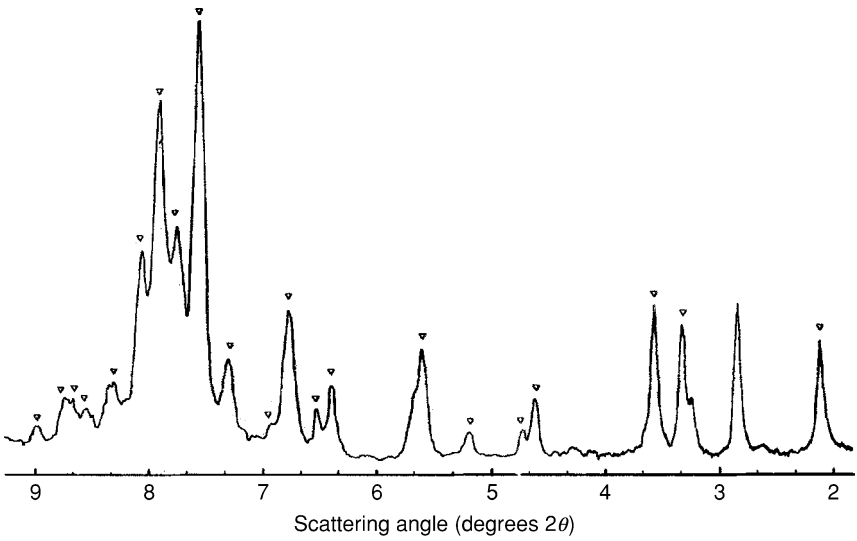

Fig. 1. X-ray powder diffraction pattern of niclosamide.

Table 1. Scattering angles and relative intensities in the X-ray powder diffraction pattern of niclosamide

Scattering angle (degrees 2θ)	Relative intensity ($I/I_{max} \times 100$)	Scattering angle (degrees 2θ)	Relative intensity ($I/I_{max} \times 100$)
13.5	3	3.74	8
11.6	8	3.58	19
9.4	27	3.47	100
7.66	36	3.34	81
6.94	14	3.20	5
6.81	32	3.18	5
6.46	37	3.12	5
5.26	14	3.08	5
5.16	6	3.06	5
4.77	5	2.99	4
4.48	26	2.87	5
4.00	17	2.81	6
3.93	12	2.68	5
3.82	36	2.65	7

3.6. Hygroscopicity

The liquid composition of niclosamide and a nonaqueous liquid carrier in an encapsulating agent was investigated [13].

3.7. Thermal methods of analysis

3.7.1. Melting behavior

The melting range of niclosamide is between 227 and 232°C, determined after drying at 100–105°C for 4 h [6,14]. Singh [15] reported a melting point of 230°C for niclosamide.

3.7.2. Differential scanning calorimetry

The differential scanning calorimetry (DSC) thermogram of niclosamide was obtained using a General V4 IC DuPont 2100. The data points represented by the curve shown in Fig. 2 were collected from 200 to 400°C using a heating rate of 5°C/min. It was found that the compound melted at 231.66°C with an enthalpy of fusion equal to 69.31 J/g.

3.7.3. Thermogravimetric analysis

van Tonder *et al.* [16] investigated the moisture adsorption and desorption behavior of three prepared crystal forms of niclosamide. These prepared forms were characterized by DSC, thermogravimetric (TG) analysis, calorimetry, Karl–Fischer titration, and X-ray diffractometry.

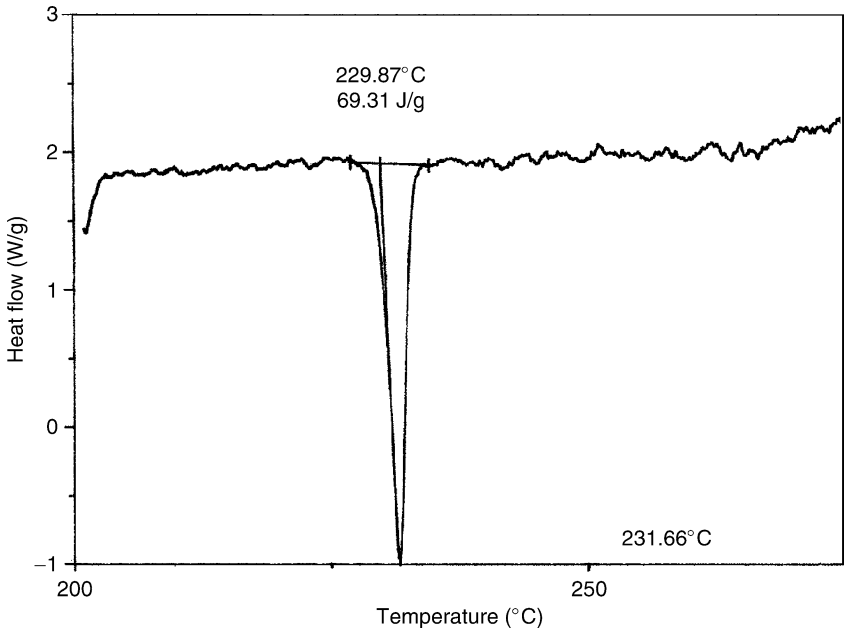

Fig. 2. Differential scanning calorimetry thermogram of niclosamide.

3.7.4. Boiling point, enthalpy of vapor, flash point, and vapor pressure

The calculated value of the boiling point of niclosamide under a pressure of 760 torr was 424.5 ± 45.0°C. The enthalpy of vapor calculated value was 70.52 ± 3.0 KJ/mol. The calculated value of flash point was found to be 210 ± 51.7°C; and the vapor pressure was calculated to be 8.35E−8 torr at 25°C [17].

Another reported study involved the preparation of four niclosamide solvates and the determination of the stability of the crystal forms in different suspension vehicles by DSC and TG analysis. Thermal analysis showed that the niclosamide solvates were extremely unstable in a PVP-vehicle and rapidly changed to monohydrated crystals. A suspension in propylene glycol was more stable and TG analysis showed that crystal transformation was less rapid [18].

3.8. Spectroscopy

3.8.1. UV–Vis spectroscopy

The UV absorption spectra of niclosamide in methanol, methanolic 0.1 N HCl and methanolic 0.1 N NaOH are shown in Fig. 3. The figures were recorded using a Perkin-Elmer double beam model 550s UV–Vis spectrophotometer. The values of the log ε_{max} (log molar extinction coefficient) at their corresponding wavelength maximum in nanometers (λ_{max}) are shown in the following table.

Solvent system	λ_{max} (nm)	log ε_{max}
Methanol	212	4.57
	234	4.47
	333	4.28
	377 inflection	4.19
Methanolic N/10 hydrochloric acid	209	4.55
	333	4.32
Methanolic N/10 sodium hydroxide	217	4.58
	234	4.58
	332	4.32
	377 inflection	4.32

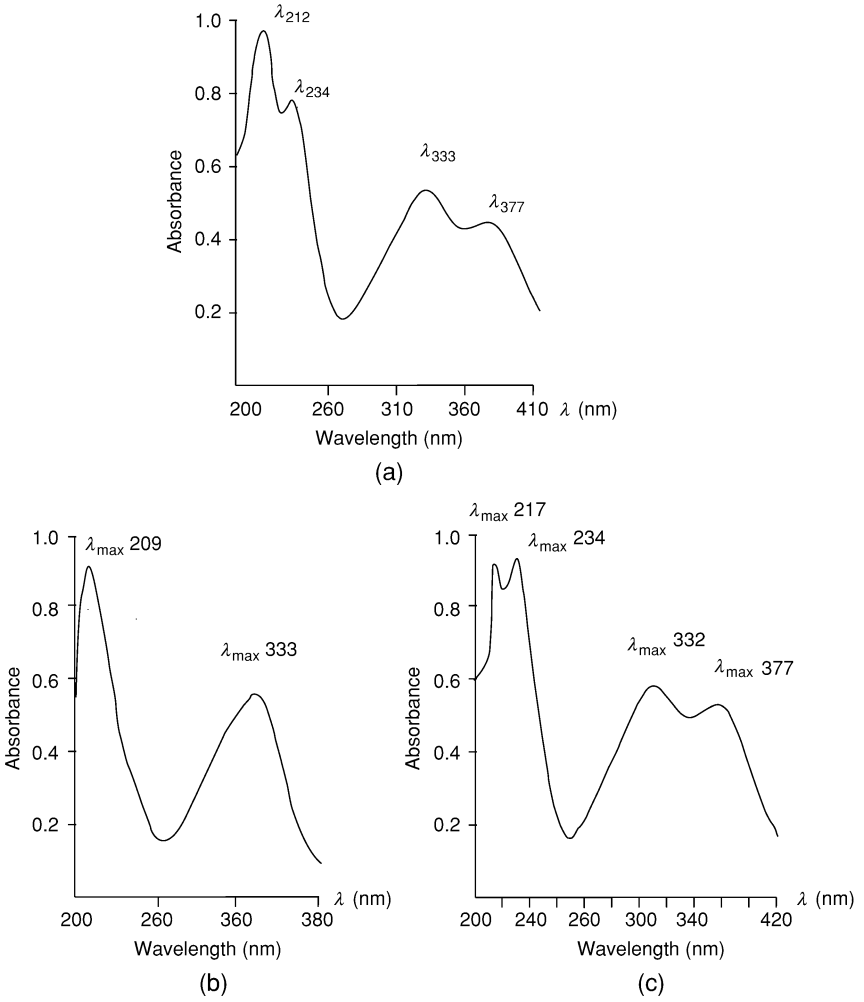

Fig. 3. Ultraviolet absorption spectrum of niclosamide dissolved in methanol (a), methanolic 0.1 M HCl (b) and methanolic 0.1 M NaOH (c).

The spectra of niclosamide in methanol (Fig. 3a) and methanolic base (Fig. 3c), show four bands with the same λ_{max} values but ε_{max} values increase in base. In methanolic acid (Fig. 3b) only two bands appeared [19]. This could be explained in terms of resonance effects as well as the dissociation of the phenolic-OH group to phenolate in base [20,21]. The possible resonance structures of niclosamide are shown below:

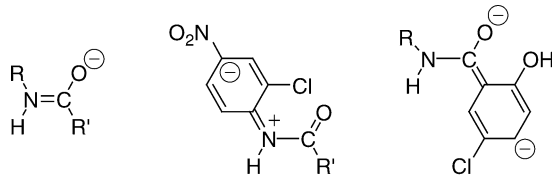

where R = $ClC_6H_3NO_2$ and R′ = ClC_6H_3OH.

The possibility of keto-enol tautomerism exists. In basic medium, the enolic form is favored. Furthermore, the presence of the CONH group in the *trans* form could be proved from the ultraviolet absorption spectrum of niclosamide in methanol.

3.8.2. *Vibrational spectroscopy*

The infrared absorption spectrum of niclosamide is shown in Fig. 4. It was obtained in a KBr disc using a Unicam SP200 infrared spectrophotometer. The principal peaks were noted at 1210, 1340, 1410, 1530, 1565, 1645, 3030, and 3270 cm^{-1}.

The broadband at 3270 cm^{-1} is due to the O–H stretching vibration of the hydroxyl group. Moreover, the N–H stretching vibration absorption for open-chain amides occurs near 3270 cm^{-1} in the niclosamide solid state.

The bands at 1410 and 1210 cm^{-1} are due to combined C–O stretching vibration and O–H in-plane deformation of hydroxyl group of niclosamide [22].

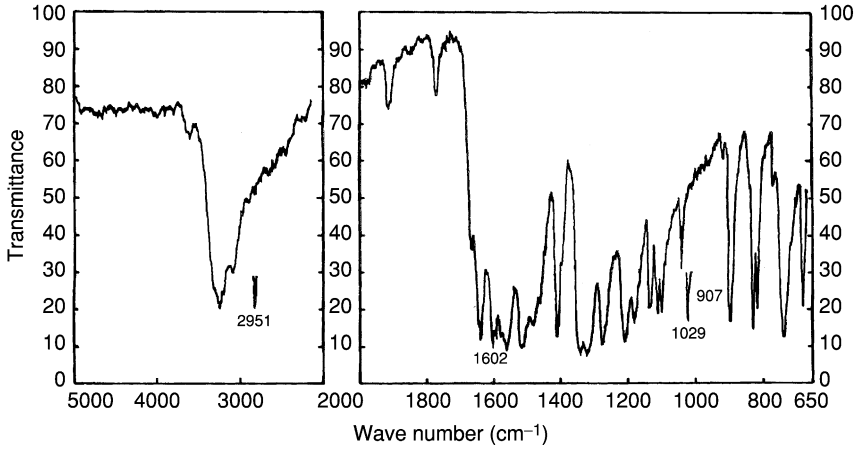

Fig. 4. Infrared absorption spectrum of niclosamide.

As niclosamide possesses the group Ph–NHCO–Ph, it shows a C=O stretching vibration (amide I band) at 1645 cm^{-1} and amide II band at 1565 cm^{-1} due to combined NH deformation and C–N stretching vibrations [22–25]. Due to presence of aromatic-type structure, niclosamide showed characteristic group frequencies for benzene derivatives. Of these, the most definite is the presence of the =C−H stretching vibration near 3030 cm^{-1} and the ring breathing vibrations in the 1600–1500 cm^{-1} region. The presence of substituents on the aromatic rings gave rise to bands in the regions 2000–1660 cm^{-1} (showing three bands characteristic of tri-substituted compounds [26]), 1600–1450 cm^{-1} (showing the splitting of the 1500 cm^{-1} band to produce that at 1480 cm^{-1}, which is the case in halogenated benzenes), 1250–1000 cm^{-1} (due to the C–H in-plane deformation mode) and 950–650 cm^{-1} (due to the out-of-plane deformation vibrations) [19].

Niclosamide shows two strong absorption bands at 1530 cm^{-1} and 1340 cm^{-1} corresponding to the asymmetric and symmetric N=O stretching vibrations [14].

3.8.3. Nuclear magnetic resonance spectrometry (NMR)

The ^{1}H NMR and the ^{13}C NMR spectra of niclosamide were obtained using a Bruker Instruments system operating at 300, 400, or 500 MHz (proton NMR), or at 75, 100, or 125 MHz (carbon NMR). Standard Bruker software was used to obtain DEPT, COSY, and BETCOR spectra. All measurements were obtained with the compound being dissolved in deuterated dimethyl sulfoxide (DMSO-d_6).

3.8.3.1. ^{1}H NMR spectrum

The full ^{1}H NMR spectrum of niclosamide is shown in Fig. 5, with various regions being expanded in Fig. 6 for easier viewing. Assignments for the resonance bands are given in Table 2. Due to difficulty in solubility of the compound, the spectrum was run at high temperature (100°C). This probably influenced the resonance of the amide proton (h, Table 2), which is so broad that it barely changed the baseline. The chemical shift of the hydroxyl proton (g, Table 2) is highly dependent upon temperature and as the spectrum was run at 100°C, the resonance of (g) might occur almost anywhere over the usual 1000 Hz range (~11.4 ppm).

3.8.3.2. ^{13}C NMR spectrum

The ^{13}C NMR spectrum of niclosamide is shown in Fig. 7 (Full ^{13}C NMR spectrum) and Fig. 8 (expanded ^{13}C NMR spectrum). The assignments for the observed bands are provided in Table 3, which are consistent with the 13 carbon contents of niclosamide.

3.9. Mass spectrometry

The mass spectrum of niclosamide was obtained utilizing an AEI single focusing mass spectrometer model MS12 with VG micromass 2S8, using an ion source temperature of 100–300°C, an electron energy of 70 eV, and with a trap current of 100 μA.

Figure 9 shows the detected mass fragmentation pattern of niclosamide. The major peaks in the spectrum occur at *m/z* 326, 291, 172, 156, 155, 154, 144, 142,

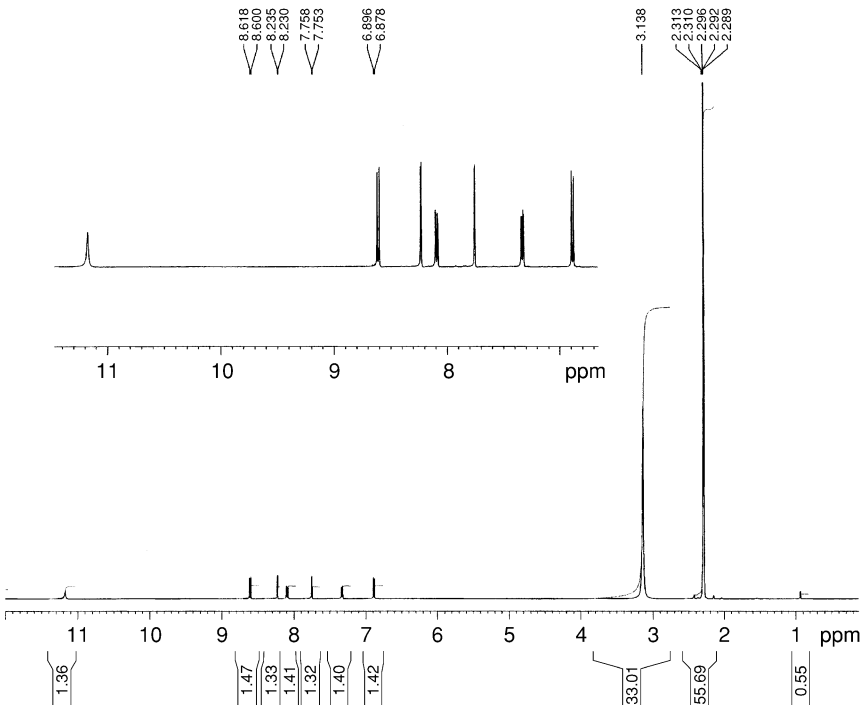

Fig. 5. Full ^{1}H NMR spectrum of niclosamide.

127, 99, and 63. The base peak appeared at *m/z* 155, along with a molecular ion peak at *m/z* 326. The mass fragmentation pattern of the compound is detailed in Table 4. The most abundant ion (the base-peak) at *m/z* 155 is due to the benzoyl cation resulting from expulsion of an amine radical; further decomposition (to *m/z* 127 then *m/z* 99) involves ejection of carbon monoxide [27–29].

4. METHODS OF ANALYSIS

4.1. British pharmacopoeia compendial methods [6]

4.1.1. Identification [6]

Test 1. To 50 mg of niclosamide add 5 mL of 1 M hydrochloric acid and 0.1 g of zinc powder, heat in a water-bath for 10 min, cool and filter. To the filtrate add 1 mL of a 5 g/L solution of sodium nitrite and allow to stand for 3 min, add 2 mL of a 20 g/L solution of ammonium sulfamate, shake, allow to stand for 3 min and add 2 mL of a 5 g/L solution of naphthylethylenediamine dihydrochloride. A violet color is produced [6].

Test 2. Heat niclosamide on a copper wire in a nonluminous flame. The flame becomes green [6].

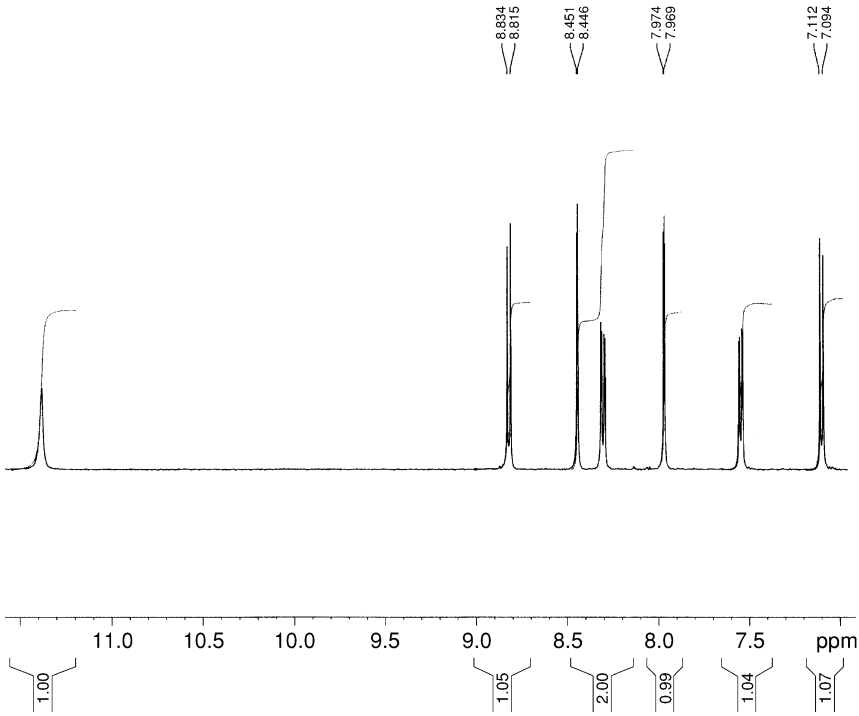

Fig. 6. Expanded ^{1}H NMR spectrum of niclosamide. NMR spectrum of niclosamide.

Table 2. Assignments for the resonance bands observed in the ^{1}H NMR spectrum of niclosamide

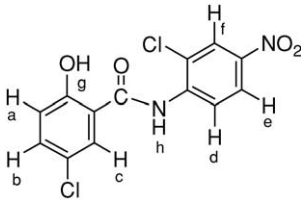

Chemical shift (ppm)	Number of protons	Multiplicity and coupling constant (J)	Assignment
7.10	1	Doublet (8.7 Hz)	Ha
7.55	1	Doublet of doublets (8.7 and 2.7 Hz)	Hb
7.97	1	Doublet (2.7 Hz)	Hc
8.45	1	Doublet (8.7 Hz)	Hf
8.30	1	Doublet of doublets (8.7 and 2.7 Hz)	He
8.82	1	Doublet (8.7 Hz)	Hd

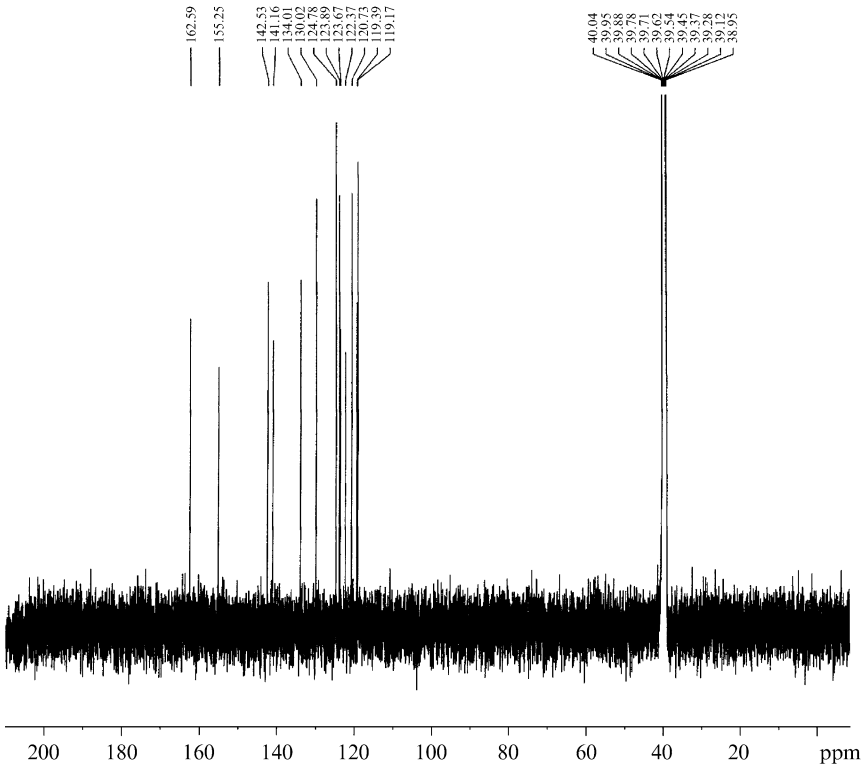

Fig. 7. Full ^{13}C NMR spectrum of niclosamide.

Test 3. Burn 20 mg of niclosamide by the oxygen flask method [6], using 5 mL of dilute sodium hydroxide solution as the absorbing liquid. The resulting solution gives a white precipitate with silver nitrate solution, which is insoluble in dilute nitric acid but soluble in dilute ammonia solution.

4.1.2. Impurity analysis [6]

4.1.2.1. 2-Chloro-4-nitroaniline

To 0.25 g of niclosamide add 5 mL of methanol, heat to boiling, cool, add 45 mL of 1 M HCl, heat again to boiling, cool, filter, and dilute the filtrate to 50 mL with 1 M HCl. To 10 mL of the solution add 0.5 mL of a 5 g/L solution of sodium nitrite and allow to stand for 3 min. Add 1 mL of a 20 g/L solution of ammonium sulfamate, shake, allow to stand for 3 min and add 1 mL of a 5 g/L solution of naphthylethylenediamine dihydrochloride. Any pinkish-violet color produced in the test solution is not more intense than that in a reference solution (100 ppm) [6].

4.1.2.2. 5-Chlorosalicylic acid

To 1.0 g of niclosamide add 15 mL of water, boil for 2 min, cool, filter through a membrane filter (nominal pore size: 0.45 μm), wash the filter and dilute the combined filtrate and washings to 20 mL with water. To 10 mL of this solution, add

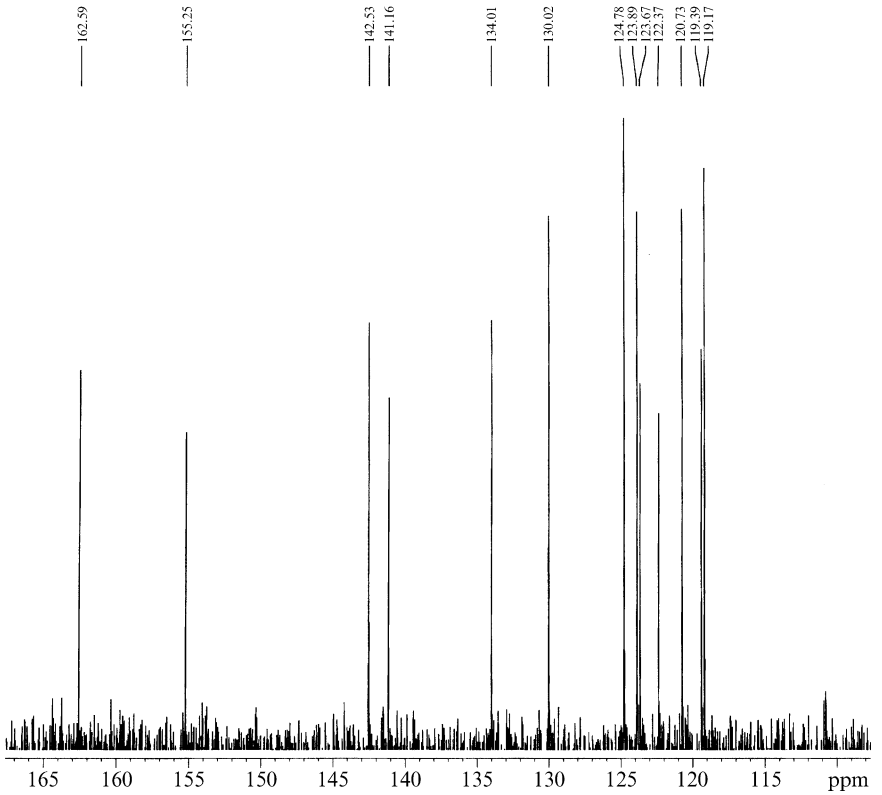

Fig. 8. Expanded ^{13}C NMR spectrum of niclosamide.

Table 3. Assignments for the resonance bands observed in the ^{13}C NMR spectrum of niclosamide

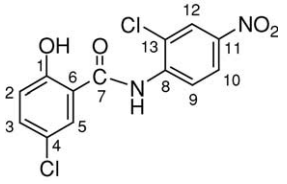

Chemical shift (ppm)	Assignment	Chemical shift (ppm)	Assignment
119.17	C2	130.02	C5
119.39	C6	134.01	C3
120.73	C9	141.16	C11
122.37	C10	142.53	C8
123.67	C12	155.24	C1
123.89	C13	162.59	C7
124.78	C4	–	–

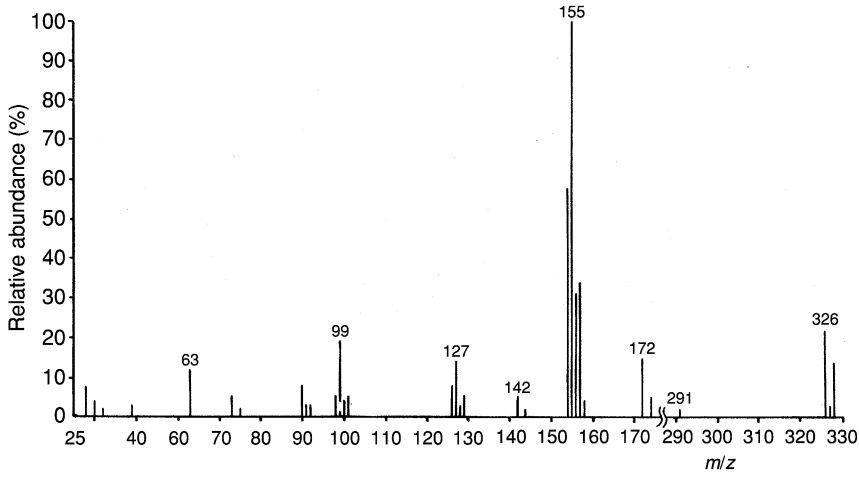

Fig. 9. Mass spectrum of niclosamide.

0.1 mL of ferric chloride solution. Any violet color produced in the test solution is not more intense than that in a reference solution (60 ppm) [6].

4.1.2.3. Chlorides

To 2 g of niclosamide add a mixture of 1.2 mL of acetic acid and 40 mL water, boil for 2 min, cool and filter. Two milliliters of the filtrate diluted to 15 mL with water complies with the limit test for chlorides (500 ppm) [6].

4.1.3. Other tests

4.1.3.1. Loss on drying [6]

Niclosamide loses 4.5–6.0% of its weight, determined on 1.0 g by drying in an oven at 100–105°C for 4 h.

4.1.3.2. Sulfated ash [6]

Not more than 0.1%, determined on 1.0 g.

4.1.4. Assay method [6]

Dissolve 0.30 g of niclosamide in 80 mL of a mixture of equal volumes of acetone and methanol. Titrate with 0.1 tetrabutylammonium hydroxide, determining the endpoint potentiometrically. One milliliter of 0.1 M tetrabutylammonim hydroxide is equivalent to 32.71 mg of $C_{13}H_8Cl_2N_2O_4$.

4.2. Titrimetric methods of analysis

4.2.1. Aqueous and potentiometric titration methods

Nickel and Weber [30] reported aqueous titrations of carboxylic acids, phenols, acidic drugs containing NH groups, cationic acids (ammonium salts) in dimethylformamide solution against 0.1 M potassium hydroxide aqueous solution as the

Table 4. Mass fragmentation of niclosamide

m/z	Relative intensity (%)	Formula	Fragment
326	22.5	$C_{13}H_8Cl_2N_2O_4$	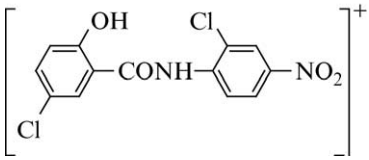
291	3	$C_{13}H_8ClN_2O_4$	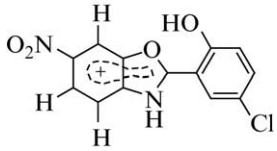
172	16	$C_6H_5ClN_2O_2$	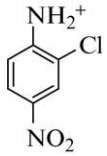
156	31	$C_7H_5ClO_2$	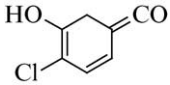
155	100	$C_7H_4ClO_2$	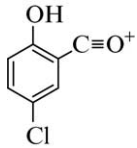
154	58	$C_7H_3ClO_2$	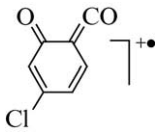
142	5	$C_5H_3ClNO_2$	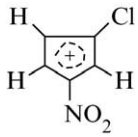
127	14	C_6H_4ClO	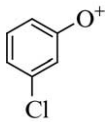
99	19.5	C_5H_4Cl	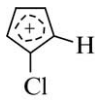
63	13	$C_5H_3^+$	

titrant. The potentiometric endpoint method was used because of its advantage in the determination of weak acids or bases. In addition, no indicator was required.

4.2.2. Nonaqueous titration methods

Twenty weakly acidic drugs, including niclosamide, were determined by a nonaqueous catalytic thermometric titration method. Catalysis of the anionic polymerization of acetonitrile was used for endpoint indication. The solvent used was a mixture of acetonitrile and dimethylformamide or pyridine, and the titrant was sodium methoxide, potassium hydroxide, tertiary butanol, or tertiary butanol–sodium nitrite. Recoveries, limits of detection and relative standard deviations were tabulated [31].

4.3. Electrochemical methods of analysis

4.3.1. Voltammetry

The electrochemical behavior of niclosamide was described on the basis of d.c. polarography, cyclic voltammetry, a.c. polarography, and differential pulse polarography, in the supported electrolytes of pH ranging from 2.0 to 12.0 [32]. A tentative mechanism for the reduction of niclosamide is proposed that involves the transfer of 4 e^-. Parameters such as diffusion coefficients and heterogeneous forward rate constant values were evaluated.

Cyclic voltammetry, square-wave voltammetry, and controlled potential electrolysis were used to study the electrochemical oxidation behavior of niclosamide at a glassy carbon electrode. The number of electrons transferred, the wave characteristics, the diffusion coefficient and reversibility of the reactions were investigated. Following optimization of voltammetric parameters, pH, and reproducibility, a linear calibration curve over the range 1×10^{-6} to 1×10^{-4} mol/dm^3 niclosamide was achieved. The detection limit was found to be 8×10^{-7} mol/dm^3. This voltammetric method was applied for the determination of niclosamide in tablets [33].

Detection of damage caused to DNA by niclosamide in schistosomiasis was investigated using an electrochemical DNA-biosensor. It showed for the first time clear evidence of interaction of niclosamide with DNA and suggested that niclosamide toxicity can be caused by this interaction, after reductive activation. The electrochemical reduction and oxidation of niclosamide involved the use of cyclic, differential, and square-wave voltammetry, at a glassy carbon electrode. It enabled the detection limit of 8×10^{-7} M [34].

Alemu *et al.* [35] developed a very sensitive and selective procedure for the determination of niclosamide based on square-wave voltammetry at a glassy carbon electrode. Cyclic voltammetry was used to investigate the electrochemical reduction of niclosamide at a glassy carbon electrode. Niclosamide was first irreversibly reduced from NO_2 to NHOH at -0.659 V in aqueous buffer solution of pH 8.5. Following optimization of the voltammetric parameters, pH and reproducibility, a linear calibration curve over the range 5×10^{-8} to 1×10^{-6} mol/dm^3 was achieved, with a detection limit of 2.05×10^{-8} mol/dm^3 niclosamide. The results of the analysis suggested that the proposed method has promise for the routine determination of niclosamide in the products examined [35].

4.3.2. Polarography

Mishra and Gode developed a direct current polarographic method for the quantitative determination of niclosamide in tablets using individually three different buffer systems, namely Mcllraine's buffers (pH 2.20−8.00), borate buffers (pH 7.80−10.00), and Britton–Robinson's buffers (pH 2.00−12.00) as well as 0.2 M sodium hydroxide. The drug was extracted from the sample with methanol, appropriate buffer was added to an aliquot and the solution then polarographed at the dropping-mercury electrode versus saturated calomel electrode at 25°C [36]. The resultant two-step reduction waves observed were irreversible and diffusion-controlled. For the quantitative determination, the method of standard addition was used. Niclosamide can be determined up to a level of 5−10 μg/mL.

Solomon and Zewde studied the polarographic behavior of niclosamide in ethanol media [37]. Niclosamide was determined qualitatively and quantitatively at 10^{-4} to 10^{-7} M in 0.1 M ammonium acetate in redistilled 95% ethanol. Direct current and differential pulse polarograms were taken at 23°C with a dropping mercury electrode of drop time 1 s, and a sweep rate of 8 mV/s, using an aqueous Ag/AgCl/Cl saturated reference electrode, and a Pt auxiliary electrode. Niclosamide in 95% ethanol gave 2 well-defined waves with half wave potential of E½ (1) = −0.4787 V and E½ (2) = −1.1138 V, respectively; these potentials were independent of niclosamide concentration. The d.c. polarogram showed a well-behaved curve only for the first wave, the second wave being ill-defined. The diffusion current (id) as measured using the differential polarographic technique for both first and second waves gave a linear id concentration curve of 10^{-4} to 10^{-7} M [37]. A differential pulse polarography method has been developed for the quantitative determination in different pharmaceutical formulations using method of standard addition [32].

Polarographic studies of a mitochondrial fraction from *Hymenolepis diminuta* showed that of four substrates tested, DL-glycerol–3-phosphate was the most rapidly oxidized, but the highest respiratory control ratio (1.7) was obtained with DL-isocitric acid. With isocitrate as substrate oxyclozanide at 1.61 nM stimulated O uptake and relieved oligomycin inhibition of adinosine diphosphate-stimulated respiration, but at concentrations above 2 μM progressively inhibited O uptake. Rafoxanide, niclosamide, 3,4,5-tribromo-salicylanilide, nitroxynil, resorantel, dichlorophen, and 2,4-dinitrophenol exhibited effects similar to those of oxyclozanide on the respiration in cestode mitochondria. The relative potencies were compared and the possible mode of action discussed [38].

Saber and Sidky [39] described polarographic estimations of Bayluscide (I) (niclosamide) or its ethanolamine salt (II). Solutions of I or II containing 80% by volume methanol (the rest was the buffer components in H_2O) yielded highly reproducible polarograms [39].

4.3.3. Coulometry

A variant of the Karl–Fischer water determination was described [40]. By heating the drug substance, the contained water was transferred into a titration cell by a carrier gas. The automated system consisted of an oven sample processor and a coulometer.

4.4. Spectroscopic methods of analysis

4.4.1. Spectrophotometry

Niclosamide was determined in bulk and pharmaceuticals by treatment with hydroquinone, β-naphthol, or resorcinol in an alkaline medium and measurement of absorbance at 380 nm [41].

Zarapkar *et al.* developed a spectrophotometric method for the determination of niclosamide by coupling with diazotized sulfamethoxyazole forming a pale yellow complex. The absorbance of the complex was measured at 380 nm to determine the drug [42].

Selective differential UV spectrophotometric method was presented for the determination of niclosamide in bulk and in its pharmaceuticals [43]. The method was based on measuring niclosamide in alkaline solutions against their neutral ethanolic solutions as blanks. The proposed method was sensitive, highly specific, and advantageous over the conventional UV assays, since the interference of the excipients, impurities, degradation products, or other accompanying drugs was nullified.

A simple spectrophotmetric method for the determination of niclosamide in bulk and dosage forms was developed [44]. It was based on the reduction of the nitro group in niclosamide to the amino group by treatment with zinc powder and dilute HCl for 15 min in 95% ethanol solution. The cold and clear filtrate reacted with *p*-benzoquinone, when a pink compound was obtained which absorbed at 506 nm.

Onur and Dinc [45] described four new spectrophotometric methods for simultaneous determination of niclosamide (I) and thiabendazole (II) in tablets and other binary mixture formulations. The method used picric acid for selective precipitation of (II) followed by determination of (I) by first-derivative spectrophotometry.

A UV spectrophotometric method for niclosamide determination in chewable tablets at 333 nm was described [46]. The excipients did not interfere in the determination.

A rapid second-derivative spectrophotometric assay procedure was described for the simultaneous determination of niclosamide and thiabendazole in tablets [47]. The derivative absorbances were measured at 354 nm for niclosamide and at 242.5 nm for thiabendazole.

Niclosamide and other some antiamebic and anthelmintic drugs were determined spectrophotometrically in pharmaceuticals based on the formation of colored species with *p-N,N*-dimethylphenylenediamine·2HCl and chloramines-T [48]. The method was simple, sensitive, and reproducible within 1%.

In another method, niclosamide was measured at 380 nm by coupling with diazotized sulfamethoxyazole in the presence of Me_3N to form a pale yellow complex [42].

Niclosamide was also determined in tablets by dissolution of the tablets in 0.1 N sodium hydroxide solution followed by measurement of the absorbance at 375 nm [49]. The methods also use 0.1 M sulfuric acid solution.

Niclosamide and its dosage forms were spectrophotometrically estimated by reaction with aqueous 4-aminophenazone in the presence of ammonia and measurement of absorbance of the resulting oxidative coupling product at 520 nm [50]. Beer's law was obeyed in the concentration range 1.25–10.0 μg/mL; the relative standard deviation was 1.51% and the recovery 98.9–99.6%. Dosage form excipients did not interfere.

Liu [51] developed a simple and rapid UV spectrophotometric method for determination of niclosamide. The drug, with or without purification by chromatography on a silica gel plate, was dissolved in anhydrous ethanol and the solution or standard was placed in a 1-cm quartz cell and analyzed at 335 nm by spectrophotometry.

Spectrophotometric determination of niclosamide and thiabendazole in their binary mixtures (e.g., tablets) was realized by precipitating thiabendazole with ammonium reineckate at pH 3.0 selectively and reading the absorbance of the solution of the precipitate in acetone at 525 nm for thiabendazole and by measuring the $dA/d\lambda$ values at 405.8 nm in the first-derivative spectra of the remaining solution for niclosamide [52].

Emara [53] developed a rapid, simple, accurate and reproducible method for the quantitative determination of niclosamide ethanolamine salt (NES), the most widely used molluscicide against snail vectors of schistosomiasis, in both distilled and natural canal waters. The biocide was extracted completely from water samples by passing through Sep-Pak C_{18} cartridge and eluting the cartridge with methanol. The eluate was then analyzed directly for NES by UV–Vis spectrophotometry at 330 nm [53].

A sensitive spectrophotometric method was reported for the determination of niclosamide and some other antiamebic and anthelmintic drugs either in pure form or in formulations. The method was based on reduction with Zn and HCl followed by reaction with metol and potassium dichromate at pH 3.0 to give a colored product having maximum absorbance at 530 nm for niclosamide [54].

A method was described for the determination of niclosamide in simulated gastric and intestinal media using spectrophotometry at 386 nm [55]. The method obeyed Lambert–Beer's law at 2–16 μg niclosamide/mL. Alkaline hydolysis of niclosamide gave two products, 5-chlorosalicylic acid and 2-chloro-4-nitroaniline. Niclosamide appeared to be stable in simulated gastric and intestinal media.

A spectrophotometric method for the quantitative determination of fenasal (niclosamide) in tablets was given [56]. The tablets were powdered and extracted with acetone at 35–45°C. The solution was treated with ethanolamine in ethanol (1:1) at pH $\leq$ 8.0; the absorbance was determined at 400 nm.

4.4.2. Colorimetry

Based on the formation of a yellow product of niclosamide in a 0.1 N NaOH medium, Kokovkin-Shcherbak and Tiraspol'skaya [57] improved the photometric determination of the drug using differential photocolorimetry. Three independent factors were taken into account: the comparative solution, the solution to be analyzed, and concentration of NaOH.

Johnson and Stephens [58] gave a historical perspective review of the use of colorimeters for conducting on-site toxicity tests and for measuring concentrations of lampricides, including niclosamide as the active ingredient of Bayluscide, in the sea lamprey control program during 1957–1999. After brief reliance on colorimetric and GC chromatography methods, high performance liquid chromatography (HPLC) is currently used for all Bayluscide analyses [58].

A modified method for determining Bayluscide in field trials was described by Strufe [59]. It involved the use of test kit containing safranin granulate and extracting with diethylcarbonate instead of ammonium acetate. The color reaction followed by a Zeiss-Ikon Polytest Colorimeter.

Three methods for quantitative analysis of niclosamide at concentrations of 0.5–2.0 ppm were given. For *in situ* analysis, safranine dye solution was added to the sample and the extraction solution added which formed the upper phase. The niclosamide content was determined by the color intensity of the upper phase. The colors were compared with blanks of known concentration. When an accurate determination was required, niclosamide was extracted from the water sample with amylacetate, a methanol solution of sodium hydroxide was added to the extraction, and the resulting yellow color was measured at 385 mμ in a spectrophotometer. Third method made use of a calibration curve [60].

4.4.3. Calorimetry

The preparation of four niclosamide solvates and the study of their physical transformation and stability of the crystal forms in different suspension vehicles by DSC and thermal gravimetry (TG) were reported [18]. Thermal analysis showed that the niclosamide solvates were extremely unstable in a propylvinylpropyline (PVP)-vehicle and rapidly changed to monohydrated crystals. A suspension in propylene glycol was more stable and TG analysis showed that crystal transformation was less rapid. In this vehicle, the crystals transformed to the anhydrate, rather than the monohydrate, since the vehicle was nonaqueous. The TEG-hemisolvate was the most stable in suspension and offered the possibility of complex exploitation [18].

In another study, the influence of moisture on the crystal forms of niclosamide obtained from acetone and ethyl acetate was reported [62]. Recrystallization of niclosamide was performed in the presence and absence of moisture. Two hydrates and their corresponding anhydrates were isolated. The hydrates obtained by the process of recrystallization from acetone (Form I) and that obtained from ethyl acetate (Form II) were classified based on differences in their dehydration profile, crystal structure, shape, and morphology. Crystals obtained in the absence of moisture were unstable, and when exposed to the laboratory atmosphere transformed to their corresponding hydrates. Differential scanning calorimetry thermograms indicate that Form I changes to an anhydrate at temperatures below 100°C, while Form II dehydrates in a stepwise manner above 140°C. This finding was further confirmed by TG analysis. Dehydration of Form II was accompanied by a loss of structural integrity, demonstrating that water molecules play an important role in maintaining its crystal structure. Form I, Form II, and the anhydrate of Form II showed no significant moisture sorption over the entire range of relative humidity. Although the anhydrate of Form I did not show any moisture uptake at low humidity, it was converted to the monohydrate at elevated humidity (>95%). All forms could be interconverted depending on the solvent and humidity conditions [62].

Application of DSC and HPLC to determine the effects of mixture composition and preparation during the evaluation of niclosamide-excipients compatibility showed that although some reactions occurred, niclosamide was compatible with a majority of common tablet excipients tested [63].

4.4.4. Photometry

The photometric determination of phenasal (niclosamide), based on the formation of a yellow product in a 0.1 N NaOH medium, was reported [57].

Khloshchanov [64] indicated by photometric analysis that the greatest concentration of phenasal was observed in cestodes of the lower third of the small intestine of sheep 4 h after oral administration of 0.2 g of the anthelmintic/kg. Increasing the dose of phenasal to 1 g/kg increased shedding of the cestodes.

4.5. Chromatographic methods of analysis

4.5.1. Electrophoresis

Kasianowicz *et al.* [65] described the determination of the transport of niclosamide protons across lipid bilayer membranes by equilibrium dialysis, electrophoretic mobility, membrane potential, membrane conductance, and spectrophotometric measurements.

4.5.2. Thin-layer chromatography

Heinisch *et al.* described methods for detecting drugs containing chlorine, bromine, or iodine that can be extracted from acidic solutions with ether, then identified with TLC using 12 solvent systems and silica gel F_{254} plates [66].

Thirteen new visualizing reagents have been used to detect niclosamide and 13 phenolic drugs following thin-layer chromatography on silica gel layers. Limits of detection, detectability index, and broadening index were determined for these drugs following use of these visualizing reagents. Aniline blue and brilliant green were the best and most universal visualizing reagents for the phenolic drugs investigated. Densitogram of selected phenolic drugs after spraying with aniline blue and brilliant green were presented [67].

The stability of niclosamide was studied in simulated gastric and intestinal juices, with and without enzymes, after incubation at 37°C. The remaining intact drug and its degradation products (2-chloro-4-nitroaniline and 5-chlorosalicylic acid) were extracted with chloroform/methanol (5:1) and determined by TLC and HPLC. The drug was stable in these media for at least 6 h [68].

Relative retention times for niclosamide and 570 drugs and related compounds on eight chromatographic systems were reported [69]. TLC employing silica gel plates, gas chromatography employing 3% OV–1 on Chromosorb W-HP, and reversed-phase high-pressure chromatography employing octadecylsilanized columns were described.

4.5.3. High performance liquid chromatography

An HPLC method was developed that confirmed the photodegradation of [^{14}C] niclosamide in sterile, pH 5, 7, and 9 buffered aqueous solutions under artificial sunlight at 25.0 ± 1.0°C [70]. These degradates were carbon dioxide and two- and four-carbon aliphatic acids formed by cleavage of both aromatic rings.

Another HPLC method was described in a series of experiments analyzing the kinetics and mechanisms of [^{14}C] niclosamide degradation in sediment and water systems [71].

A stability-indicating HPLC method has been described for niclosamide in artificial gastric and intestinal juices [68].

Comparative study of fluorescence CYPs assays of niclosamide with that obtained by conventional HPLC assay using human liver microsomes and recombinant CYPs was developed [72].

A simple, specific, and accurate reversed-phase HPLC method for the assay of niclosamide and several anthelmintics in veterinary products was reported [73]. The method afforded rapid and efficient separation, good resolution, and identification of the examined compounds, alone or combined. The method was used to quantify these drugs, alone or in combination, in tablet, powder, and liquid formulations.

The *in vitro* uptake of L-[^{3}H] glutamate by tissue slices of cestode *H. diminuta*, denuded of tegument, was investigated [74]. Acidic amino acids, imipramine, and fluoxetine were effective inhibitors of high- and low-affinity uptake, whereas L-[^{3}H] glutamate receptor legands, neurotransmitters, and some anthelmintics generally were not. The concentrations present in, and the metabolism of L-[^{3}H] glutamate by, tissue slices was examined by HPLC.

Rainbow trout and channel catfish were exposed to a nominal concentration of 0.02 mg/L of niclosamide for a period of approximately 12 h. Samples of fillet tissue were collected from each fish species before treatment and at 6, 12, 18, 24, 48, 96, and 192 h after exposure. The fish were dissected, homogenized, extracted, and analyzed by HPLC [75].

The effects of soil depth and moisture on pesticide photolysis were studied. Moist soil at depth of 3, 2.5, 2, 1.5, 1, and 0.5 mm were each dosed at 2.5 μg/g with ^{14}C-niclosamide and photolyzed under a xenon lamp at constant temperature. Samples were removed after 20, 40, 110, and 153 h of continuous irradiation. The decrease in percent of niclosamide and the appearance of degradates were followed by analyzing the soil extracts by HPLC [76].

Shreier *et al.* [77] developed an HPLC method for the determination of Bayluscide residues in muscle fillet tissues of fish exposed to Bayluscide and 3-(trifluoro-methyl)-4-nitrophenol during sea lamprey control treatments in the Great Lakes (USA).

Laboratory trials during lampricide application (0.5–5.8 mg/L, 24-h exposure) with rainbow trout confirmed that field formulations of lampricides induce hepatic mixed function oxygenase enzymes activity. Mixed function oxygenase induction was associated with the 3-trifluoromethyl-4-nitrophenol formulation, and not the 2′,5-dichloro–4′-nitrosalicylanilide (Bayer 73) component of the field application. Bioassays were successfully confirmed with HPLC [78].

A screening test for niclosamide, pharmaceuticals, drugs, and insecticides with high performance reversed-phase liquid chromatography retention data of 560 compounds were given [79]. The relative retention times were calculated as the ratio of retention times of compound and reference compound, 5-(*p*-methylphenyl)-5-phenylhydantoin. The UV detector wavelength was 220 nm, where most of the compounds gave a good response. Two solvent programs and a prepacked column C-18 SIL-X-10 were used for the analysis.

Relative retention times for niclosamide and 570 drugs and related compounds on eight chromatographic systems were reported. Reversed-phase high-pressure chromatography employing octadecylsilanized columns was described [69].

Muir and Grift described a method for the determination of niclosamide in river water and sediment. River water was extracted by shaking with ethylacetate [80]. Sediment was shaken with methanol–water (4:1), the mixture was centrifuged, and

Table 5. HPLC methods for the analysis of niclosamide

Material	Column	Mobile phase (flow rate)	Detector	Reference
Dosage form	5 µm Silosorb-600 (15 cm × 0.6 cm)	Hexane/Dioxane (17:3) (2 mL/min)	At 254 nm	[61]
	4 µm NovaPak C_{18} column (15 cm × 3.9 mm i.d.)	Phosphate buffer of pH 3.6/methanol (3:1) (1 mL/min)	At 254 nm	[63]
Rainbow trout and channel catfish fillet tissue	5 µm Phenomenex Prodigy ODS-3 column (15 cm × 4.6 mm i.d.) equipped with a YMC ODS AQ guard column	Gradient elution: (1 mL/min) ACN/58 mM sodium acetate buffer of pH 3.8 (30% ACN held for 5 min to 100% ACN in 25 min and to 30% ACN in 3 min	Diode-array detection at 360 and 335 nm	[77]
River water and sediment	μ-Bondapak-NH_2 (30 cm × 4.2 mm i.d.)	Methanol/water (80:20) or acetonitrile/water (60:40) (2 mL/min)	At 313 nm	[80]
	Lichrosorb Si 60 (25 cm × 4.2 mm)	Hexane/isopropanol (95:5) (1.5 mL/min)	At 313 nm	[80]

the methanol evaporated. The sediment extract was then partitioned with methylene chloride and the extracts were cleaned up on a Florisil column. Niclosamide could be analyzed, after methylation with methyl iodide, by gas chromatography with electron-capture or alkali-flame detection, or directly by high pressure liquid chromatography with UV absorbance (313 nm) detection. Recoveries of niclosmide were 99–116% in fortified river water and 73–126% in fortified sediment samples [80].

Malan *et al.* [63] applied HPLC to show that niclosamide was compatible with a majority of common tablet excipients tested (Table 5).

4.5.4. Gas chromatography

Determination of niclosamide by gas chromatography, indicated that niclosamide showed relatively slower degradation either in the case of niclosamide or its mixture with herbicides [6].

Muir and Grift [80] determined the methylated derivative of niclosamide on a Tracor 560 GC equipped with an alkali-flame detector (AFD) and a ^{63}Ni electron capture detector (ECD). A 1.8 m × 4 mm i.d. glass column packed with 5 % OV-1 on Chromosorb W-HP and at 260°C was used with both detectors. Carrier gas (N_2, ECD; He, AFD) flow rate was 40 mL/min for both detectors. Detector and inlet oven temperatures were 350 and 250°C, respectively, for the ECD; and 275 and 250°C, respectively, for the AFD. The AFD had air and hydrogen flows of 120 and 4.0 mL/min, respectively.

A sensitive method was described for the detection and estimation of residues of niclosamide in bananas involving extraction of niclosamide, purification of the extract by solvent partition and column chromatography, formation of the heptafluorobutyryl derivative of 2-chloro-4-nitroaniline in 99% yield, and determination of the derivative by gas liquid chromatography with electron capture detection.

Recoveries from fortified bananas were 89 and 79% at levels of 0.02 and 0.2 mg/kg, respectively [81]. The sensitivity of the method was such that 0.6 pg of the pure derivative could be detected.

Niclosamide, formulated as the ethanolamine salt, was determined in formulations and the impact of residues on the environment assessed [82]. Efficient (>85%) phase-transfer, *N,O*-dimethylation of niclosamide and the synthesized 5-deschloro analog internal standard, followed by gas–liquid chromatography separation and electron-capture detection, permitted the determination of as little as 10 ppb analyte in fortified, stagnant water.

A gas–liquid chromatographic (GLC) method was described for determining residues of Bayer 73 (2-aminoethanol salt of niclosamide) in fish muscle, aquatic invertebrates, mud, and water by analyzing for 2-chloro-4-nitroaniline, a hydrolysis product of Bayer 73 [83]. Residues were extracted with acetone–formic acid (98 + 2), and partitioned from water samples with chloroform. After sample cleanup by solvent and acid–base partitioning, the concentrated extract was hydrolyzed with 2N NaOH and H_2O_2 for 10 min at 95°C. The 2-chloro-4-nitroaniline was then partitioned hexane–ethyl ether (7 + 3) and determined by electron capture GLC. Average recoveries were 88% for fish, 82% for invertebrates, 82% for mud, and 98% for water at 3 or more fortification levels.

Other GC methods for determination of niclosamide were also described [58,69].

4.6. Determination in body fluids and tissues

In addition to unchanged niclosamide, niclosamide-*O*-glucuronide was detected in bile, 2′,5-dichloro–4′-aminosalicylanilide was detected in urine and feces, and conjugates of the latter, including its *N*-glucuronide, were also detected by mass spectrometry in the urine of intact or biliary cannulated rats given ^{14}C-labeled niclosamide orally [84]. The high level of excretion of metabolites in urine and bile indicated considerable gastrointestinal absorption of niclosamide.

5. STABILITY

Graebing *et al.* [70] studied the photodegradation of [^{14}C]niclosamide in sterile, pH 5, 7, and 9 buffered aqueous solutions under artificial sunlight at 25.0 ± 1.0°C. Photolysis in pH 5 buffer was 4.3 times faster than in pH 9 buffer and 1.5 times faster than in pH 7 buffer. In the dark controls, niclosamide degraded only in the pH 5 buffer. After 360 h of continuous irradiation in pH 9 buffer, the HPLC chromatographic pattern of the degradates was the same regardless of which ring contained the radiolabel. These degradates were confirmed to be carbon dioxide and two- and four-carbon aliphatic acids formed by cleavage of both aromatic rings. Carbon dioxide was the major degradates, comprising similar 40% of the initial radioactivity in the 360 h samples from both labels. The other degradates formed were oxalic acid, maleic acid, glyoxylic acid and glyoxal. In addition, in the chloronitroaniline-labeled irradiated test solution, 2-chloro-4-nitroaniline was observed and identified after 48 h of irradiation but was not detected thereafter. No other aromatic compounds were isolated or observed in either labeled test system [70].

Rodriguez *et al.* [68] studied the stability of niclosamide in artificial gastric and intestinal juices. The gastric juice contained sodium chloride and hydrochloric acid with or without pepsin. The intestinal juice contained sodium phosphate with or without pancreatin. Niclosamide was incubated with the juices at 37°C for 6 h. The remaining intact drug and its degradation products (2-chloro-4-nitroaniline, 5-chlorosalicylic acid) were extracted with chloroform/methanol (5:1) and determined by TLC and HPLC. The drug was stable in these media for at least for 6 h.

Frank *et al.* [76] studied the effects of soil depth and moisture on niclosamide photolysis. Moist soil at depths of 3, 2.5, 2, 1.5, 1, and 0.5 mm were dosed at 2.5 μg/g with ^{14}C-niclosamide and photolysed under a xenon lamp at constant temperature. Samples were removed after 20, 40, 110, and 153 h of continuous irradiation. The decrease in percent of niclosamide and the appearance of degradates were followed by analyzing the soil extracts by HPLC. A corresponding set of experiments used air-dried soil. An experiment was also performed using initially moist soil, which was permitted to dry during photolysis but returned to moist conditions at each sampling. Qualitative and quantitative differences were found in the rate and route of degradation of niclosamide under these conditions. These differences have resulted from a combination of reduced photochemical activity and microbial population in dry soil. The half-lives of niclosamide in the dry soils were two and five times longer than those in the moisture-maintained soil. There was also a noticeable difference in the half-lives in soil of different depths. Moisture-maintained soil showed a uniform linear increase in half-life from 95 to 195 h as soil depth increased from 0.5 to 3.0 mm. With air-dried soil the half-lives were greatly dependant on soil depth, showing a much broader range of 199 h at 0.5 mm to 1064 h in 3.0 mm soil. An experiment design was described which maintained soil temperature and moisture to present conditions [76].

van Tonder *et al.* [85] studied the effect of polymorphism and pseudopolymorphism on the physical stability of niclosamide suspensions. Through recrystallization from organic solvents an anhydrated, monohydrated, and three solvated crystal forms of niclosamide were prepared. The crystal forms were characterized by DSC and TG analyses. It was determined that the physical instability of aqueous niclosamide suspensions of these crystal forms depended on the transformation of the drug powder to a poorly water-soluble monohydrate. Recommended approaches for the development of suspension with these crystal forms are indicated and their application and pitfalls in suspension formulation are discussed.

In a further study in isothermal stability testing, Wollmann *et al.* [86] indicated that the water of crystallization (5.53%) of niclosamide had no effect on stability, and the half-life claimed can be extended to 10 years.

6. CLINICAL APPLICATIONS

6.1. Pharmaceutical applications

Niclosamide is an anthelmintic, which is active against various intestinal tapeworms. It is the drug of choice for tapeworm infections due to *Taenia Saginata*, *Diphyllobothrium Latum*, and *Taenia Solium*. Niclosamide is particularly effective

for the treatment of luminal adult tapeworm infections due to its efficacy when given orally as a single daily dose or in a limited number of daily doses [3,8,87–89]. Niclosamide appears to be second-line therapy to praziquantel for *Hymenolepis Nana* (dwarf tapeworm) infections [89]. The usual adult dose for the treatment of tapeworms is 2 g as a single dose; the pediatric dose for children weighing between 11 and 34 kg is 1 g as a single dose, and 1.5 g for those over 34 kg [3,8,87–93].

6.2. ADME profile

Niclosamide is not significantly absorbed from the gastrointestinal tract [94]. However, no specific data for pharmacokinetic parameters for niclosamide is available in literature. The metabolic fate of the small amount of drug that is absorbed is unknown but presumably it is metabolized in the liver, possibly to less active forms.

A review discussing anthelmintic activity, pharmacokinetics, toxicity, side effects, and clinical use of niclosamide and other anthelmintic agents is reported [95].

6.3. Mechanism of action

Niclosamide inhibits oxidative phosphorylation and stimulates adenosine triphosphatese activity in the mitochondria of cestodes, killing the scolex and proximal segments of the tapeworm both *in vitro* and *in vivo*. The scolex of the tapeworm, then loosened from the gut wall, may be digested in the intestine and thus may not be identified in the stool even after extensive purging [90,91]. Niclosamide is not appreciably absorbed from the gastrointestinal tract [92,93] and the side effects have primarily been limited to gastrointestinal symptoms.

6.4. Dosing information

The usual adult dose for the treatment of *T. saginata* (beef tapeworm), *D. latum* (fish tapeworm) and *Dipylidium caninum* (dog tapeworm) is 2 g as a single dose. The pediatric dose for children weighing between 11 and 34 kg is 1 g as a single dose, and 1.5 g for those over 34 kg. For the treatment of *H. nana* (dwarf tapeworm), the usual adult dose is 2 g (4 tablets) as a single daily dose for 7 days. The tablets should be chewed thoroughly and taken after a light meal. If segments of cestodes or ova are present after 7 days, therapy may be continued to ensure the infestation is eradicated [96].

ACKNOWLEDGEMENTS

The author wishes to express his gratitude and thanks to Prof. Dr Abdullah A. Al-Badr, for his invaluable advice, assistance, encouragement, and constant guidance during the course of this work. Appreciation is also extended to Mr Tanvir A. Butt, for his secretarial assistance.

REFERENCES

[1] R. G. Alfonso (ed.), *Remington: The Science and Practice of Pharmacy*, 19th edn., Mack Publishing Co., Easton, USA, 1995, p. 1339.
[2] S. Budavari (ed.), *The Merck Index*, 13th edn., Merck and Co., NJ, 2001, p. 1167.
[3] J. E. F. Reynolds (ed.), *Martindale, the Extra Pharmacopoeia*, 31st edn., The Royal Pharmaceutical Society, London, 1996, p. 120.
[4] A. C. Moffat (ed.), *Clarke's Isolation and Identification of Drugs*, 2nd edn., The Pharmaceutical Press, London, 1988, p. 805.
[5] Swiss Pharmaeutical Society (ed.), *Index Nominum 2000. International Drug Directory*, 17th edn., Medpharm GmbH Scientific Publishers, Stuttgart, 2000, p. 728.
[6] *British Pharmacopoeia 2000 CD-Rom*, Vol. 1. Her Majesty's Stationary Office, London, 2000.
[7] E. Bekhli, *Med. Prom. SSSR*, 1965, **19**, 25.
[8] S. Budavari (ed.), *Merck Index*, 12th edn., Merck and Co, NJ, 1996, p. 6357.
[9] E. C. van Tonder, T. S. P. Maleka, W. Liebenberg, M. Song, D. E. Wurster and M. M. de Villiers, *Int. J. Pharm.*, 2004, **269**, 417.
[10] A. Monkiedje, A. J. Englande and J. H. Wall, *J. Environ. Sci. Health, Part B: Pesticides, Food Contam. Agric. Wastes*, 1995, **B30**, 73.
[11] K. Westesen and B. Siekmann, Patent written in Pharmacia AB, Sweden, 1994, p. 78.
[12] M. R. Caira, E. C. van Tonder, M. M. de Villiers and A. P. Lotter, *J. Inclusion Phenomena Mol. Recog. Chem.*, 1998, **31**, 1.
[13] C. M. Harvey, *Brit. UK Pat. Appl.*, 1989, 14.
[14] *European Pharmacopoeia*, 4th edn., Council of Europe, Strasbourg, France, 2001, p. 1624
[15] H. Singh, *Indian J. Chem., Section B: Organic Chem. Including Med. Chem.*, 1997.
[16] E. C. van Tonder, T. S. P. Maleka, W. Liebenberg, M. Song, D. E. Wurster and M. M. de Villiers, *Int. J. Pharm.*, 2004, **269**, 417.
[17] Calculated using Advanced Chem. Development (ACD/Labs) Software Solaris V4.67 (1994–2004 ACD/Labs).
[18] M. M. de Villiers, M. D. Mahlatji, S. F. Malan, E. C. van Tonder and W. Liebenberg, *Die Pharmazie*, 2004, **59**, 534.
[19] B. M. H. Al-Hadiya, Spectrometric and Spectrophotometric Analysis of Some Anthelmintics, Master of Science thesis, the School of Pharmacy and Pharmacology, University of Bath, UK, 1981.
[20] A. Kotera, S. Shibata and K. Sone, *J. Am. Chem. Soc.*, 1955, **77**, 6185.
[21] A. L. Sklar, *J. Chem. Phys.*, 1939, **7**, 984.
[22] L. J. Bellamy, *Infra-Red Spectra of Complex Molecules*, 2nd edn., John Wiley and Sons, New York, 1975.
[23] H. A. Szymanski, *IR Theory and Practice of Infrared Spectroscopy*, Plenum Press, New York, 1964.
[24] K. Miyazawa, T. Shlmanouchi and S. Mizushima, *J. Chem. Phys.*, 1958, **29**, 611.
[25] U. Shiedt, *Angew. Chem.*, 1954, **66**, 609.
[26] C. W. Young, R. B. Duvall and N. Wright, *Anal. Chem.*, 1951, **23**, 709.
[27] H. Budzikiewicz, C. Djerassi and D. H. Williams, *Mass Spectrometry of Organic Compounds*, Holden-Day, Inc., London, 1967.
[28] D. Goldsmith, D. Becher, S. Sample and C. Djerassi, *Tetrahedron, Suppl.*, 1966, **7**, 145.
[29] J. L. Catter, *J. Chem. Soc.*, 1964, **5477**; 1965, **5742**.
[30] P. Nickel and W. Weber, *PZ Wissenschaft*, 1989, **2**, 13.
[31] Q. Wu, Q. Yang and R. Yu, *Nanjing Yaoxueyuan Xuebao*, 1983, **3**, 63.
[32] C. Sridevi and S. J. Reddy, *J. Indian Chem. Soc.*, 1991, **68**, 263.
[33] H. Alemu, N. M. Khoabane and P. F. Tseki, *Bull. Chem. Soc. Ethiopia*, 2003, **17**, 95.
[34] F. C. Abreu, M. O. F. Goulart and A. M. Oliveira Brett, *Biosensors Bioelectron.*, 2002, **17**, 913.
[35] H. Alemu, P. Wagana and P. F. Tseki, *Analyst*, 2002, **127**, 129.
[36] A. K. Mishra and K. D. Gode, *Indian Drugs*, 1985, **22**, 317.
[37] T. Solomon and H. Zewde, *Sinet*, 1981, **4**, 31.
[38] R. E. Yorke and J. A. Turton, *Z. Parasitenkunde*, 1974, **45**, 1.
[39] T. M. H. Saber and M. M. Sidky, *J. Chem. United Arab Republic*, 1970, **13**, 369.
[40] R. Schlink, C. Dengler, P. Kirschenbuhler and K. H. Surborg, *GIT-Fachzeitschrift*, 2003, **47**, 141.

[41] S. S. Zarapkar and P. M. Deshpande, *Indian J. Pharm. Sci.*, 1989, **51**, 136.
[42] S. S. Zarapkar, S. R. Mehra and R. V. Rele, *Indian Drugs*, 1989, **26**, 360.
[43] H. G. Daabees, *Anal. Lett.*, 2000, **33**, 639.
[44] S. A. Abdel Fattah, *Spectrosc. Lett.*, 1997, **30**, 795.
[45] F. Onur and E. Dinc, *Scientia Pharmaceutica*, 1996, **64**, 151.
[46] E. R. M. Kedor-Hackmann, M. M. F. Nery and M. I. R. M. Santoro, *Revista de Ciencias Farmaceuticas*, 1994, **15**, 141.
[47] F. Onur and N. Tekin, *J. Faculty Pharmacy Gazi University*, 1994, **11**, 33.
[48] C. S. P. Sastry, M. Aruna, A. R. M. Rao and A. S. R. P. Tipirneni, *Chemia Analityczna*, 1991, **36**, 153.
[49] B. V. Lopatin, N. B. Lopatina and A. F. Bekhli, *Farmatsiya*, 1989, **38**, 75.
[50] C. P. S. Sastry, M. Aruna and A. R. M. Rao, *Indian Drugs*, 1988, **25**, 348.
[51] C. Liu, *Yaowu Fenxi Zazhi*, 1983, **3**, 56.
[52] F. Onur and N. Tekin, *Anal. Lett.*, 1994, **27**, 2291.
[53] L. H. Emara, *J. AOAC Int.*, 1993, **76**, 847.
[54] C. S. P. Sastry, M. Aruna and A. R. M. Rao, *Talanta*, 1988, **35**, 23.
[55] N. Bergisadi and D. Sarigul, *Acta Pharmaceutica Turcica*, 1986, **28**, 51.
[56] V. A. Kholoshchnov, *Voprosy Botaniki i Fizioloii Rastenii*, 1973, **3**, 73.
[57] N. I. Kokovkin-Shcherbak and S. G. Tiraspol'skaya, *Farmatsiya*, 1975, **24**, 44.
[58] D. A. Johnson and B. E. Stephens, *J. Great Lakes Res.*, 2003, **29**(Suppl. 1), 521.
[59] R. Strufe, *Pflanzenschutz-Nachr.* "Bayer", 1963, **16**, 221.
[60] R. Strufe, *Bull. World Health Org.*, 1961, **25**, 503.
[61] O. M. Solodka and G. A. Donets, *Farm. Zh (Kiev)*, 1990, **6**, 58.
[62] R. V. Manek and W. M. Kolling, *AAPS PharmSciTech*, 2004, **5**, E14.
[63] C. E. Malan, M. M. deVilliers and A. P. Lotter, *J. Pharm. Biomed. Anal.*, 1997, **15**, 549.
[64] V. A. Khloshchanov, *Mater. Izuch. Eff. Fenasala Kishechnykh Tsestodozakh Zhvachnykh Zhivotn*, 1972, **2**, 74.
[65] J. Kasianowicz, R. Benz and S. McLaughlin, *J. Membrane Biol.*, 1987, **95**, 73.
[66] G. Heinisch, H. Matous, W. Rank and R. Wunderlich, *Scientia Pharmaceutica*, 1981, **49**, 472.
[67] A. Pyka, D. Gurak and K. Bober, *J. Liq. Chromatogr. Rel. Technol.*, 2002, **25**, 1483.
[68] E. J. Ch. Rodriguez, M. G. Penichet, R. G. Nunez and I. H. Chaves, *Revista Mexicana de Ciencias Farmaceuticas*, 1998, **29**, 30.
[69] T. Daldrup, F. Susanto and P. Michalke, *Fresenius' Z. Anal. Chem.*, 1981, **308**, 413.
[70] P. W. Graebing, J. S. Chib, T. D. Hubert and W. H. Gingerich, *J. Agric. Food Chem.*, 2004, **52**, 870.
[71] P. W. Graebing, J. S. Chib, T. D. Hubert and W. H. Gingerich, *J. Agric. Food Chem.*, 2004, **52**, 5924.
[72] T. E. Bapiro, A. C. Egnell, J. A. Hasler and C. M. Masimirembura, *Drug Metabolism Disposition*, 2001, **29**, 30.
[73] E. C. van Tonder, M. M. de Villiers, J. S. Handford, C. E. P. Malan and J. L. du Preez, *J. Chromatogr.,* A, 1996, **729**, 267.
[74] R. A. Webb, *Comp. BioChem. Physiol., Part C*, 1986, **85 C**, 151.
[75] V. K. Dawson, T. M. Schreier, M. A. Boogaard, N. J. Spanjers and W. H. Gingerich, *J. Agric. Food Chem.*, 2002, **50**, 6780.
[76] M. P. Frank, P. Graebing and J. S. Chib, *J. Agric. Food Chem.*, 2002, **59**, 2607.
[77] T. M. Shreier, V. K. Dawson, Y. Choi, N. J. Spanjers and M. A. Boogaard, *J. Agric. Food Chem.*, 2000, **48**, 2212.
[78] K. R. Munkittrick, M. R. Servos, J. L. Parrott, V. Martin, J. H. Carey, P. A. Flett and G. J. Van Der Kraak, *J. Great Lakes Res.*, 1994, **20**, 355.
[79] T. Daldrup, P. Michalka and W. Boehme, *Chromatogr. Newslett.*, 1982, **10**, 1.
[80] D. C. G. Muir and N. P. Grift, *Int. J. Environ. Anal. Chem.*, 1980, **8**, 1.
[81] J. S. Johnson and G. B. Pickering, *Pesticide Sci.*, 1979, **10**, 531.
[82] F. C. Churchill II and D. N. Ku, *J. Chromatogr.*, 1980, **189**, 375.
[83] C. W. Luhning, P. D. Harman, J. B. Sills, V. K. Dawson and J. L. Allen, *J. Assoc. Off. Anal. Chem.*, 1979, **62**, 1141.
[84] L. A. Griffith and V. Facchini, *Recent Dev. Mass Spectrom. Biochem. Med.*, 1979, **2**, 121.
[85] E. C. van Tonder, M. M. de Villiers, A. P. Loetter, M. R. Caira and W. Liebenberg, *S. Afr. Pharmazeutische Industrie*, 1998, **60**, 722.

[86] H. Wollmann, M. Patrunky and M. Zimmermann, *Zentralblatt fuer Pharmazie, Pharmakotherapie und Laboratoriumsdiagnostik*, 1983, **122**, 571–579.
[87] Z. H. Zidan, F. M. A. Ragab and K. H. A. Mohamed, *J. Egypt. Soc. Parasitol.*, 2002, **32**, 285.
[88] *USP DI, Vol. I: Drug Information for Health Care Providers*, 13th edn., United State Pharmacopieal Convention, Inc., p. 2171.
[89] Anon., Drugs for parasitic infections. *Med. Lett. Drugs Ther.*, 1988, **30**, 15.
[90] G. Lenoir, *Toxicity Arch. Fr. Pediatr.*, 1985, **42**, 965.
[91] R. D. Pearson and E. L. Hewlett, *Ann. Intern. Med.*, 1985, **102**, 550.
[92] AMA Department of Drugs, *AMA Drug Evaluations*, 6th edn., American Medical Association, Chicago, IL, 1986.
[93] A. G. Gilman, L. S. Goodman and J. W. Rall, *et al.* (eds) *Goodman and Gilman's The Pharmacological Basis of Therapeutics*, 7th edn., Macmillan Publishing Co., New York, 1985.
[94] Technical Information: Niclocide (R), niclosamide, Miles Laboratories, West Haven, CT, 1981.
[95] D. A. Denham ''Anthelmintics'', in *Antibiotics and Chemotherapy* (ed. F. O'Grady), 7th edn., Churchill Livingstone, Edinburgh, UK, p. 513.
[96] Product Information: Niclocide (R), niclosamide, Miles Laboratories, West Haven, CT, 1994.

Oxytetracycline: Analytical Profile

Mochammad Yuwono and Gunawan Indrayanto

Assessment Service Unit, Faculty of Pharmacy, Airlangga University, Dharmawangsa Dalam, Surabaya 60286, Indonesia

Contents

1. INTRODUCTION

Oxytetracycline is available as oxytetracycline ($C_{22}H_{24}N_2O_9$; MW 460.4) [1–3], oxytetracycline hydrochloride ($C_{22}H_{24}N_2O_9 \cdot HCl$; MW 496.9) [1,2,4–8], oxytetracycline dihydrate ($C_{22}H_{24}N_2O_9 \cdot 2H_2O$; MW 496.4) [1,2], and oxytetracycline calcium ($[C_{22}H_{24}N_2O_9]_2 \cdot Ca$), MW 958.9) [1,4].

PROFILES OF DRUG SUBSTANCES, EXCIPIENTS, AND RELATED METHODOLOGY, VOLUME 32
ISSN: 0099-5428

DOI: 10.1016/S0099-5428(05)32003-X

Molecular structure. The molecular structure of oxytetracycline is as follows:

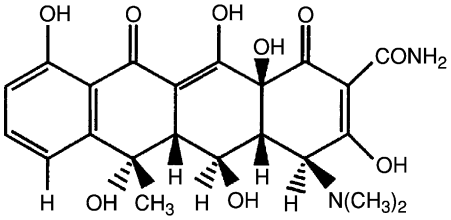

Oxytetracycline

Chemical name. (4S, 4aR, 5aR, 6S, 12aS)-4-(Dimethylamino)1, 4, 4a, 5, 5a, 6, 11, 12a-octahydro-3, 5, 6, 10, 12a-hexahydroxy-6-methyl-1, 11-dioxo-2-naphthacenecarboxyamide. CAS Reg. 2058-46-0 (as mono HCl), 6153-64-6 (as dihydrate), 15251-48-6 (as calcium salt).

Oxytetracycline occurs as yellow crystals or crystalline powder, has a bitter taste and is odorless. Oxytetracycline hydrochloride should have potency not less than 835 μg $C_{22}H_{24}N_2O_9$ per mg [1], whilst for oxytetracycline not less than 832 μg/g [1]; or 95.0–102.0% as anhydrous substance [2]; or not less than 88.0% of $C_{22}H_{24}N_2O_9$ calculated as anhydrous basis [3,4]. For oxytetracycline calcium, it should contain not less than 90.0% and not more than 100.5% [2], or 865 μg $C_{22}H_{24}N_2O_9$ per mg [1]. Oxytetracycline was produced by the growth of certain strain of *Streptomyces rimosus* or obtained by other means.

Oxytetracycline preparations for oral administration should contain not less than 90% or not more than 120% [1] or not less than 90% and not more than 110% [2], of the labeled amount. For ointment, the requirements are not less than 90.0% and not more than 115% (for oxytetracycline HCl and Hydrocortisone ointment, or 120% for other ointment. For ophthalmic suspension mixture with hydrocortisone acetate, its content should contain not less than 90% and not more than 110% [1].

2. COMPENDIAL METHODS OF ANALYSIS

2.1. Identification

2.1.1. Bulk drug substance

Two identification tests for oxytetracycline hydrochloride are given in the USP 28 [1], one being an ultraviolet absorption test and the other a color test. European Pharmacopoeia [2], British Pharmacopoeia (BP) 2003 [4], International Pharmacopoeia [5], and Pharmacopoeia of the People's Republic of China [6] described a thin-layer chromatography and color tests for identification of oxytetracycline hydrochloride and oxytetracycline dihydrate. For identification of oxytetracycline calcium, USP 28 [1] used Method II under identification of tetracycline <193>, whilst BP 2003 [4] described a TLC, color test, and calcium test as the method of identification.

2.1.1.1. Ultraviolet absorption

The absorptivity of 20 μg/mL test solution of oxytetracycline hydrochloride in 0.1 N hydrochloric acid at 353 nm should be between 96% and 104% of that of oxytetracycline RS. It is calculated on the anhydrous base and the potency of the reference standard being taken into account [1], whilst its absorption maximum in KCl solution (0.05 N KCl + 0.01 N HCl) is 353 nm with the absorbance 0.54–0.58 [4].

2.1.1.2. Color test

A light to deep red color is produced when oxytetracycline hydrochloride, oxytetracycline dihydrate, or oxytetracycline calcium is dissolved in sulfuric acid [1–5], and the color becomes yellow after water is added to the solution [1,2,4–7].

Any opalescence in the solution of 10 mg test substance (oxytetracycline dihydrate) in a mixture of 1 mL of dilute nitric acid R and 5 mL of water R added with 1 mL of silver nitrate solution R2 is not more intense than that in a mixture of 1 mL of dilute nitric acid R, 5 mL of a 21 mg/L solution of potassium chloride R and 1 mL of silver nitrate solution R2 [1,2].

2.1.1.3. Thin-layer chromatographic method

A summary of TLC methods for identification of oxytetracycline is given in Table 1.

2.1.2. Oxytetracycline in pharmaceutical preparations

For identification of oxytetracycline in pharmaceutical preparations, USP 28 [1] describes Method II under identification of tetracycline <193> (see Table 1), BP 2003 [4] describes a TLC and color test.

2.2. Impurity analyses

2.2.1. Light-absorbing impurities

The light-absorbing impurities of oxytetracycline hydrochloride and oxytetracycline dihydrate [2,4,6] are detected using a UV-spectrophotometric method. In all the compendia, the absorbance of a solution of 2.0 mg/mL in a mixture of 1 volume of hydrochloric acid solution (0.1 mol/L) and 99 volumes of methanol at 430 nm not greater than 0.50 is required; the absorbance of a solution of 10 mg/mL in the same solvent at 490 nm is not greater than 0.20. The measurements are carried out within 1 h of the preparation of the solutions.

2.2.2. Related substances

Oxytetracycline (OTC) and oxytetracycline hydrochloride (OTC HCl) may contain the impurities 4-epi-oxytetracycline (EOTC), tetracycline (TC) and 2-acetyl-2-decarboxamido-oxytetracycline (ADOTC) [2,4]. According to European Pharmacopoeia, oxytetracycline hydrochloride may also contain anhydro-oxytetracycline (AOTC), α-apo-oxytetracycline (α-AOTC), β-apo-oxytetracycline (β-AOTC). The structures are shown in Fig. 1.

To determine the related substances of OTC and OTC HCl, a liquid chromatographic method is described using a column (25 cm × 4.6 mm i.d.) packed

Table 1. Summary of compendial methods for TLC identification

Stationary phase	Mobile phase	Detection	Reference substances	Reference
Oxytetracycline (hydrochloride)				
Octyl silinized silica gel	0.5 M oxalic acid pH 2.0–ACN–MeOH (80:20:20)	UV	CTC HCl + DOX hyclate + OTC + TC HCl	[1]
Octadecylsilyl silica F 254 Plate R	ACN–MeOH–63 g/L oxalic acid pH 2 (20:20:60)	UV 254 nm	OTC HCl + TC + minocycline HCl	[4]
Silica gel H	Water–MeOh–CH_2Cl^2 (6:35:59)	UV 365 nm	OTC HCl + demeclocycline HCl	[2]
Silica gel G/0.1 M Na_2EDTA	200 ml mixture of aceton–$CHCl_3$–EtOA (1:2:2) and 5 mL 0.1 M Na_2EDTA (pH 7)	NH_3 (UV 365 nm)	OTC HCl + TC HCl + CTC HCl	[7]
Kieselguhr	200 ml mixture of aceton–$CHCl_3$–EtOA (1:2:2) and 5 mL 4% Na_2EDTA (pH 7)	NH_3 (UV 365 nm)	OTC HCl + TC HCl + CTC HCl	[5]
Oxytetracycline calcium				
Silica gel 60 sprayed with 10 M NaOH (110°C, 1 h)	H_2O–MeOH–CH_2Cl_2 (6:35:59) pH to 7.0 with 10% Na_2EDTA	UV 365	OTC HCl + demeclocycline HCl	[4]
Oxytetracycline dihydrate				
Octadecylsilyl silica F 254 Plate R	ACN–MeOH–63 g/L oxalic acid pH 2 (20:20:60)	UV 254 nm	OTC HCl + TC + Minocycline HCl	[4]

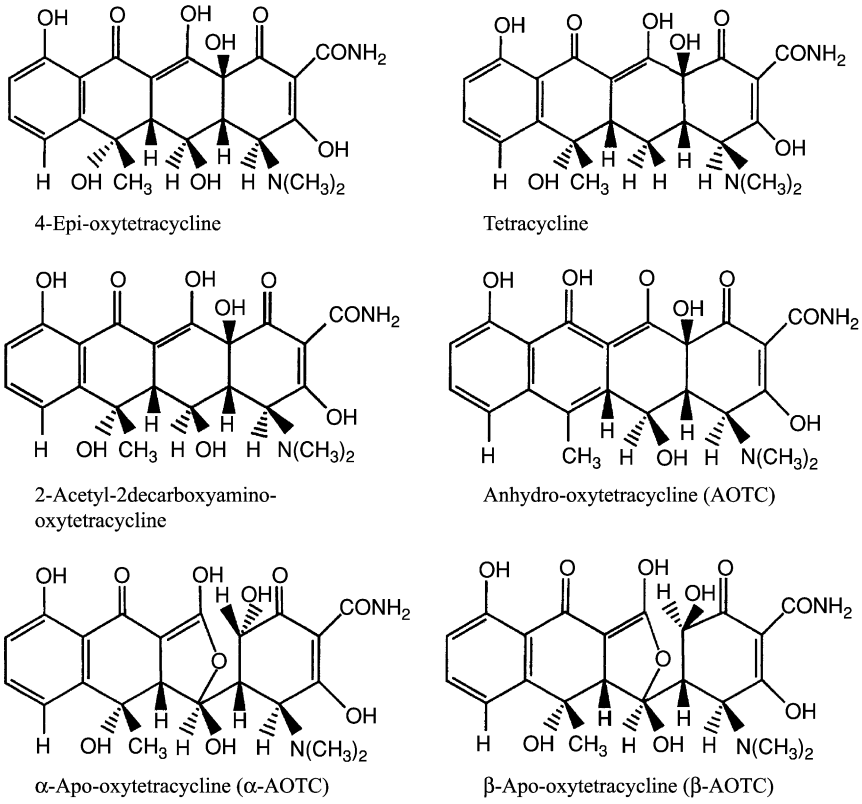

Fig. 1. Structures of substances related to oxytetracycline.

with styrene-divinylbenzene copolymer R (8–10 μm). A buffer solution prepared by mixing 60.0 g of 2-methyl–2 propanol R with 60 mL of 0.33 M phosphate buffer solution pH 7.5 R, 50 mL of a 10 g/L solution of tetrabutylammonium hydrogen sulfate R adjusted pH 7.5 with dilute sodium hydroxide solution R, 10 mL of a 0.4 g/L solution of sodium edetate R and diluted to 1000 mL with water is used as mobile phase. The temperature of the column is maintained at 60°C, whereas the flow rate and the detector are set at 1.0 mL/min and 254 nm, respectively [4].

OTC and OTC HCl should contain not more than 2% of ADOTC, 2% of TC, 0.5% of EOTC and 2% in total of AOTC, α-AOTC, *β*-AOTC [2,4].

2.2.3. Sulfated ash

The sulfated ash in oxytetracycline is determined using the general test method:

British Pharmacopoeia 2003: method <2.4.14> [4]
European Pharmacopoeia: method <2.4.14> [2]
Indian Pharmacopoeia 1996: Appendix <3.22> [7]

All above compendial specifications are not more than 0.5%.

2.2.4. *Heavy metals*

According to BP 2003 [4], European Pharmacopoeia [2], a 0.5 g of test substance complies with limit test C (50 ppm). The standard is prepared using 2.5 mL of lead standard solution (10 ppm Pb).

2.3. Assay methods

2.3.1. *Oxytetracycline bulk drug substance*

The USP 28 [1], European Pharmacopoeia [2], BP 2003 [4], and Indian Pharmacopoeia 1996 [7] use the liquid chromatography method as described above in Section 2.2.2 for the assay of oxytetracycline. The International Pharmacopoeia 1988 [5], Pharmacopoeia of the People's Republic of China [6], Indian Pharmacopoeia [7], and Indonesian Pharmacopoeia [8] use a microbiological method. This methodology will be described in more detail in a later section.

2.3.2. *Oxytetracycline in pharmaceutical preparations*

For assaying oxytetracycline content in injections, tablets, capsules, ointments, and oral suspensions, the United States Pharmacopoeia 28 [1] uses a liquid chromatography method described in the assay under oxytetracycline. For oxytetracycline and Nystatin capsules and for oral suspension, United States Pharmacopoeia 28 [1] uses a microbiological method listed under antibiotics-microbial assays <81>.

3. ELECTROCHEMICAL METHOD

Kurzawa and Kowalczyk-Marzec [9] described electrochemical titration methods for the determination of OTC in commercial preparations commonly used in veterinary medicine. A relative standard deviation (RSD) below 1.0% was reported using $NH_4Mo_7O_{24}$, $NaVO_3$, NaOH, $AgNO_3$, and $FeCl_3$ as titrants of conductometric, potentiometric, and cyclic voltammetric titration methods. Standard additions and potentiometric titration using oxytetracycline hydrochloride-selective electrodes were demonstrated by Issa *et al.* [10] to determine OTC HCl in pure solutions and in pharmaceutical preparations. The ion-selective electrode used was reported having a Nernstian response within 1.02×10^{-6} to 1.02×10^{-2} mol/L of OTC. The response is unaffected by the change of pH over the range from 4 to 11.

Couto *et al.* [11] developed a flow injection system with potentiometric detection for determination of TC, OTC, and CTC in pharmaceutical products. A homogeneous crystalline CuS/Ag_2S double membrane tubular electrode was used to monitor the Cu(II) decrease due to its complexation with OTC. The system allows OTC determination within a $49.1–4.9 \times 10^3$ ppm and a precision better than 0.4%. A flow injection method for the assay of OTC, TC, and CTC in pharmaceutical formulations was also developed by Wangfuengkanagul *et al.* [12] using electrochemical detection at anodized boron-doped diamond thin-film electrode. The detection limit was found to be 10 nM (signal-to-noise ratio = 3).

Sun *et al.* [13] developed a selective electrode for the determination of OTC hydrochloride. The electrode is constructed of a plasticized PVC membrane

containing three types of ion-pairs as the electroactive substance, i.e., OTC-tetraphenylborate, OTC-phosphotungstate, and OTC-silicotungstate. The sensor was successfully used for the analysis of OTC in pharmaceutical formulations by using direct potentiometry.

4. SPECTROSCOPIC METHODS OF ANALYSIS

Galego and Arroyo [14] described a simultaneous spectrophotometric determination of OTC, hydrocortisone, and nystatin in the pharmaceutical preparations by using "ratio spectrum-zero crossing derivate" method. The calculation was performed by using multivariate methods such as partial least squares (PLS)-1, PLS-2, and principal component regression (PCR). This method can be used to resolve accurately overlapped absorption spectra of those mixtures.

Samola and Urleb [15] reported qualitative and quantitative analysis of OTC using near-infrared (NIR) spectroscopy. Multivariate calibration was performed on NIR spectral data using principle component analysis (PCA), PLS-1, and PCR.

Fernandez-Gonzáles *et al.* [16] described a method for determination of OTC in medicated premixes and feeds by second-derivative synchronous spectrofluorometry. The assay based on the reaction of oxytetracycline with divalent metal ion (Ca^{2+}) at pH 6–10 to form a yellow complex that can be analyzed by synchronous spectrofluorometry ($\Delta\lambda = 115$ nm). Rao *et al.* [17] described a spectrophotometric method for the determination of OTC in pharmaceutical formulations based on the color reaction with uranium, which was detected at 413 nm.

5. CHEMILUMINESCENCE METHODS

In recent years, the chemiluminescence method has been developed for the determination of OTC, TC, and CTC. The chemiluminescence can be achieved by direct reaction or by energy-transfer mechanism. As a ligand, OTC with europium(III) forms an OTC–Eu(III) complex under mild alkaline condition. Rakicioglu *et al.* [18] reported the increased fluorescence intensity of the europium(III)–TC when the system was oxidized by hydrogen peroxide. The europium-sensitized fluorescence with EDTA as co-ligand and cetyltrimethylammonium chloride as surfactant was used to determine OTC, TC, CTC, and doxycycline (DC) in aqueous solutions. The method was reported sensitive with detection limit of 5×10^{-10} mol/L for oxytetracycline [19]. A europium-sensitized time-resolved lumininescence method was described by Chen *et al.* [20] for the determination of oxytetracycline in catfish muscles. The recovery and the limit of detection were reported to be 92–112% and 3–7 ng/g, respectively. Han *et al.* [21] developed a chemiluminescence method for the assay of OTC, TC, and CTC in pharmaceutical formulations based on an enhancement of the tetracyclines upon chemiluminescence light emission of tris(2,2′-bipyridine)ruthenium(II) by potassium permanganate using Mn(II) as catalyst. The limit of detection for oxytetracycline was reported at 2.0×10^{-8} g/mL. Zheng *et al.* [22] developed a simple electrogenerated chemiluminescence method for the determination of OTC, TC, and CTC in pharmaceutical formulations. The method was based

on the chemiluminescence reaction of the electrogenerated bromine near to the surface of the platinum electrode with H_2O_2 and tetracyclines. The detection limit (signal to noise ratio = 3) of the method was 7.0×10^{-8} g/mL for OTC.

6. CAPILLARY ELECTROPHORESIS

Capillary electrophoresis (CE) has recently become a very valuable tool for pharmaceutical analysis due to its high-resolution speed and the very small sample volume needed. For analysis of OTC, the use of CE has also been reported. Tjørnelund and Hansen [23] developed a simple method for the assay of OTC in ointments by means of capillary electrophoresis. The OTC in the sample was reported to be well separated from related impurities and degradation products using nonaqueous capillary electrophoretic technique as metal chelate compound with magnesium ion. The use of nonaqueous capillary electrophoresis media offers the advantages to provide a very simple method by injecting the solvent used for a single extraction step with an organic solvent. The method was then validated for the analysis of oxytetracycline contained in a drug ''Hydrocortisone with Terramycin ointment''. The recovery obtained was close to 100% with precision lesser than 3.6% [24]. Li *et al.* [25] developed a capillary electrophoresis method that provides a sufficient separation of OTC, TC, and demeclocycline (DMC) from their respective impurities within an analysis time of only 15 min.

A high performance capillary electrophoresis (HPCE) was described for the separation and simultaneous determination of OTC, TC, CTC, DC, and chloramphenicol in honey. The use of buffer pH 3.2 containing 0.02 mol/L Na_2HPO_4 and 0.01 mol/L citric acid with addition of 4% (v/v) *N*-methylmorpholine and 12% (v/v) acetonitrile demonstrated a good separation of these five antibiotics within 20 min. The proposed method gave detection limit (signal to noise ratio > 5) of 20 μg/L for OTC [26].

Capillary zone electrophoresis coupled with fast cyclic voltammetric detection was developed by Zhou *et al.* [27] for the separation and determination of OTC, TC, and CTC antibiotics. All compounds were well separated by optimization of pH and complexation with a boric acid–sodium tetraborate buffer. The detection limit using fast on-line cyclic voltammetric detection with Hg-film-microm electrode was 1.5×10^{-6} mol/L for OTC (signal to noise ratio > 2). A continuous flow manifold coupled on-line to a capillary electrophoresis system was developed by Nozal *et al.* [28] for determining the trace levels of OTC, TC, and DC in surface water samples.

7. MICROBIOLOGICAL AND IMMUNOLOGICAL METHODS

United States Pharmacopoeia 28 [1] describes a microbiological method under antibiotics–microbial assays for the analysis of OTC and nystatin capsules, OTC and nystatin for oral suspension, OTC HCl and hydrocortisone ointment, and OTC HCl and polymyxin B sulfate ointment. The methods are relative rather than absolute, which are based on the determination of the level of oxytetracycline by a microbiological response to a series of standard oxytetracycline concentrations by a

strain of test microorganism. Among other test organisms and assay media investigated by Tsai and Kondo [29], the combination of *Bacillus subtilis* and minimum medium (MM) showed the greatest sensitivity for screening OTC. Microbiological methods are simple, versatile, and relatively cheap. However, they are time consuming and poor in terms of sensitivity and specificity. The immunoassay approaches such as radioimmunoassays (RIAs) and enzyme-linked immunosorbent assays (ELISAs) are methods that offer more sensitive and selective results than do microbiological methods. The RIA methods involve the specific binding of antibiotics to receptors and the quantitation is obtained by measuring of radioactivity: H^3 or C^{14}. Young and Carlson [30] applied the radioimmunoassay technique for routine monitoring of OTC in water and wastewater. ELISA's are different from heterogeneous RIAs in that antigen or antibody is labeled with an enzyme in place of a radioisotope. An application of ELISA was reported by Aga *et al.* [31] in determining the fate of tetracyclines in land-applied livestock for the analysis of oxytetracycline in different foods such as milk, honey, and meat. The immunoassay methods have a limited application because of the unique reagent and antibody. Interferences may occur when OTC is measured in the presence of other antibiotics. Some microbial and immunological test kits such as Delvotest®, Ridascreen®, Charm II® are now commercially available and widely used for screening the oxytetracycline residue in different foods such as milk, honey, and meat [32–34].

8. CHROMATOGRAPHIC METHODS OF ANALYSIS

8.1. Thin-layer chromatography

Krzek *et al.* [35] reported the qualitative identification and quantitative analysis of the mixtures of OTC, tiamulin, lincomycin, and spectinomycin in the veterinary preparations by using TLC/densitometry. As stationary phase, they used precoated TLC aluminum sheets, and the mobile phases were mixtures of 10% citric acid solution, hexane, ethanol (80:1:1, v/v), and *n*-butanol, ethanol, chloroform, 25% ammonia (4:5:2:5, v/v). The other application of TLC or HPTLC for analyzing OTC in the various samples is summarized in Table 2 [36].

8.2. High performance liquid chromatography

HPLC methods have been widely used for the analysis of OTC in different samples. As described above in the Section 2.3, the HPLC method is described in most of compendia [1,2,4,7] for determination of OTC in bulk drug substances and in some pharmaceutical preparations. The application of HPLC methods for the analysis of antibiotics including oxytetracycline has been recently reviewed by Diaz-Cruz *et al.* [37] and Lunn [38]. A summary of HPLC method for the analysis of OTC is presented in Table 3.

The separations of OTC have been carried out, in most instances, with reversed phase (RP) and polymeric ODS column. One difficulty in the analysis of OTC using RP-HPLC is the interaction of OTC with metal ions to form chelate complexes and the adsorption of OTC on RP columns, which consequently leads to severe peak

Table 2. Analysis of oxytetracycline by TLC (data cited from CBS 1.09, 2003, Camag)

Stationary phase	Mobile phase	Detection	Samples
Silica gel	$CHCl_3$–MeOH–5% aqueous EDTA (13:4:1); pre-developing: 5% aqueous EDTA	UV 366 nm	Milk
Silica gel	$CHCl_3$–MeOH (10:1) with traces NH_3	UV 254 and 366 nm	Animal feed
Silica gel	$CHCl_3$–MeOH–water (65:25:5); pre-developing: saturated aqueous Na_2EDTA	UV 254 nm	Pharmaceuticals
Silica gel	EtOA–acetone–water (60:20:6)	NH_3	Pharmaceuticals
Silica gel treated with 0.27 M Na_2EDTA	$CHCl_3$–MeOH–acetone–ammonia 1% (5:11:25:9)	Fluorescence (365, 440 nm)	Pharmaceuticals
Silica gel treated with EDTA/NaOH	CH_2Cl_2–MeOH–Water (58: 35: 7)	UV 365 nm	Bulk drug
Silica gel treated with 10% EDTA	CH_2Cl_2–MeOH–water (59:35:7)	UV 254 or 280 nm; fluorescence (366, 400 nm)	Food
Cellulose added with 5 g $MgCl_2$ 6 H_2O + 0.3 M Na_2EDTA in 100 mL water and 2 mL acetic acid	IPA–acetone–water (75:15:15)	NH_3 observed with UV 365 nm	Clinical samples
RP-8	$CHCl_3$–MeOH–5% aqueous EDTA (65:20:5, lower phase) and MeOH–ACN–0.5 M aqueous oxalic acid pH (3:1:1:4)	0.2 M aqueous oxalic acid and 10% TEA observed with UV 366 nm	Honey
RP-8	MeOH–ACN–0.5 M aqueous oxalic acid (1:1:4)	FAB-MS	Milk

tailing and inconsistent analyte recoveries. To avoid these problems, the mobile phase containing complexing agent such as EDTA [39–41] or oxalic acid [42–45] is generally used. Monser and Darghouth [46] described a HPLC method using porous graphitic carbon column to separate simultaneously the common tetracyclines including OTC and 6-epi-doxycycline in bulk powder and pharmaceutical preparations. The column was reported to show the successful baseline separation of the tetracyclines examined in less than 12 min using isocratic elution. The polymer based stationary phases have recently been used for the determination of oxytetracycline in different samples. The use of polymeric column requires usually viscous organic modifiers such as EDTA and/or tetrabutylammonium ion pairing reagents. Additionally, the system is mostly operated at an elevated column temperature [1,2,47,48].

Table 3. Summary of HPLC conditions for the analysis of oxytetracycline

Column	Mobile phase	Detection	Analyte(s) and sample	Extraction and cleanup	Detection limit (DL), quantitation limit (QL) and recovery (Rec)	Reference
Chromsper C8	ACN–oxalic acid 0.01 M (aq. pH 2.0; 20:80)	Fluorescence 385 nm/500 nm	OTC and TC in salmon muscle	Extraction with EDTA–Mcllvaine buffer pH 4.0; cleanup with polymeric SPE	QL = 50 μg/kg, Rec = 83.9–93%	[51]
Polymer Labs. PLRP-S	Gradient: A: 0.001 M oxalic acid, 0.5% formic acid + 3% THF in water, B = THF	Positive ESI-MS/MS	OTC, CTC, TC, DC, and its 4-epimer in pig tissues	Extraction with sodium succinate solution, protein removal with TCA, SPE cleanup on polymeric RP column	DL = 0.5–4.2 ng/g	[57]
Polymer Labs. PLRP-S	A: 0.1% TFA in water B: ACN	UV 350 nm	OTC in water, biofilter sand, sediment, trout tissues	Dilution with acidic buffer containing EDTA, cleanup with Polymeric SPE cartridge	DL = 0.04 ppm (trout); 0.03 ppm (biofilter sand); 1 ppm (sediment), 0.003 ppm (water) Rec = 82–108%	[48]
RP C-18	Water, 5% formic acid, ACN, MeOH (23:40:25:12)	ESI–MS/MS	OTC, TC, CTC in lagoon water	Polymeric SPE and C–18 cartridge	DL = 3.6 μg/L Rec = 86–110%	[59]
Polymer Labs. PLRP-S	0.01M oxalic acid–ACN (75:25, v/v)	UV 360 nm	Animal tissues	Extraction with oxalic buffer followed by chelation and deproteination, cleanup with styrene-divinylbenzene cartridge	Rec: 76–87%	[77]
Supelcosil LC-18-DB column	pH 2.3 H_3PO_4–ACN (76:24, v/v)	UV 355 nm	Ovine milk	Extraction with ACN and cleanup with CH_2Cl_2 and hexane	DL = 5.2 ng/ml QL = 17.5 ng/ml Rec = 85.8–98.9%	[52]

(*Continues*)

Table 3. (*Continued*)

Column	Mobile phase	Detection	Analyte(s) and sample	Extraction and cleanup	Detection limit (DL), quantitation limit (QL) and recovery (Rec)	Reference
Polymer Labs. PLRP-S column	Gradient: Sol. A = 0.1 M KH_2PO_4–0.01 M citric acid–0.01 M EDTA, B = ACN–MeOH–buffer (25:10:65, v/v)	UV 350 nm	Egg, animal tissues	Extraction with EA, evaporated, reconstituted in MeOH, online MCAC cleanup	DL = 3 μg/kg 91–94% (egg) 101–104% (animal tissues)	[40]
Polymer Labs. PLRP-S column	Gradient: A = 0.02 M H_3PO_4 and 0.01 M sodium 1-decansulfonate B = ACN	UV–DAD 355 nm	OTC, TC, CTC, DC in eggs and broiler meat	Extraction with CH_2Cl_2 and petroleum ether	DL = 2.2 ng/g (OTC, eggs) QL = 13.0 ng/g (OTC, eggs) Rec = 76%	[49]
High purity C-18 silica column; Inertsil ODS2	Gradient: A: ACN–H_2O (10:90) containing 0.04% (v/v) heptafluorobutyric acid, 10 mM oxalic acid and 10 μM EDTA ammonium salt B: ACN–H_2O (90:10) containing 0.04% (v/v) heptafluorobutyric acid, 10 mM oxalic acid and 10 μM EDTA ammonium salt	APCI-MS	OTC, TC, CTC and its isomers in muscle and kidney	Extraction with glycine-HCl buffer, cleanup with isolute cyclohexyl cartridge	DL = 10 ng/g (muscle); 20 ng/g (kidney) Rec = 56–74%	[39]
Zorbax SB C-18	Mixture of 0.001 M EDTA, 0.05 M citric acid, 0.013 M	UV 353 nm	Fish muscles	Extraction with McIlvaine buffer pH	QL = 0.04 μg/g Recovery = 33–35%	[78]

	trisodium citrate and 0.1 M KNO_3–DMF–ACN (65:25:10)			4.0 containing EDTA, addition of TCA		
RP LUNA C18	ACN–0.01 M oxalic acid (85:15, v/v)	UV 355 nm	OTC and Its 4′ epimer in edible tissues from Turkeys	Extracted with McIlveine buffer (pH 4.0) and cleanup by MCAC	DL of OTC = 4.7 g/kg (muscle); 11.0 g/kg (liver), 9.3 g/kg (kidney)	[50]
LiChroSpher 100 RP 18E	ACN–0.02 M orthophosphoric acid (24:76, v/v), pH 2.3	UV 355 nm	OTC and OA in blue mussel (Mytilus edulis)	Extraction with methanolic oxalic acid sol (pH 1.4)	0.012 μg/g (OTC) Rec = 65.4% (OTC)	[44]
Silasorb C8	MeOH–0.01 M oxalic acid, pH 3.0 (30:70, v/v)	UV 250 nm	OTC in pharmaceutical formulation	Dilution with MeOH	DL: 2 ng; QL = 10 ng (injected onto the column)	[61]
Hypercarb porous graphitic carbon carbon	0.05 M potassium phosphate buffer (pH 2.0)–ACN (40:60)	UV 268 nm	OTC, DC, CTC, MC in pharmaceutical products	Tablets: dissolution in mobile phase; ointments: addition of cyclohexane and extracted with buffer solution	Rec = 98.8% (OTC, ointment); 99.8–101% (tablet)	[46]
Inertsil C8	0.1 M ammonium acetate (pH 3.0)–ACN (75:25, v/v)	UV 350 nm	OTC in bovine kidney and medicated milk replacer	Extraction: McIlvaine buffer–EDTA solution, cleanup with SPE column	Rec: 84–98%	[76]
LiChrosorb RP 18	MeOH–ACN–0.01 M oxalic acid (17.5:17.5:65, %)	UV–DAD	OTC, TC, CTC in meat, milk, and cheese	Extraction with buffer solution, cleanup with SPE or MSPD	Rec = 48–86% (SPE) Rec = 89–93% (MSPD); DL = 15–22 ng/g (SPE); 30 ng/g (MSPD)	[73]
RP ODS hypersil column	ACN–0.05 M sodium phosphate monobasic dihydrate pH 2.2 (22:78, v/v),	Electrochemical detection, 400 mV	OTC, TC, CTC, MC, DC in ovine milk	Extraction with ACN and hexane	12.5 ng/ml (OTC) Rec = 88% (OTC)	[53]

(*Continues*)

Table 3. (*Continued*)

Column	Mobile phase	Detection	Analyte(s) and sample	Extraction and cleanup	Detection limit (DL), quantitation limit (QL) and recovery (Rec)	Reference
RP C–18	0.05 M KH_2PO_4 buffer (pH 2.5)–ACN (84:16, v/v)	Amperometric detection at 1.2 V	OTC, TC, CTC, DMC, DC, MC, MNC in bulk powders and pharmaceutical preparations	Dilution with mobile phase	DL = 0.1–1.0 ng/µl; Rec = 99.1–100.4%	[54]
Xterra MS C18	Gradient: A: MeOH, H_2O (5:95, v/v) added with formic acid (0.08 M) B: MeOH, water (95:5, v/v) added with formic acid (0.08 M)	ESI–MS/MS	OTC, EOTC, TC, ETC, ADOTC, α-AOTC, β-AOTC in ointments	Extraction with hexane–0.08 M formic acid (1:1, v/v)	DL = 0.78 mg/l (OTC); QL = 2.60 mg/L (OTC); Rec: 90–112%	[60]
MacMod Hydrobond PS C8	0.01 M formic acid–ACN–MeOH (75:18:7)	UV 370 nm; ESI–MS/MS	OTC, TC, CTC in shrimps and whole milk	Extraction with succinic acid, cleanup with OASIS HLB SPE column	DL = 25–400 ng/g (shrimps); 50–300 ng/g (milk)	[62]
Polymer Labs. PLRP-S	Mixture of 0.1 M KH_2PO_4, 0.01 M citric acid and 0.01 M EDTA	UV 350 nm	OTC, TC, CTC, and DMC in sheep liver and cattle kidney	Extraction with succinate buffer, dilution with EDTA–pentanesulphonic buffer, cleanup with C8 or XAD–2 SPE cartridge and MCAC	DL = 10 µg/kg (OTC)	[81]
Spherisorb ODS1	0.025 M oxalic acid solution–ACN–THF (75:22:5:2.5, v/v/v)	UV 355 nm	OTC in bryophyte	Extraction with acetone and MacIlvaine buffer (50:50, v/v) saturated with EDTA	DL = 30 ng/g QL = 100 ng/g Rec: 48%	[64]

UV detection, diode-array detector (DAD) and fluorescence have been the detection techniques used, coupled to HPLC for the analysis of OTC. UV detection is set at 355 nm [49–51], 350 nm [40], or at 353 nm [52]. Using the diode array detector [49] offers advantages that the target peak can be identified by its retention time and absorption spectrum. Compared to UV detection, fluorescence detection is generally more specific and is less interfered by other compounds in the sample matrix [51]. A HPLC method with electrochemical detection has also been suggested recently. Zhao *et al.* [53] described HPLC with a coulometric electrode array system for the analysis of OTC, TC, CTC, DC, and methacycline (MC) in ovine milk. An amperometric detection coupled with HPLC was developed by Kazemifard and Moore [54] for the determination of tetracyclines in pharmaceutical formulations.

For confirmatory assay, liquid chromatography–tandem mass spectrometry (LC–MS/MS) is becoming more frequently used in the analysis of OTC owing to its high sensitivity and ability. Electrospray ionization (ESI) [55–57] and atmospheric pressure chemical ionization (APCI) [41] methods combined with tandem mass spectrometry are favored because of their higher sensitivity and better reproducibility. Hamscher *et al.* [58] developed a method for the determination of persistent TC residues in soil fertilized with manure by HPLC tandem mass spectrometry, MS–MS, and confirmation by MS–MS–MS. Zhu *et al.* [59] developed an LC–tandem mass spectrometry for the analysis of common tetracyclines in water. The detection limit for oxytetracycline was 0.21 μg/L. Lykkeberg *et al.* [60] used LC–MS/MS for determination of oxytetracycline and its impurities EOTC, TC, ETC, ADOTC, α-AOTC, and β-AOTC.

The HPLC analysis of OTC in bulk substances and pharmaceutical formulations is done generally without any problems in the sample preparation step [1,2]. Papadoyannis *et al.* [61] described a HPLC method for the determination of OTC in commercial pharmaceuticals, in which samples were simply diluted in the appropriate solvent. The main difficulty of the oxytetracycline analysis especially in biological materials comes from the matrix samples, since OTC may be strongly bound to protein and metal ions in the sample. Therefore, various extraction and cleanup procedures have been developed to achieve the best separation and accuracy. Buffer solutions containing weak acids and chelating agents and solid-phase extraction cartridges are generally used for the extraction and cleanup of the analyte from the sample [62]. Furusawa [63] introduced a nonorganic solvent for extraction of OTC from milk samples. Delépée and Pouliquen [64] used ion-paired solid-phase extraction for the determination of OTC in the bryophyte *Fontinalis antipyretica*. The extraction and cleanup of antibiotics used in agriculture was reviewed by Oka *et al.* [65] and presented more detail in later section.

9. DETERMINATION OF OTC RESIDUES IN FOOD AND FISHERIES PRODUCTS

Oxytetracycline is a broad-spectrum antibiotic, which has been used worldwide in veterinary medicine and in aquaculture for the prevention and treatment of disease and as feed additives to promote growth. The maximum residue limits (MRLs) of OTC and relative substances as described by the US Food and Drug Administration [66] and European Union [67] are presented in Table 4.

Table 4. The maximum residue limit (MRL) of oxytetracycline and related substances [66,67]

Antibiotics	Marker residue	Animal species	MRL (ppm) EC	MRL (ppm) US FDA	Target tissues
OTC	Sum of parent drug (and its 4-epimer)*	All food producing species	0.1	2	Muscle
			0.3	6	Liver
			0.6	12	Kidney
			0.1	0.3	Milk
			0.2	n.a.**	Eggs
TC	Sum of parent drug (and its 4-epimer)*	All food-producing species	0.1	2	Muscle
			0.3	6	Liver
			0.6	12	Kidney
			0.1	n.a.	Milk
			0.2	n.a.	Eggs
CTC	Sum of parent drug (and its 4-epimer)*	All food-producing species	0.1	2	Muscle
			0.3	6	Liver
			0.6	12	Kidney
			0.1	n.a.	Milk
			0.2	0.4	Eggs
DC	Doxycycline	Bovine	0.1	n.a.	Muscle
			0.3	n.a.	Liver
			0.6	n.a.	Kidney
		Porcine, poultry	0.1	n.a.	Muscle
			0.3	n.a.	Skin + fat
			0.3	n.a.	Liver
			0.6	n.a.	Kidney

EC = European Comission; US FDA = United State Food and Drug Administration;* for EC
** data not available.

Numerous analytical methods for antibiotics residues in foods and fisheries products have been reported in the literature over past 25 years or more. Most of them require multistep sample preparation and cleanup. The analysis of OTC residues often presents difficulties mainly due to their trace levels in biological samples and to the complexity of the sample matrixes. Immunoassays have been used as methods for OTC analysis, but this method is only semiquantitative and less selective. Several commercially microbial inhibition or immunological kit tests have been developed for screening OTC in food samples [34,68,69]. Moats *et al.* [33] compared a radioimmunoassay (Charm II®) test with HPLC method for detection of oxytetracycline residues in milk sample. Mascher *et al.* [32] reported the ELISA kit Ridascreen® "Tetracycline" for semiquantitative determination of oxytetracycline residues in honey. The detection limit was reported lower than 50 ppb. Such test kit can detect the whole group of antibiotics, so that it is not selective and needs further confirmation using HPLC or LC-MS. An excellent review of test kit technology for antibiotics used in agriculture was made by Boison and MacNeil [70]. A solid phase fluorescence immunoassay (SPFIA) has been recently introduced for the analysis of antibiotics including OTC residues in milk, in bovine and in porcine kidneys. The SPFIA is suggested as an alternative to classical inhibition test for screening oxytetracycline. The limit detection for oxytetracycline was 300 ppb [71].

OTC can be well separated from TC, DC, and its impurities by means of capillary electrophoresis [25]. However, the use of CE in the analysis of OTC residues is restricted because of the low concentration sensitivity of this technique [28]. HPLC is by far the most widely used method for the analysis of OTC residues in food and fisheries products. Chromatographic analysis of tetracycline including OTC analysis in foods was reviewed by Oka *et al.* [65] and MacNeil [72]. HPLC methods for the analysis of OTC are summarized in Table 2.

Since OTC is strongly bound to the protein of biological materials, it is difficult to extract the OTC residues into organic solvent. Reported methods involve generally long and tedious sample extraction and cleanup including liquid–liquid extraction, solid-phase extraction (SPE) [73,74], or matrix solid phase dispersion (MSPD) [73,75]. The majority of investigators used acidic buffers at pH 2–4 combined with solid-phase extraction (SPE) for extraction and cleanup of OTC residues from food and fisheries products. SPE provides not only to eliminate interfering substances but also to concentrate samples and improve the accuracy of the method. SPE using the reversed-phase octadecyl (C_{18}) cartridge is the most widely used to clean up the samples. A problem such as low percentage recovery appears when the RP C18 cartridge is used due to the interaction of OTC with residual silanol and metal ions in silica-based sorbants. To overcome these problems, chelating agents are often used for the pretreatment of the C18 cartridge or added to the eluent of the cartridge. Oka *et al.* [75] and Kijak *et al.* [76] used a 0.1-M EDTA–McIlvaine buffer that resulted in more consistent recoveries for TCs extracted from samples. Blanchflower *et al.* [41] described the use of a glycine buffer for C18 extraction of TCs from muscle and kidney samples. Posyniak *et al.* [77] validated a procedure for simultaneous determination of OTC, TC, and CTC residues in animal tissues using oxalic a styrene-divinylbenzene column for SPE cleanup. The Use of this cartridge was reported to give higher and more reproducible recovery of analytes compared with other SPE sorbants. One-step liquid chromatographic method has been published by Coyne *et al.* [78] for OTC analysis of fish muscles. In that method, the fish muscle was homogenized in MacIlvaine buffer (pH 4.0) containing EDTA followed by precipitation of proteins using trichloroacetic acid (TCA). For the spiked concentration ranged from 0.04 to1.0 μg/g, the percentage recovery of 33–35% and the precision between 1.9% and 7.5% were reported. The addition of TCA as an additional protein-denaturing step was reported to decrease the SPE column blockade [51]. A comparison between SPE and MSPD as pre-separation technique has also been discussed for the determination of OTC, TC, and CTC in meat, milk, and cheese [73]. In this study, SPE was performed using Sep-Pak RP–18 cartridges, whilst Bakerbond C–18 bulk LC packing (40 μm, 60 Å) was used for MSPD. The extraction recoveries of OTC were reported to range from 52% to 90% for SPE and from 79% to 93% for MSPD at concentration levels between 100 ng/g and 1000 ng/g samples. Some authors used copolymeric SPE cartridges to serve a simplified sample cleanup for the analysis of OTC in shrimps and milk, salmon muscle, animal tissues, and products [51,62]. Cheng *et al.* [79] described a simple method using cartridges containing a macroporous polymer, poly(divinylbenzene-co-*N*-vinylpyrrolidone) for the determination of OTC in porcine serum. In that method, the use of this sorbant was reported to give better recovery than reversed silica-based sorbants.

This cleanup procedure was also applied for routine analysis of TCs in ground water and lagoon water samples [59] and for shrimps [77].

The use of ion-pairing liquid chromatography was reported to minimize sample cleanup of the OTC residues analysis in eggs and broiler meat [49]. The study involved using a polymeric analytical column, which demonstrated higher accuracy and lower peak tailing compared to silica-based bonded column. A selective cleanup technique by metal chelate affinity chromatography (MCAC) has been introduced for the cleanup of OTC in food, serum, and urine samples [40,50,80]. The technique was based on the interaction of OTC with metal ions to form chelate compounds, which usually results in lower accuracy of the more conventional SPE methods. The original technique was then miniaturized by Capolongo *et al.* [50] adopting a mini SPE column and applied for the cleanup of tissue samples for the analysis of oxytetracycline and its 4′-epimer. The MCAC has been developed by Stubbings *et al.* [81] as an online cleanup procedure prior to HPLC (MCAC-HPLC). Cooper *et al.* [40] reported that MCAC-HPLC shows higher throughput, higher recovery, and lower detection limit for the determination of oxytetracycline compared to off-line MCAC-HPLC.

The LC–MS/MS method has been recently developed by Andersen *et al.* [62] for simultaneous determination of OTC residues in shrimp and whole milk. The analysis was based on the extraction of the samples with succinic acid followed by cleanup using a copolymeric solid phase extraction column and confirmation of the residues using electrospray ionization LC–MS/MS. Using this method OTC, TC, and CTC were confirmed in shrimp samples from 25 to 400 ng/g. The multi-residue analysis of tetracycline antibiotics including OTC, TC, CTC, DC, and their 4-epimers in pig tissues was reported by Cherlet *et al.* [57] using liquid chromatography combined with positive-ion electrospray ionization mass spectrometry. The samples were treated with sodium succinate solution (pH 4.0) followed by protein removal with trichloroacetic acid and paper filtration. A polymeric reversed phase cartridge was used for the cleanup to obtain an extract suitable for LC–MS/MS analysis. Using a PLRP-S polymeric reversed column, the method was reported to give the limit detection between 0.5 and 4.5 ng/g.

For the analysis of OTC residues and its related substances in food and fisheries products, LC–MS/MS is presently the most modern and promising method due to its high sensitivity, reproducibility, and specificity.

10. LIST OF ABBREVIATIONS

ADOTC	2-acetyl-2-decarboxamido-oxytetracycline
AOTC	anhydro-oxytetracycline
α-AOTC	α-apo-oxytetracycline
β-AOTC	β-apo-oxytetracycline
APCI	atmospheric pressure chemical ionization
BP	British Pharmacopoeia
CTC	chlortetracycline
DC	doxycycline

DMC	demeclocycline
ELISA	enzyme-linked immunosorbent assays
EOTC	4-epi-oxytetracycline
ESI	electrospray ionization
LC	liquid chromatography
LC-MS	liquid chromatography–mass spectrometry
MC	methacycline
MCAC	metal chelate affinity chromatography
MSPD	matrix solid phase dispersion
OTC	oxytetracycline
RIAs	radioimmunoassays
SPE	solid phase extraction
TC	tetracycline
USP	United States Pharmacopoeia

REFERENCES

[1] *United States Pharmacopoeia 28*, United States Pharmacopoeial Convention, Inc., Rockville, MD, 2004, pp. 1387–1392.
[2] *European Pharmacopoeia*, 4th edn., Council of Europe, Strasbourg, France, 2001, pp. 1693–1696.
[3] *Japanese Pharmacopoeia*, 14th edn., Society of Japanese Pharmacopoeia, Japan, 2001, p. 665.
[4] *British Pharmacopoeia 2003*, Vol. I, The Stationary Office, London, UK, 2003, pp. 1401–1405.
[5] *The International Pharmacopoeia*, 3rd edn., Vol. 3, World Health Organization, Geneva, 1988, pp. 231–237.
[6] *Pharmacopoeia of the People's Republic of China*, Vol. II, Chemical Industry Press, Beijing, 1997, pp. 439–440.
[7] *Indian Pharmacopoeia 1996*, Vol. 1, The Controller of Publications, Delhi, 1996, pp. 543–548.
[8] *Farmakope Indonesia (Indonesian Pharmacopoeia)*, Edisi IV, Departemen Kesehatan Republik Indonesia, Jakarta, 1995, pp. 639–640.
[9] M. Kurzawa and A. Kowalczyk-Marzec, *J. Pharm. Biomed. Anal.*, 2004, **35**, 95–102.
[10] Y. M. Issa, A. L. El-Ansary and A. S. Tag-Eldin, *Microchim. Acta*, 2000, **135**, 97–104.
[11] C. M. C. M. Couto, J. L. F. C. Lima, M. Conceição, B. S. M. Montenegro and S. Reis, *J. Pharm. Biomed. Anal.*, 1998, **18**, 527–533.
[12] N. Wangfuengkanagul, W. Siangproh and O. Chailapakul, *Talanta*, 2004, **64**, 1183–1188.
[13] X. X. Sun, X. Zhang and H. Y. Aboul-Enein, *Il Farmaco*, 2004, **59**, 307–314.
[14] J. M. L. Galego and J. P. Arroyo, *Anal. Chim. Acta*, 2002, **460**, 85–97.
[15] N. Samola and U. Urleb, *Anal. Chim. Acta*, 2000, **410**, 203–210.
[16] R. Fernandez-Gonzáles, M. S. Garcia-Falcón and J. Simal-Gándara, *Anal. Chim. Acta*, 2002, **455**, 143–148.
[17] M. B. Rao, P. S. Ramamurthy, V. S. Rao, M. Basanti Rao and V. Suryanarayana Rao, *Indian J. Pharm. Sci.*, 1996, **58**, 254–255.
[18] Y. Rakicioglu, J. H. Perrin and S. G. Schulman, *J. Pharm. Biomed. Anal.*, 1999, **20**, 397–399.
[19] N. Arnaud and J. Georges, *Analyst*, 2001, **126**, 694–697.
[20] G. Chen, M. J. Schneider, A. M. Darwish, S. J. Lehotay and D. W. Freeman, *Talanta*, 2004, **64**, 252–257.
[21] H. Han, Z. He and Y. Zeng, *Anal. Sci.*, 1999, **15**, 467–470.
[22] X. Zheng, Y. Mei and Z. Zhang, *Anal. Chim. Acta*, 2001, **440**, 143–149.
[23] J. Tjørnelund and S. H. Hansen, *J. Chromatogr. A*, 1997, **779**, 235–243.
[24] J. Tjørnelund and S. H. Hansen, *J. Pharm. Biomed. Anal.*, 1997, **15**, 1077–1082.

[25] Y. M. Li, A. Van Schepdael, E. Roets and J. Hoogmartens, *J. Pharm. Biomed. Anal.*, 1997, **15**, 1063–1069.
[26] T. B. Chen, W. H. Deng, W. H. Lu, R. M. Chen and P. F. Rao, *Chinese J. Chromatogr.*, 2001, **19**, 91–93.
[27] J. Zhou, G. C. Gerhardt, A. Baranski and R. Cassidy, *J. Chromatogr. A*, 1999, **839**, 193–201.
[28] L. Nozal, L. Arce, B. M. Simonet, A. Rios and M. Valcárcel, *Anal. Chim. Acta.*, 2004, **517**, 89–94.
[29] C. E. Tsai and F. Kondo, *J. Food Protection*, 2001, **64**, 361–366.
[30] S. Young and K. Carlson, *Water Res.*, 2004, **38**, 3155–3166.
[31] D. S. Aga, R. Goldfish and P. Kulsrestha, *Analyst*, 2003, **128**, 658–662.
[32] A. Mascher, S. Lavagnoli and M. Curatolo, *Apidologie*, 1996, **27**, 229–233.
[33] W. A. Moats, K. L. Anderson, J. E. Rushing and D. P. Wesen, *Am. J. Vet. Res.*, 1995, **56**, 795–800.
[34] P. Popelka, J. Nagy, P. Popelka, S. Marcinčák, H. Różanska and J. Sokol, *Bull. Vet. Inst. Pulawy*, 2004, **48**, 273–276.
[35] J. Krzek, A. Kwiecien, M. Starek, A. Kierszniewska and W. Rzeszuko, *J. AOAC Int.*, 2000, **83**, 1502–1506.
[36] *Camag Bibliographic Service*, version 1.08, Camag, Muttenz, 2003.
[37] M. S. Diaz-Cruz, M. L. Lopez de Alda and D. Barceló, *Trends Anal. Chem.*, 2003, **22**, 340–351.
[38] G. Lunn, *HPLC Methods for Pharmaceutical Analysis*, Vol. 4, Wiley-Interscience Publication, John Wiley & Sons, Inc., New York, 2000, pp. 1250–1256.
[39] N. Furusawa, *J. Chromatogr. A*, 1999, **839**, 247–251.
[40] A. D. Cooper, G. W. F. Stubbings, M. Kelly, J. A. Tarbin, W. H. H. Farrington and G. Shearer, *J. Chromatogr. A*, 1998, **812**, 321–326.
[41] W. J. Blanchflower, R. J. McCracken, A. S. Haggan and D. G. Kennedy, *J. Chromatogr. B*, 1997, **692**, 351–360.
[42] G. J. Reimer and L. M. Young, *J. Assoc. Off. Anal. Chem.*, 1990, **73**, 813–817.
[43] V. M. Moreti, G. L. Albertini, F. Bellagamba, U. Luzzana, G. Serrini and F. Valfre, *Analyst*, 1994, **119**, 2749–2751.
[44] H. Pouliquen, D. Gouelo, M. Larhantec, N. Pilet and L. Pinault, *J. Chromatogr. B*, 1997, **702**, 157–162.
[45] M. Touraki, P. Rigas, P. Pergandas and C. Kastritsis, *J. Chromatogr. B*, 1995, **663**, 167–171.
[46] L. Monser and F. Darghouth, *J. Pharm. Biomed. Anal.*, 2004, **23**, 353–362.
[47] H. Pouliquen, D. Keita and L. Pinault, *J. Chromatogr.*, 1992, **627**, 287–293.
[48] M. C. Carson, G. Bullock and J. Bebak-Williams, *J. AOAC Int.*, 2002, **85**, 2, 341–348.
[49] H. De Ruyck, H. De Ridder, R. Van Rentergem and F. Van Wambeke, *Food-Addit. Contam.*, 1999, **16**, 2, 47–56.
[50] F. Capolongo, A. Santi, L. Tomasi, P. Anfosi, M. Missagia and C. Montesissa, *J. AOAC Int.*, 2002, **85**, 8–14.
[51] A. L. Pena, C. M. Lino, M. Irene and N. Silviera, *J. AOAC Int.*, 2003, **86**, 5, 925–929.
[52] G. Boatto, A. Pau, M. Palomba, L. Arenare and R. Cerri, *J. Pharm. Biomed. Anal.*, 1999, **20**, 321–326.
[53] F. Zhao, X. Zhang and Y. Gan, *J. Chromatogr. A*, 2004, **1055**, 109–114.
[54] A. G. Kazemifard and D. E. Moore, *J. Pharm. Biomed. Anal.*, 1997, **16**, 689–696.
[55] S. P. Khong, Y. A. Hammel and P. A. Guy, *Rapid Commun. Mass Spectrom.*, 2005, **19**, 493–502.
[56] M. L. Loke, S. Jespersen, R. Vreeken, H. Sørensen and J. Tjørnelund, *J. Chromatogr. B*, 2003, **783**, 11–23.
[57] M. Cherlet, M. Schelkens, S. Croubels and P. De Backer, *Anal. Chim. Acta*, 2003, **492**, 199–213.
[58] G. Hamscher, S. Sczesny, H. Höper and H. Nau, *Anal. Chem.*, 2002, **74**, 1509–1518.
[59] J. Zhu, D. D. Snow, D. A. Cassada, S. J. Monson and R. F. Spalding, *J. Chromatogr. A*, 2001, **98**, 177–186.
[60] A. K. Lykkeberg, B. Halling-Sørensen, C. Cornett, J. Tjørnelund and S. H. Hansen, *J. Pharm. Biomed. Anal.*, 2004, **34**, 325–332.
[61] I. N. Papadoyannis, V. F. Samanidou and L. A. Kovatsi, *J. Pharm. Biomed. Anal.*, 2000, **23**, 273–280.
[62] W. C. Andersen, J. E. Roybal, S. A. Gonzales, S. B. Turnipseed, A. P. Pfenning and L. R. Kuck, *Anal. Chim. Acta*, 2004, **529**, 145–150.
[63] N. Furusawa, *LC-GC North America*, 2003, **21**, 362–364.

[64] R. Delépée and H. Pouliquen, *Anal. Chim. Acta*, 2003, **475**, 117–123.
[65] H. Oka, H. Nakazawa, K.-I. Harada and J. D. MacNeil (eds.) *Chemical Analysis of Antibiotics Used in Agriculture*, AOAC International, Arlington, 1995.
[66] *U.S. Food and Drug Administration, Code of Federal Regulation*, Title 21, Part 556, Sections 150, 500, and 720, US Government Printing Office, Washington, DC, 2003, Chap. 1; http://www.accessdata.fda.gov/scripts/cdrh/cfdocs/cfcfr/CFRSearch.cfm? fr=556.500 (April 30, 2005).
[67] *Commision Regulation (EC) No 1570/98*, European Commission, *Official Journal of the European Communities*, L 205, Brussels, July 17, 1998; http://www.europa.eu.int/eur-lex/en/archive/1998/l_20519980722en.html (April 30, 2005).
[68] J. Kurittu, S. Lonnberg, M. Virta and M. Karp, *J. Food Prot.*, 2000, **63**, 953–957.
[69] K. De wasch, L. Okerman, S. Croubels, H. De Brabander, J. Van Hoff and P. De Backer, *Analyst*, 1998, **123**, 2737–2741.
[70] J. O. Boison and J. D. MacNeil, New Test Kit Technology, in: H. Oka, H. Nakazawa, K.-I. Harada and J. D. MacNeil (eds), *Chemical Analysis of Antibiotics Used in Agriculture*, AOAC International, Arlington, 1995, pp. 77–119.
[71] L. Okerman, K. D. Wasch and J. Van Hoof, *J. AOAC Int.*, 2003, **86**, 2, 236–240.
[72] J. D. MacNeil, *J. AOAC Int.*, 2002, **85**, 252–253.
[73] E. Brandšteterová, P. Kubalec, L. Bovanová, P. Simko, A. Bednáriková and L. Macháčková, *Z. Lebensm. Unters. Forsch, A*, 1997, **205**, 311–315.
[74] N. Furusawa, *Talanta*, 2003, **59**, 155–159.
[75] H. Oka, Y. Ito, T. Goto, T. Minami, I. Yamamoto and H. Matsumoto, *J. AOAC Int.*, 2003, **86**, 494–500.
[76] P. J. Kijak, C. V. Cope and W. M. Pedersoli, *J. AOAC Int.*, 1999, **82**, 1329–1333.
[77] A. Posyniak, J. Zmudzki, R. L. Ellis, S. Semeniuk and J. Niedzielska, *J. AOAC Int.*, 1999, **82**, 4, 862–865.
[78] R. Coyne, Ø. Bergh and O. B. Samuelsen, *J. Chromatogr. B*, 2004, **810**, 325–328.
[79] Y.-F. Cheng, D. J. Phillips and U. Neue, *Chromatographia*, 1997, **44**, 187–190.
[80] W. H. H. Farrington, J. Tarbin, J. Bygrave and G. Shearer, *Food Addit. Contam.*, 1991, **8**, 55–64.
[81] G. Stubbings, J. A. Tarbin and G. Shearer, *J. Chromatogr. B*, 1996, **679**, 137–145.

Penicillamine: Physical Profile

Abdulrahman Al-Majed, Fathallah Belal, Saeed Julkhuf, and Hussein El-Subbagh

Department of Pharmaceutical Chemistry, College of Pharmacy, King Saud University, P.O. Box 2457, Riyadh 11451, Saudi Arabia

Contents

PROFILES OF DRUG SUBSTANCES, EXCIPIENTS, AND RELATED METHODOLOGY, VOLUME 32
ISSN: 0099-5428

DOI: 10.1016/S0099-5428(05)32004-1

1. DESCRIPTION

1.1. Nomenclature

1.1.1. Chemical names [1]

3-Mercapto-(D)-valine; β,β-dimethylcysteine; α-amino-β-methyl-β-mercaptobutyric acid; β-thiovaline.

1.1.2. Nonproprietary names [2]

Penicillamine is the United States-adopted name for (D)-penicillamine.

1.1.3. Proprietary names [1,2]

Cuprimine; Cuprenil; Depamine; Mercaptyl; Pendramine; Depen; Distamine; DMC; Trolovol; Kelatin; Metalcaptase.

1.2. Formulae [1]

1.2.1. Empirical formula, CAS number, and molecular weight

Penicillamine	$C_5H_{11}NO_2S$	[52-67-5]	149.21
Penicillamine·HCl	$C_5H_{11}NO_2S·HCl$	[- - - - -]	185.50

1.2.2. Structural formula

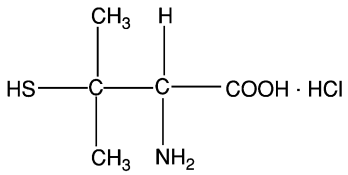

1.3. Elemental analysis

The theoretical elemental composition of penicillamine is as follows:

Carbon	40.20%
Hydrogen	7.43%
Nitrogen	21.45%
Oxygen	9.39%
Sulfur	21.49%

1.4. Appearance

Penicillamine is a white or almost white, finely crystalline powder, having a slight characteristic odor and a slightly bitter taste [3].

2. PHYSICAL CHARACTERISTICS

2.1. Ionization constant

The titration curve of penicillamine hydrochloride at 25 °C revealed the presence of three ionizable groups with pK_a values of 1.8 (carboxyl group), 7.9 (α-amino group), and 10.5 (*β*-thiol group). Recently, the ionization constants for the acidic functions of (D)-penicillamine were verified by pH titration at 37 °C and 0.15 M ionic strength [2]. A 1% solution in water has a pH of 4.5–5.5 [3].

2.2. Solubility characteristics

Penicillamine is freely soluble in 9 parts of water, slightly soluble in 530 parts of ethanol (alcohol), slightly soluble in other alcohols, and practically insoluble in chloroform and ether at 20 °C [2].

2.3. Optical activity

The enantiomers of this drug differ in their efficacy and activity, with (D)-penicillamine being the enantiomer required for pharmaceutical preparations. The (*L*)-enantiomer is toxic, and its absorption by the human body is more than the (*D*)-enantiomer. While both enantiomers of penicillamine are desulfhydrated by (*L*)-cysteine desulfhydrase, only the (l)-isomer inhibits the action of this enzyme [2].

The reported optical rotation values for (D)-penicillamine are:

$[\alpha] = -63\,^{\circ}\text{C} = 0.1$ in pyridine
$[\alpha] = -61.3\,^{\circ}\text{C} = 2.5$ in 1.0 M NaOH

The specific rotation range required by official compendia is between (−58 °C and −68 °C), determined in a 5% solution in 1.0 M NaOH at 25 °C [1,2].

2.4. Particle morphology

Under the polarizing microscope, both polymorphs of (*D*)-penicillamine were seen as anisotropic crystals, with Form I existing as needles and Form II as plates.

2.5. Crystallographic properties

Two polymorphs of (*D*)-penicillamine are known [2], with the existence of these being confirmed using infrared spectroscopy and X-ray crystallography. It was reported that Form I has a minimum between its IR peaks at 1078 and 1101 cm^{-1} that are less intense than the adjacent peaks at about 1050 and 1160 cm^{-1}, while Form II has an absorption peak at 1092 cm^{-1} which is more intense than the adjacent peaks at about 1050 and 10160 cm^{-1} [2].

The X-ray powder diffraction pattern of (*D*)-penicillamine was obtained using a Siemens XRD-5000 diffractometer, and the powder pattern is shown in Fig. 1. A summary of the crystallographic data deduced from the pattern of (*D*)-penicillamine is located in Table 1.

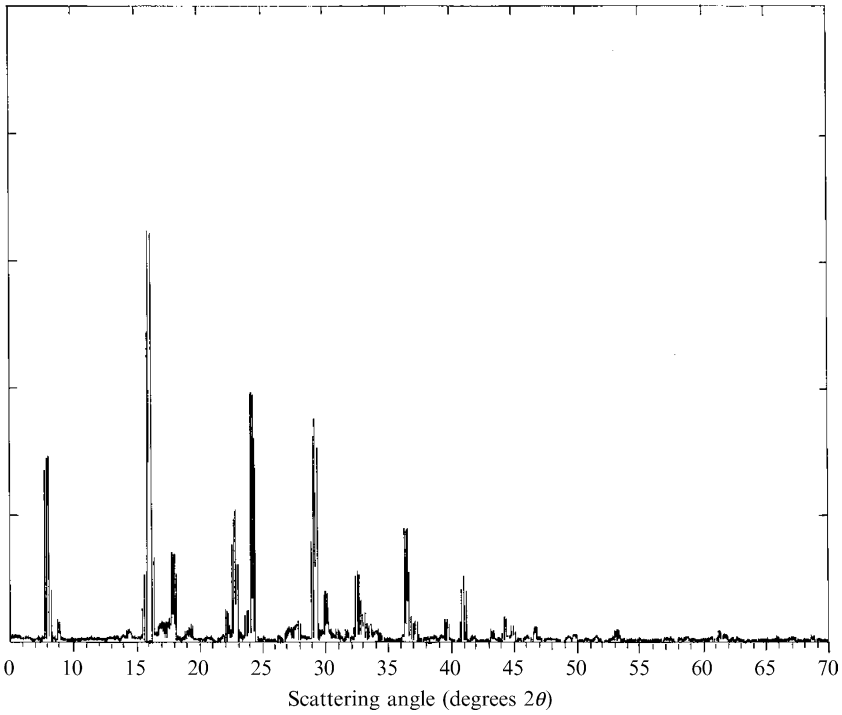

Fig. 1. X-ray powder diffraction pattern of (D)-penicillamine.

2.6. Hygroscopicity

Penicillamine is obtained as hygroscopic crystals.

2.7. Thermal methods of analysis

2.7.1. Melting behavior

The melting point temperatures reported for penicillamine are: m.p. = 198, 198.5, and 212 °C [2].

2.7.2. Thermogravimetry

The only thermal event in the differential thermal analysis curve of (*D*)-penicillamine is the melting endotherm at 185 °C. Either polymorph of (*D*)-penicillamine gives the same endotherm [2].

2.8. Spectroscopy

2.8.1. Vibrational spectroscopy

The infrared absorption spectrum of (*D*)-penicillamine was obtained using a Perkin-Elmer infrared spectrophotometer. The spectrum shown in Fig. 2 was obtained with

Table 1. Crystallographic data from the X-ray powder diffraction pattern of (*D*)-penicillamine

Scattering angle (degrees 2θ)	*d*-spacing (Å)	Relative intensity (%)	Scattering angle (degrees 2θ)	*d*-spacing (Å)	Relative intensity (%)
8.023	11.0107	45.12	8.875	9.9551	4.84
16.088	5.5044	100.00	17.992	4.9251	21.87
19.336	4.5867	4.31	22.203	4.0005	7.57
22.856	3.8876	32.33	24.251	3.5670	50.56
27.839	3.2020	5.33	29.220	3.0537	54.80
30.049	2.9717	12.34	31.705	2.8199	2.97
32.537	2.7495	17.55	33.021	2.7104	7.11
36.485	2.4507	27.97	37.139	2.2689	5.65
10.996	2.1997	15.27	43.333	2.08963	2.54
11.275	2.0441	73.25	5.05	44.923	2.0161
3.85	45.711	1.9130	43.87	3.52	53.170
1.7212	3.17	21.312	1.5107	31.87	2.63
58.752	1.3642	1.41	16.088	5.5044	100.00
24.251	3.5570	50.55	29.220	3.0537	54.80
8.023	11.0107	45.12	22.856	3.8875	32.33
36.485	2.4507	27.97	17.992	4.9261	21.87
32.537	2.7496	17.55	40.995	2.1997	15.27
30.045	2.9717	12.34	22.203	4.0005	5.67
33.021	2.7104	7.11	44.275	2.0441	6.05
39.593	2.2589	5.65	37.139	2.4188	5.37
27.829	2.2020	5.33	8.875	9.9551	4.84
19.336	4.5857	4.31	44.923	2.0151	3.85
46.711	1.9430	3.82	53.170	1.7212	3.17
31.705	2.8199	2.97	43.333	2.0863	2.54
51.312	1.5107	2.53	68.752	1.3542	1.41

the compound being compressed in a KBr pellet, and the assignments for the major IR absorption bands are shown in Table 2.

2.8.2. Nuclear magnetic resonance spectroscopy

2.8.2.1. ^{1}H NMR spectrum

The ^{1}H NMR spectrum of (*DL*)-penicillamine in D_2O was obtained on a Bruker 500 MHz instrument, and the resulting spectrum is shown in Fig. 3. Confirmation of the spectral assignments was derived from a COSY experiment (see Fig. 4), and these assignments are summarized in Table 3.

Two singlet bands were observed at chemical shifts of 1.37 and 1.45 ppm, each of which integrated for three protons, and were assigned to the two methyl groups. A singlet at 3.59 ppm, integrated for one proton, was assigned to the CH function. The COSY experiment showed a small degree of long range coupling between the two methyl groups and the CH group.

2.8.2.2. ^{13}C NMR spectrum

The noise-modulated broadband decoupled ^{13}C NMR spectrum of (*DL*)-penicillamine is shown in Fig. 5. Two methyl carbons were found to resonate at chemical shifts of 27.7 and 30.2 ppm, in addition to a CH carbon at 64.6 ppm. Two quaternary

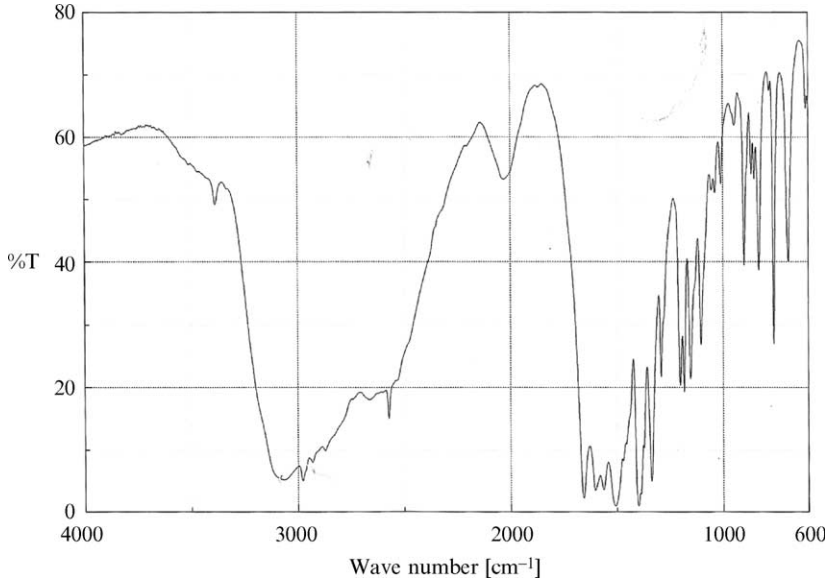

Fig. 2. Infrared absorption spectrum of (*D*)-penicillamine.

Table 2. Assignments for the main infrared absorption bands of penicillamine

Energy (cm^{-1})	Band assignment
3066	$-NH_3^+$
2932	$-NH_3^+$
2662	$-SH$
1655	$-CO_2$
1291	$-CO_2$

absorptions were observed at 43.8 and 171.5 ppm. These assignments were confirmed by DEPT and HSQC experiments (Fig. 6), and summarized in Table 4.

2.8.3. Mass spectrometry

The mass spectrum of (*DL*)-penicillamine was obtained utilizing a Shimadzu PQ 0–5000 mass spectrometer. The detailed mass fragmentation pattern is shown in Fig. 7, where a base peak was observed at *m*/*z* 75. The proposed mass fragmentation pattern of (*DL*)-penicillamine is summarized in Table 5. It is worth mentioning that the drug did not show a molecular ion peak. A proposed scheme of the MS fragmentation pattern of (*DL*)-penicillamine is shown in Fig. 8.

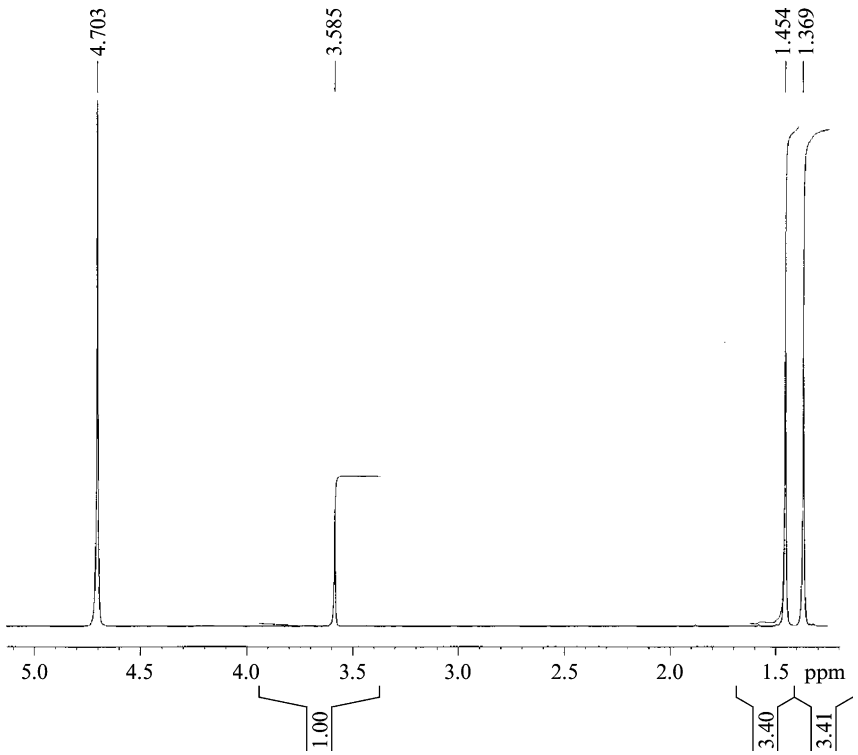

Fig. 3. ^{1}H NMR spectrum of (*D*)-penicillamine.

3. STABILITY

3.1. Solid-state stability

Penicillamine is relatively stable in both light and air, so the conventional storage conditions are that it should be stored in a well container, protected from light [1, 4]. Penicillamine is relatively stable *in vivo* as well.

3.2. Solution-phase stability

Aqueous solutions of (*D*)-penicillamine are comparatively stable at pH 2–4, and it degrades slowly by first order or pseudo-first order kinetics in aqueous solutions. A 3% solution of penicillamine hydrochloride stored under nitrogen in a sealed container at 20 °C decomposed to the extent of about 10% per year [2].

3.3. Stability in biological fluids

Under *in vivo* conditions, the free thiol has also been found in plasma and urine of patients with rheumatoid arthritis after treatment with the drug. It was also found

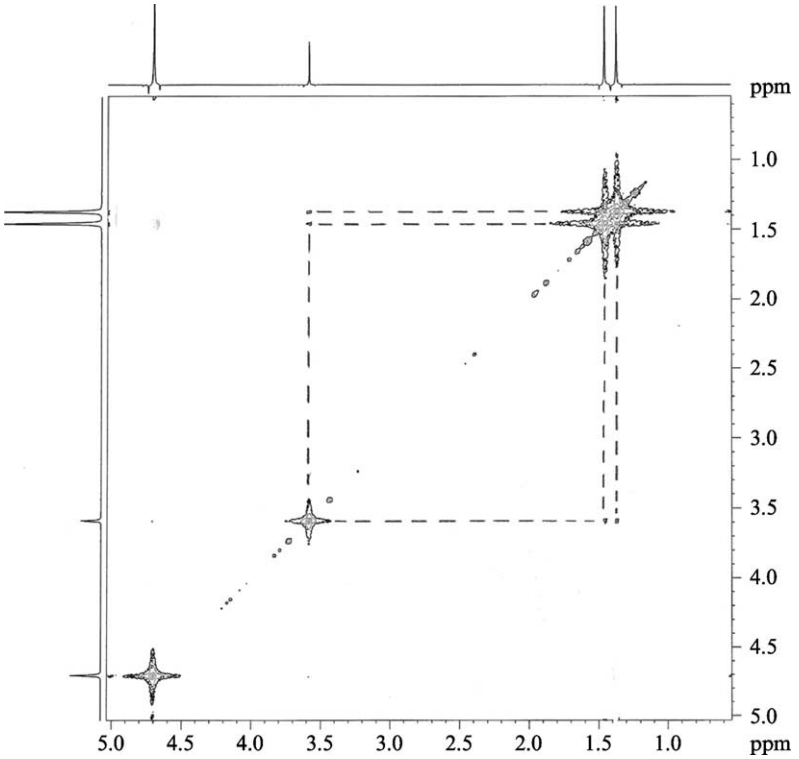

Fig. 4. COSY-NMR spectrum of (*D*)-penicillamine.

Table 3. Summary of assignments for the ^{1}H NMR spectrum of (*D*)-penicillamine

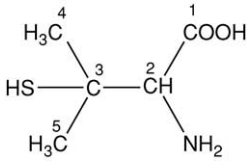

Chemical shift, relative to TMS (ppm)*	Number of protons	Multiplicity	Assignment
1.37	3	s	$-CH_3$
1.45	3	s	$-CH_3$
3.59	1	s	$-CH$

*Signal at 4.70 ppm is for D_2O.

the stable copper–(*D*)-penicillamine complex shows a high superoxide reactivity, which may be responsible for the therapeutic effects in rheumatoid arthritis [2].

3.4. Incompatibilities with functional groups

The three functional groups of penicillamine enable it to take part in a number of chemical reactions.

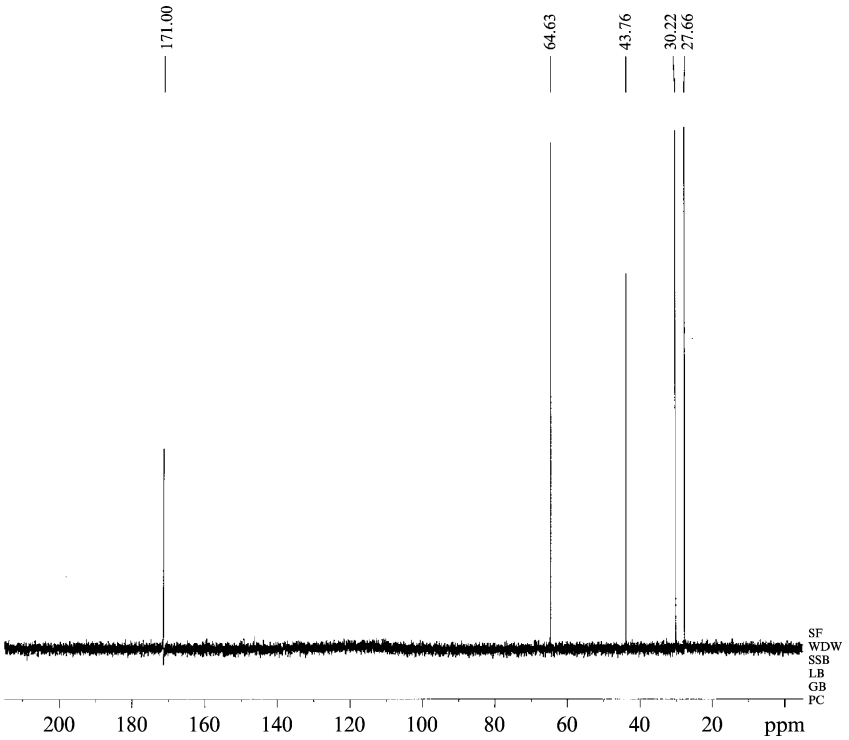

Fig. 5. ^{13}C NMR spectrum of (*D*)-penicillamine.

3.4.1. Chelation of metals

Penicillamine is known to form complexes of varying stability with several metal ions. In neutral solution, penicillamine complexes with mercury, lead, nickel, and copper are relatively more stable than those of zinc, iron, and manganese. The three functional groups of penicillamine may be engaged in the formation of metal complex, and the resultant compounds may be polymeric in structure.

3.4.2. Sulfydryl–disulfide exchange

Xu *et al.* [5] described the effect of (*D*)-penicillamine on the binding of several anti-acetylcholine receptor monoclonal antibodies to the *Torpedo acetylcholine* receptor. Penicillamine is covalently incorporated into the acetylcholine receptor through SS exchange at the cysteine residues of the α-subunit, altering the antigenic structure of the receptor. This effect on the structure of the native receptor at the neuromuscular junction may be responsible for the establishment of the autoimmune response to the acetylcholine receptor in (*D*)-penicillamine-induced myasthenia gravis. Cysteine and penicillamine interact to form penicillamine-cysteine mixed disulfide complexes [6]:

$$\mathrm{PenSH} + \mathrm{CysS} = \mathrm{SCys} \overset{K = 0.13}{\longleftrightarrow} \mathrm{PenS} = \mathrm{SCys} + \mathrm{CysSH}\cdot$$

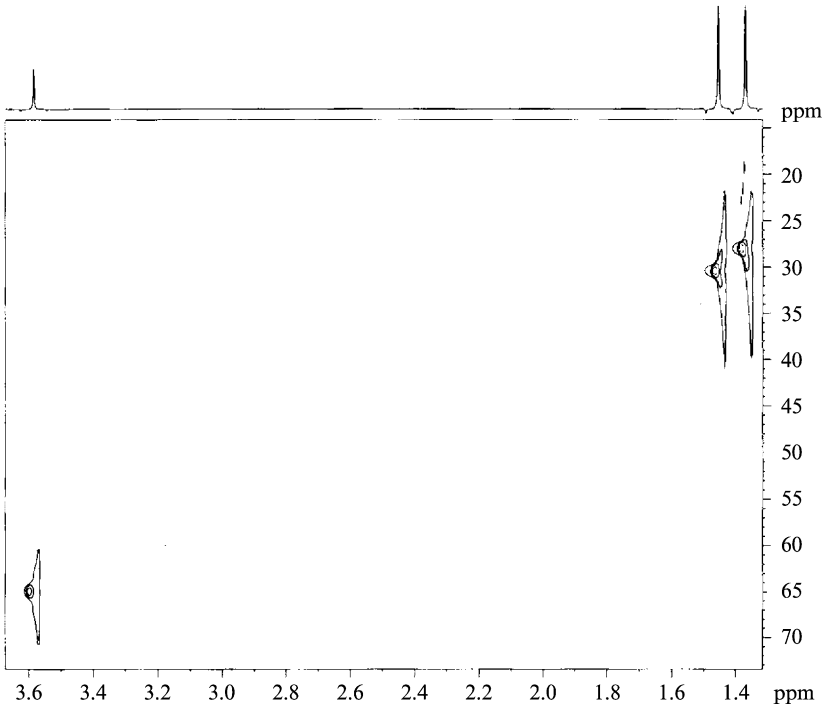

Fig. 6. HSQC NMR spectrum of (*D*)-penicillamine.

Table 4. Summary of assignments for the ^{13}C NMR spectrum of (*DL*)-penicillamine

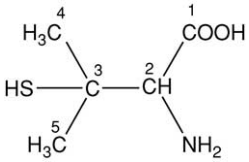

Chemical shift, relative to TMS (ppm)	Assignment (carbon number)
27.7, 30.2	4, 5
43.8	3
64.6	2
171.5	1

3.4.3. Thiazolidine formation

Penicillamine reacts with pyridoxal-5-phosphate to form a thiazolidine derivative, and is able to displace many amino acids from their Schiff base complexes, forming stable compounds of this type. The reactivity of the thiol group of penicillamine is less than that of cysteine, probably because of steric hindrance by the adjacent methyl groups of penicillamine, which in consequence is less rapidly oxidized *in vivo* [7].

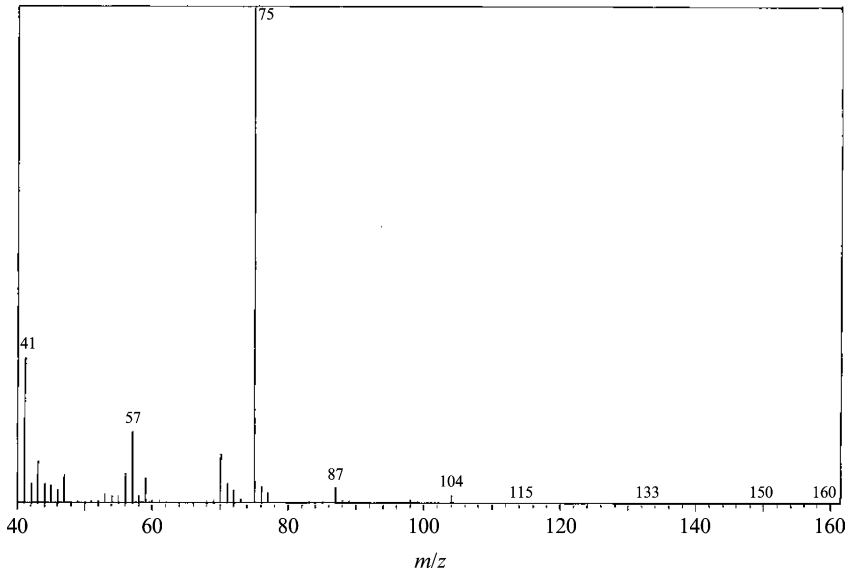

Fig. 7. Mass spectrum of (*D*)-penicillamine.

Table 5. Mass spectrometry fragmentation pattern of (*D*)-penicillamine

m/z	Relative intensity (%)	Fragment
104	1.7	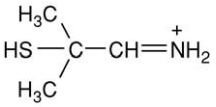
87	3.4	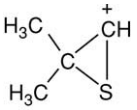
75	100	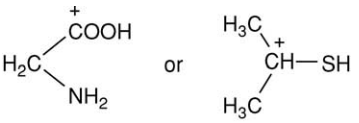
57	15	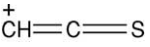
41	29	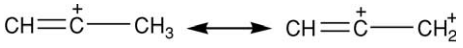

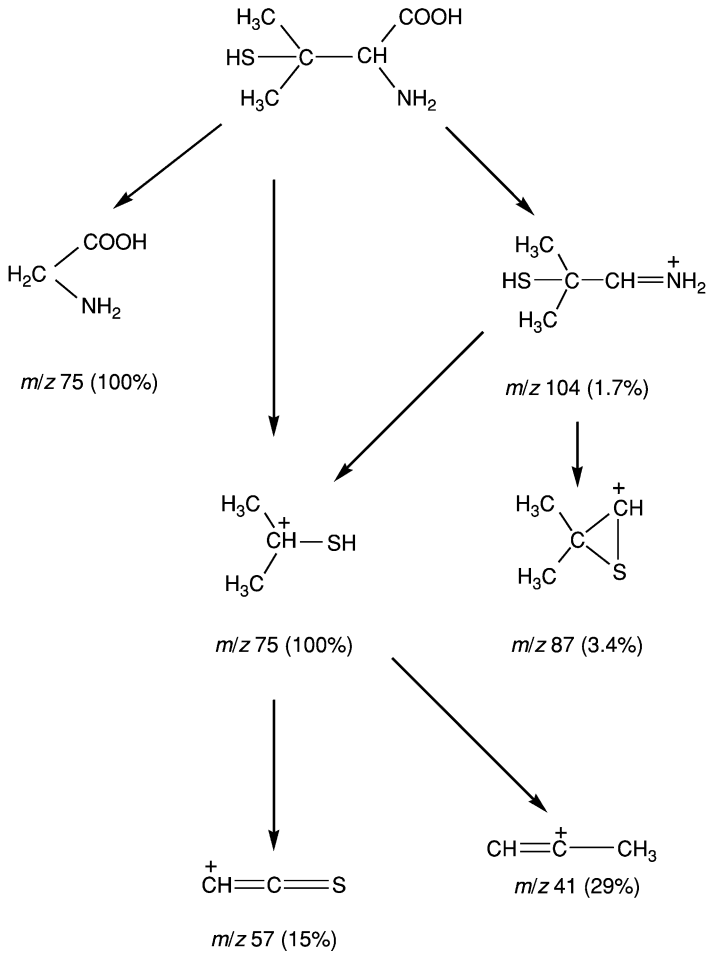

Fig. 8. Proposed mass fragmentation pattern of (*DL*)-penicillamine.

REFERENCES

[1] S. Budavari (ed.), *The Merck Index*, 12th edn., Merck and Co., 1996, p. 1218.
[2] C. C. Chiu and L. T. Grady, Penicillamine, in *Analytical Profile of Drug Substances* (ed. K. Florey), Vol. 10, Academic Press, 1981, pp. 601–637.
[3] K. Parfitt, in *Martindale, the Complete Drug Reference*, 32nd edn., Pharmaceutical Press, Massachusetts, 1999, p. 988.
[4] *European Pharmacopeia*, 3rd edn., The Council of Europe Strasburg, 2001, p. 1242.
[5] Q. Xu, R. H. Fairclough and D. P. Richman, *Ann. N. Y. Acad. Sci.*, 1993, **681**, 335–338, *Chemical Abstracts*, 1993, **119**, 131164e.
[6] *Drug Facts and Comparisons*, Wolters Kluwer Co., St. Louis, 2000, pp. 592–595.
[7] E. C. Huskisson (ed.), *Anti-Rheumatic Drugs,* Praeger Publishers, New York, 1983, pp. 523–524.

Penicillamine: Analytical Profile

Abdulrahman Al-Majed, Fathallah Belal, and Saeed Julkhuf

Department of Pharmaceutical Chemistry, College of Pharmacy, King Saud University, P.O. Box 2457, Riyadh 11451, Saudi Arabia

Contents

PROFILES OF DRUG SUBSTANCES, EXCIPIENTS, AND RELATED METHODOLOGY, VOLUME 32
ISSN: 0099-5428

DOI: 10.1016/S0099-5428(05)32005-3

1. COMPENDIAL METHODS OF ANALYSIS

1.1. Identification [1,2]

The following identification tests are listed in the compendia:

a. Addition of phosphotungstic acid solution to a penicillamine solution gives a deep blue coloration. The test entails dissolving a 40 mg sample in 4 mL of water R and 2 mL of phosphotungstic acid solution R. The color is observed after a 5 min standing time.

b. Addition of acetone–hydrochloric acid solution to a penicillamine solution gives a white precipitate. Dissolve 0.5 g of sample in a mixture of 0.5 mL of hydrochloric acid R and 4 mL of warm acetone R, cool in iced water, and initiate crystallization by scratching the walls of the tube with a glass rod. A white precipitate is formed, which is filtered with the aid of vacuum, washed with acetone R, and dried with suction. A 10 mg/mL solution of the precipitate is dextrorotatory.

1.2. Physical methods of analysis [2]

1.2.1. Solution appearance

Dissolve 2.5 g in carbon dioxide-free water R, and dilute to 25 mL with the same solvent. The solution is clear, and not more intensely colored than intensity 6 of the range of reference solutions of the most appropriate color.

1.2.2. pH

Dissolve 2.5 g in carbon dioxide-free water R, dilute to 25 mL with the same solvent, and the dilute 1 mL of this solution to 10 mL with carbon dioxide-free water R. The pH of this solution is 4.5–5.5.

1.2.3. Specific optical rotation

Dissolve 0.500 g in 1 M sodium hydroxide, and dilute to 10.0 mL with the same solvent. The specific optical rotation is -61.0° to -65.0°, calculated with reference to the dried substance.

1.3. Impurity analysis [2]

Examine the sample by thin-layer chromatography, using silica gel G R as the coating substance. Dissolve 10 mg of the substance to be examined in 4 mL of water R as a test solution, and dissolve 10 mg of penicillamine reference substance in 4 mL of water R as a reference solution. Apply 2 μL of each solution separately to the plate. Develop over a path of 10 cm using a mixture of 18 volumes of glacial acetic acid R, 18 volumes of water R, and 72 volumes of butanol R. Dry the plate at 100–105 °C for 5–10 min, and expose to iodine vapor for 5–10 min. The principal spot in the chromatogram obtained with the test solution is similar in position, color, and size to the principal spot in the chromatogram obtained with the reference.

1.4. Assay methods

The British Pharmacopoeia [2] describes a potentiometric titration method for the determination of penicillamine as the pure drug substance. The method is performed by dissolving 100 mg of the substance in 30 mL of anhydrous acetic acid. The mixture is titrated with 0.1 M perchloric acid, and the endpoint determined potentiometrically. Each milliliter of 0.1 M perchloric acid is equivalent to 14.92 mg of $C_6H_{11}NO_2S$.

The British Pharmacopoeia [2] also describes a method for determination of penicillamine tablets. Weigh and powder 20 tablets. Dissolve a quantity of the powder containing 100 mg of penicillamine as completely as possible in 50 mL of water and filter. Add 5 mL of 1 M sodium hydroxide to the filtrate and 0.2 mL of a 0.1% (w/v) solution of dithizone in 96% ethanol. Titrate with 0.02 M mercury(II) nitrate *VS*; each mL of 0.02 M mercury(II) nitrate *VS* is equivalent to 5.968 mg of $C_6H_{11}NO_2S$.

2. TITRIMETRIC METHODS OF ANALYSIS

2.1. Aqueous titration methods

Rizk *et al.* [3] used 2,3-dichloro-5,6-dcyano-*p*-benzoquinone as a redox titrant in the aqueous titration of penicillamine. Finely ground tablets were mixed with H_2O and the mixture was filtered. The filtrate (or an injectable solution) was diluted with H_2O and acidified with H_3PO_4 before titration with the redox titrant. The titration was conducted in anhydrous acetic acid using thiethylperazine dihydrochloride as the indicator. The endpoint was detected by a color change to green, and recoveries of penicillamine were 98.4–100.5%.

2.2. Nonaqueous titration methods

Vollmer *et al.* [4] compared the Hg(II) acetate method described in the Code of Federal Regulations for the determination of penicillamine in bulk drug and formulations with (i) a nonaqueous lithium methoxide titration, (ii) a nonaqueous $HCLO_4$ titration, and (iii) a colorimetric method with hydroxylamine. Method (ii) was unsatisfactory for bulk determinations. Method (i) was less precise than the Hg(II) acetate method, but gave satisfactory results for bulk drug and capsule samples. Method (iii) was the only method that gave satisfactory results in the presence of EDTA.

2.3. Potentiometric titration

Motonaka *et al.* [5] described a potentiometric method for the titration of (*D*)-penicillamine with an iodide-selective electrode. An excess of methanolic 0.05 M iodine was added to a sample containing 8 μg to 6.2 mg of (*D*)-penicillamine. The solution was then diluted to 50 mL with H_2O, and titrated with 0.1 mM to 0.1 M $AgNO_3$. For 6 mg of (*D*)-penicillamine, the coefficient of variation was less than 0.3%.

3. ELECTROCHEMICAL METHODS ANALYSIS

3.1. Stripping voltammetry

Forsman [6] described the stripping-voltammetric pattern of penicillamine at a hanging-mercury-drop electrode in the presence of Cu(II). Studies were reported of the anodic and cathodic stripping of cysteine and penicillamine at a hanging-mercury-drop electrode in acetate buffer solution (pH 4.6) containing Cu(II). The compounds form a Cu complex that is adsorbed on the mercury drop, and an anodic-stripping peak at +0.08 V versus the SCE is observed for both substances. This peak is due to formation of an adsorbed Hg(II) complex from the accumulated Cu(II) complex. An additional anodic-stripping peak at ~+0.1 V is observed for penicillamine. Both substances exhibit a cathodic-stripping peak at ~−0.4 V, which corresponds to reduction of the Cu(II) complex. A study was described of the potential dependence of the accumulation of Hg and Cu complexes of cysteine, with use of cathodic stripping with a normal pulse potential ramp.

Banica *et al.* [7] studied the effect of adding Ni(II) as an aid in the detection of penicillamine. The catalytic-Ni(II) method enables detection of the analyte with better selectivity compared to other indirect cathodic-stripping-voltammetric methods.

Ion *et al.* [8] described a method for the determination of (*D*)-penicillamine using cathodic stripping voltammetry (CSV) in which the drug is detected by its catalytic effect on Ni(II) reduction. Differential-pulse CSV with a hanging Hg-drop electrode, a 50 mV pulse height, a 0.5 s pulse interval, and a potential scan speed 10 mV/s to give a peak at –0.6 V. The supporting electrolyte was either phosphate–acetate buffer or 0.05 M MOPS buffer (adjusted to pH 7 with NaOH) containing 0.5 mM $NiSO_4$. The three-electrode cell had an Ag/AgCl (3 M KCl) reference electrode and pure N_2 was used to expel O_2 from the test solution. The detection limit for the drug was 15 nM, with detection of *N*-acetylcysteine also being possible without mutual interference in the phosphate–acetate buffer system.

3.2. Cyclic voltammetry

Wangfuengkanagul and Chailapakul [9] described the electroanalysis of (*D*)-penicillamine at a boron-doped diamond thin film (BDD) electrode using cyclic voltammetry. The BDD electrode exhibited a well-resolved and irreversible oxidation voltammogram, and provided a linear dynamic range from 0.5 to 10 mM with a detection limit of 25 μM in voltammetric measurement. In addition, penicillamine has been studied by hydrodynamic voltammetry and flow injection analysis with amperometric detection using the BDD electrode.

3.3. Polarography

Fogg and Fayad [10] studied the polarographic behavior of penicillamine by differential pulse polarography. The anodic polarographic wave was shown to be diffusion-controlled, and a linear calibration plot was obtained in citrate–phosphate buffer (pH 2.5) over the range 0.1–5.0 $\times$ 10^{-6} M. The peak potential varied linearly over the pH range 2–8, although the peak current was highly dependent

on the pH. The current exhibited maximum values at pH 3 and 10 (4.7 and 3.8 μA, respectively), with a minimum value of 3.2 μA at a pH of 7.

Lopez-Fonseca *et al.* [11] discussed the theory of reverse pulse polarography and the technique was applied in the determination of penicillamine electrochemically coated on a dropping-mercury electrode. Using long drop times and short pulses, the drug can be determined at levels as low as 50 nM in the presence of Cu(II), and the technique compares well with normal-pulse and differential-pulse polarography.

4. SPECTROSCOPIC METHODS OF ANALYSIS

4.1. Spectrophotometry

Besada [12] described a spectrophotometric method for determination of penicillamine by reaction with nitrite and Co(II). Penicillamine is first treated with 1 M $NaNO_2$ (to convert the amino-group into a hydroxy-group), then with 0.1 M $CoCl_2$, and finally the absorbance of the brownish-yellow complex obtained is measured at 250 nm. The process is carried out in 50% aqueous ethanol, and the pH is adjusted to 5.4–6.5 for maximum absorbance. The calibration graph is linear over the concentration range of 0.25–2.5 mg per 50 mL, and the mean recovery ($n = 3$) of added drug is 99.7%. Cystine, cysteine, methionine, and other amino acids do not interfere.

Besada *et al.* [13] described spectrophotometric methods for determination of penicillamine in pure and dosage forms. Penicillamine was measured spectrophotometrically in 0.1 M HCl (at 195 nm) or in 0.1 M NaOH (at 238 nm). Both methods gave recoveries of 100% with good precision. For determination of the drug in tablets, in the presence of excipients, ground samples were extracted with each of these solvents and the difference in absorbance at 238 nm between the two solutions were measured. The recovery of the drug from commercial tablets was 99.8%, with a coefficient of variation of 0.38%. The three methods were suitable for 4–130 ppm of the drug.

Walash *et al.* [14] described a kinetic spectrophotometric method for determination of several sulfur containing compounds including penicillamine. The method is based on the catalytic effect on the reaction between sodium azide and iodine in aqueous solution, and entails measuring the decrease in the absorbance of iodine at 348 nm by a fixed time method. Regression analysis of the Beer's law plot showed a linear graph over the range of 0.01–0.1 μg/mL for penicillamine with a detection limit of 0.0094 μg/mL.

Amarnth and Amarnth [15] described a specific method for the determination of penicillamine and cysteine. Treatment with 1,1-thiocarbonyl diimidazole converts penicillamine to 5,5-dimethyl-2-thioxothiazolidine-4-carboxylic acid. The detection limit is 2 pmol of the drug per injection, and the detector response is linear up to 1 nmol.

4.2. Colorimetry

Al-Majed [16] described a simple colorimetric method for the determination of (*D*)-penicillamine in pure form and in pharmaceutical formulations that is based on coupling between (*D*)-penicillamine and 2,6-dichloroquinone-4-chlorimide (DCQ) in

dimethyl sulfoxide to yield a product having a yellow color and with a maximum absorbance at 431 nm. Regression analysis of the Beer's law plot showed good correlation ($r = 0.9998$) with a linear graph over the range of 4–20 μg/mL, and a detection limit of 0.15 μg/mL. The method results were accurate and reproducible, and specific for intact drug even in the presence of some interfering substances. The recovery was 101.6%, with a residual standard deviation of 1.57%.

Besada and Tadros [17] used an oxidant to develop iodate as a simple colorimetric method for the assay of penicillamine. Sample solutions containing 0.4–2 mg of penicillamine were mixed with 2 mL of aqueous 2% KIO_3 and 30% H_2SO_4, and the mixture was shaken for 1 min. The liberated iodine was extracted with CCl_4 (3×10 mL) and the combined extracts were diluted to 50 mL with CCl_4. After this, the absorbance at 520 nm (molar absorptivity = 1280) was measured against a reagent blank. Beer's law was obeyed over the ranges studied, the method was characterized by an average recovery of 99.7%, and the coefficient of variation was 0.4–1.2 mg ($n = 5$). The method was applied for the determination of penicillamine in capsules.

Issopoulos and coworkers [18,19] used two systems for the determination of micromolar concentrations of (*D*)-penicillamine. The first method is based on the oxidation of penicillamine by Fe(III) in the presence of 1,10-phenanthroline, which yields the Fe(II)/phenanthroline complex having an absorption maximum at 510 nm. The absorbance was constant over the pH range 4.0–8.0, and the complex was stable for at least 24 h. The optimum range of the drug is 2–15 μg/mL. In the second method, a coupled redox-complexation reaction was developed by taking 0.1–2 mL of the sample and mixing with 5 mL H_2O, 5 mL 0.902 mM Fe(III) solution, 5 mL acetic acid/sodium acetate buffer (pH 4.6), and 5 mL 0.307 mM 2,4,6-tris-(2-pyridyl)-1,3,5-triazine solution. The mixture was diluted to 25 mL with H_2O, heated on a water bath at 50 °C for 25–30 min, cooled, and the absorbance measured at 595 nm. Beer's law was obeyed for 1.7–25 μM of (*D*)-penicillamine. The relative standard deviation ($n = 5$) was 0.97–2.42% over the range of 0.5–2 μg/mL. Recoveries were 99.14% for the bulk drug substance, and 103.83–108.5% for drug product in capsules.

Buyuktimkin and Buyuktimkin [20] described a spectrophotometric method of assay of penicillamine and its tablets. An aqueous solution of 100 mg/mL of penicillamine was added to ethanolic 5 mM Sanger reagent (1-fluoro-2,4-dinitrobenzene), solid $NaHCO_3$, and water. The solution was diluted and heated at 70 °C for 45 min. After cooling, the solution was diluted with 3% ethanolic HCl. The absorbance of the resulting yellow complex was measured at 355 nm (molar absorptivity = 19,721). Recovery of the drug from commercial tablets was 99.1 ± 0.7%.

Raggi *et al.* [21] described a spectrophotometric analysis method with ammonium tetrachloropalladate for penicillamine in pharmaceutical formulations. An aqueous solution of penicillamine (298 μg/mL) was treated with 1.5 mL of 20 mM $(NH_4)_2PdCl_4$ in 1 M HCl. The mixture was diluted to 10 mL, and the absorbance measured at 403 nm after 20 min. The method has a recovery of 98.8%, and was used to determine penicillamine in aqueous extracts of capsules.

Fakhr Eldin *et al.* [22] described a simple sequential spectrophotometric method for the assay of penicillamine. The method is based on the complex formed when the drug is reacted with Fe(III) solution in hydrochloric acid media. The deep blue colored drug–Fe(III) complex is monitored at a maximum wavelength of 600 nm.

A linear range of 25–300 ppm of the drug was obtained with a relative standard deviation of less than 0.98%.

4.3. Fluorimetry

Byeon *et al.* [23] described a fluorimetric method for (D)-penicillamine using 9-fluorenylmethyl pentafluorophenyl carbonate and acetonitrile. Capsules containing penicillamine were extracted with water and then filtered. The solution was incubated at 70 °C for 40 min with borate buffer solution. After cooling, the mixture was extracted with diethyl ether and the fluorescence of the aqueous phase measured at (excitation = 260 nm, emission = 313 nm). The calibration graph was linear for 0.4–5.0 μM of penicillamine with a coefficient of variation of 0.4%.

A specific and sensitive fluorimetric method was proposed by Al-Majed for the determination of (D)-penicillamine in its pure state and in its dosage forms [24]. The method is based on the coupling between (D)-penicillamine and 4-fluoro-7-nitrobenzo-2-oxa-1,3-diazole, and analysis of the fluorescent product was measured at an excitation wavelength of 465 nm and an emission wavelength of 530 nm. The fluorescence intensity was found to be a linear function of the drug concentration over the range of 0.6–3 μg/mL, and the detection limit was 2 ng/mL (13 nM).

Al-Ghannam *et al.* [25] described a simple fluorimetric procedure for determination of three pharmaceutical compounds containing thiol groups, including penicillamine. In this method, the drugs are treated with 1,2-naphthoquinone-4-sulfonic acid. The later compound is reduced to 1,2-dihydroxynaphthalene-4-sulfonic acid, which is measured fluorimetrically (excitation = 318 nm, emission = 480 nm). The method is sensitive to 0.5–4.5 μg/mL, with a detection limit of 0.05 μg/mL (S/N = 2).

Pérez Ruiz *et al.* [26] determined penicillamine and tiopronin in pharmaceutical preparations by flow injection fluorimetry. The procedure is based on the oxidation of these drugs by thallium(III), whereupon the fluorescence of Tl(I) produced in the oxidation of penicillamine is monitored using excitation at 227 nm and emission at 419 nm. A linear calibration graph for penicillamine was obtained between 3×10^{-7} and 8×10^{-6} M.

5. CHROMATOGRAPHIC METHODS OF ANALYSIS

5.1. Thin-layer chromatography

Kovacs-Hadady and Kiss [27] studied the chromatographic characteristics of thiazolidinecarboxylic acid derivatives, formed by reaction of (D)- and (L)-penicillamine with various substituted benzaldehydes and heterocyclic aldehydes in order to evaluate the aldehydes as derivatizing agents for separation of the penicillamine enantiomers. The TLC method of Martens *et al.* [28] was used. Transformation to thiazolidine carboxylic acids with benzaldehyde and substituted benzaldehydes was not complete, so formaldehyde is still the preferred reagent for separation of the enantiomers.

Martens *et al.* [28] reported a system for resolving the optical isomers, and determining the enantiomeric purity of (D)-penicillamine by thin-layer chromatography.

Penicillamine (50 mg) was mixed with 50 mg of formaldehyde, 50 μL of concentrated HCl, and 2.5 mL of propan-2-ol, and the solution heated at 60 °C for 2 h. An aliquot of the reaction mixture was subjected to TLC on a Chiralplate (Macherey–Nagel) with a mobile phase of methanol–H_2O–acetonitrile (1:1:4). Detection was made using 0.1% ninhydrin reagent, and the limit of detection was approximately 0.5%. Good separation of (*D*)- and (*L*)-penicillamine was achieved.

5.2. Gas chromatography

Penicillamine is a polar nonvolatile molecule and therefore derivatization is a requirement for analysis by gas chromatography. Abe *et al.* [29] described stereoselective GC phases for immobilized chiral polysiloxanes with (*S*)-leucine derivatives as the chiral selector. Five chiral GC phases were prepared, and which were analogous to Chirasil-Val but containing leucine as an amino acid bonded to *t*-butylamide or a 1-arylethylamide (aryl = α-naphthyl or phenyl). These selector compounds were immobilized by bonding to a methylsilicone using 1,3,5,7-tetramethyl-1,3,5,7-tetravinylcyclotetrasiloxane and dicumyl peroxide as cross-linking agents with curing at 170 °C. The resulting stationary phases were evaluated as 0.12–0.14 μm coatings on column (10 m × 0.25 mm i.d.) programmed as appropriate in the range 100–160 °C with He (1 mL/min) as a carrier gas and a 1:3 split ratio.

Penicillamine was determined by Rushing *et al.* [30] as its hydrochloride salt in animal feeding-stuffs and as the salt or free base in aqueous solution by GLC following a single-step double derivatization with diazomethane–acetone. *N,N*-diethylaniline was used as internal standard. The GLC was carried out on a glass column (90 cm × 2 mm) of 5% of SP2100 on Supelcoport (100–120 mesh) operated at 110° with He as carrier gas (25 mL/min) and a rubidium-sensitized N–P detector. There were no interfering peaks and the drug and the internal standard were eluted in ~2 and ~1.5 min, respectively. The method was used to study the stability of the salt or the base in water and the salt in feeding-stuffs.

5.3. High performance liquid chromatography

Biffar *et al.* [31] determined penicillamine in its encapsulated formulations. A solution (1.25 mg/mL) of the contents of 10 capsules in 0.1% Na_2EDTA solution was analyzed by HPLC on an ASI column (30 cm × 4 mm) of ODS (10 μm), using 1 mM Na hexanesulfonate in 50 mM phosphate buffer (pH 3.0) as the mobile phase (1.7 mL/min) and UV detection at 210 nm. The coefficient of variation ($n = 10$) was 0.16%, the analyte recovery ($n = 6$) was 100.2%, and the detection limit was 40 ng. Good agreement was obtained with results obtained by the standard titrimetric method.

Merino-Merino *et al.* [32] used the OPA reagent (*o*-phthaldehyde condensed with 2-mercaptoethanol) to separate penicillamine enantiomers after their derivatization. Racemic and (*D*)-penicillamine were dissolved in aqueous 0.5 M NaOH, and treated with the derivatizing solution (methanolic *o*-phthaldehyde and 2-mercaptoethanol in 0.4 M potassium borate buffer solution of pH 10). The reaction mixture was set aside for 2 min at room temperture, whereupon a portion of solution was analyzed by HPLC. The method used a Cyclobond column (25 cm × 4.6 mm) maintained at 5 °C, a mobile phase of ethanol/1% triethylammonium acetate (1:1; pH 4.5) eluted at

1.0 mL/min, and fluorescence detection at 450 nm (excitation at 355 nm). Good resolution between the (*D*)- and (*L*)-enantiomers was achieved, and the calibration graphs were linear from 5 (the detection limit) to at least 200 μg/mL of each derivatized enantiomer. The coefficients of variation ($n = 7$) were 6.7 and 5.3% for the derivatized (*D*)- and (*L*)-penicillamine enantiomers, respectively. The applicability of the method for the determination of the drug in tablets was tested.

Nakashima *et al.* [33] used *N*-[4-(6-dimethylamino-2-benzofuranyl)-phenyl]-maleimide to separate penicillamine enantiomers on a chiral stationary phase. Standard solutions of the (*D*)- and (*L*)-penicillamine enantiomers were prepared in acetonitrile. A (*D*)-penicillamine capsule (containing 1 mg of drug in the 235 mg contents) was dissolved in 10 mL H_2O and diluted to 8 μM with acetonitrile. The sample solutions (50 μL) were derivatized by heating at 60 °C for 30 min with 150 μL of 200 μM *N*-[4-(6-dimethylamino-2-benzofuranyl)phenyl] maleimide in acetonitrile and 200 μL borate buffer (pH 8.5). After cooling, a 10 μL portion of the reaction mixture was analyzed by HPLC on a 5 μm Sumichiral OA-2500S column (25 cm × 4.6 mm i.d.; Sumika Chemical Analysis Service, Osaka, Japan), using 75% aqueous methanol containing 0.15 M ammonium acetate and 0.05 M tetra-*n*-butylammonium bromide as the mobile phase (elution at 1 mL/min). Fluorescence detection at 455 nm (excitation at 360 nm) was used, and the calibration graphs were linear from 2.50 pmol per injection with detection limits of 290 and 350 fmol for the (*D*)- and (*L*)-penicillamine enantiomers, respectively. The (*D*)-penicillamine capsule product was shown by the method to be free of (*L*)-penicillamine. Other thiol compounds can be determined by the method by making slight modifications of the eluent.

Favaro and Fiorani [34] used an electrode, prepared by doping conductive C cement with 5% cobalt phthalocyanine, in LC systems to detect the pharmaceutical thiols, captopril, thiopronine, and penicillamine. FIA determinations were performed with pH 2 phosphate buffer as the carrier stream (1 mL/min), an injection volume of 20 μL, and an applied potential of 0.6 V versus Ag/AgCl (stainless steel counter electrode). Calibration curves were developed for 5–100 μM of each analyte, and the dynamic linear range was up to approximately 20 μM. The detection limits were 76, 73, and 88 nM for captopril, thiopronine, and penicillamine, respectively. LC determinations were performed using a 5-μm Bio-Sil C18 HL 90-5S column (15 cm × 4.6 mm i.d.) with 1 mM sodium 1-octanesulfonate in 0.01 M phosphate buffer/acetonitrile as the mobile phase (1 mL/min) and gradient elution from 9:1 (held for 5 min) to 7:3 (held for 10 min) in 5 min. The working electrode was maintained at 0.6 V versus Ag/AgCl, and the injection volume was 20 μL. For thiopronine, penicillamine, and captopril, the retention times were 3.1, 5.0, and 11.3 min, and the detection limits were 0.71, 1.0, and 2.5 μM, respectively.

According to a Macherey–Nagel application note [35], a mixture of 20 ng each of (*L*)-cysteine, (*L*)-glutathione, and (*L*)-penicillamine was resolved in less than 12 min by HPLC. The method used a Nucleosil 100-5SA column (15 cm × 4.6 mm i.d.) with aqueous 4.5 g/L ammonium citrate–6 g/L phosphoric acid at pH 2.2 as the mobile phase (eluted at 1 mL/min) and electrochemical detection at a gold electrode polarized at +800 mV.

Bystryakov *et al.* [36] described a double detection method to determine aliphatic thiols by HPLC. A solution of 0.1–1 mg/mL of such compounds in the mobile phase was analyzed by HPLC using a of Nucleosil C18 micro-column (5 μm; 6.2 cm × 2 mm)

with phosphate buffer solution (pH 2.0) or phosphate buffer solution (pH 2.0) – ethanol as mobile phase (50 or 100 μL/min). Detection was by consecutive detection, consisting of spectrophotometry at 210 nm and voltammetry with use of a two-Pt electrode system at 0.8 V. Operating conditions and chromatograms were given for the determination of penicillamine, unithiol, and *N*-acetyl-cysteine. The use of coupled spectrophotometric and electrochemical detection gave good selectivity in the determination of drugs containing mercapto-groups in the presence of disulfides.

5.4. Ion-pair chromatography

Goetze *et al.* [37] used an ion-pair reagent technique to separate the complexes of different amino acids, including penicillamine. Separation of the complexes by HPLC with different amino acids on the C18/RP columns was unsatisfactory unless an ion-pair reagent (e.g., 15–20 mM sodium dodecylsulfate) was added to the mobile phase, and the acetonitrile concentration was optimized in each instance. For the separation of different complexes with one amino acid (such as penicillamine), the *cis*- and *trans*-complexes, as well as smaller amounts of other reaction products, were separated on the Nucleosil 5C18 column with an acetonitrile gradient in a buffer solution of pH 3.8. Preparative separation of these complexes for characterization by NMR was also achieved with use of trifluoroacetic acid as ion-pair reagents. The NH_2 column gave similar results to the others with this ion-pairing reagent.

5.5. Electrophoresis

5.5.1. Paper electrophoresis

Solution equilibria of Fe(III)/Cr(III) in methionine and Fe(III)/Cr(III) in methionine/penicillamine complex systems were studied by paper electrophoresis and were reported by Tewari [38]. The formation of 1:1:1 mixed ligand complexes is inferred, and the stability constants of the complexes at 35 °C and 0.1 M ionic strength were 6.80 ± 0.09 (Fe(III)–methionine–penicillamine) and 4.60 ± 0.16 (Cr(III)–methionine–penicillamine), respectively.

Tewari [39] described an electrophoretic method to be used in the study of mixed ligand complexes in solutions, including those of penicillamine. Paper strips (30 × 1 cm) were soaked in electrolyte, spotted with Cr(III), Fe(III), or glucose solution, sandwiched between metal plates maintained at 35°C, and left to stand for 15 min. The protruding ends of the strips were then dipped in electrolyte for 60 min with a 240 V potential applied to the metal plates. For binary complexes, the electrolyte was 0.1 M $HClO_4$/0.01 M methyl cystine (MC), and the experiment was repeated at various pH values. For ternary complexes, the electrolyte was 0.1 M $HClO_4$/0.1 M MC containing varying amounts of 0.1 M penicillamine, adjusted to pH 8.5 with NaOH. Spots were detected on the strips using potassium ferrocyanide solution for Fe(III) and 1-(2-pyridylazo)-2-naphthol for Cr(III). $AgNO_3$ in acetone and an ethanolic 2% NaOH solution were used to detect glucose. The distances migrated by the metal spots were measured relative to the glucose spots, and the results used to calculate stability constants for the complexes.

An electrophoretic method was described by Srivastava *et al.* [40] to study equilibria of the cited mixed ligand complex systems in solution. Stability constants of the Zn(II) and Cd(II) complexes were 5.36 and 5.18 (log *K* values), respectively, at an ionic strength of 0.1 and a temperature of 35 °C.

An ionophoretic method was described by Tewari [41] for the study of equilibria in a mixed ligand complex system in solution. This method is based on the movement of a spot of metal ion in an electric field with the complexants added in the background electrolyte at pH 8.5. The concentration of the primary ligand (nitrilotriacetate) was kept constant, while that of the secondary ligand (penicillamine) was varied. The stability constants of the metal–nitrilotriacetate–penicillamine complexes have been found to be 6.26 ± 0.09 and 6.68 ± 0.13 (log *K* values) for the Al(III) and Th(IV) complexes, respectively, at 35 °C and an ionic strength of 0.1 M.

5.5.2. Capillary electrophoresis

Gotti *et al.* [42] reported an analytical study of penicillamine in pharmaceuticals by capillary zone electrophoresis. Dispersions of the drug (0.4 mg/mL for the determination of (D)-penicillamine in water containing 0.03% of the internal standard, *S*-methyl-L-cysteine, were injected at 5 kPa for 10 seconds into the capillary (48.5 cm × 50 μm i.d., 40 cm to detector). Electrophoresis was carried out at 15 °C and 30 kV, with a pH 2.5 buffer of 50 mM potassium phosphate and detection at 200 nm. Calibration graphs were linear for 0.2–0.6 μg/mL (detection limit = 90 μM). For a more sensitive determination of penicillamine, or for the separation of its enantiomers, a derivative was prepared. Solutions (0.5 mL, final concentration 20 μg/mL) in 10 mM phosphate buffer (pH 8) were mixed with 1 mL of methanolic 0.015% 1,1′-[ethylidenebis-(sulfonyl)]bis-benzene and, after 2 min, with 0.5 mL of pH 2.5 phosphate buffer. An internal standard (0.03% tryptophan, 0.15 mL) was added and aliquots were injected. With the same pH 2.5 buffer and detection at 220 nm, calibration graphs were linear for 9.3–37.2 μg/mL, with a detection limit of 2.5 μM. For the determination of small amounts of (L)-penicillamine impurity, the final analyte concentration was 75 μg/mL, the pH 2.5 buffer contained 5 mM beta-cyclodextrin and 30 mM (+)-camphor-10-sulfonic acid, with a voltage of 20 kV, and detection at 220 nm. Calibration graphs were linear for 0.5–2% of the toxic (L)-enantiomer, with a detection limit of 0.3%.

Russell and Rabenstein [43] described a speciation and quantitation method for underivatized and derivatized penicillamine, and its disulfide, by capillary electrophoresis. Penicillamine and penicillamine disulfide were determined by capillary electrophoresis on a capillary (24 cm × 25 μm i.d. or 50 cm × 50 μm i.d. for underivatized thiols) with detection at 357 nm (200 nm for underivatized thiols). The run buffer solution was 0.1 M phosphate (pH 2.3). Detection limits were 20–90 μM without derivatization, and 5–50 μM after derivatization. Calibration graphs were linear from 1 μM to 5 mM thiols.

5.6. Flow injection analysis

Zhang *et al.* [44] determined penicillamine via a FIA system. A 50 μL sample was injected into an aqueous carrier stream of a flow injection manifold and mixed with

reagent streams of 10 mM quinine in 0.1 M H_2SO_4 (4 mL/min) and 2 mM Ce(IV) in 0.1 M H_2SO_4 (4 mL/min). The chemiluminescence intensity of the product was measured, and the calibration graph was linear for 2–200 μM penicillamine. The detection limit was 15 pmol, and the relative standard deviation ($n = 10$) was less than 4% for 20 μM analyte. The method was applied to the analysis of pharmaceuticals, and recoveries of 50 μM in tablets were 93–101%.

Garcia *et al.* [45] determined penicillamine in pharmaceutical preparations by FIA. Powdered tablets were dissolved in water, and the solution was filtered. Portions (70 μL) of the filtrate were injected into a carrier stream of water that merged with a stream of 1 mM $PdCl_2$ in 1 M HCl for determination of penicillamine. The mixture was passed though a reaction coil (180 cm long) and the absorbance was measured at 400 nm. Flow rates were 1.2 and 2.2 mL/min for the determination of penicillamine, the calibration graphs were linear for 0.01–0.7 mM, and the relative standard deviation ($n = 10$) for 0.17 mM analyte was 0.8%. The method was sufficiently selective, and there were no significant differences between the labeled contents and the obtained results.

Vinas *et al.* [46] also determined penicillamine by chemiluminescence – flow injection analysis. The sample was dissolved in water, and a portion of resulting solution was introduced into an FIA system consisting of 5 mM luminol in 0.1 M KOH–boric acid buffer (pH 10.4), 50 μM Cu(II), and 10 mM H_2O_2 eluted at 7.2 mL/min. Chemiluminescent detection was used, the calibration graphs were linear from 0.1 to 10 mM of penicillamine, and the coefficients of variation were from 1.2% and 2.1%.

Vinas *et al.* [47] determined penicillamine routinely by using batch procedures and FIA. A capsule was dissolved in water, diluted to 250 mL, and a suitable portion of the solution treated with 1 mM Co(II) solution (2.5 mL) and 2 M ammonium acetate (2.5 mL). The mixture was diluted to 25 mL and the absorbance of the yellow complex was determined at 360 nm. Calibration graphs were linear for 0.02–0.3 mM of penicillamine. The method was modified for flow injection analysis using peak-height or peak-width methods, but in both cases the flow rates were maintained at 3.3 mL/min. For the peak-height technique, calibration graphs were linear for 0.1–2 mM, and the sampling frequency was 150 samples per hour. For the peak-width method, the response was linear for 50 μM to 0.1 M, and this method was particularly useful for routine determinations.

FIA determinations of penicillamine was performed by Favaro and Fiorani [48] with phosphate buffer (pH 2) as the carrier stream (eluted at 1 mL/min), an injection volume of 20 μL, and an applied potential of 0.6 V versus Ag/AgCl (stainless steel counter electrode). The calibration curves were presented for 5–100 μM of the analyte, the dynamic linear range was up to approximately 20 μM, and the detection limits was 88 nM for penicillamine.

6. DETERMINATION IN BODY FLUIDS AND TISSUES

Zhang *et al.* [49] determined penicillamine in urine by the coupled technique of chemiluminescence detection and liquid chromatography. The urine sample was adjusted to pH 2 with 2 M H_2SO_4 and centrifuged at 3000 rpm for 5 min. A 12 mL

volume of the supernatant was passed through a single-use C18-type Sep-Pak cartridge. The first 10 mL of the eluate was discarded, and the last 2 mL was collected for analysis by ion-pair reversed-phase LC. The chromatography was performed on a Rosil C18 column (15 cm × 4.6 mm i.d., 5 μm particle size) with an injection volume of 100 μL, 1 g/L octanesulfonic acid sodium salt, and 0.4 mM EDTA in 0.2 M acetate buffer at pH 3 as the mobile phase (eluted at 1 mL/min). The chemiluminescence detection was developed by postcolumn addition of 2 mM Ce(IV) in 100 mM H_2SO_4 (4 mL/min) and 100 mM quinine in 100 mM H_2SO_4 (4 mL/min). The calibration graph was linear for 2–2000 μM penicillamine, the detection limit was 1 μM, and the relative standard deviation ($n = 10$) for 10–50 μM penicillamine was less than 5%. The method was used in a pharmacokinetic study entailing the analysis of urine samples given by human volunteers over a 25 h period after the oral administration of penicillamine.

Haj-Yehia and Benet [50] described a fluorimetric method for determination of penicillamine in tissues. Rat tissues (tabulated; 50–100 mg) were homogenized in 1 mL of ice-cold 20 mM EDTA in 20% acetonitrile, and the mixtures were centrifuged at 4000 × *g* for 5 min at 4 °C. The supernatants were adjusted to 1–2.5% sample concentration with borate buffer (pH 8.4). Portions (0.1 mL) were mixed with 0.1 mL of 50 μM *N*-acetylcysteine (internal standard), 0.1 mL of 0.25 mM 2-(4-*N*-maleimidophenyl)-6-methoxybenzofuran in acetonitrile, and 0.7 mL borate buffer (pH 8.4). After 1 h the mixtures were diluted with 1 mL of mobile phase; 10-μL portions were analyzed by a HPLC system consisting of a 5 μm Ultrasphere-ODS column (25 cm × 4.6 mm i.d.), a mobile phase of 10 mM KH_2PO_4 containing 0.1% sodium hexanesulfonate (adjusted to pH 4.5), and fluorescence detection at 390 nm (excitation at 310 nm). Calibration graphs were linear for 0.5–5 nmol aliphatic thiols, and the detection limits were 2–75 fmol. The method was applied to the determination of sulfhydryl-containing drugs (*N*-acetylcysteine and penicillamine) and endogenous thiols (cysteine and glutathione) in biological samples.

Wakabayashi *et al.* [51] determined penicillamine in serum by HPLC. Serum (0.1 mL) was vortex-mixed for 30 s with 50 μL of 0.1% EDTA and 0.2 mL of 10% TCA. The solution was centrifuged at 1500 × *g* and filtered. A 5 μL portion was analyzed on a Shodex C18 column (15 cm × 4.6 mm i.d.), using a mobile phase of 19:1 methanolic 0.05 M phosphate buffer (pH 2.8) containing 1 mM sodium octylsulfate and 10 μM EDTA. Liver or kidney samples were similarly extracted, and the extracts were cleaned up on a Bond-Elut cartridge prior to HPLC analysis. Detection was effected with an Eicom WE-3G graphite electrode maintained at +0.9 V versus Ag/AgCl. The calibration graph was linear up to 500 ng, and the detection limits were 20 pg. For 1 μg of penicillamine added to serum, liver, or kidney, the respective relative standard deviations ($n = 5$) were 3.6, 5.1, and 4.4%.

Rabenstein and Yamashita [52] determined penicillamine and its symmetrical and mixed disulfides by HPLC in biological fluids. Plasma and urine were deproteinized with trichloroacetic acid, and HPLC was performed on a column (25 cm × 4.6 mm) or Biophase ODS (5 μm) with a mobile phase comprising 0.1 M phosphate buffer (pH 3) and 0.34 mM Na octylsulfate at 1 mL/min. Detection was with a dual Hg–Au amalgam electrode versus a Ag–AgCl reference electrode. (*D*)-penicillamine and homocysteine were determined at the downstream electrode at +0.15 V, and homocystine, penicillamine–homocysteine, and penicillamine disulfides were first reduced

to thiols at the upstream electrode (−1.10 V) before detection downstream. Calibration graphs were linear from 5 to 45 μM (penicillamine), 5 to 40 μM (homocysteine), 2 to 30 μM (penicillamine/homocysteine) in phosphate buffer solution.

(*D*)-penicillamine is separated from serum by treatment with EDTA in the presence of HPO_3 and centrifugation as described by Nakashima *et al.* [53]. Reaction of the mercapto group with the cited compound is then carried out in borate buffer solution (pH 8.5) at 60 °C for 30 min. (*D*)-penicillamine is determined on a column (15 cm × 4.6 mm) of ODS-80TM (Toyo Soda Co.) using a mobile phase of 2.5 mM imidazole buffer (pH 7.7) – acetonitrile (1:1) containing 10 mM tetrabutylammonium bromide eluted at 0.8 mL/min. After fluorimetric detection at 455 nm (excitation at 360 nm), the detection limit is 50 fmol of penicillamine in a 20-μL injection, and the calibration graph is linear up to 12 pmol. The recovery of (*D*)-penicillamine from serum was 91.8%.

Yamashita and Rabenstein [54] also determined penicillamine and its disulfide in plasma by HPLC. Plasma was deproteinized with an equal volume of cold 5% trichloroacetic acid, the mixture was centrifuged, and the supernatant solution was filtered (0.2 μm filter). The solution was treated with thiol–disulfide internal standard solution and a portion (20 μL) was analyzed by HPLC on a column (25 cm × 4.6 mm) of Partisil ODS-3 (5 μm) or of Biophase ODS (5 μm), with a guard column (4 cm × 4.6 mm) of Partisil ODS-3 (10 μm). The mobile phase (eluted at 1 mL/min) was phosphate buffer (pH 3) containing 0.8 mM sodium octyl sulfate and 3% aqueous methanol. Detection was electrochemical, using dual Au–Hg amalgam electrodes in series. The thiols were detected at the downstream electrode, and the disulfides were reduced at the upstream electrode and then detected as for the thiols. The calibration graphs were linear up to 25, 60, and 1500 μM for reduced penicillamine, (*D*)-penicillamine-glutathione mixed disulfide, and oxidized penicillamine, respectively. Detection limits were in the picomol range for all compounds except penicillamine disulfide, which had a detection limit of 600 pmol. The method was also applied in the analysis of urine.

Wronski [55] described a method to separate and resolve penicillamine from physiological fluids. To urine (100 mL) was added 60 g of $(NH_4)_2SO_4$, the solution was filtered, mixed with 2 g of Na_2SO_3, and 1 mL of 0.1 M EDTA in 20% triethanolamine, and shaken with 5–20 mL of 0.01–0.06 M tributyltin hydroxide in octane for 5 min. A portion (5–8 mL) of the organic phase was shaken with 0.2 mL of HCl in 20% glycerol solution. A portion of the aqueous phase (5–10 μL per cm of the strip width) was applied to cellulose gel, and electrophoretic separation was performed by the technique described previously. The thiol spots were visualized with *o*-hydroxymercuri benzoic acid–dithiofluorescein and densitometry with a 588-nm filter.

Webb *et al.* [56] determined free penicillamine in the plasma of rheumatoid arthritis patients. Plasma ultrafiltrate was mixed with trichloroacetic acid and 4-aminobenzoic acid as internal standards, and HPLC mobile phase to determine total reduced penicillamine. Plasma was vortexed with trichloroacetic acid, the precipitated protein was removed after 15 min by centrifuging, and the supernatant solution was filtered and mixed with 4-aminobenzoic acid. In each instance, a 50-μL portion of solution was analyzed on a 25-cm column of Spherisorb-NH_2 (5 μm) at 25 °C, with an electrochemical detector having dual porous graphite electrodes set at

0.0 and +0.8 V, respectively. The ion-pairing mobile phase was that described by Abounassif and Jefferies but with the omission of EDTA. The detection limit was 0.3 μM penicillamine. Sources of error were identified as oxidative loss and changes in ratio of free to protein-bound penicillamine after sample collection.

Marnela *et al.* [57] used an amino acid analyzer using fluorescence detection to determine penicillamine in urine. Urine is analyzed on a Kontron Chromakon 500 amino acid analyzer containing a column (20 cm × 3.2 mm) of AS7O resin in the Li (I) form. Buffers containing LiOH, citric acid, methanol, HCl, and Brij 35 at pH 2.60, 3.20, and 3.60 are used as mobile phases (0.4 mL/h). The fluorescence reagent is prepared by the method of Benson and Hare. Detection is at 450 nm (excitation at 350 nm). The analyte response is linear from 0.025 to 10 mM, with a limit of detection of 25 μM.

Mann and Mitchell [58] described a simple colorimetric method for estimation of (*D*)-penicillamine in plasma. Blood containing 2–50 μg of penicillamine was mixed with 0.1 M EDTA solution in tromethamine buffer solution. 0.1 mL of this solution was adjusted to pH 7.4 and centrifuged. To a portion of the plasma was added 3 M HCL, the mixture was freeze-dried, and a suspension of the residue in ethanol was centrifuged. The supernatant liquid was mixed with tromethamine buffer solution (pH 8.2) and 10 mM 5,5′-dithiobis-(2-nitrobenzoic acid) in phosphate buffer solution (pH 7.0), the mixture was shaken with ethyl ether, and the absorbance of the separated aqueous layer was measured at 412 nm. The mean recovery was 60% (four determinations), and the calibration graph was linear for the cited range.

Usof *et al.* [59] utilized the derivatizing agent NPM and reversed-phase HPLC as a method for analysis of (*D*)-penicillamine. The relative standard deviation for within-precision and between-precision of 500 nM standard (*D*)-penicillamine were 2.27% and 2.23%, respectively. Female Sprague–Dawley rats were given 1 g/kg (*D*)-penicillamine I.P., and the amounts of (*D*)-penicillamine in the samples were subsequently determined. The assay is rapid, sensitive, and reproducible for determining it in biological samples.

Beales *et al.* [60] determined penicillamine and other thiols in urine by this method. To prevent oxidation of penicillamine, EDTA was added to the urine. A 20-μL sample was injected on to a 4.5-cm precolumn of Hypersil-ODS (5 μm) attached to an analytical column (10 cm× 4.6 mm) of the same material. The mobile phase (1 mL/min) consisted of heptanesulfonic acid and Na_2EDTA in water at pH 4. Disulfides in the elute were reduced in a column (15 cm × 4.6 mm) containing dihydrolipoamide-bonded glass beads, and then passed into the postcolumn reactor, a column (15 cm × 2 mm) of 40-μm glass beads. Ellman reagent (5,5′-dithiobis-(2-nitrobenzoic acid) and tripotassium citrate (pH 7.4)) was fed into the reactor at 0.5 mL/min., and detection of the yellow anion formed was at 412 nm. Homocysteine was used as internal standard. Calibration graphs were linear for thiols over the range of 10–150 ng on the column, and in the range 0–1 μg for penicillamine.

Lankmayr *et al.* [61] reported a method for the determination of penicillamine in serum. 1 mL of ethanol was added to 0.5 mL of serum that had been mixed with 50 μL of 0.3 M EDTA. After shaking and centrifuging the mixture, 1 mL of the supernatant solution was added to 2 mL of 0.067 M phosphate buffer (pH 8.2) and 0.2 mL of methanolic dansylaziridine (10 mg/mL), and the mixture was heated at

60 °C for 1 h. A 100 μL portion of the solution was injected onto a column (15 cm× 3.2 mm) of LiChroscob RP-18 (7 μm) for HPLC at room temperature, using acetonitrile–0.033 M phosphate buffer of pH 8.2 (1:2) containing 0.05% of ethylenediamine as the mobile phase (eluted at 1 mL/min). Fluorimetric detection involved excitation at 338 nm and measurement at 540 nm (or with a 430 nm cutoff filter). For 50–300 ng of drug injected on to the column, the coefficient of variation was 7–8%. The method permits a simple determination of (*D*)-penicillamine in serum at therapeutic levels.

Zygmunt *et al.* [62] determined penicillamine(I) containing sulfhydryl in the presence of glutathione(II) and cysteine(III) in urine or serum. The sample was deproteinized by adding 25% of its volume of acetonitrile–70% perchloric acid (4:1) and centrifuging. The clear solution was analyzed on a stainless-steel column (25 cm × 4.6 mm) containing Partisil 10 SCX, with a stainlesssteel guard column (5 cm × 4.6 mm) containing 37–44-μm LC-8 Pellicular Packing (Supelco). The mobile phase (eluted at 0.9 mL/min.) was 1% aqueous methanol buffered at pH 2.3 (10 mM citrate), and the detector was equipped with a dropping-mercury electrode, operated at +50 mV versus a silver–AgCl (1 M LiCl) electrode. The detection limit for penicillamine or cysteine was 0.6 μM, and 0.8 μM for glutathione. The detector response was linear for concentrations up to 0.1 mM.

Bergstrom *et al.* [63] used HPLC for determination of penicillamine in body fluids. Proteins were precipitated from plasma and hemolyzed blood with trichloroacetic acid and metaphosphoric acid, respectively, and, after centrifugation, the supernatant solution was injected into the HPLC system via a 20-μL loop valve. Urine samples were directly injected after dilution with 0.4 M citric acid. Two columns (5 cm × 0.41 cm and 30 cm × 0.41 cm) packed with Zipax SCX (30 μm) were used as the guard and analytical columns, respectively. The mobile phase (2.5 mL/min) was deoxygenated 0.03 M citric acid–0.01 M Na_2HPO_4 buffer, and use was made of an electrochemical detector equipped with a three-electrode thin-layer cell. The method was selective and sensitive for mercapto-compounds. Recoveries of penicillamine averaged 101% from plasma and 107% from urine, with coefficients of variation equal to 3.68 and 4.25%, respectively. The limits of detection for penicillamine were 0.5 μm and 3 μm in plasma and in urine, respectively. This method is selective and sensitive for sulfhydryl compounds.

Shaw *et al.* [64] described a (*D*)-penicillamine detection method in blood samples that had been treated with EDTA, deproteinized with trichloroacetic acid, and analyzed within 1 h. Penicillamine was detected at a vitreous-carbon electrode operated at +800 mV after HPLC separation. A linear calibration graph was obtained, and the method had a limit of detection equal to 5–20 ng. The method was useful in clinical and in pharmacokinetic studies.

Nishiyama and Kuninori [65] described a combination method of assay for penicillamine using HPLC and postcolumn reaction with 6,6′-dithiodi(nicotinic acid). Thiols were separated by HPLC on a reversed-phase column (25 cm × 4.6 mm) packed with Fine Sil C18-10, with 33 mM KH_2PO_4 (adjusted to pH 2.2 with H_3PO_4) or 33 mM sodium phosphate (pH 6.8) as the mobile phase. Detection was by postcolumn derivatization with 6,6′-dithiodi(nicotinic acid), and measurement of the absorbance of the released 6-mercaptonicotinic acid was made at 344 nm. The detection limit for penicillamine was 0.1 nmol. A comparison was made with a

method involving postcolumn derivatization with 5,5′-dithiobis-(2-nitrobenzoic acid).

Miners *et al.* [66] described a fluorescence method for (*D*)-penicillamine in plasma after derivatization with *N*-[4-(benzoxazol-2-yl)phenyl]maleimide and high performance liquid chromatography. Penicillamine is derivatized in acidified (pH 5) protein-free plasma solution with the cited reagent to give a stable fluorescent product. Chromatography is carried out using a column of micro Bondapak C18, and methanol–0.1 mM sodium acetate (12:13) as the mobile phase (flow rate of 2 mL/min). Detection by fluorescence at 360 nm (excitation at 319 nm) yielded linear calibration graphs that were linear over the range of 1–500 μM in plasma, and having a limit of detection of 0.25 μM. The method is suitable for pharmacokinetic studies.

REFERENCES

[1] C. C. Chiu and L. T. Grady Penicillamine, in *Analytical Profile of Drug Substances* (ed. K. Florey), Vol. 10, Academic Press, New York, 1981, pp. 601–637.
[2] *European Pharmacopeia*, 3rd edn., 2001, p. 1242.
[3] M. S. Rizk and N. A. Zakhari, *Farmaco, Ed. Prat.*, 1986, **41**, 75–82.
[4] P. J. Vollmer, J. Lee and T. G. Alexander, *J. Assoc. Off. Anal. Chem.*, 1980, **63**, 1191–1194.
[5] J. Motonaka, S. Ikeda and N. Tanaka, *Bunseki Kagaku*, 1982, **31**, 669–674.
[6] U. Forsman, *J. Electroanal. Chem.*, 1983, **152**, 241–254; *Anal. Abstr.*, March 1984, **46**, (3), [3D150].
[7] F. G. Banica, A. G. Fogg, A. Ion and J. C. Moreira, *Anal. Lett.*, 1996, **29**, 1415–1429.
[8] A. Ion, F. G. Banica, A. G. Fogg and H. Kozlowski, *Electroanal. (NY)*, 1996, **8**, 40–43.
[9] N. Wangfuengkanagul and O. Chailapakul, *Talanta*, 2002, **58**, 1213–1219.
[10] A. G. Fogg and N. M. Fayad, *Anal. Chim. Acta*, 1980, **113**, 91.
[11] J. M. Lopez-Fonseca, A. Otero and J. C. Garcia-Monteagudo, *Talanta*, 1988, **35**, 71–73.
[12] A. Besada, *Anal. Lett.*, 1988, **21**, 435–446.
[13] A. Besada, N. B. Tadros and Y. A. Gawarious, *Anal. Lett.*, 1987, **20**, 809–820.
[14] M. I. Walash, A. M. Metwally, A. A. El-Brashy and A. A. Abdelal, *IL Farmaco*, in press.
[15] V. Amarnth and K. Amarnth, *Talanta*, 2002, **56**, 745–751.
[16] A. A. Al-Majed, *J. Pharm. Biomed. Anal.*, 1999, **21**, 827–833.
[17] A. Besada and N. B. Tadros, *Mikrochim. Acta*, 1987, **II**, 225–228.
[18] P. B. Issopoulos and P. T. Economou, *Anal. Chim. Acta*, 1992, **257**, 203–207; *Anal. Abstr.*, December 1992, **54**, (12), [12G137].
[19] P. B. Issopoulos and S. E. Salta, *IL Farmaco*, 1997, **52**, 113–118; *Anal. Abstr.*, September 1997, **59**, (9), [9G168].
[20] N. Buyuktimkin and S. Buyuktimkin, *Pharmazie*, 1985, **40**, 581–582.
[21] M. A. Raggi, L. Nobile, V. Cavrini and A. M. Di Pietra, *Boll-Chim-Farm.*, 1986, **125**, 295–297.
[22] O. S. Fakhr Eldin, A. J. Haider, S. M. Z. Al-Lawati, A-Kindy, M. N. Imad Eldin and B. S. Salama, *Talanta*, 2003, **61**, 221–231.
[23] S. Y. Byeon, J. K. Choi and G. S. Yoo, *Yakche-Hakhoechi*, 1990, **20**, 73–78.
[24] A. A. Al-Majed, *Anal. Chim. Acta*, 2000, **408**, 169–175.
[25] Sh. M. Al-Ghannam, A. M. El-Brashy and Al-Farhan, *IL Farmaco*, 2002, **57**, 625–629.
[26] T. Pérez Ruiz, C. Martínez-Lozano, V. Tomás and C. Sidrach de Cardona, *J. Pharm. Biomed. Anal.*, 1996, **15**, 33–38.
[27] K. Kovacs-Hadady and I. T. Kiss, *Chromatographia*, 1987, **24**, 677–679.
[28] J. Martens, K. Guentherm and M. Schickedanz, *Arch. Pharm.*, 1986, **319**, 461–465, *Anal. Abstr.*, August, 1986, 48 [8E98].
[29] I. Abe, K. Terada, T. Nakahara and H. Frank, *J. High Resolut. Chromatogr.*, 1998, **21**, 592–596; *Anal. Abstr.*, April 1999, **61**, (4), [4B14].
[30] L. G. Rushing, E. B. Hansen and H. C. Thompson, *J. Chromatogr., Biomed. Appl.*, 1985, **337**, 37–46.

[31] S. Biffar, V. Greely and D. Tibbetts, *J. Chromatogr.*, 1985, **318**, 404–407.
[32] I. Merino-Merino, E. Blanco-Gonzalez and A. Sanz-Medel, *Mikrochim. Acta*, 1992, **107**, 73–80.
[33] K. Nakashima, T. Ishimaru, N. Kuroda and S. Akiyama, *Biomed. Chromatogr.*, 1995, **9**, 90–93.
[34] G. Favaro and M. Fiorani, *Anal. Chim. Acta*, 1996, **332**, 249–255.
[35] Macherey–Nagel, *Application Note*, 2001, **A–1243**, 2.
[36] V. P. Bystryakov, S. N. Lanin and A. P. Arzamastsev, *Khim. Farm. Zh.*, 1991, **25**, 81–84.
[37] H. J. Goetze, W. S. Sheldrick and A. F. M. Siebert, *Fresenius' J. Anal. Chem.*, 1993, **346**, 634–638.
[38] B. B. Tewari, *J. Chromatogr. A*, 1998, **793**, 220–222.
[39] B. B. Tewari, *Biomed. Chromatogr.*, 1996, **10**, 221–224.
[40] S. K. Srivastava, V. K. Gupta, B. B. Tiwari and I. Ali, *J. Chromatogr.*, 1993, **635**, 171–175.
[41] B. B. Tewari, *J. Chromatogr. A*, 2001, **910**, 181–185.
[42] R. Gotti, R. Pomponio, V. Andrisano and V. Cavrini, *J. Chromatogr. A.*, 1999, **844**, 361–369.
[43] J. Russell and D. L. Rabenstein, *Anal. Biochem.*, 1996, **242**, 136–144.
[44] Z. D. Zhang, W. R. G. Baeyens, X. R. Zhang and G. Van-der-Weken, *Analyst*, 1996, **121**, 1569–1572.
[45] M. S. Garcia, C. Sanchez-Pedreno, M. I. Albero and V. Rodenas, *J. Pharm. Biomed. Anal.*, 1993, **11**, 633–638.
[46] P. Vinas, I. Lopez-Garcia and J. A. Martinez-Gil, *J. Pharm. Biomed. Anal.*, 1993, **11**, 15–20.
[47] P. Vinas, J. A. Sanchez-Prieto and M. Hernandez-Cordoba, *Microchem. J.*, 1990, **41**, 2–9.
[48] G. Favaro and M. Fiorani, *Anal. Chim. Acta*, 1996, **332**, 249–255.
[49] Z. Zhang, W. R. G. Baeyens, X. Zhang, Y. Zhao and G. Van Der Weken, *Anal. Chim. Acta*, 1997, **347**, 325–332.
[50] A. I. Haj-Yehia and L. Z. Benet, *J. Chromatogr. B, Biomed. Appl.*, 1995, **666**, 45–53.
[51] H. Wakabayashi, S. Yamato, M. Nakajima and K. Shimada, *J. Pharm. Biomed. Anal.*, 1994, **12**, 1147–1152.
[52] D. L. Rabenstein and G. T. Yamashita, *Anal. Biochem.*, 1989, **180**, 259–263.
[53] K. Nakashima, M. Muraoka, S. Nakatsuji and S. Akiyama, *Rinsho. Kagaku.*, 1988, **17**, 51–54.
[54] G. T. Yamashita and D. L. Rabenstein; *J. Chromatogr., Biomed. Appl.*, **83** (2 (*J. Chromatogr.*, **491**)), 341–354.
[55] M. Wronski, *Chem. Anal. (Warsaw)*, 1989, **34**, 213–219; *Anal. Abstr.*, June 1991, **53**, [6F165].
[56] B. A. Webb, S. J. Richardson and I. Haslock, *Ann. Clin. Biochem.*, 1988, **25**, 186–191.
[57] K. M. Marnela, H. Isomaki, R. Takalo and H. Vapaatalo, *J. Chromatogr., Biomed. Appl.*, 1986, **53**, (1 (*J. Chromatogr.*, **380**)), 170–176.
[58] J. Mann and P. D. Mitchell, *J. Pharm. Pharmacol.*, 1979, **31**, 420–421; *Anal. Abstr.*, January 1980, **38**, (1), [1D42].
[59] M. Usof, R. Neal, N. Aykin and N. Ercal, *Biomed. Chromatogr.*, 2000, **14**, 535–540; *Anal. Abstr.*, July 2001, **63**, (7), [7G214].
[60] D. Beales, R. Finch, A. E. M. McLean, M. Smith and I. D. Wilson, *J. Chromatogr., Biomed. Appl.*, 1981, **226**, 498–503; *Anal. Abstr.*, July 1982, **43**, (1), [1D114].
[61] E. P. Lankmayr, K. W. Budna, K. Mueller, F. Nachtman and F. Rainer, *J. Chromatogr., Biomed. Appl.*, 1981, **222**, 249–255; *Anal. Abstr.*, September 1981, **41**, (3).
[62] B. Zygmunt, H. B. Hanekamp, P. Bos and R. W. Frei, *Fresenius' Z. Anal. Chem.*, 1982, **311**, 197–200; *Anal. Abstr.*, November 1982, **43**, (5), [5D115].
[63] R. F. Bergstrom, D. R. Kay and J. G. Wagner, *J. Chromatogr., Biomed. Appl.*, 1981, **222**, 445–452; *Anal. Abstr.*, November 1981, **41**, (5), [5D170].
[64] I. C. Shaw, A. E. M. Mclean and C. H. Boult, *J. Chromatogr.*, 1983, **275**, 206–210; *Anal. Abstr.*, February 1984, **46**, (2), [2D114].
[65] J. Nishiyama and T. Kuninori, *Anal. Biochem.*, 1984, **138**, 95–98.
[66] J. O. Miners, I. Fearnley, K. J. Smith, D. J. Birkett, P. M. Brooks and M. W. Whitehouse, *J. Chromatogr., Biomed. Appl.*, 1983, **275**, 89–96.

Penicillamine: Adsorption, Distribution, Metabolism, and Elimination Profile

Abdulrahman Al-Majed, Fathallah Belal, and Saeed Julkhuf

Department of Pharmaceutical Chemistry, College of Pharmacy, King Saud University, P.O. Box 2457; Riyadh 11451, Saudi Arabia

Contents

1. USES AND APPLICATIONS

The (*D*)-enantiomer of penicillamine is used clinically in man either as the hydrochloride or as the free amino acid [1], although the (*L*)-enantiomer also forms chelation complexes. Penicillamine is an effective chelator of copper, mercury, zinc, and lead, and other heavy metals to form stable, soluble complexes that are readily excreted in the urine [2,3].

Penicillamine has also been used in cystinuria and for the treatment of rheumatoid arthritis. Discovery of its chelating properties led to its use in patients with Wilson's disease (hepatolenticular degeneration) and heavy-metal intoxications. Penicillamine is administered by mouth and should be taken on an empty stomach [4].

2. PHARMACOKINETICS

2.1. Absorption

Penicillamine is well absorbed (40–70%) from the gastro-intestinal tract and, therefore, has a decided advantage over many chelating agents. Food, antacids, and iron reduce its absorption, so it should be taken on an empty stomach. Preferably, the

PROFILES OF DRUG SUBSTANCES, EXCIPIENTS, AND RELATED METHODOLOGY, VOLUME 32
ISSN: 0099-5428

DOI: 10.1016/S0099-5428(05)32006-5

substance should be administered 1 h or more before meals, 2 h after meals, and more than 1 h apart from any other drug, food, or milk [2, 5].

2.2. Distribution

Peak concentrations in the blood are obtained between 1 and 3 h after administration. Unlike cysteine (its nonmethylated parent compound), penicillamine is somewhat resistant to attack by *cysteine desulfhydrase* or *L-amino acid oxidase*. As a result, penicillamine is relatively stable *in vivo* [7,2].

2.3. Metabolism

Penicillamine is reported to be more than 80% bound to plasma protein. The compound is metabolized in the liver. *N-acetylpenicillamine* is more effective than penicillamine in protecting against the toxic effect of mercury, presumably because it is even more resistant to metabolism [7,2].

2.4. Elimination

Penicillamine is eliminated primarily via the urinary tract as penicillamin-disulfide, cysteine-penicillamine, homocysteine-penicillamine, or *S*-methyl-D-penicillamine. Studies with radiolabelled (*D*)-penicillamine indicate that the drug is rapidly eliminated via the kidney, with 80% of urinary excretion occurring within 10 h. Animal studies indicate that penicillamine is rapidly eliminated from the liver and kidneys, but is cleared slowly from collagen-and elastin-rich tissues such as skin and bone. Due to extensive binding in these tissues, excretion of drug and its metabolites persists for weeks or months following cessation of therapy [6]. Elimination is biphasic with an initial elimination half-life of about 1–3 h followed by a slower phase, suggesting gradual release from tissues [7].

3. PHARMACOLOGICAL EFFECTS [5]

3.1. Mechanism of action

Rheumatoid arthritis. The mechanism of action of penicillamine in rheumatoid arthritis is unknown. Penicillamine markedly lowers IgM rheumatoid factor, but produces no significant depression in absolute levels of serum immunoglobulins. It does dissociate macroglobulins (rheumatoid factor). The drug may decrease cell-mediated immune response by selectively inhibiting T-lymphocyte function. Penicillamine may also act as an anti-inflammatory agent by inhibiting release of lysosomal enzymes and oxygen radicals, protecting lymphocytes from the harmful effects of hydrogen peroxide formed at inflammatory sites.

Wilson's disease. Penicillamine is a chelating agent that removes excess copper in patients with Wilson's disease. From *in vitro* studies that indicate that one atom of copper combines with two molecules of penicillamine, it would appear that 1 g of

Table 1. Penicillamine drug interactions

Precipitant drug	Object drug*	Effect	Description
Penicillamine	Digoxin	↓	Digoxin serum may be reduced, possibly decreasing its pharmacological effects. The digoxin dose may need to be increased.
Penicillamine	Gold therapy, antimalarial or cytotoxic drugs, oxyphenbutazone or phenylbutazone	↑	Do not use these drugs in patients who are concurrently receiving penicillamine. These drugs are associated with similar serious hematologic and renal reactions.
Penicillamine	Gold salts	↑	Patients who have had gold salt therapy discontinued due to a major toxic reaction may be at greater risk of serious adverse reactions with penicillamine, but not necessarily of the same type. However, this is controversial.
Antacids	Penicillamine	↓	The absorption of penicillamine is decreased by 66% with coadministration of antacids.
Iron salts	Penicillamine	↓	The absorption of penicillamine is decreased by 35% with coadministration of iron salts.

* ↑ = object drug increased. ↓ = object drug decreased.

penicillamine should be followed by the excretion of almost 200 mg of copper. However, the actual amount excreted is almost 1% of this.

Cystinuria. Penicillamine reduces excess cystine excretion in cystinuria. Penicillamine with conventional therapy decreases crystalluria and stone formation, and may decrease the size of or dissolving existing stones. This is achieved by disulfide interchange between penicillamine and cystine, resulting in a substance more soluble than cystine and readily excreted.

3.2. Toxicity [2]

The main disadvantage of penicillamine for short-term use as a chelating agent is the concern that it might cause anaphylactic reactions in patients allergic to penicillin. With long-term use, penicillamine induces several cutaneous lesions, including urticaria, macular or popular reactions, pemphigoid lesions, lupus erythematosis, dermatomyositis, adverse effects on collagen, and other less serious reactions, such as dryness and scaling. Cross-reactivity with penicillin may be responsible for some episodes of urticarial or maculopapular reactions with generalized edema, pruritus, and fever.

The hematological system also may be affected severely. Reactions include leukopenia, aplastic anemia, and agranulosytosis. These may occur at any time during therapy, and they may be fatal.

Renal toxicity induced by penicillamine is usually manifested as reversible proteinuria and hematuria, but may progress to nephrouritic syndrome with membraneous glomerulopathy.

Toxicity to the pulmonary system is uncommon, but severe dyspnea has been reported from penicillamine-induced bronchoalveolitis. Myasthenia gravis has been induced by long-term therapy with penicillamine.

3.3. Drug interactions [5]

A summary of drug interactions with penicillamine is found in Table 1.

It has been found that the absorption of penicillamine is decreased by 52% when taken with food.

REFERENCES

[1] J. T. Scott, *Copeman's Textbook of the Rheumatic Diseases*, Churchill Livingstone, New York, 6th edn., 1986, p. 525.
[2] J. G. Hardman, A. G. Gilman and L. E. Limbird, *Goodman and Gilman's Pharmacological Basis of Therapeutics*, McGraw-Hill Companies, Inc., New York, 9th edn., 1996, p. 1667.
[3] *Drug Information for the Health Care Professional* (USP DI)^{R}, The United States of Pharmacopeial Convention, Inc., Rockville, Vol. I, 16th edn., 1996, p. 2297.
[4] A. A. Al-Majed, *Anal. Chim. Acta*, 2000, **408**, 169–175.
[5] *Drug Facts and Comparison*, A Wolters Kluwer Company, St. Louis, 2000, pp. 592–595.
[6] S. Budavari (ed.), *The Merck Index*, 12th edn., Merck and Co., NJ, 1996, p. 1218.
[7] K. Parfitt, *Martindale, The Complete Drug Reference*, Pharmaceutical Press, Massachusetts, 32nd edn., 1999, p. 988.

Primaquine Diphosphate: Comprehensive Profile

Abdullah A. Al-Badr

Department of Pharmaceutical Chemistry, College of Pharmacy, King Saud University, P.O. Box 2457, Riyadh-11451, Kingdom of Saudi Arabia

Contents

PROFILES OF DRUG SUBSTANCES, EXCIPIENTS, AND RELATED METHODOLOGY, VOLUME 32
ISSN: 0099-5428

DOI: 10.1016/S0099-5428(05)32007-7

1. DESCRIPTION

1.1. Nomenclature

1.1.1. Chemical names

N^4-(6-methoxy-8-quinolinyl)-1,4-pentanediamine diphosphate.
N^4-(6-methoxy-8-quinolinyl)-1,4-diaminopentane diphosphate.
(*RS*)-8-(4-amino-1-methylbutylamino)-6-methoxy quinoline diphosphate.
1,4-Diaminopentane, N^4-(6-methoxy-8-quinolinyl) diphosphate.
1,4-Pentanediamine, N^4-(6-methoxy-8-quinolinyl) diphosphate [1–6].

1.1.2. Nonproprietary names

Base: Primaquine, Primaquin, Primaquinum, Primaquina.
Phosphate: Primaquine phosphate, Primaquine (diphosphate de), Primaquini diphosphas, Primaquinbisdihydrogenphosphat, Primaquine diphosphate, Difosfato de Primaquina, Primachina Fosfato, Primaquinum Phosphoricum SN-13272 [1–6].

1.1.3. Proprietary names

PMQ-Inga, Primachina fosfato, Primaquine [1–6].

1.2. Formulae

1.2.1. Empirical formula, molecular weight, and CAS number

Primaquine	$C_{15}H_{21}N_3O$	259.35	[90–34–6]
Primaquine diphosphate	$C_{15}H_{21}N_3O{\cdot}2H_3PO_4$	455.34	[63–45–6]
Primaquine oxalate	$C_{15}H_{21}N_3O{\cdot}C_2H_2O_4$	349.39	–

1.2.2. Structure

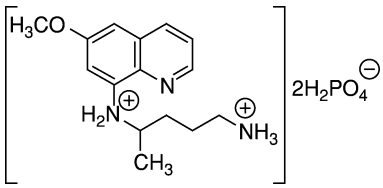

1.3. Elemental composition

Primaquine	C 69.47%;	H 8.16%;	N 16.20%;	O 6.17%.	
Primaquine diphosphate	C 39.56%;	H 5.93%;	N 9.23%;	O 31.65%;	P 13.63%.
Primaquine oxalate	C 58.44%;	H 6.63%;	N 12.03%;	O 22.90%	

1.4. Appearance

Primaquine: A viscous liquid.
Primaquine diphosphate: orange-red or orange crystalline powder, odorless and has bitter taste, solution is acid to litmus.
Primaquine oxalate: Yellow crystals from 80% ethanol.

1.5. Uses and application

Primaquine is an 8-aminoquinoline antimalarial agent, which is effective as tissue schizontocide against intrahepatic forms of all types of malaria parasite and is used to produce radical cure of *vivax* and *ovale* malarias. When primaquine is used for radical cure of *vivax* and *ovale* malarials, a course of treatment with a blood schizontocide must be given first to kill any erythrocytic parasite. Primaquine phosphate is then administered by mouth, usually in a dose equivalent to 15 mg of the base daily for 14 days but higher doses or longer courses may be required to overcome resistance in some strains of *Plasmodium vivax*. World Health Organization has advised that a treatment period of 21 days should be employed to achieve radical cure in most of South-East Asia and Oceania. A suggested dose for children is 250 mg/kg body weight daily for 14 days. Regimens of 30 mg (children, 500–750 μg/kg body weight) once every 7 days for 8 weeks have been suggested to minimize haemolysis in patients with glucose-6-phoshate dehydrogenase deficiency [3].

Primaquine is also gametocytocidal and a single dose of 30–45 mg has been suggested to prevent transmission of *falciparum* malaria particularly in areas where there is a potential for reintroduction of malaria. Primaquine is also used in the treatment of *Pneumocystis carinii* pneumonia in AIDS patients in combinations with clindamycin [3].

Primaquine should be administered cautiously to actually ill patients with any serious systemic disease characterized by a tendency to granulocytopenia such as rheumatoid arthritis or lupus erythematosus. The drug should be used with care in patients with glucose-6-phosphate dehydrogenase deficiency. Primaquine should be withdrawn if signs of haemolysis or methaemoglobinaemia occur and the blood

count should be monitored periodically. Primaquine should not be administered concomitantly with drugs liable to induce haemolysis or bone marrow depression. Mepacrine may increase the plasma concentrations of primaquine, resulting in a higher risk of toxicity, and it has been recommended that these drugs should not be used concomitantly [3].

2. METHODS OF PREPARATION

Elderfield *et al.* [7] prepared primaquine diphosphate as follows.

1,4-Dibromopentane **1** (460 g) and potassium phthalimide **2** (278 g) and 1.5 L acetone was refluxed for 24 h with stirring, the potassium bromide was filtered off, and the filtrate fractionated gave 67% 4-bromo-1-phthalimidopentane **3** as pale yellow oil. 6-Methoxy-8-aminoquinoline **4** (348 g) and 4-bromo-1-phthalimidopentane **3** (296 g) in 1 L ethanol was refluxed for 72 h with stirring. The mixture was cooled, diluted with diethyl ether and filtered, the residue of 6-methoxy-8-aminoquinoline hydrobromide was washed with diethyl ether, the combined filtrate and washings was washed with aqueous potassium carbonate and water, dried and evaporated, the dark brown residue was boiled in ethanol with decolorizing carbon and filtered. The filtrate was cooled and the crystal deposit was recrystallized from ethanol and gave the 4-phthalimido-1-methyl butyl amino analog **5** of primaquine. 6-Methoxy-8-aminoquinoline (17.4 g) **4**, 4-bromo-1-phthalimidopentane **3** (29.6 g), ethanol (30 mL) and phosphate buffer, pH 8, (100 mL) was heated for 79 h with stirring at 75–80 °C yielded 49% of crude 4-phthalimido-1-methyl butyl amino analog **5** of 6-methoxy-8-(4-amino-1-methyl butylamino)quinoline (primaquine) **6**. Compound **5** was refluxed for 2 h in ethanol with the equivalent amount of hydrazine hydrate and extracted with ethanol, the extract was treated with swirling with the calculated amount of 85% phosphoric acid, the precipitated orange oil was treated with ethanol, and the crystal material was recrystallized from 90% ethanol yielded 80% of primaquine diphosphate **6**. When primaquine base, in diethyl ether, was treated with 1 mol equivalent of oxalic acid in ethanol and the precipitate recrystallized from 80% ethanol gave primaquine oxalate.

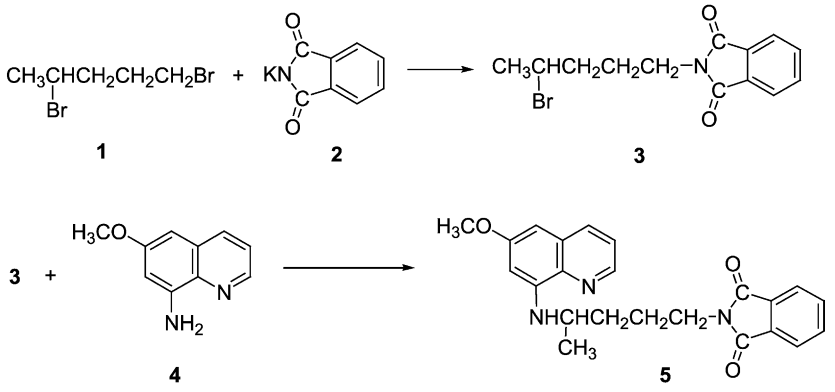

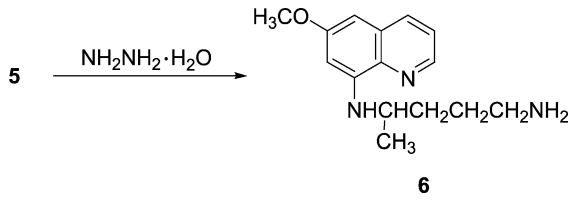

Chu *et al.* reported the synthesis of primaquine diphosphate [8] as follows.

4-Bromo-1-phthalimidopentane **3** was obtained in 72–82 g yield by refluxing 92 g of 1,4-dibromopentane **1**, 55.5 g of potassium phthalimide **2**, and 200 mL dry acetone on a steam bath for 30 h. Compound **3** (30 g) and 42 g 6-methoxy-8-aminoquinoline **4** refluxed at 130−135 °C for 6 h, extracted with benzene to separate insoluble 6-methoxy-8-aminoquinoline hydrobromide, the residue from evaporation of the benzene was refluxed with stirring with 100 mL of an alcoholic solution of 6 g hydrazine hydrate for 4 h, the solution was concentrated, made acidic to congo red with 8 N hydrochloric acid, filtered, and washed with boiling water. The combined filtrate and washings was concentrated, made alkaline, extracted with benzene, and distilled *in vacuo* to give 20.5 g primaquine **6**, which was treated with 19 mL 85% phosphoric acid in absolute ethanol, formed 42.5% primaquine diphosphate.

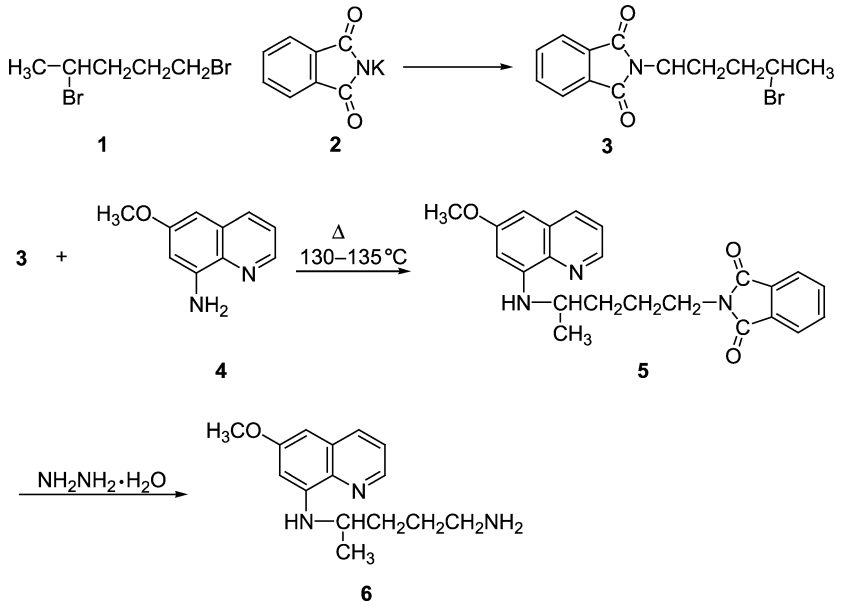

3. PHYSICAL CHARACTERISTICS

3.1. Solubility characteristics

Primaquine base: Soluble in ether, moderately soluble in water.

Primaquine diphosphate: Soluble 1 in 16 of water, practically insoluble in ethanol, chloroform, and ether.

3.2. X-ray powder diffraction pattern

The X-ray powder diffraction pattern of primaquine diphosphate was performed using a Simons XRD-5000 diffractometer. Table 1 shows the values of the scattering angles (degrees 2θ), the interplanar d-spacings (Å), and the relative intensities (%) for primaquine diphosphate, which were automatically obtained on a digital printer. Figure 1 shows the X-ray powder diffraction pattern of the drug, which was carried out on a pure sample of the drug.

3.3. Thermal methods of analysis

3.3.1. Melting behavior

Primaquine diphosphate melts at about 197–198 °C and primaquine oxalate melts at 182.5–185 °C. Primaquine as a base is viscous liquid that boils at 175–179 °C. Primaquine oxalate m.p. 182.5–185 °C.

3.3.2. Differential scanning calorimetry

The differential scanning calorimetry (DSC) thermogram of primaquine diphosphate was obtained using a DuPont TA-9900 thermal analyzer attached to a DuPont Data unit. The thermogram shown in Fig. 2 was obtained at a heating rate of 10 °C/min, and was run from 50 to 300 °C. The compound was found to melt at 209.8 °C.

3.4. Spectroscopy

3.4.1. UV–Vis spectroscopy

The ultraviolet spectrum of primaquine diphosphate in methanol (0.0016%) shown in Fig. 3 was recorded using a Shimadzu Ultraviolet visible spectrometer 1601 PC. The drug exhibited two maxima at 361 and 266.1 nm. Clarke reported the following: aqueous acid −265 nm (A 1%, 1 cm = 579a), 282 nm (A 1%, 1 cm = 574a), and 334 nm [2].

3.4.2. Vibrational spectroscopy

The infrared (IR) absorption spectrum of primaquine diphosphate was obtained as KBr disc using a Perkin-Elmer infrared spectrometer. The infrared spectrum is shown in Fig. 4 and the principal peaks are at 2946, 1612, 1469, 1430, 1384, 1200, 1050, 956, 815, and 760 cm^{-1}. The assignments of the infrared absorption bands of primaquine diphosphate are shown in Table 2. Clarke reported the following principal peaks at 1611, 1595, 815, 1230, 1572, and 1170 cm^{-1} (KBr disk) [2].

3.4.3. Nuclear magnetic resonance spectrometry

3.4.3.1. ^{1}H NMR spectra

The proton nuclear magnetic resonance (NMR) spectra of primaquine diphosphate was obtained using a Bruker instrument operating at 300, 400, or 500 MHz.

Table 1. Crystallographic data from the X-ray powder diffraction pattern of primaquine diphosphate

Scattering angle (degrees 2θ)	*d*-spacing (Å)	Relative intensity (%)	Scattering angle (degrees 2θ)	*d*-spacing (Å)	Relative intensity (%)
5.698	15.4976	4.90	5.945	14.8540	0.18
6.117	14.4356	0.22	10.320	8.5644	3.35
11.313	7.8149	100.00	12.260	7.2134	1.92
14.467	6.1176	3.97	15.318	5.7794	0.78
16.975	5.2190	45.33	17.765	4.9887	0.64
18.355	4.8295	1.15	18.998	4.6674	3.22
19.471	4.5552	2.60	20.000	4.4358	1.37
20.675	4.2925	14.76	21.611	4.1088	0.82
21.844	4.0655	1.64	22.650	3.9225	27.50
23.533	3.7773	0.75	24.121	3.6866	3.72
24.391	3.6463	2.79	25.083	3.5473	0.83
25.586	3.4787	1.18	25.840	3.4451	0.75
26.458	3.3660	0.72	27.3566	3.2332	3.19
29.295	3.0461	10.47	29.680	3.0075	0.72
30.204	2.9565	0.31	31.188	2.8654	2.21
31.520	2.8360	0.20	32.334	2.7665	0.43
32.818	2.7268	0.27	34.230	2.6174	9.36
34.514	2.5965	3.88	34.880	2.5701	1.17
35.593	2.5202	0.23	36.460	2.4623	0.39
39.040	2.3053	0.48	40.148	2.2442	3.34
40.509	2.2250	4.10	41.990	2.1499	0.33
42.528	2.1240	6.16	43.218	2.0916	0.63
43.625	2.0730	0.90	44.0.46	2.0542	2.17
45.093	2.0089	0.39	45.526	1.9908	1.71
46.162	1.9649	9.46	46.813	1.9390	0.39
47.677	1.9059	0.49	48.834	1.8634	0.35
49.983	1.8232	0.38	50.736	1.7979	0.67
52.353	1.7461	0.60	53.085	1.7238	0.42
53.800	1.7025	0.31	55.431	1.6562	0.15
56.765	1.6204	0.59	58.689	1.5718	0.79
59.018	1.5638	0.86			

Standard Bruker Software was used to execute the recording of DEPT, COSY, and HETCOR spectra. The sample was dissolved in DMSO-d_6 and all resonance bands were referenced to tetramethylsilane (TMS) internal standard. The ^{1}H NMR spectra of primaquine diphosphate are shown in Figs. 5–8. The ^{1}H NMR assignments of primaquine diphosphate are shown in Table 3.

3.4.3.2. ^{13}C NMR spectra

The ^{13}C NMR spectra of primaquine diphosphate were obtained using a Bruker instrument operating at 75, 100, or 125 MHz. The sample was dissolved in DMSO-d_6 and tetramethylsilane (TMS) was added to function as the internal standard. The ^{13}C NMR spectra are shown in Fig. 9. The HSQC and HMBC spectra are shown in Figs. 10 and 11, respectively. The DEPT 90 and DEPT 135 are shown in Figs. 12 and 13, respectively. The assignments for the observed resonance bands associated with the various carbons are provided in Table 4.

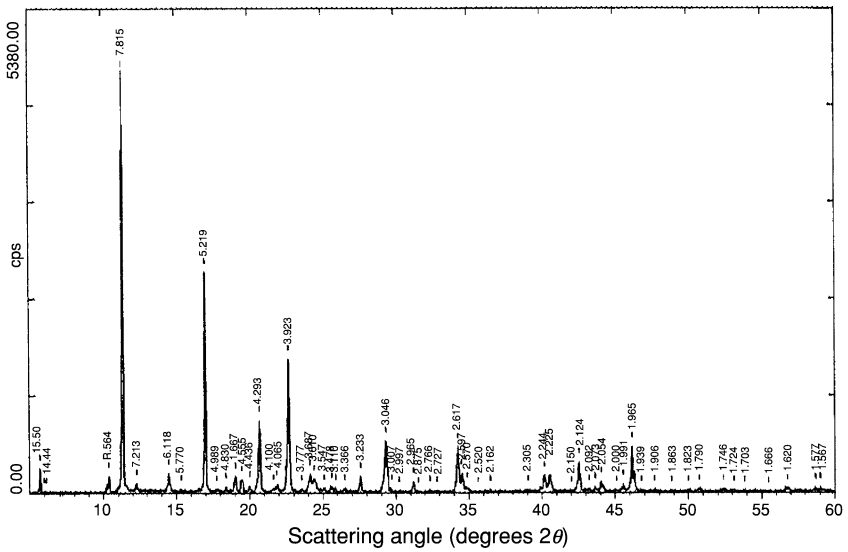

Fig. 1. The X-ray powder diffraction pattern of primaquine diphosphate.

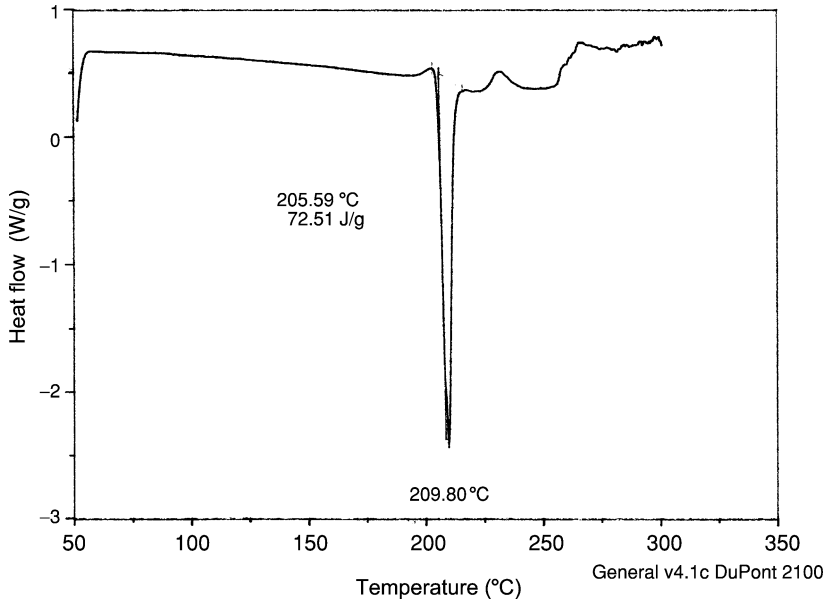

Fig. 2. Differential scanning calorimetry thermogram of primaquine diphosphate.

3.5. Mass spectrometry

The mass spectrum of primaquine diphosphate was obtained using a Shimadzu PQ-5000 mass spectrometer. The parent ion was collided with helium as a carrier gas. Figure 14 shows the detailed mass fragmentation pattern for primaquine diphosphate. Table 5 shows the proposed mass fragmentation pattern of the drugs. Clarke reported the following principal peaks at *m/z* 201, 81, 98, 175, 259, 176, 202, and 242 [2].

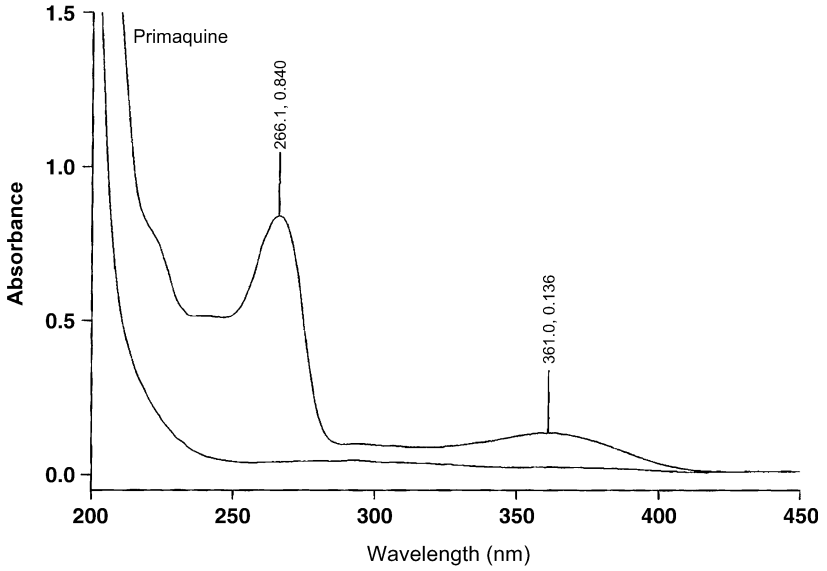

Fig. 3. Ultraviolet absorption spectrum of primaquine diphosphate.

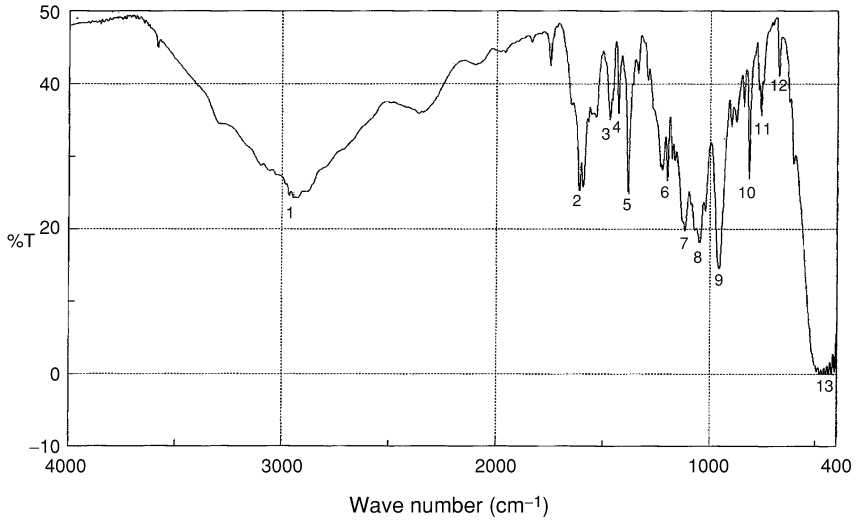

Fig. 4. The infrared absorption spectrum of primaquine diphosphate (KBr pellet).

4. METHODS OF ANALYSIS

4.1. Compendial method of analysis

4.1.1. British pharmacopoeia compendial methods [3]

4.1.1.1. Primaquine phosphate

Primaquine phosphate contains not less than 98.5% and not more than the equivalent of 101.5% of (*RS*)-8-(4-amino-1-methylbutylamino)-6-methoxyquinoline diphosphate, calculated with reference to the dried substance.

Table 2. Vibrational assignments for primaquine diphosphate infrared absorption bands

Frequency (cm^{-1})	Assignments
3300–3150	NH_2 and NH stretch
2946–2900	CH_3 and CH_2 stretch
1612	 stretch
1469, 1430	CH_2 bending
1384, 1200	C–H bending
1050	C–O stretch
956, 815, 760	C–H bending

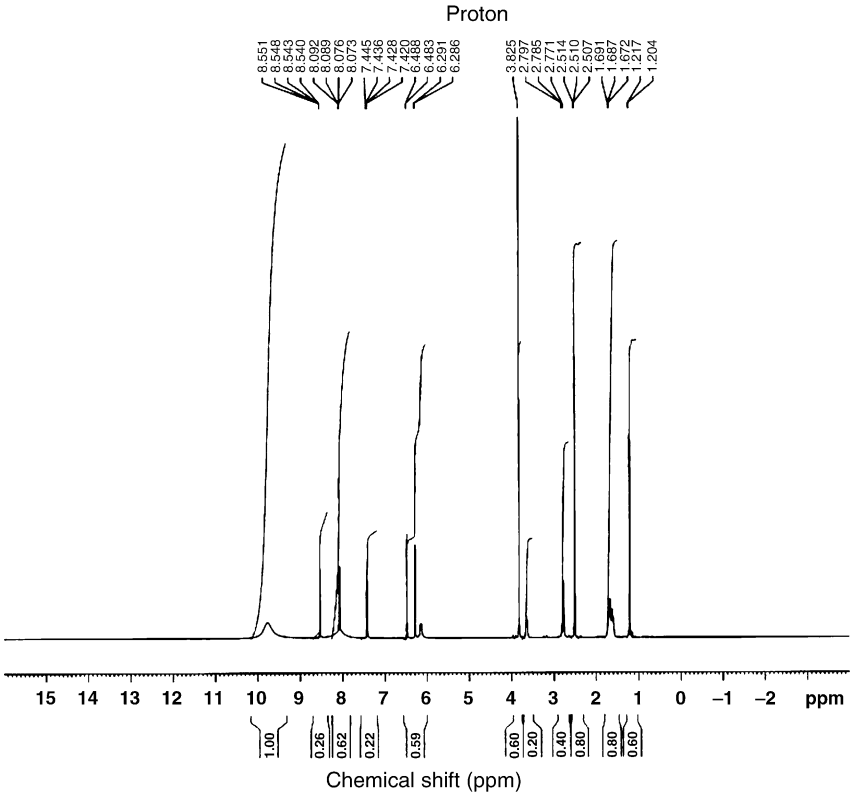

Fig. 5. The ^1H NMR spectrum of primaquine diphosphate in DMSO-d_6.

Identification

Test 1: Dissolve 15 mg of primaquine phosphate in 0.01 M *hydrochloric acid* and dilute to 100 mL with the same acid. Examined between 310 and 450 nm, according to the general procedure (2.2.25), the solution shows two absorption maxima, at 332

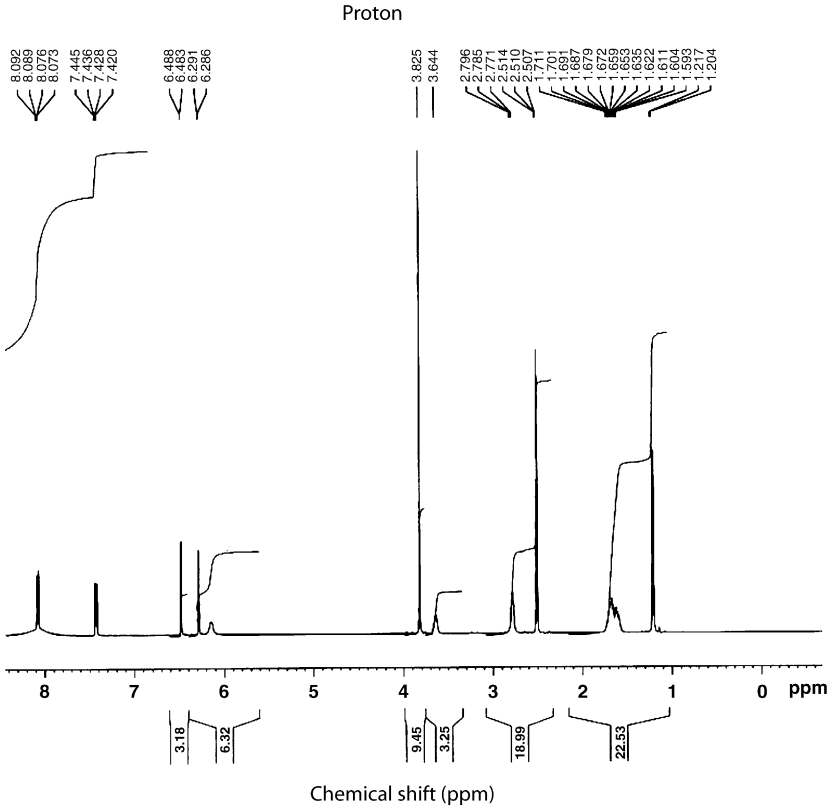

Fig. 6. Expanded ^{1}H NMR spectrum of primaquine diphosphate in DMSO-d_6.

and 415 nm. The specific absorbances at the maxima are 45–52 and 27–35, respectively. Dilute 5 mL of the solution to 50 mL with 0.01 M *hydrochloric acid*. Examined between 215 and 310 nm, the solution shows three absorption maxima, at 285, 265, and 282 nm. The specific absorbances at the maxima are 495–515, 335–350, and 330–345, respectively.

Test 2: Examine by infrared absorption spectrophotometry, according to the general procedure (2.2.24), comparing with spectrum obtained with *primaquine diphosphate* Chemical Reference Substance (*CRS*). Examine the substance as discs prepared as follows: dissolve separately 0.1 g of primaquine diphosphate and the reference substance in 5 mL of *water R*, add 2 mL of *dilute ammonia R* and 5 mL of *chloroform R* and shake; dry the chloroform layer over 0.5 g of *anhydrous sodium sulfate R*; prepare a blank disc using about 0.3 g of *potassium bromide R*, apply dropwise to the disc 0.1 mL of the chloroform layer, allowing the chloroform to evaporate between applications; dry the disc at 50 °C for 2 min.

Test 3: Examine by thin-layer chromatography, as specified in the general procedure (2.2.27), using as the coating substance a suitable silica gel with a fluorescent indicator having an optimal intensity at 254 nm.

Carry out all operations as rapidly as possible protected from light. Prepare the test and reference solutions immediately before use.

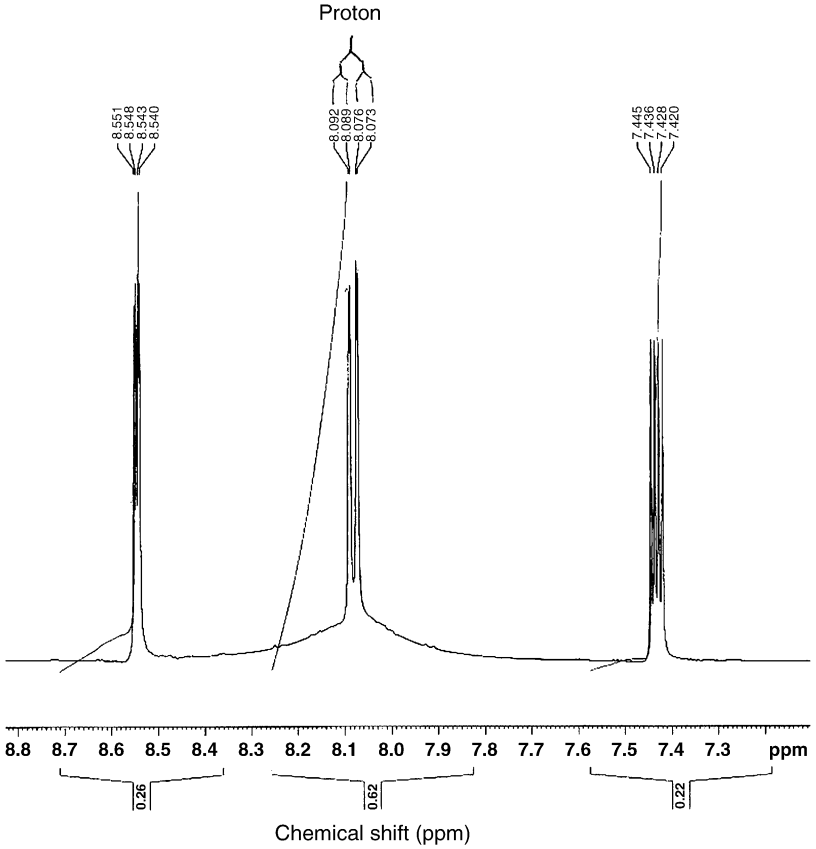

Fig. 7. Expanded ^{1}H NMR spectrum of primaquine diphosphate in DMSO-d_6.

Test solution: Dissolve 0.2 g of primaquine diphosphate in 5 mL of *water R* and dilute to 10 mL with *methanol R*. Dilute 1 mL of the solution to 10 mL with a mixture of equal volumes of *methanol R* and *water R*.

Reference solution: Dissolve 20 mg of primaquine diphosphate CRS in 5 mL of water R and dilute to 10 mL with *methanol* R.

Carry out prewashing of the plate with a mixture of 1 volume of *concentrated ammonia R*, 40 volumes of *methanol R* and 60 volumes of *chloroform R*. Allow the plate to dry in air. Apply separately to the plate 5 μL of each solution. Develop over a bath of 15 cm using the mixture of solvents prescribed for prewashing. Allow the plate to dry in air and examine in ultraviolet light at 254 nm. The principal spot in the chromatogram obtained with the test solution is similar in position and size to the principal spot in the chromatogram obtained with the reference solution.

Test 4: Dissolve 50 mg of primaquine diphosphate in 5 mL of *water R*. Add 2 mL of *dilute sodium hydroxide solution R* and shake with two quantities, each of 5 mL, of *chloroform R*. The aqueous layer, acidified by addition of *nitric acid R*, gives reaction (b) of phosphates, as described in the general procedure (2.3.1).

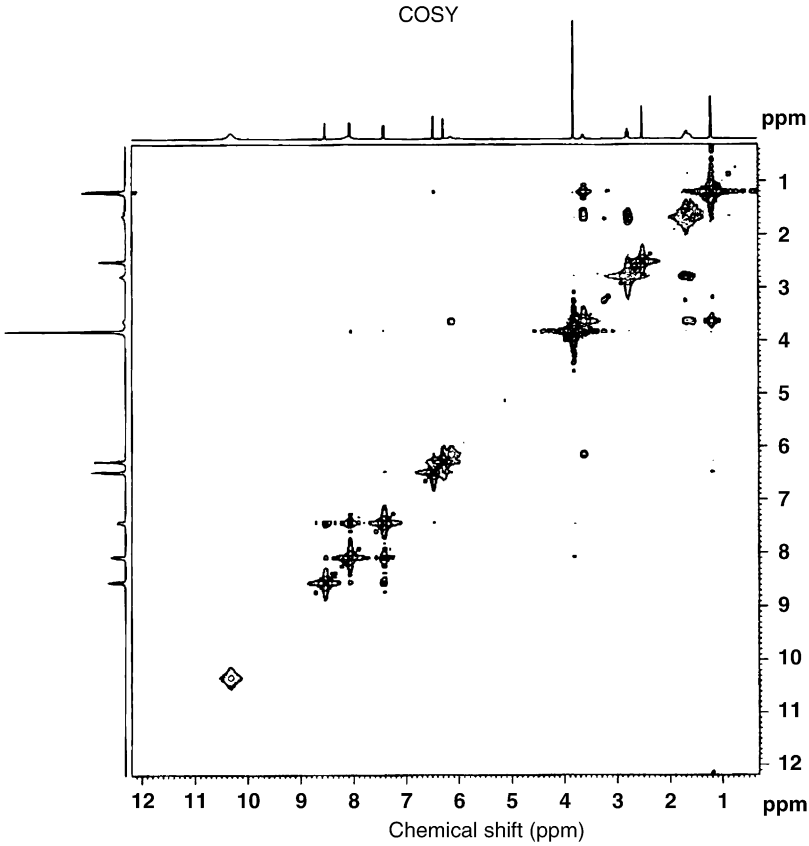

Fig. 8. COSY ^{1}H NMR spectrum of primaquine diphosphate in DMSO-d_6.

Tests

Related substances. Examine by liquid chromatography as described in the general procedure (2.2.29).

Test solution: Dissolve 50 mg of primaquine diphosphate in *water R* and dilute to 5 mL with the same solvent. To 1 mL of this solution add 0.2 mL of *concentrated ammonia R* and shake with 10 mL of the mobile phase. Use the clear lower layer.

Reference solution (a): Dissolve 50 mg of *primaquine diphosphate CRS* in *water R* and dilute to 5 mL with the same solvent. To 1 mL of this solution, add 0.2 mL of *concentrated ammonia R* and shake with 10 mL of the mobile phase. Use the clear lower layer.

Reference solution (b): Dilute 3 mL of the test solution to 100 mL with the mobile phase.

Reference solution (c): Dilute 1 mL of the test solution to 10 mL with the mobile phase. Dilute 1 mL of this solution to 50 mL with the mobile phase.

The chromatographic procedure may be carried out using:

– a column 0.2 m long and 4.6 mm in internal diameter packed with *silica gel* for *chromatography R* (10 μm).

Table 3. Assignments of the resonance bands in the ^{1}H NMR spectrum of primaquine diphosphate

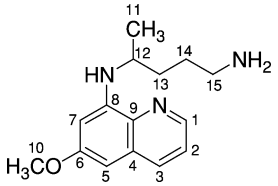

Chemical shift (ppm, relative to TMS)	Number of protons	Multiplicity*	Assignment (proton at carbon number)
9.6–9.90	2	bs	NH_2
8.54–8.55	1	m	1
8.07–8.09	2	dd	3 and NH
7.42–7.44	1	q	2
6.48	1	s	7
6.29	1	s	5
3.82	3	s	10
3.64	1	bs	12
2.77–2.79	2	t	15
1.59–1.71	2	m	13 and 14
1.20–122	3	t	11

*s, singlet; dd, double doublet; m, multiplet; bs, broad singlet; q, quartet.

– a mixture of 0.1 volume of *concentrated ammonia R*, 10 volumes of *methanol R*, 45 volumes of *chloroform R*, and 45 volumes of *hexane R* as the mobile phase at a flow rate of 3 mL/min.
– as detector a spectrophotometer set at 261 nm.
– a loop injector.

Inject 20 µL of each solution and continue the chromatography for at least twice the retention time of primaquine. In the chromatogram obtained with the test solution, the sum of the areas of any peaks, apart from the principal peak, is not greater than the area of the principal peak in the chromatogram obtained with reference solution (b) (3%). Disregard peak due to solvent and any peak whose area is less than that of the principal peak in the chromatogram obtained with reference solution (c). The test is not valid unless in the chromatogram obtained with reference solution (a), just before the principal peak there is a peak whose area is about 6% of that of the principal peak and the resolution between these peaks is not less than 2; in the chromatogram obtained with reference solution (c) the signal-to-noise ratio of the principal peak is not less than five.

Loss on drying. When the experiment is carried out according to the general procedure (2.2.32), not more than 0.5% is determined on 1 g by drying in an oven at 100–105 °C.

Assay

Dissolve 0.2 g of primaquine phosphate in 40 mL of *anhydrous acetic acid R*, heating gently. Titrate with 0.1 M *perchloric acid* determining the endpoint

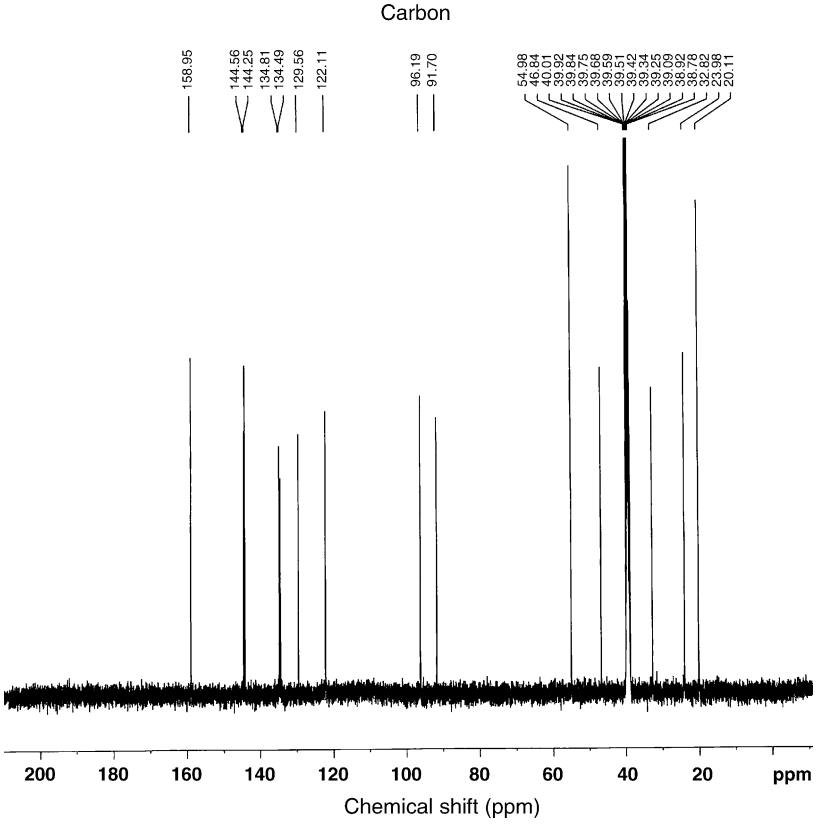

Fig. 9. ^{13}C NMR spectrum of primaquine diphosphate in DMSO-d_6.

potentiometrically as described in the general procedure (2.2.20). One milliliter of 0.1 M *perchloric acid* is equivalent to 22.77 mg of $C_{15}H_{27}N_3O_9P_2$.

Storage

Store protected from light.

4.1.2. United States pharmacopoeia compendial methods [4]

4.1.2.1. Primaquine phosphate

Primaquine phosphate contains not less than 98% and not more than 102% of $C_{15}H_{21}N_3O{\cdot}2H_3PO_4$ calculated on the dried basis.

Identification

Test 1: Infrared absorption. This test must be carried out according to the general procedure <197K>. The spectrum obtained from the sample of primaquine phosphate should be identical with that spectrum obtained from *USP Primaquine Phosphate RS*.

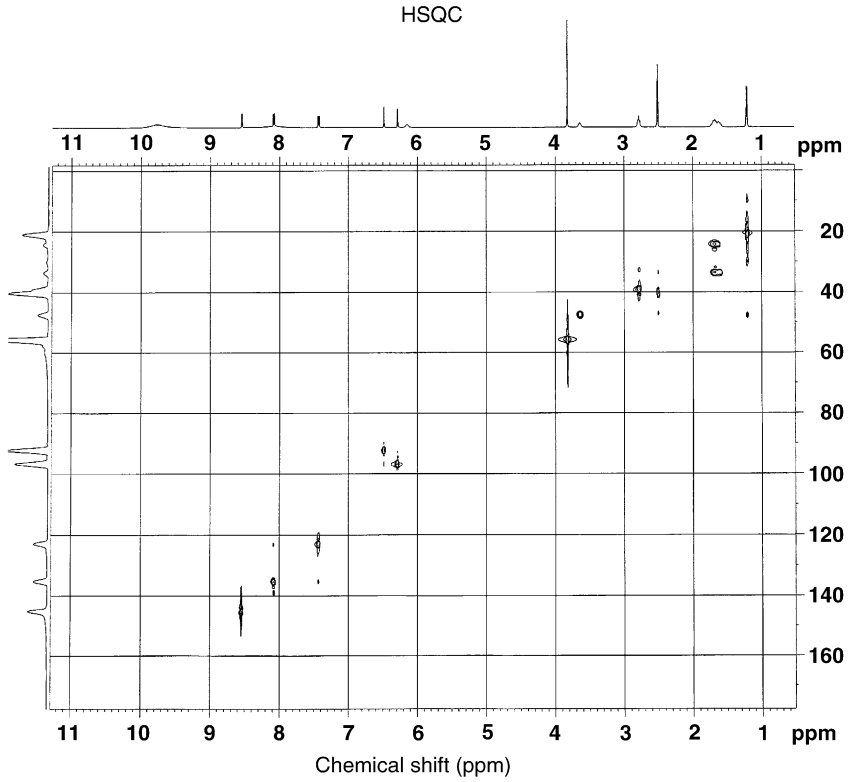

Fig. 10. The HSQC NMR spectrum of primaquine diphosphate in DMSO-d_6.

Test 2: The residue obtained by ignition of primaquine phosphate responds to the test for pyrophosphate as described under phosphate, the test must be carried out as described in the general procedure <191>.

Loss on drying. By following the general procedure <731>, dry primaquine phosphate at 105 °C for 2 h. It loses not more than 1% of its weight.

Organic volatile impurities. By following method 1 in the general procedure <467>: meets the requirements.

Assay

Dissolve about 700 mg of primaquine phosphate, accurately weighed, in about 75 mL of water in a beaker, add 10 mL of hydrochloric acid, and proceed as directed under Nitrite Titration in the general procedure <451>, beginning with "cool to about 15 °C". Each milliliter of 0.1 M sodium nitrite is equivalent to 45.53 mg of $C_{15}H_{21}N_3O{\cdot}2H_3PO_4$.

4.1.2.2. Primaquine phosphate tablets

Primaquine phosphate tablets contain not less than 93% and not more than 107% of the labeled amount of $C_{15}H_{21}N_3O{\cdot}2H_3PO_4$.

Packaging and storage. Preserve in well-closed, light-resistant container.

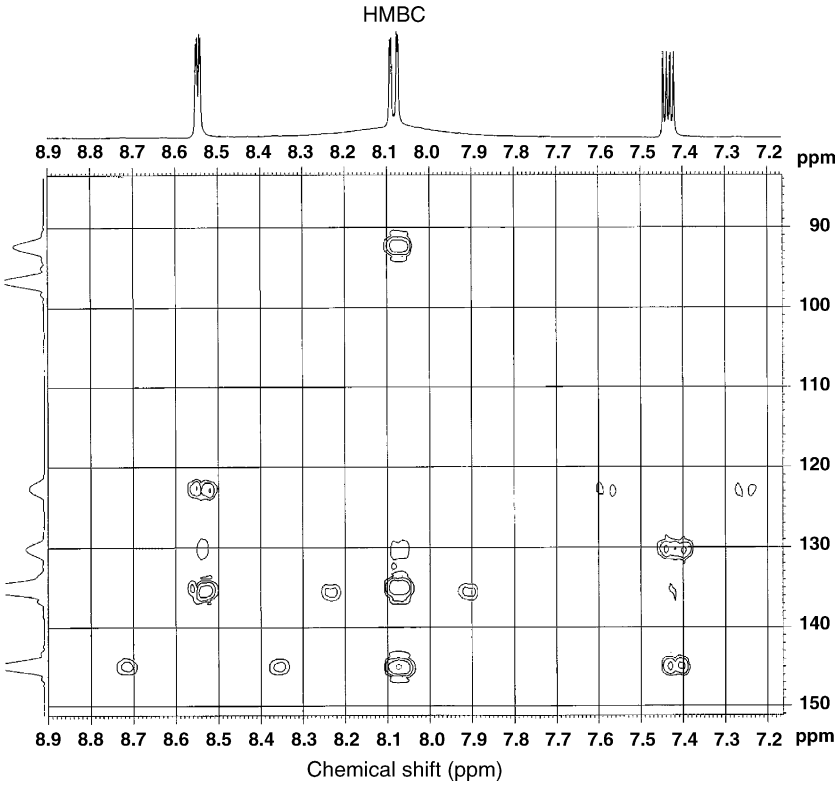

Fig. 11. The HMBC NMR spectrum of primaquine diphosphate in DMSO-d_6.

USP Reference Standards <11>. *USP Primaquine Phosphate RS.*

Identification

Digest a quantity of finely powdered tablets, equivalent to about 25 mg of primaquine phosphate, with 10 mL of water for 15 min, and filter.

Test 1: Dilute 0.1 mL of the filtrate with 1 mL of water, and add one drop of gold chloride TS: a violet blue color is produced at once.

Test 2: To the remainder of the filtrate add 5 mL of trinitrophenol TS: a yellow precipitate is formed. Wash the precipitate with cold water, and dry at 105 °C for 2 h: the picrate melts between 208 °C and 215 °C. [*Caution: Picrate may explode.*]

Dissolution. To be carried out according to the general procedure <711>:

Medium: 0.01 N Hydrochloric acid; 900 mL.
Apparatus 2: 50 rpm.
Time: 60 min.

Determine the amount of $C_{15}H_{21}N_3O{\cdot}2H_3PO_4$ dissolved by employing the following method:

1-Pentanesulfonate sodium solution: Add about 961 mg of sodium-1-pentanesulfonate and 1 mL of glacial acetic acid to 400 mL of water, and mix.

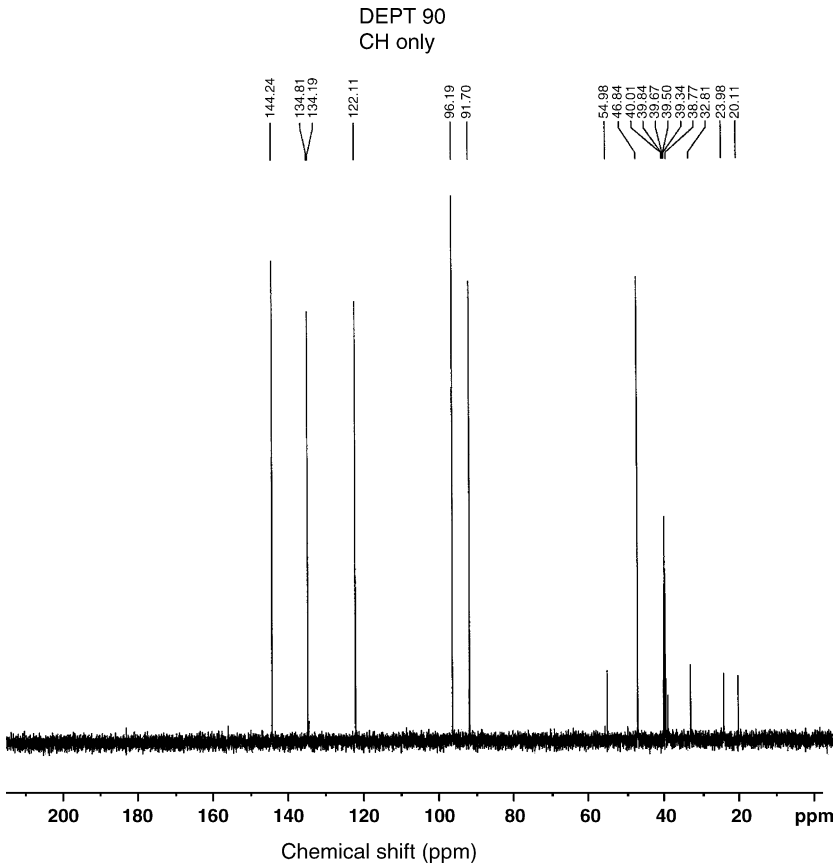

Fig. 12. The DEPT 90 ^{13}C NMR spectrum of primaquine diphosphate in DMSO-d_6.

Mobile phase: Prepare a filtered and degassed mixture of methanol and *1-pentanesulfonate sodium solution* (60:40). Make adjustments if necessary (see *system suitability under Chromatography* <621>).

Chromatographic system: See Chromatography <621>.

The liquid chromatograph is equipped with a 254 nm detector and a 3.9 mm × 30 cm column that contains packing L1. The flow rate is about 2 mL/min. Chromatograph replicate injections of the Standard solution and record the peak responses as directed for *procedure*: the relative standard deviation is not more than 3%.

Procedure: Separately inject into the chromatograph equal volumes (about 20 μL) of the solution under the test and a Standard solution having a known concentration of *USP primaquine phosphate RS* in the same *Medium* and record the chromtograms. Measure the responses for the major peak, and calculate the amount of $C_{15}H_{21}N_3O{\cdot}2H_3PO_4$ dissolved.

Tolerances: Not less than 80% (*Q*) of the labeled amount of $C_{15}H_{21}N_3O{\cdot}2H_3PO_4$ is dissolved in 60 min.

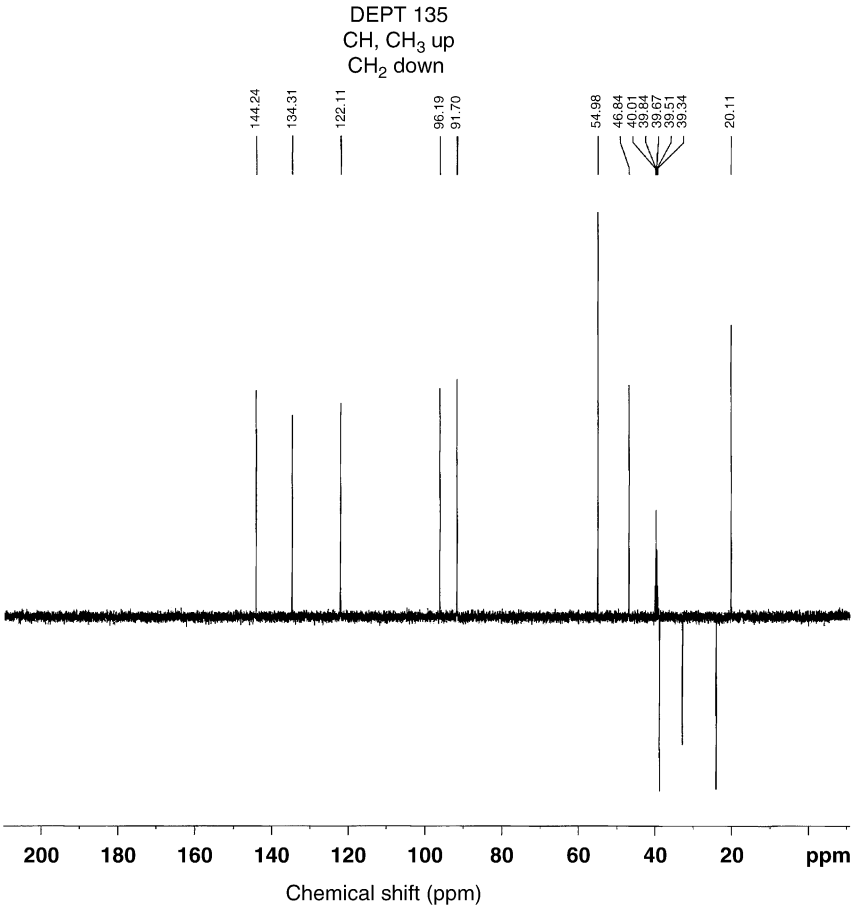

Fig. 13. The DEPT 135 ^{13}C NMR spectrum of primaquine diphosphate in DMSO-d_6.

Uniformity of dosage units. When the test is carried out as directed in the general procedure <905>: meet the requirements.

Procedure for content uniformity: Transfer 1 tablet, previously crushed or finely powdered, to a beaker, add 5 mL of hydrochloric acid and about 25 g of crushed ice, then add water to bring the total volume to about 50 mL. Proceed as directed under *Nitrite Titration* under the general procedure <451>, beginning with "slowly titrate", and using as the titrant 0.01 M sodium nitrite VS, freshly prepared from 0.1 M sodium nitrite. Concomitantly perform a blank titration, and make any necessary correction. Each milliliter of 0.01 M sodium nitrite is equivalent to 4.553 mg of $C_{15}H_{21}N_3O{\cdot}2H_3PO_4$.

Assay

Weigh and finely powder not less than 30 tablets. Weigh accurately a portion of the powder, equivalent to about 700 mg of primaquine phosphate, and transfer to a

Table 4. Assignments for the resonance bands in the ^{13}C NMR spectrum of primaquine diphosphate

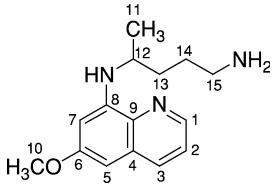

Chemical shift (ppm relative to TMS)	Assignment (carbon number)	Chemical shift (ppm relative to TMS)	Assignment (carbon number)
158.95	6	91.70	7
144.56	8	54.98	10
144.25	1	46.84	12
134.81	9	38.77	15
134.49	3	32.82	14
129.56	4	23.98	13
122.11	2	20.11	11
96.19	5		

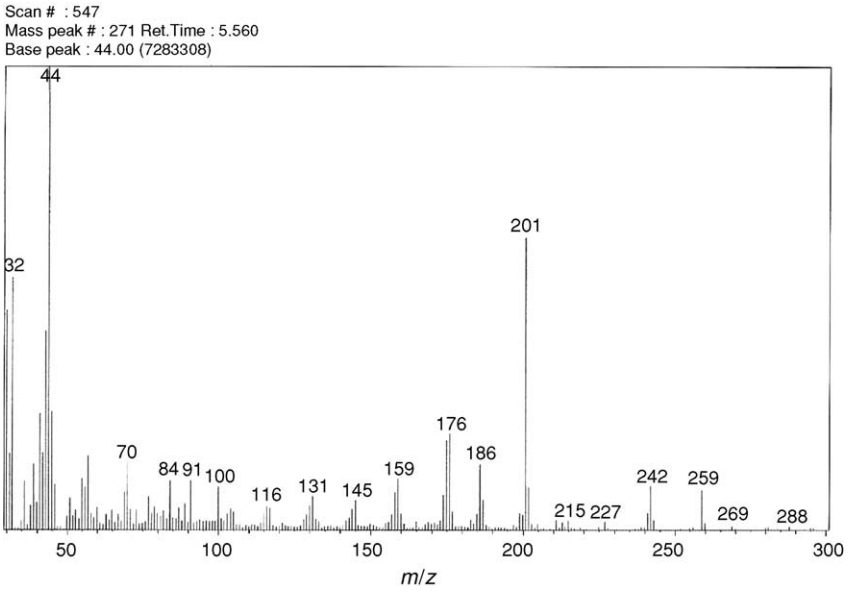

Fig. 14. Mass spectrum of primaquine diphosphate.

beaker. Add 50 mL of water and sufficient hydrochloric acid to provide about 5 mL in excess, and proceed as directed under *Nitrite Titration* as described in the general procedure <451>, beginning with "cool to about 15 °C". Each milliliter of 0.1 M sodium nitrite is equivalent to 45.53 mg of $C_{15}H_{21}N_3O{\cdot}2H_3PO_4$.

Table 5. Mass spectral fragmentation pattern of primaquine diphosphate

m/z	Relative intensity (%)	Fragment	
		Formula	Structure
259	9	$C_{15}H_{21}N_3O$	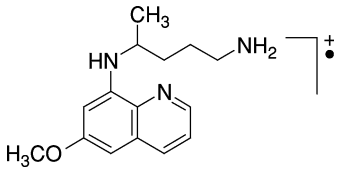
243	2	$C_{14}H_{17}N_3O$	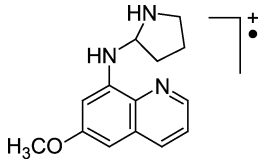
242	10	$C_{14}H_{16}N_3O$	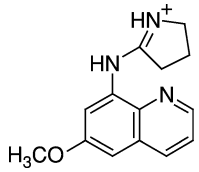
215	2	$C_{12}H_{13}N_3O$	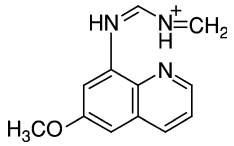
201	62	$C_{12}H_{13}N_2O$	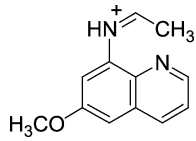
186	14	$C_{11}H_{10}N_2O$	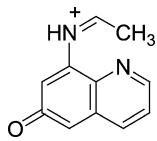
175	19	$C_{10}H_{11}N_2O$	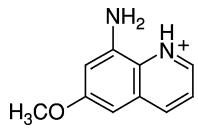
174	7	$C_{10}H_{10}N_2O$	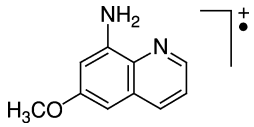

(*Continues*)

Table 5. (*Continued*)

m/z	Relative intensity (%)	Fragment	
		Formula	Structure
159	11	$C_9H_7N_2O$	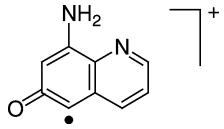
145	7	$C_9H_9N_2$	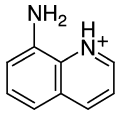
116	4	C_8H_6N	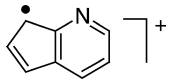
131	8	$C_8H_7N_2$	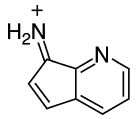
100	5	$C_5H_{12}N_2$	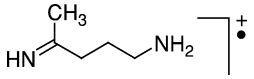
91	10	C_6H_5N	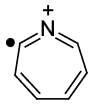
84	9	$C_4H_8N_2$	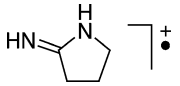
70	14	C_4H_8N	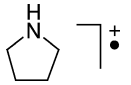
44	100	C_2H_6N	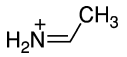
32	53	CH_4O	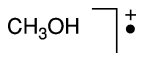
30	53	CH_4N	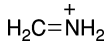

4.2. Reported methods of analysis

4.2.1. Identification

Clarke recommended the following three identification tests [2]:

Test 1: Dissolve 10 mg of primaquine diphosphate in 5 mL of water and add 1 mL of a 5% solution of ceric ammonium sulfate in dilute nitric acid, a violet color is produced (distinction from chloroquine) [2].

Test 2: Mandelin's Test: Dissolve 0.5 g of ammonium vanadate in 1.5 mL of water and dilute to 100 mL with *sulfuric acid*. Filter the solution through glass wool. Add a drop of the reagent to the primaquine phosphate sample on a white tile. A orange → violet color is produced [2].

Test 3: Marquis Test: Mix 1 volume of *formaldehyde solution* with 9 volumes of *sulfuric acid*. Add a drop of the reagent to the primaquine phosphate sample on a white tile; an orange color is produced [2].

4.2.2. Titrimetric methods

Nickel used nitromethane and acetonitrile for the titration of primaquine and other basic pharmaceuticals in various solvents with 0.05 N perchloric acid in dioxane [9]. Half-neutralizaton potentials were determined in acetonitrile, methyl nitrite, and acetic acid anhydride with respect to pyramidon, arbitrarily taken as 500 mV and were shown in a table.

Walash *et al.* [10] determined primaquine and other quinoline drugs in bulk and in pharmaceuticals by a titrimetric method. The method is based on reaction with 1,3-dibromo-5,5-dimethylhydantoin or *N*-bromosuccinimide as the titrant. Primaquine was determined either by usual titration or by potentiometric titration with the brominating agents. The recovery was approximately 100%. The method was simple, precise, and accurate.

Ahmad and Shukla [11] determined primaquine and other antimalarial aminoquinolines by vanadium titration. The drugs were determined by oxidation with aqueous ammonium vanadate solution and back titration of the unconsumed reagent with aqueous acidic ammonium ferrous sulfate with *N*-phenyl anthranilic acid indicator.

Yang *et al.* [12] determined the ionization constants of primaquine by a titrimetric method and studied its coordination ratio with vitamin C. The ionization constants of primaquine in 50% (v/v) ethanol in water determined at 25 °C in the ionic strength range of 5×10^{-3} to 5×10^{-2} mol/L are given. The coordination ratio of primaquine to vitamin C is determined by continuous variation and mole ratio methods based on pH and conductance measurements to be 1:1, indicating that the coordination compound formed in the solution is mainly a 1:1 compound.

Hufford *et al.* [13] determined the dissociation constants of primaquine by titration with 0.1 N hydrochloric acid in acetonitrile–water mixture and values were extrapolated to water by using linear regression analysis.

4.2.3. Conductometric methods

Papovic *et al.* [14] used a conductometric method for the determination of primaquine phosphate. This method is recommended with perchloric acid, silicotungstic acid, and sodium hydroxide as titrants. Conductometric curves obtained with

various titrants differ in their shapes, depending on the changes occurring in conductivity of the solution before and after the titration endpoint, and their character is such that the titration endpoint can be accurately and reproducibly determined. In titration with perchloric acid, no individual protonations were observed on conductometric curves and only one inflexion point appeared although both the nitrogen atoms were protonated. Moreover, in the titration of primaquine phosphate with silicotungstic acid one inflexion point was obtained. With sodium hydroxide, deprotonation was effected only on the primary amine of the drug.

Amin and Issa [15] described a conductometric and indirect atomic absorption spectrometric methods for the determination of primaquine phosphate and other antimalarial agents. The method is based on the formation of their ion-associates with [Cd^{2+}, Co^{2+}, Mn^{2+}, and Zn^{2+}] thiocyanate, ammonium reineckate, and/or sodium cobaltinitrate. The molar combining ratio reveal that (1:1) (drug:reagent) ion-associates are formed for all reagents except for ammonium reineckate which forms (1:2) ion-associates with all studied drugs. The optimum conditions for the ion-association have been studied. Conductometric method was applied for the drug determination of the suggested drugs in bulk powders, whereas indirect atomic absorption spectrometric method, depending on the measurement of the excess metal ion present in supernatant solutions after precipitation of the ion associates is used to calculate the drug concentration. Optimum concentrations ranges for the determination of primaquine and the drugs under consideration were 0.46–12.9 and 0.155–3.87 mg using conductometric and indirect atomic absorption spectral methods, respectively. These procedures have been applied successfully to the analysis of these drugs in formulations and the results are favorably comparable to the official methods.

4.2.4. Spectrophotometric methods

Abou-Ouf *et al.* [16] described a spectrophotometric method for the determination of primaquine phosphate in pharmaceutical preparation. Two color reactions for the analysis of primaquine phosphate dosage form, which are based on 2,6-dichloroquinone chlorimide and 1,2-naphthoquinone-4-sulfonate, were described. The reactions depend on the presence of active centers in the primaquine molecule. These are the hydrogen atoms at position 5 of the quinoline nucleus and the primary amino group of the side chain. The method was applied to tablets of primaquine phosphate and a combination of primaquine phosphate and amodiaquine hydrochloride.

Prasad *et al.* [17] recommended a spectrophotometric assay method for the determination of primaquine in plasma.

Hassan *et al.* [18] used a spectrophotometric method for the simultaneous determination of primaquine with amodiaquine mixtures in dosage forms. Crushed tablets containing primaquine phosphate and amodiaquine hydrochloride were extracted with 0.1 M hydrochloric acid, and the mixture was filtered. A portion of the filtrate was diluted with 0.1 M hydrochloric acid, and the absorbance of this solution was measured at 282 and 342 nm against hydrochloric acid.

Sulaiman and Amin [19] used a spectrophotometric method for the determination of primaquine and chloroquine with chloranil. Treat the sample solution with 5 mL

each of 0.05 M borate buffer (pH 9) and 1 mM chloranil and dilute to 25 mL with water. Heat the stoppered flask at 65 °C for 20 min, cool to room temperature and measure the absorbance at 305 nm versus a reagent blank. The epsilon value for primaquine phosphate is 20.000.

Chatterjee *et al.* [20] quantitatively separated primaquine from amodiquine by a selective precipitation method. A powdered sample containing primaquine and amodiaquine was dissolved in 0.01 N hydrochloric acid 4 N ammonia was added to precipitate amodiaquine. The mixture was filtered and the combined filtrate and washings containing primaquine was diluted with water and 0.1 N hydrochloric acid. The absorbance of this solution was measured at 282 nm versus a solvent blank.

Abdel-Salam *et al.* [21] described a sensitive and simple spectrophotometric method for the determination of primaquine and other antimalarial drugs. The method is based on the formation of complexes between iodine (as an acceptor) and the basic drug in chloroform solution. Optimum conditions were established for the determination of primaquine, in pure form or in pharmaceutical preparation. Results were accurate and precise.

Vishwavidyalaya *et al.* [22] used a difference-spectrophotometric method for the estimation of primaquine phosphate in tablets. One portion of powdered tablets, equivalent to 7.5 mg of primaquine phosphate, was extracted with hydrochloric acid–potassium chloride buffer (pH 2) and a second portion was extracted with phosphate buffer (pH 10). Primaquine phosphate was determined from the difference in absorbance of the acid and alkaline extracts at 254.2 nm. The calibration graph was rectilinear from 2 to 14 μg/mL of primaquine phosphate. Recovery was 98.6% and no interference was observed from excipients. Results compared with those by the British Pharmacopoeial method.

Min *et al.* [23] determined primaquine phosphate, in tablets, by an ultraviolet spectrophotometric method. Sample was treated with 0.01 M hydrochloric acid and the resulting solution (500 μg/mL) was diluted to 50 mL with 0.01 M hydrochloric acid. The absorbance of the solution was measured at 265 nm versus a reagent blank. Beer's law was obeyed from 8 to 20 μg/mL of primaquine phosphate. Recovery was 100.2% ($n = 5$) and the coefficient of variation was 0.5%. Results were consistent with those obtained by a pharmacopoeial method.

Refaat *et al.* [24] used a spectrophotometric method for the determination of primaquine, and 16 other tertiary amine drugs, in bulk or in pharmaceuticals. The method involved the condensation of malonic acid with acetic anhydride in the presence of a tertiary amine in an aliphatic or a heterocyclic system. The condensation product is highly fluorescent and allows the spectrofluorimetric determination of the drug in the ng/mL ranges ($\lambda_{ex} = 415$ nm and $\lambda_{em} = 455$ nm). The product is also colored and allows the spectrophotometric determination of the drug and the other tertiary amine drugs ($\lambda_{max} = 333$ nm). Results of analysis of pure drugs and their dosage forms by these methods are in good agreement with those of the official British Pharmacopoeia and United States Pharmacopoeial procedures.

Artemchenko *et al.* [25] used a spectrophotometric method with *p*-quinone chlorimide in isopropanol in a pH 8 universal buffer for the determination of primaquine.

Talwar *et al.* [26] described a difference spectrophotometric method for the estimation of primaquine phosphate in tablets. The method is based on the

measurement of the absorbances at 265.5 and 281.3 nm (acidic solution) and 259 nm (alkaline solution). The λ_{max} of difference spectra was 254.2 nm. Beer's law was obeyed in the concentration range 2−14 μg/mL. The recovery was 98.62−99.19%.

4.2.5. Spectrofluorimetric methods

Refaat *et al.* [24] used a spectrophotometric method for the determination of primaquine, and 16 other tertiary amine drugs, in bulk or in pharmaceuticals. The method involved the condensation of malonic acid with acetic anhydride in the presence of a tertiary amine in an aliphatic or a heterocyclic system. The condensation product is highly fluorescent and allows the spectrofluorimetric determination of the drug in the ng/mL ranges ($\lambda_{ex} = 415$ nm and $\lambda_{em} = 455$ nm).

Gu *et al.* [27] used a spectrofluorimetric method for the determination of the long-acting antimalarial primaquine octanoate.

Aaron *et al.* [28] described a photochemical fluorimetric method for the determination of primaquine absorbed on silica gel chromatoplates.

Tsuchiya *et al.* [29] used a photochemical fluorimetric method for the determination of primaquine in a flowing solvent with application to blood serum. The standard or sample solution, as a 1:1 mixture of phosphoric acid solution (containing primaquine) and dioxan, was placed in a separating funnel and allowed to flow through a photochemical reactor and fluorescence cell at 0.3 mL/min. Serum (1 mL) was centrifuged after adding 1 mL of trichloroacetic acid and the supernatant solution (1 mL) was diluted to 50 mL with 0.7 M phosphoric acid–dioxan (1:1). The fluorescence background of serum was very low, allowing detection limit of $<$0.1 μg/mL.

Ibrahim *et al.* [30] described a fluorimetric method for the determination primaquine and two other aminoquinoline antimalarial drugs using eosin. Powdered tablets or ampule contents containing the equivalent of 50 mg of the drug was extracted with or dissolved in water (100 mL). A 10 mL aliquot was mixed with 10 mL of aqueous ammonia, 1 mL of 0.001% eosin (C.I. acid red 87) in dichloroethane, and dichloroethane was added to volume. Primaquine was determined fluorimetrically at 450 nm (excitation at 368 nm). Calibration graphs were rectilinear for 0.1–5 μg/mL of primaquine. Recoveries were quantitative. The method could be readily adapted for determination of the drug in biological fluids.

Cheng *et al.* reported the use of a synchronous fluorimetric method for the determination of primaquine in two-component antimalarial tablets [31]. Ground tablets were dissolved in water and the mixture was filtered. The fluorescence intensities of chloroquine phosphate and primaquine phosphate, in the filtrate, were measured at 380 nm (excitation at 355 nm) and 505 nm (excitation at 480 nm), respectively. The calibration graphs were linear from 1 to 8 μg/mL of chloroquine phosphate and 10 to 110 μg/mL of primaquine phosphate. The mean recoveries were 98.2–101.49% and the relative standard deviations were 2.23%.

4.2.6. Colorimetric methods

Fuhrmann and Werrbach [32] used a field test for the quantitative detection of primaquine in urine. Filter urine and place 10 mL in a 50-mL graduated cylinder. Add 1 mL of 25% ammonium hydroxide and 20 mL ammonium acetate and shake

immediately and thoroughly for 3 s. Allow to stand for 10–20 min, and transfer 15 mL of the ammonium acetate to a 25-mL measuring cylinder. Add 10 mL of 0.2 N sulfuric acid, shake, and after layer separation, withdraw 3 mL of the sulfuric acid without adherence of the ammonium acetate. Put the acid extract in a test tube; add 0.25 mL of diazo reagent (10 mL of a solution containing 4 g sulfanilic acid, 12 mL hydrochloric acid and water to 800 and 0.25 mL of 0.5% sodium nitrite). After 10 min, add 0.5 mL of Fehling reagent (40 g sodium hydroxide and 140 g sodium potassium tartarate per liter), mix, and determine the orange-red color colorimetrically or photometrically (Hg 436 filter). Determine the concentration by reference to a standard curve, which is linear in the range 0.3–2.1 mg% primaquine.

Rao and Rao [33] used a rapid, sensitive, and simple colorimetric method for the estimation of primaquine phosphate. The method is based on its reaction with sodium vandate to give a pink color, which has an absorbance maximum at 550 nm. Beer's law is obeyed for 2–30 μg/mL.

Issa *et al.* [34] used 2,3-dichloro-5,6-dicyano-*p*-benzoquinone for the spectrophotometric determination of primaquine and other antimalarials. The drugs were determined in tablets by a spectrophotometric method based on the reaction with 2,3-dichloro-5,6-dicyano-*p*-benzoquinone and measurement of the absorbance at 460 nm. The reaction occurred fastest in methanol and acetonitrile to yield a radical anion, which was detected by electron spin resonance. The color attained its maximum intensity after 5 min and remained stable for at least 1 h. The absorbance versus concentration curve obeyed Beer's law in the concentration range 1–4 mg per 100 mL. The recovery was 99.9–102.6%.

De Faria and Santos [35] studied primaquine diphosphate and its oxidation product by visible, ultraviolet, Raman and electron paramagnetic resonance spectroscopy as well as cyclic voltammetry. The doubly protonated form of the drug is oxidized to a radical that absorbs strongly in the visible region at 552 nm. Such a species is highly reactive, and its time-decay is mainly due to its interaction with the nonoxidized drug. Another radical can be generated at higher pH, possibly originating from the singly protonated form of the drug.

El-Ashry *et al.* [36] studied the complex formation between the bromophenol blue, primaquine, and other important aminoquinoline antimalarials. The colorimetric method used was described as simple and rapid and is based on the interaction of the drug base with bromophenol blue to give a stable ion-pair complex. The spectra of the complex show maxima at 415–420 nm with high apparent molar absorptivities. Beer's law was obeyed in the concentration range 1–8, 2–10, and 2–12 μg/mL for amodiaquine hydrochloride, primaquine phosphate, and chloroquine phosphate, respectively. The method was applied to the determination of these drugs in certain formulations and the results were favorably comparable to the official methods.

John *et al.* [37] described a colorimetric method for the estimation of primaquine phosphate. Sample solutions of different dilutions (0.15–0.6 mL) of the drug (6–24 μg/mL) were treated with 5 mL of 1% cerric ammonium sulfate in dilute nitric acid and made up to 25 mL with water. The absorbance of the resulting light purple solution was measured at 480 nm after similar 30 min. Beer's law was obeyed from 5–30 μg/mL of primaquine phosphate. The method is applicable to bulk formulations in addition to tablets and capsule formulation.

Amin and Issa [38] described a simple, rapid, accurate, and sensitive spectrophotometric method for the microdetermination of primaquine phosphate and other aminoquinoline antimalarials. The method is based on the interaction of these drugs with calmagite indicator to give a highly colored ion-pair complex that exhibit maximum absorption at 666 nm for primaquine phosphate. Beer's law is obeyed in the concentration range 1–33 μg/mL for primaquine phosphate. For more accurate analysis, the Ringbom optimum concentration range is 3–30 μg/mL for primaquine phosphate. The method was applied to the determination of primaquine and the other two antimalarial agents in certain formulations, with results that compared favorably with those obtained by the official methods.

Hassan *et al.* [39] used a sensitive color reaction method for the determination of primaquine in pharmaceutical preparation. Primaquine was treated with diazo-*p*-nitroaniline in acidic medium to give an orange-yellow product with an absorbance maximum at 478 nm. When the medium was made alkaline, bathochromic, and hypochromic shifts occurred; the new maximum was located at 525 nm. The mean percentage recoveries for authentic samples amounted to 100 and 100.21 by the acid and alkaline procedures, respectively ($P = 0.05$). Both reactions could be used to determine primaquine salts in pharmaceutical preparations. The results obtained were in good agreement with those of the official methods. Recoveries were quantitative by both methods.

Sastry *et al.* [40] described a spectrophotometric method for the determination of primaquine and other antimalarial drug using quinones. The drug was determined as a (1:1) complexes with embelin (2,5-dihydroxy-3-undecyl-1,4-benzoquinone), 2,5-dihydroxy-1,4-benzoquinone, or chloranilic acid. Samples of tablets, injection, or syrup containing 50 mg of the drug were dissolved in or diluted with 10 mL of water and the solution was filtered and mixed with 2 mL of 1 M sodium hydroxide and the precipitated free base were extracted into chloroform (4 × 20 mL). The combined chloroform extracts were washed with water (2 × 20 mL), dried over sodium sulfate and diluted to 100 mL with chloroform, then diluted with chloroform to contain 100 μg/mL of the drug. Aliquots of these solutions (containing 20–200 μg of the free base) were mixed with 2 mL of a 0.5% solution of embelin, 2,5-dihydroxy-1,4-benzoquinone or chloranilic acid in chloroform at 30 ± 5 °C and diluted with chloroform and after 2 min, the absorbance was measured at 520 nm for embelin, 500 nm for 2,5-dihydroxy-1,4-benzoquinone or 540 nm for chloranilic acid. The Beer's law ranges, regression equations, correlation coefficient, and coefficient of variation were 1.99% for complexes of primaquine with embelin and were tabulated.

Sastry *et al.* [41] used a new spectrophotometric method for the estimation of primaquine, using 3-methylbenzothiazolin-2-one hydrazone. An aqueous extract of the sample of powdered tablets (containing 50 μg/mL of primaquine phosphate was mixed with 1 mL each of aqueous 8.5 mM 3-methylbenzothiazolin-2-one hydrazone and 11.84 mM CeIV (in 0.72 M sulfuric acid), the mixture was diluted to 10 mL, and the absorbance was measured at 510 nm versus a reagent blank. Beer's law was obeyed for 0.7–12 μg/mL of the drug; and for 50 μg, the coefficient of variation was 0.52% ($n = 8$). Other antimalarials and pharmaceutical adjuvants did not interfere.

Sastry *et al.* [42] reported the use of an extractive spectrophotometric method for the determination of primaquine and other antimalarial agents using Fast Green FCF (C.I. Food Green 3) or Orange II (C.I. Acid Orange 7). Sample solution

containing 20 μg/mL of primaquine was mixed with phthalate buffer solution (pH 5) and aqueous 0.5% C.I. Food Green 3. After dilution with water, the aqueous solution was extracted with chloroform and the absorbance of the chloroform layer was measured at 630 nm. Instead of C.I. Food Green 3 and phthalate buffer solution, aqueous 0.5% C.I. Acid Orange 7 and 0.1 M hydrochloric acid were also used with absorbance measurement at 495 nm.

Mahrous *et al.* [43] determined primaquine and other antimalarials by use of chloranilic acid for the colorimetry. Primaquine was treated with 0.2 chloranilic acid solution in acetonitrile to give a purple solution with absorption maximum at 522 nm. Beer's law was obeyed from 0.04 to 0.2 mg/mL. Analysis of pharmaceutical formulation by this method is as accurate as the official method.

El-Kommos and Emara [44] described a spectrophotometric method, for the determination of primaquine and other secondary aromatic amines pharmaceuticals, using 3-methylbenzothiazolin-2-one hydrazone. The method is based on oxidative coupling reaction of 3-methylbenzothiazolin-2-one hydrazone.

Rao *et al.* [45] determined primaquine phosphate, in pharmaceutical dosage forms, by using a colorimetric method. Powdered tablets containing the equivalent of 100 mg of primaquine phosphate were heated with 25 mL of water for 10 min, the solution was cooled and filtered, and 10 mL portion of the filtrate was diluted 10-fold with water. A 5-mL portion of this solution was mixed with 5 mL of pH 5 buffer solution, 1 mL of 0.08% amidopyrine solution in aqueous 95% alcohol and 2 mL of aqueous 0.1% sodium periodate. After 10 min, 0.5 mL of aqueous sodium metabisulfite solution was added and the absorbance was measured at 580 nm. Beer's law was obeyed between 4 and 43 μg/mL of primaquine phosphate. Recoveries were quantitative.

Rao *et al.* [46] reported the use of a spectrophotometric method for the determination of primaquine phosphate with ninhydrin. Standard solution of 0.01% primaquine phosphate solution (3 mL) or solution prepared from the drug or its tablets was mixed with 2 mL of water, 5 mL of 2-methoxyethanol and then with 4 mL of ninhydrin reagent. The mixture was boiled for 35 min, and, after cooling and dilution to 25 mL with water, the absorbance was measured at 570 nm versus a reagent blank. Beer's law was obeyed from 4 to 20 μg/mL with recoveries of 99.4–100.2% for 25 mg of primaquine phosphate.

El-Kommos and Emara [47] determined primaquine and other secondary aromatic amines pharmaceuticals by a spectrophotometric method using 4-dimethyl amino cinnamaldehyde. The reaction of the reagent with primaquine and with the other amines was investigated. Powdered tablets were extracted with methanolic 0.1 M perchloric acid. The extract was mixed 1:1 with methanolic 0.2% of 4-dimethyl amino cinnamaldehyde and the mixture was diluted with methanol before measurement of the absorbance at 670 nm for primaquine phosphate. Beer's law was obeyed for 2–20 μg/mL of primaquine. The pink and green color formed with primaquine was stable for at least 24 h. Recoveries were good. Amodiaquine did not interfere with the determination of primaquine.

Sastry *et al.* [48] described a new spectrophotometric method for the estimation of primaquine, using 4-aminophenazone (4-aminoantipyrine). Aliquots of primaquine solution were mixed with 2 mL of methanolic 0.5% of 4-aminoantipyrine. After 5 min, 5 mL of 0.1% sodium periodate was added, and, after 3 min, the solution was

diluted to 25 mL with water. The absorbance was measured at 580 nm versus a reagent blank within 30 min. Beer's law was obeyed from 2 to 34 μg/mL of primaquine. The coefficient of variation ($n = 6$) was 0.9% at 600 μg of primaquine.

Ibrahim *et al.* [49] described a spectrophotometric method for the determination of primaquine and other antimalarial agents in pharmaceuticals. Powdered tablet or ampule contents containing 25 mg of primaquine phosphate, was dissolved in water and the solution was made alkaline with 6 M ammonia before extraction with chloroform. The extract was evaporated to dryness and the residue was dissolved in acetonitrile. A portion of the solution was mixed with 0.04% tetracyanoethylene solution in acetonitrile and diluted to volume with acetonitrile. After 10 min, the absorbance was measured at 415 nm for primaquine. Beer's law was obeyed from 2 to 12 mg/mL. The results agreed well with those of the United State Pharmacopoeia XX method.

Sastry *et al.* [50] estimated primaquine in its tablet formulation. Powdered tablets equivalent to 100 mg of primaquine phosphate were dissolved in water, filtered, and filtrate was diluted to 100 mL with water. Portions of the solution were shaken with 3 mL of 5 mM brucine–0.16 M sulfuric acid, 1.5 mL of 5 mM sodium periodate and 2 mL of 1.2 M sulfuric acid and diluted to 9 mL with water. The solution was set aside for 20 min in a boiling water bath, cooled, and diluted to 10 mL with water. The absorbance was measured at 510 nm versus a reagent blank. Beer's law was obeyed from 20 to 140 μg/mL of primaquine phosphate. The coefficient of variation was 1.56% ($n = 8$). Recovery was 99.2%.

El-Brashy [51] reported the determination of primaquine and other antimalarials via charge-transfer complexes. Powdered sample of primaquine phosphate was dissolved in water and the solution was adjusted to an alkaline pH with 6 M ammonia and extracted with chloroform. The extract was dried with anhydrous sodium sulfate, filtered, and evaporated to dryness under nitrogen and the residue was dissolved in acetonitrile. Portions of the solution were mixed with 0.2% 7,7,8,8-tetracyanoquinodimethane, diluted with acetonitrile, and set aside for 10 min before the absorbance was measured at 845 nm versus a reagent blank. The calibration graphs were linear from 0.4 to 3 μg/mL and recovery was 98%.

Baker *et al.* [52] reported the use of a colorimetric method for the determination of primaquine metabolites, in urine.

4.2.7. Nuclear magnetic resonance spectrometric methods

Clark *et al.* [53] subjected primaquine to metabolic studies using microorganisms. A total of 77 microorganisms were evaluated for their ability to metabolize primaquine, of these, 23 were found to convert primaquine to one or more metabolites (thin-layer chromatography analysis). Preparative scale fermentation of primaquine with four different microorganisms resulted in the isolation of two metabolites, identified as 8-(3-carboxy-1-methylpropylamino)-6-methoxyquinoline and 8-(4-acetamido-1-methylbutylamino)-6-methoxyquinoline. The structures of the metabolites were proposed, based primarily on a comparison of the ^{13}C NMR spectra of the acetamido metabolite and the methyl ester of the carboxy metabolite with that of primaquine. The structures of both metabolites were confirmed by direct comparison with authentic samples.

Singh *et al.* [54] used a ^{13}C NMR spectrometric method and reported the chemical shifts of primaquine and chloroquine. The signals are assigned on the basis of substituent effects on benzene shifts, intensities, multiplicities in single-frequency off-resonance decoupled and the comparison with structurally related compounds.

Hufford *et al.* [13] used a ^{13}C NMR spectroscopic method for the assignments of dissociation constants of primaquine. The first and second dissociation constants of primaquine were determined by titration with 0.1 N hydrochloric acid in acetonitrile–water mixtures and values were extrapolated to water by using linear regression analysis. The assignments of the dissociation constants were unambiguously achieved by studying the ^{13}C NMR spectral data obtained with monohydrochloride, dihydrochloride, and trihydrochloride salts.

McChesney and Sarangan [55] reported that primaquine undergoes unexpectedly rapid aromatic proton exchange with the medium. At pH <4, the exchange of carbon number 5 in the quinoline ring system is so fast as to be unmeasurable by proton NMR methods. At pH 6–6.5 the half-life for exchange is 4–5 min. This unexpectedly high rate of proton exchange with a medium may provide an important clue to the biological activity of primaquine.

Hufford and Baker [56] reported the assignments of the ^{13}C NMR spectra of three derivatives of primaquine namely 4-methylprimaquine, 5-methoxy-4-methylprimaquine, and 5-methoxyprimaquine. These assignments were based on comparison with those of primaquine, proton-coupled data, and selective long-range proton decoupling.

Hufford *et al.* [57] used proton and ^{13}C NMR spectrometric data to establish the novel sulfur-containing microbial metabolite of primaquine. Microbial metabolic studies of primaquine using *Streptomyces roseochromogenus* produced an *N*-acetylated metabolite and a methylene-linked dimeric product, both of which have been previously reported, and a novel sulfur-containing microbial metabolite. The structure of the metabolite as an S-linked dimer was proposed on the basis of spectral and chemical data. The molecular formula $C_{34}H_{44}N_6O_4S$ was established from field-desorption mass spectroscopy and analytical data. The ^{1}H- and ^{13}C NMR spectra data established that the novel metabolite was a symmetrical substituted dimer of primaquine *N*-acetate with a sulfur atom linking the two units at carbon 5. The metabolite is a mixture of stereoisomers, which can equilibrate in solution. This observation was confirmed by microbial synthesis of the metabolite from optically active primaquine.

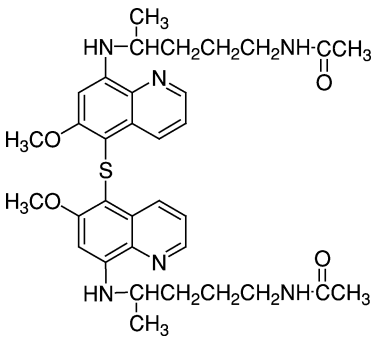

Perussi *et al.* [58] studied the interaction of primaquine and chloroquine with ionic micelles as studied by ^{1}H NMR and electronic absorption spectroscopy. The characteristic of binding of primaquine and chloroquine to the micelles of surfactants with different charge of head groups were studied by ^{1}H NMR and optical absorption of spectroscopy. Cetyltrimethylammonium chloride was used as a cationic surfactant, sodium dodecyl sulfate as an anionic surfactant and *N*-hexadecyl-*N,N*-dimethyl-3-ammonio-1-propanesulfonate as zwitterionic. The pK values and binding constants were estimated. Interaction with sodium dodecyl sulfate significantly increases an apparent pK of primaquine and chloroquine. The chemical shift patterns and values of binding constants in the presence of different surfactants show that the mode of interaction of charged drugs with micelles is nonspecific, since the complexes formed are similar for different types of surfactants.

4.2.8. Culometric method

Berka *et al.* [59] described an accurate and reproducible coulometric method, with chlorine electrogenerated at the anode, for the determination of micro quantities of primaquine phosphate. Titration was carried out in an anode compartment with a supporting electrolyte of 0.5 M sulfuric acid–0.2 M sodium chloride and methyl orange as indicator. One coulomb was equivalent to 1.18 mg of primaquine phosphate. The coefficients of variation for 0.02–0.5 mg of primaquine phosphate were 1–5%. Excipients did not interfere.

4.2.9. Polarographic methods

Zhan and Mao [60] used a simple, fast, and selective alternating current oscilloscopic polarographic titration method for the determination of primaquine and other alkaloid phosphate in pharmaceutical preparation. The titration was carried out with a standard lead solution in hexamethylene tetramine buffer containing 1 M sodium chlorate (pH 5.5). The results obtained by this method are comparable to those obtained by pharmacopoeial method.

Zhan [61] reported the use of an oscillopolarographic method for the determination of primaquine phosphate and other drugs in pure form and in pharmaceutical preparations. The sample solution was mixed with potassium bromide and 6 M hydrochloric acid and the mixture was titrated with 0.1 M sodium nitrite. A micro platinum electrode and a platinum electrode were used as indicators and reference electrodes, respectively. The mean recoveries were 96.88–99.88%. Results agreed well with those obtained by the Chinese Pharmacopoeia method.

Saad *et al.* [62] reported that electrodes based on polyvinyl chloride matrix membranes containing one of three macrocyclic crown ethers with dioctyl phenyl phosphonate solvent mediator and, in some instances, anion excluder have been studied for their potentiometric response to the primaquinium cation. Primaquine-selective electrodes based on dibenzo(18-crown-6) gave sub-Nernstian responses while those based on dibenzo(24-crown-8) and dibenzo(30-crown-10) exhibited good electrochemical characteristics, such as Nernstian responses, fast dynamic response times (30 s), a wide range of working pH (pH 4–10) and good selectivity over many metal cations, chloroquine, and sulfonamide drugs. The addition of 50% mole ratio anion excluder, relative to the sensor, not only led to an improvement in

the electromotive force stability, but also produced, in most instances, improved selectivity characteristics for both the dibenzo(24-crown-8) and dibenzo(30-crown-10) based electrodes. Determination of primaquine diphosphate (4.5–453 μg/cm^3) using the standard additions method resulted in a mean recovery and relative standard deviation of 107% and 8%, respectively. Determination of primaquine in pharmaceutical preparation is also described.

Mohamed [63] investigated the complexation behavior of amodiaquine and primaquine with Cu(II) by a polarographic method. The reduction process at dropping mercury electrode in aqueous medium is reversible and diffusion controlled, giving well-defined peaks. The cathodic shift in the peak potential (E_p) with increasing ligand concentrations and the trend of the plot of $E_{½}$ versus log C_x indicate complex formation, probably more than one complex species. The composition and stability constants of the simple complexes formed were determined. The logarithmic stability constants are: log $B_1 = 3.56$; log $B_2 = 3.38$, and log $B_3 = 3.32$ [Cu(II)–primaquine at 25 °C].

4.2.10. X-ray analysis

Yu *et al.* [64] established the S-configuration for (+)-primaquine, prepared from the racemate by chemical resolution, by solid-state X-ray analysis of the (+)-1-phenylethylurea obtained with R-(+)-1-phenylethylisocyanate.

4.2.11. Atomic absorption spectroscopy

Amin and Issa [15] described an indirect atomic absorption spectrometric method for the determination of primaquine and other antimalarials. The method is based on the formation of their ion-associates with [Cd^{2+}, Co^{2+}, Mn^{2+}, and Zn^{2+1}] thiocyanate, ammonium reineckate, and/or sodium cobaltinitrate.

Hassan *et al.* [65] used a method for the determination of primaquine and other antimalarials, through ternary complex formation. The analytical aspects of the reaction between the widely used antimalarial drugs with cobalt and thiocyanate to form ternary complexes are described. Alternatively, determination of the cobalt content of the nitrobenzene extract using atomic absorption spectroscopy provided an indirect method for the determination of the drugs. Both methods are applied to the analysis of pharmaceutical preparation and the results obtained agreed well with those obtained with official methods.

4.2.12. Chromatographic methods

4.2.12.1. Thin-layer chromatography methods

Fusari *et al.* [66] described a qualitative thin-layer chromatography (TLC) elution technique, for the assay of primaquine and other pharmaceuticals.

Zheng and Sun [67] used a thin-layer chromatographic method for the analysis of primaquine and other quinoline derivatives. The drug and other compounds were chromatographed on silica gel GF_{254} plate, with methanol:aqueous 25–28% ammonia (200:3) and chloroform:dichloromethane:diethylamine (4:3:1), as mobile phases. Spots were located under ultraviolet radiation. The detection limit was 1–2 μg/mL. Total separation could be achieved by the use of two plates and the respective mobile phase.

Dwivedi *et al.* used a thin-layer chromatographic densitometric and ultraviolet spectrophotometric methods for the simultaneous determination of primaquine and a new antimalarial agent, CDRI compound number 80/53 [68]. The new antimalarial agent, compound 80/53 is unstable in acidic conditions where it is converted into primaquine. To conduct stability studies of this compound, thin-layer chromatography densitometric and ultraviolet spectrophotometric determination methods were developed. These methods are also suitable of the determination of compound 80/53 or primaquine in bulk and pharmaceutical dosage forms.

Dwivedi *et al.* [69] used a high-performance thin-layer chromatographic method for the simultaneous analysis of primaquine, bulaquine, and chloroquine. The high performance thin-layer chromatography workstation comprised of Automatic TLC sampler-III equipped with 50 μL Hamilton syringe, TLC Scanner-3, equipped with mercury, tungsten, and deuterium lamp for scanning of TLC plates. The separation was achieved on thin-layer plates of precoated Si-gel 60 F_{254} (20 cm × 20 cm, 0.2 mm). The plates were scanned at wavelength of 254 nm. Data was acquired and processed using a CATS4-HPTLC software. The solvent system used was hexane–diethylether–methanol–diethylamine in the ratio of (37.5: 37.5:25:0.5). TLC was performed at 27 ± 3 °C in a Camag TLC twin trough glass chamber.

Clarke [2] recommended the following three thin-layer chromatography systems [70].

System 1

Plates. Silica gel G, 250 μm thick, dipped in, or sprayed with, 01 M potassium hydroxide in methanol, and dried.

Mobile phase. Methanol:strong ammonia solution (100:1.5).

Reference compounds. Diazepam R_f 75, chlorprothixene R_f 56, codeine R_f 33, atropine R_f 18.

$R_f = 19$ Acidified iodoplatinate solution, positive [70].

System 2

Plates. This system uses the same plates as system 1 with which it may be used because of the low correlation of R_f values.

Mobile phase. Cyclohexane:toluene:diethylamine (75:15:10).

Reference compounds. Dipipanone R_f 66, pethidine R_f 37, desipramine R_f 20, codeine R_f 06.

$R_f = 13$ Acidified iodoplatinate solution, positive [70].

System 3

Plates. This system uses the same plates as systems 1 and 2 with which it may be used because of the low correlation of R_f values.

Mobile phase. Chloroform:methanol (90:10).

Reference compounds. Meclozine R_f 79, caffeine R_f 58, dipipanone R_f 33, desipramine R_f 11.

$R_f = 05$ Acidified iodoplatinate solution, positive [70].

4.2.12.2. Gas chromatographic methods

Clarke [2] reported the following gas chromatographic system [71].

Column. 2.5% SE-30 on 80–100 mesh chromosorb G (acid-washed and dimethyldichlorosilane-treated), 2 cm × 4 mm internal diameter glass column, it is essential that the support is fully deactivated.

Column temperature. Normally between 100 and 300 °C. As an approximate guide, the temperature to be used is the retention index ÷10.

Carrier gas. Nitrogen at 45 mL/min.

Reference compounds. *n*-Alkanes with an even number of carbon atoms. Retention index: 2314 [71].

Rajagopalan *et al.* [72] described an electron-capture gas chromatographic assay method for the determination of primaquine in blood. The method involves derivatization with heptafluorobutyric anhydride to form the diheptafluorobutyramide derivative after a single extraction at alkaline pH. The derivatives are quantitated by electron-capture gas chromatography. Blood levels of primaquine as low as 8 ng/mL can be measured with good precision.

4.2.12.3. Gas chromatography–mass spectrometric methods

Baty *et al.* [73] studied several substituted 8-aminoquinoline related to primaquine and the known antimalarial drugs, by gas chromatography–mass spectrometry method. 5,6-Dihydroxy-8-aminoquinoline, a possible metabolite of primaquine, can be detected by single ion-monitoring after conversion to trimethylsilyl ether derivative. The mass spectra obtained in this study indicate that there are certain ions which are characteristic of trimethylsilyl ethers of hydroxylated 8-aminoquinolines and 5,6-dimethoxy-8-aminoquinolines. These compounds should thus be amenable to analysis if they were produced during *in vivo* metabolism studies. Using selected ion-monitoring, the derivatized compounds can be detected at submicrogram levels.

Greaves *et al.* [74] used a selected ion-monitoring assay method for the determination of primaquine in plasma and urine using gas chromatography–mass spectrometric method and a deuterated internal standard. After freeze-drying and extraction with trichloroethylene, the sample plus internal standard was reacted with Tri Sil TBT (a 3:3:2 by volume mixture of trimethylsilylimidazole, *N,O*-bis-(trimethylsilylacetamide and trimethylchlorosilane) and an aliquot injected to the gas chromatograph-mass spectrometer. The gas chromatographic effluent was monitored at *m*/*z* 403, and *m*/*z* 406, the molecular ions of the bis-tetramethylsilane ethers of primaquine and 6-trideuteromethoxy primaquine.

4.2.12.4. High performance liquid chromatography–mass spectrometric methods

Nitin *et al.* [75] developed and validated a sensitive and selective liquid chromatography–tandem mass spectrometric method (LC–MS–MS) for the simultaneous estimation of bulaquine and its metabolites primaquine in monkey plasma. The mobile phase consisted of acetonitrile–ammonium acetate buffer (20 mM, pH 6) (50:50, v/v) at a flow rate of 1 mL/min. The chromatographic separations were achieved on two Spheri cyano columns (5 μm, 30 cm × 4.6 mm), connected in

series. The quantitation was carried out using a Micromass LC–MS–MS with an electrospray source in the multiple reaction monitoring mode. The analytes were quantified from the summed total ion value of their two most intense molecular transitions. Another method was also used by the same authors. A simple liquid–liquid extraction method with 2 × 1 mL *n*-hexane-ethyl acetate–dimethyl octyl amine (90:10:0.05, v/v) was utilized. The method was validated in terms of recovery, linearity, accuracy, and precision (within- and between-assay variation). The recoveries from spiked control samples were ≥90% and 50% for bulaquine and primaquine, respectively. Linearity in plasma was observed over a dynamic range of 1.56–400 and 3.91–1000 ng/mL for bulaquine and primaquine, respectively.

4.2.12.5. High-pressure liquid chromatographic methods

Dua *et al.* [76] carried out some chromatographic studies on the isolation of peroxydisulfate oxidation products of primaquine. A 100 μL sample (0.25 mg/mL) of primaquine and 100 μL of potassium peroxydisulfate (0.24 mg/mL) were mixed and 5 μL portions injected onto a μ-Bondapak C_{18} (5 μm) column (30 cm × 3.9 mm) column 5, 15, 30, and 40 min after the start of oxidation. Analytes were eluted (1 mL/min) with acetonitrile–methanol–1 M perchloric acid (30:7:1.95) and detected at 254 nm. The product of a semipreparative oxidation performed on a 10-fold scale were crudely separated on a column (100 cm × 2 cm) filled with Bio-Gel P-2 and each colored band, identified visually, analyzed by high performance liquid chromatography. Fractions with similar peak profiles were pooled, rechromatographed on Bio-Gel P-2 and checked by high performance liquid chromatography until pure compounds were obtained. Eight oxidation compounds were obtained at 90% purity and the structures of five major products were determined by infrared, nuclear magnetic resonance, and mass spectrometry. Two products, 6-methoxy-5,8-bis-(4-amino-1-methylbutylamino)quinoline and 5,5-bis-[6-methoxy-8-(4-amino-1-methylbutylamino)quinoline] exhibited a threefold to fourfold increase in gametocytocidal activity of primaquine.

Dua *et al.* [77] also develoed a reversed-phase high performance liquid chromatographic method using acetonitrile–methanol–1 M perchloric acid–water (30:9:1:95, v/v) at a flow rate of 1.5 mL/min on a μ-Bondapak C_{18} column with an ultraviolet detection at 254 nm, for the separation of primaquine, its major metabolite carboxyprimaquine and other metabolites such as *N*-acetylprimaquine, 4-hydroxyprimaquine, 5-hydroxy primaquine, 5-hydroxy-6-methoxy primaquine and demethyl primaquine, and also other antimalarials. The calibration graphs were linear in the range 0.025–100 μg/mL for primaquine and 4−1000 μg/mL for caroxyprimaquine. The within-day and day-to-day coefficients of variation averaged 3.65 and 6.95%, respectively, for primaquine; and 3 and 7.52%, respectively, for carboxyprimaquine in plasma. The extraction recoveries for primaquine and carboxyprimaquine were 89% and 83%, respectively.

Jane *et al.* [78] used a high performance liquid chromatographic method for the analysis of primaquine and other basic drugs on silica columns using nonaqueous ionic eluents. Unmodified silica columns together with nonaqueous ionic eluents give stable and flexible systems for the analysis of primaquine and the other basic drug compounds by high performance liquid chromatography. Low wavelength ultraviolet and fluorescence detection are used and fluorescence is optimized by

postcolumn pH change or derivatization of some primary aliphatic amines with *o*-phthaldialdehyde. A novel feature is that electrochemical oxidation can be used for the detection of most analytes. Retention and relative response data (UV, 254 nm and electrochemical, +1.2 V) were generated for primaquine and 161 other compounds, using a 125-mm Spherisorb S5W silica column and methanolic ammonium perchlorate (10 mM, pH 6.7) as eluent. This system can be used isocratically in qualitative analyses as well as for quantitative work, when either the wavelength or the applied potential can be adjusted to optimize the response.

Parkhurst *et al.* [79] described a high performance liquid chromatographic method for the simultaneous determination of primaquine and its metabolites from plasma and urine samples, utilizing acetonitrile deproteinization, and direct injection onto a cyano column. Levels of 100 ng/mL per 20 μL injection could be quantitated. Preliminary pharmacokinetic analysis is reported for two human subjects after oral doses of 60–90 mg primaquine diphosphate. Two apparent plasma metabolites and two possible urinary metabolites are also reported.

Wheals used isocratic multicolumn high performance liquid chromatography as a technique for qualitative analysis and its application to the characterization of primaquine and other basic drugs using an aqueous methanol solvent [80]. A variety of high performance liquid chromatographic packing materials were prepared and their chromatographic properties compared for the separation of primaquine and the other basic drugs using a single solvent system. The three most promising packing materials (silica, a mercapto propyl modified silica and a propyl sulfonic acid modification) were subsequently used to provide retention volume data for a large number of drugs.

Clark *et al.* [81] determined the time course of *N*-acetylation of primaquine by *Streptomyces roseochromogenous* and *Streptomyces rimosus* by quantitative high performance liquid chromatographic analyses of the culture broths. The *N*-5-bistrifluoroacetyl derivative of primaquine was used as an internal standard in the analysis for the quantitation of primaquine *N*-acetate in microbial culture broths. *S. roseochromogenous* forms the highest level of primaquine *N*-acetate at 24–36 h after substrate addition, while *S. rimosus* is slower in its acetylation, peaking at 3 days after substrate addition. The formation of a novel dimeric compound from the reaction of primaquine with 8-(4-phthalimido-1-methylbutylamino)-6-methoxy quinoline is also reported.

Baker *et al.* [82] used high performance liquid chromatographic method for the analysis of the metabolism of primaquine. Using rats, dosed with 20 mg/kg of primaquine diphosphate (11.4 mg/kg), it was found that the drug underwent a metabolic oxidative deamination to give 8-(3-carboxy-1-methylpropylamino)-6-methoxyquinoline. The presence of this new mammalian metabolite was verified using high performance liquid chromatography, gas chromatography, and mass spectral methods. A quantitative high performance liquid chromatographic method for the determination of primaquine and the carboxylic acid metabolite in plasma using only 50 μL of whole blood from the rat was developed and the method could be used to detect levels as low as 0.05 μg/mL of the metabolite. Following intravenous administration of the drug, the plasma levels of primaquine fell very rapidly and after 30 min, the levels of the metabolite was much higher than those of primaquine.

Hufford *et al.* [83] studied the stereochemistry of dimeric microbial metabolites of primaquine. The dimeric microbial metabolite **1** of (±)-primaquine was shown by high performance liquid chromatography to be composed of a mixture of three compounds, which were separated. Heating of these three compounds demonstrated that they exhibit atropisomerism. Synthesis of the dimeric metabolite **1** from (−)-primaquine showed only two compounds by high performance liquid chromatography. These experiments demonstrated the presence of three enantiomeric pairs of diastereoisomers of the dimeric metabolite **1**. The other dimeric microbial metabolite **2** was shown by high performance liquid chromatography to be composed of a mixture of two compounds, which could be separated but equilibrated back to the original mixture. Synthesis of metabolite **2** from optically active primaquine produced only the compound with a longer retention time in the high performance liquid chromatography. Mixing of metabolite **2** prepared from (+)-primaquine with that prepared from (−)-primaquine produced the two compounds. The experiments demonstrate that the two compounds are an enantiomeric pair and meso-isomer, which equilibrate through a novel mechanism.

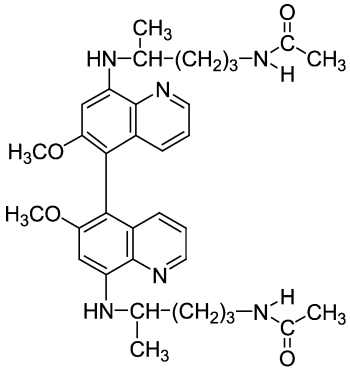

Metabolite **1**

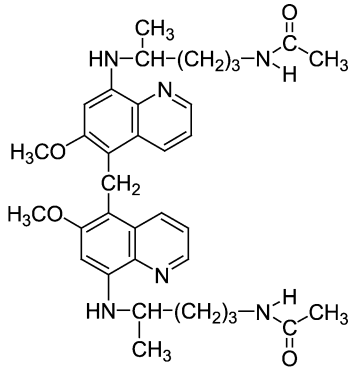

Metabolite **2**

Katori *et al.* [84] used a high performance liquid chromatographic method for the determination of primaquine phosphate tablets. Chromatography on a TSK Gel-4 (octadecylsilanized) column was used to determine the active ingredient in tablets and injections for treating tropical diseases. The mobile phase used is 26% acetonitrile in 0.05-M pH-3 phosphate buffer and the drug was detected at 260 nm. The peak area and peak height reproducibilities were $\leq$1.69%, and results compared well with those of other methods.

Okamoto *et al.* [85] performed the optical resolution of primaquine and other racemic drugs by high performance liquid chromatography using cellulose and amylose tris-(phenylcarbamate) derivatives as chiral stationary phases. Primaquine and other compounds were effectively resolved by cellulose and/or amylose derivatives having substituents such as methyl, tertiary butyl, or halogen, on the phenyl groups.

Sidhu *et al.* [86] developed a reliable and simple high performance liquid chromatographic method for the routine analysis of pharmaceutical dosage forms using a C_{18} Bondapak reversed-phase column with a binary solvent system consisting of

acetonitrile and 0.05 M potassium dihydrogen phosphate. Standardized extraction procedures for drugs in various dosage forms were developed and applied to a wide range of current pharmaceutical formulations.

Rao *et al.* [87] developed a high performance liquid chromatographic method for the determination of primaquine phosphate in pharmaceutical dosage form. A μ-Bondapak NH_2 column with chloroform–methanol (60:40) as eluent was selected with sulfalene as internal standard. The method was convenient with recovery of approximately 100% for primaquine.

Taylor *et al.* [88] developed a general separation strategy, involving solid-phase extraction followed by reversed-phase ion-pairing high performance liquid chromatography with an organic counter ion for primaquine and a set of 10 widely used antimalarial drugs and metabolites. The basis underlying the separation has been explored and work, including quantitative data, has been carried out on illustrative separations, which form the basis of novel quantitative assays of groups of antimalarials that are relevant to current prophylaxis and treatment of malaria.

Liu and Wu [89] used a high performance liquid chromatographic method for the simultaneous determination of primaquine and pyronaridine in plasma. The two drugs were extracted with ethyl acetate from alkalinized plasma or whole blood of rabbits and determined by high performance liquid chromatography, using methanol–0.05 M citric acid–disodium hydrogen phosphate pH 3/buffer solution (10:100) and detection at 254 nm. The detection limit was 3 ng. The calibration curve was linear at 0.05−0.50 μg/mL. The average recovery was 83.21 and 65.23 for pyronaridine and primaquine, respectively, and the coefficient of variation was $<5\%$.

Li *et al.* [90] used a normal phase high performance liquid chromatographic process to separate and detect primaquine in blood and liver after a single intravenous dose of the hepatic targeting agent neoglycoalbumin–primaquine conjugate and primaquine phosphate in mice. 6-Methoxy-8-(4-aminobutyrylamino)quinoline, synthesized and identified by the authors, was used as an internal standard to be added to the biological samples obtained from mice at different times after giving neoglycoalbumin–primaquine or primaquine phosphate. The mixture was extracted with ether after alkalinization in the primaquine phosphate group. In the neoglycoalbumin–primaquine group, the biological samples must be hydrolysed by heating under nitrogen and acid condition in a domestic pressure cooker before extraction. The extracts were evaporated to dryness under nitrogen, and then dissolved in the mobile phase (chloroform–methanol–ammonium hydroxide, 86.8:12.5:0.7). The results showed that the hepatic primaquine collecting ratio and the retention time of primaquine in liver in the neoglycoalbumin–primaquine group were higher and longer than those of the primaquine phosphate group. The results also point out that neoglycoalbumin–primaquine has lower targeting property.

Fang *et al.* [91] studied the enantiomeric separation of primaquine and 10 other drugs having a primary amino group using high performance liquid chromatography with a chiral Crownpak CR (+) column. The enantiomers of primaquine and the other drugs were separated by high performance liquid chromatography with Crownpak CR (+) column. By decreasing the column temperature, the elution of the analytes was delayed and enantioselectivity (resolution) was improved, but by increasing the methanol content, the elution of the analytes became more rapid, and the enantioselectivity was decreased.

Dwivedi *et al.* [69] used high performance liquid chromatographic assay method for the simultaneous analysis of primaquine, bulaquine, and chloroquine. The high performance liquid chromatographic system was equipped with 250 binary gradient pumps, a Rheodyne model 7125 injector with a 20-μL loop, and 235 diode-array detectors. The high performance liquid chromatographic separation was achieved on a reversed-phase select-B C_8 Lichrospher analytical column (25 cm × 4 mm, 5 μm). Column effluent was monitored at 265 nm. Data was acquired and processed using an IndTech HPLC interface and software. The mobile phase was 0.01 M sodium acetate buffer pH 5.6 and acetonitrile (45:55). Both the solutions were filtered in degassed before use. Chromatography was performed at 27 ± 3 °C at a flow rate of 1 mL/min.

Jawahar *et al.* [92] developed and validated a precise and reproducible high performance liquid chromatographic method for simultaneous determination of bulaquine and its metabolite primaquine in rabbit plasma. The method, applicable to 0.5 mL plasma, involves double extraction of samples with *n*-hexane:isopropanol (98:2) containing dimethyloctylamine (0.1%). Separations were accomplished by reversed-phase liquid chromatography using a Spheri-5-cyano column with a low pressure gradient with mobile phase consisting of ammonium acetate buffer (50 mM, pH 6) and acetonitrile with dimethyloctylamine. The method was sensitive with a limit of quantitation of 20 ng/mL in rabbit plasma for both bulaquine and primaquine and the recoveries were >85% and >45%, respectively.

Dean *et al.* [93] used a high performance liquid chromatographic method for the simultaneous determination of primaquine and carboxyprimaquine in plasma with electrochemical detection. After the addition of the internal standard, plasma was deproteinized by the addition of acetonitrile. Nitrogen-dried supernatants, resuspended in mobile phase were analyzed on a C_8 reversed-phase column. Limits of detection for primaquine and carboxyprimaquine were 2 and 5 ng/mL with quantitation limits of 5 and 20 ng/mL, respectively. The assay sensitivity and specificity are sufficient to permit quantitation of the drug in plasma for pharmacokinetics following low dose (30 mg, base) oral administration of primaquine, typically used in the treatment of malaria and *P. carinii* pneumonia.

The other high performance liquid chromatographic systems [94–105] are shown in Table 6.

4.2.12.6. Capillary electrophoresis methods

Fan *et al.* [106] developed a high performance capillary electrophoresis method for the analysis of primaquine and its trifluoroacetyl derivative. The method is based on the mode of capillary-zone electrophoresis in the Bio-Rad HPE-100 capillary electrophoresis system; effects of some factors in the electrophoretic conditions on the separation of primaquine and trifluoroacetyl primaquine were studied. Methyl ephedrine was used as the internal standard and the detection was carried out at 210 nm. A linear relationship was obtained between the ratio of peak area of sample and internal standard and corresponding concentration of sample. The relative standard deviations of migration time and the ratio of peak area of within-day and between-day for replicate injections were <0.6% and 5.0%, respectively.

Ng *et al.* [107] described a simple and rapid systematic optimization scheme, known as overlapping resolution mapping scheme, which make use of nine

Table 6. High performance liquid chromatography conditions of the methods used for the determination of primaquine diphosphate

Column	Mobile phase [Flow rate]	Detection	Remarks	Reference
20 cm × 6 mm of Partisil ODS III (10 μm)	pH 3.5, water–acetonitrile–methanol (6:3:1), containing 0.5 mM octanesulfonic acid [1.5 m/min]	Not given	Reversed-phase HPLC for analysis of the drug in biological fluids. Detection limit of the drug in plasma 1 ng/mL.	[94]
25 cm × 3.9 mm of μ-Bondapak CN	Acetonitrile–0.08 M citrate (77:23, pH 5), [1 mL/min]	Dual electrode electrochemical detection	Analysis of the drug and metabolites in human plasma and urine.	[95]
Fused-silica column (15 cm × 4.6 mm) of Spherisorb S5W	0.1 mL chloroform–methanol–aqueous 25% ammonia (868:125:7) [1.5 mL/min]	254 nm	Normal phase HPLC analysis in whole blood and urine.	[96]
Stainless steel column (25 cm × 4.6 mm) of YWG-$C_{18}H_{37}$ (10 μm)	Aqueous 85% methanol; [1.5 mL/min]	267 nm	Reversed-phase HPLC analysis in rabbit serum.	[97]
Whatman PX-5/25 ODS 25 cm × 4.6 mm Pirkle type 1A column	Hexane–propan–2-ol-acetonitrile (170:21:15), [1 mL/min]	Not given	Separation of enantiomers and diastereoisomers of the drug and its metabolites.	[98]
30 cm × 3.9 mm of μ-Bondapak phenyl	Acetonitrile–0.01 M KH_2PO_4 (pH 3.8)–anhydrous acetic acid (58:141:1) [2 mL/min]	278 nm	Analysis in tablets. Dextromethorphan used as internal standard.	[99]
30 cm × 3.9 mm of Bondapak NH_2	Chloroform–methanol (3:2) [1 mL/min]	254 nm	In tablets dosage forms.	[100]
15 cm × 6 mm of ODS (5 μm)	Methanol–water–anhydrous acetic acid (800:200:5) containing 0.5 mM–sodium dodecyl sulfate [1 mL/min]	340 nm	Determined primaquine with chloroquine simultaneously.	[101]
25 cm × 4 mm of Lichrosorb RP-8 (10 μm), fitted with a precolumn of the same material	0.2062 g of KH_2PO_4 and 0.2625 g of K_2HPO_4 in water–acetonitrile–methanol (1:1:2) [1 mL/min]	254 nm	Analysis of tablets. Results agreed well with B. P. method. Recovery was 102%.	[102]
15 cm × 4.6 mm of Asahipak ODP-50 at 40°C (0.45 μm)	70 mM phosphate buffer of pH 5.8–acetonitrile (77:23) containing 10 mg/L of Na_2–EDTA [0.8 mL/min]	Electrochemical	Analysis of primaquine and carboxyprimaquine in calf plasma.	[103]
Cartridge column (10 cm × 4.6 mm) of C_{18} (5 μm) equipped with a pre-column (3 cm × 4.6 mm) of C_{18}	Acetonitrile–0.05 K_2HPO_4 of pH 6–tetrahydrofuran (60:39:1) containing *N*, *N*′-dimethyl octylamine (0.5 mL/L) [0.7 mL/min]	269 nm	Determined the drug as a metabolite of a new drug, CDRI compound 8053, simultaneously, in serum.	[104]
Normal phase silica column	Chloroform–methanol–ammonia solution (86.8:12.5:0.7)	254 nm	Assay of primaquine and hepatic targeting neoglycoalbumin–primaquine in whole blood and liver of mouse by reversed-phase HPLC.	[105]

preliminary experiments to predict the optimum capillary electrophoresis separation conditions for primaquine and other antimalarial agents. In this investigation, the validity of the overlapping resolution mapping scheme is verified by choosing the optimum separation conditions predicted by the scheme in the separation of a group of 12 amino acids derivatized with the *N*-tert-butoxycarbonyl functional group, primaquine and a group of six other antimalarial agents. The effect of the buffer composition on the separation is discussed.

Taylor and Reid [108] reported that the separations of primaquine and 10 other antimalarial drugs and metabolites are shown by capillary-zone electrophoresis at low pH and by micellar electrokinetic chromatography at high pH. Capillary-zone electrophoresis is shown to be superior to micellar electrokinetic chromatography in resolution capability for these compounds under the conditions examined. Both are shown to provide different selectivities to those obtained by ion-pair reversed-phase high performance liquid chromatography. The effect of sample injection solvent is examined in capillary-zone electrophoresis and it is shown that field-amplified sample injection is effective for these compounds. It is shown that injection of sample in an organic solvent such as methanol augments the stacking of analytes resulting in lower detection limit. The limit of detection of some of the antimalarial agents in a urine matrix is reported.

Stalcup and Agyei [109] investigated heparin, the naturally occurring polydisperse and polyanionic glycosaminoglycan, as a chiral selector for capillary-zone electrophoresis. Baseline separations were obtained for a variety of underivatized drugs including primaquine and other antimalarial agents. Analysis was carried out at a pH of 4.5 or 5 using 2% heparin (w/w) in a 10-mM phosphate buffer under an applied voltage of 15 kV. All of the solutes successfully resolved contained at least two nitrogens with one of the nitrogens incorporated in a heterocyclic aromatic ring. Furthermore, successful resolution seemed to require that the nitrogens be somewhat distant from each other in the molecule. In addition to electrostatic interactions, solute size may also play a role in the heparin chiral recognition mechanism.

Nishi *et al.* [110] used dextran and dextrin as chiral selectors in capillary-zone electrophoresis. Polysaccharides such as dextrins, which are mixtures of linear α-(1,4)-linked D-glucose polymers, and dextrans, which are polymers of D-glucose units linked predominantly by α-(1,6) bonds, have been employed as chiral selectors in the capillary electrophoretic separation of enantiomers. Because these polymers are electrically neutral, the method is applicable to ionic compounds. The enantiomers of basic or cationic drugs such as primaquine were successfully separated under acidic conditions. The effects of molecular mass and polysaccharide concentration on enantioselectivity were investigated.

Phinney *et al.* [111] investigated the application of citrus pectins, as chiral selectors, to enantiomer separations in capillary electrophoresis. Successful enantioresolution of primaquine and other antimalarials, was achieved by utilizing potassium polypectate as the chiral selector. Changes in pH, chiral additive concentration, and capillary type were studied in relation to chiral resolution. The effect of degree of esterification of pectin materials on chiral recognition was evaluated.

Bortocan and Bonato [112] presented a capillary electrophoresis method for the enantioselective analysis of primaquine and its metabolite carboxyprimaquine. The method is used for the simultaneous determination of the drug and its metabolite, in

rat-liver mitochondrial fraction, suitable for *in vitro* metabolic studies. The drug and the metabolite were extracted by liquid–liquid extraction using ethyl ether. The enantiomers were resolved in a fused-silica capillary, 50 μm inside diameter and 24 cm of effective length, using an electrolyte solution consisting of 20 mmol/L sodium phosphate solution, pH 3, and 10% (w/v) maltodextrin. Hydrodynamic sample injection was used with a 10 s injection time at a pressure of 50 mbar. The applied voltage was 22 kV and the capillary temperature was controlled at 20°. Detection was carried out at 264 nm. Under these conditions, the enantiomeric fractions of the drug and of its metabolite were analyzed within 6 min. The extraction procedure was efficient in removing endogenous interferents and low values (<10%) for the coefficients of variation and deviation from theoretical values were demonstrated for both within-day and between-day assays. The method allows the analysis of primaquine and carboxyprimaquine enantiomers as low as 100 and 40 ng/mL, respectively. After validation, the method was used for an *in vitro* metabolic study of primaquine. The results showed the enantiomer (−)-primaquine was preferentially metabolized to (−)-carboxyprimaquine.

5. STABILITY

Kristensen *et al.* [113] studied the photochemical degradation of primaquine in an aqueous medium. The investigation was done using a medium simulating *in vivo* conditions, therefore, the effect of light of wavelength 320–600 nm on primaquine in phosphate buffer solution of pH 7.4 was studied. Primaquine formed seven major and several minor decomposition products. At concentrations above 4×10^{-5} secondary reactions seemed to occur, leading to the formation of a very high number of degradation products. The isolated degradation products emphasized that the quinoline ring remained intact after exposure of the drug to light, however, irradiation caused various cleavages of the side chain. It was concluded that degradation products of primaquine are not photochemically inert but may participate in secondary reactions and the two main photodecomposition products are not likely to be formed *in vivo* but may be formed *in vitro* after light exposure of drug formulations. The main photochemical degradation products were isolated by means of preparative thin-layer chromatography. The samples were identified by mass spectrometry (chemical ionization, electron impact and high resolution), ^{1}H NMR spectroscopy, and gas chromatography–mass spectrometry.

Chyan *et al.* [114] studied and compared the photophysical and redox properties of primaquine and dibucaine. Absorption and emission spectra and amperometric cyclic voltammograms of the two drugs were recorded at different concentrations and pH values. Primaquine at 77 K aggregates to form an excited-state double-proton-transfer dimer at concentrations higher than 5×10^{-5} M and in the pH range 2.5−5.5. The electrochemical instability of primaquine is probably associated with the observation that the 1×10^{-4} M primaquine in acetonitrile displays a highly accentuated signal of cyclic voltammogram in the reduction reaction H^{+}. The proton dissociative nature of primaquine supports the nuclear magnetic resonance measurement that the exchange of carbon-5 aromatic proton in primaquine at pH <4 is unusually fast. The acidic nature of primaquine, resulting from the

dissociation of carbon-5 aromatic proton, could assist the uptake of the antimalarial drugs. The spectroscopic investigations of native bacteriorhodopsin and delipidated deionized bacteriorhodopsin incorporated with the two drugs show that primaquine affects its lipid and denatures the purple membrane. The results are discussed in light of the pharmacological actions of the two drugs.

Gaudette and Coatney [115] reported that primaquine phosphate was unstable when subjected to dry heat of 100 °C in the presence of sodium chloride for 24 h, when boiled in water for 24 h and when heated for 24 h at 100 or 200 °C in melted hydrogenated vegetable oil. These findings exclude the use of primaquine phosphate as a salt additive in cooking. Primaquine phosphate was isolated from the test preparations at alkaline pH by extraction into ethylene chloride, after which primaquine phosphate was returned to an aqueous phase by shaking with 0.1 N sulfuric acid; the concentration of primaquine phosphate was then determined spectrophotometrically. The ultraviolet absorption curve of primaquine phosphate has maxima at 224, 266, 282, and 300 nm, and minima at 216, 250, 276, and 310 nm. A solution containing 10 γl/mL has an optical density of 0.375 at 282 nm; optical densities were proportional to concentrations.

Cheng *et al.* [116] reported that the structure of primaquine phosphate irradiated with 0.7−10 Mrad remained unchanged. The energy transfer action of the quinolyl group was considerable due to its resonance stabilization. Radiation-induced degradation of polyl(vinyl alcohol) decreased in the presence of primaquine phosphate but the degradation mechanism was unaffected. The content of primaquine phosphate showed linear relationship with degradation parameters of poly(vinyl alcohol).

Kristensen [117] studied the photochemical stability and phototoxicity of primaquine *in vitro*. The irradiation of primaquine in aqueous mediums causes cleavage of the side chain, leaving the quinoline structure unchanged. Both primaquine and the photodecomposition products absorb ultraviolet–visible light and might cause phototoxic reactions. Primaquine binds to melanin *in vitro*. Primaquine has photohemolytic properties in the ultraviolet–visible region, indicating that it is a potential photosensitizer. Hence, the *in vivo* hemolysis might be light induced.

Kristensen *et al.* [118] studied the influence of molecular oxygen and oxygen radicals on the photoreactivity of primaquine. Oxygen is directly involved in the photodecomposition of the drug. Flushing with helium gas prior to and during irradiation to suppress the oxygen level of the medium, retards the degradation rate of primaquine (followed by high performance liquid chromatography) and leads to the formation of only two degradation products (identified by mass spectrometry) compared to eight main and several minor products under normal atmospheric conditions. Flushing with oxygen gas, prior to and during irradiation to increase the oxygen content of the medium, accelerates the degradation rate of primaquine. Primaquine produces oxygen radicals (hydroxyl and superoxide) during photolysis, while the photoproducts of primaquine seem likely to induce singlet oxygen formation (detected by addition of radical scavenger). Sensitization reactions involving singlet oxygen lead to decomposition of primaquine (followed by high performance liquid chromatography). On the basis of these results, photochemical reaction mechanisms of primaquine are postulated and discussed. At physiological conditions (aqueous, neutral pH, oxygen rich), primaquine has large potential to

decompose after light absorption. The photoreaction seems to be initiated at the quinoline nitrogen atom. The ability to form intramolecular hydrogen bond seems to be essential for the luminescence properties of the drug. Phosphorescence lifetime of primaquine is about 5 μs. Fast chemical reactions may occur from the short-lived triplet state of the drug, but the excited compound can diffuse only a limited distance prior to de-excitation. This can be important concerning light-induced adverse effects that may appear after medication with primaquine.

Moore and Hemmens [119] studied the photosensitization of primaquine and other antimalarial agents. The drugs were tested for *in vitro* photosensitizing capability by irradiation with 365 nm ultraviolet light in aqueous solutions. The ability of these compounds to photosensitize the oxidation of 2,5-dimethylfuran, histidine, trypotophan, or xanthine, and to initiate the free radical polymerization of acrylamide was examined in the pH range 2–12. Primaquine does not have significant photochemical activity in aqueous solution.

Motten *et al.* [120] carried out some photophysical studies on primaquine and other antimalarial drugs. The drugs were irradiated with light ($\lambda < 300$ nm) and electron paramagnetic resonance and laser flash photolysis studies were conducted to determine the possible active intermediates produced. Each antimalarial drug produced at least one electron-paramagnetic resonance adduct with the spin-trap 5,5-dimethyl-1-pyrroline N-oxide in benzene or a nitrogen-centered radical adduct only (primaquine). In ethanol, only primaquine quenched singlet oxygen efficiently (2.6×10^8 M^{-1} s^{-1} in D_2O, pD7).

6. PHARMACOKINETICS

Greaves *et al.* [121] studied the plasma kinetics and urinary excretion of primaquine phosphate in volunteers after single and multiple dose regimes. The kinetic parameters were similar in glucose 6-phosphate dehydrogenase normal subjects from Thailand, glucose-6-phosphate dehydrogenase deficient subjects from Thailand, and in Caucasians. In the Caucasians subjects, approximately 1% of the dose was excreted in the urine. The kinetic parameters obtained from multiple dose studies were very similar to those obtained from single-dose studies.

Greaves *et al.* [122] also studied urinary primaquine excretion and red cell methemoglobin levels in man following a primaquine:chloroquine regimen. Red cell methemoglobin levels were found to be significantly raised in healthy subjects given a 14-day course of primaquine with chloroquine on the first 3 days. The methemoglobin levels were not related the quantity of primaquine excreted. No primaquine could be detected in plasma at 24 h following the last three daily doses.

Fletcher *et al.* [123] used a sensitive and specific gas chromatography–mass spectrometry method for the assay of primaquine in plasma and urine for studying the plasma kinetics. Preliminary studies on the effects of single and multiple oral doses were carried out. In both cases, the drug was completely removed from plasma in 24 h. The concentration of primaquine in plasma usually reached a peak 1–2 h after oral administration. The plasma elimination half-life was about 4 h.

Ward *et al.* [124] studied the pharmacokinetics of primaquine after acute and chronic administration of the drug to healthy Thai volunteers. After acute dosage

(15 mg, orally) mean peak plasma concentrations of 65 ng/mL were achieved within 2 h. Thereafter plasma drug concentrations declined monoexponentially with a mean elimination half-life of 4.4 h. The mean oral clearance was 37.6 L/h. These values are in broad agreement with values obtained in healthy Caucasians after administration of an equivalent dose of primaquine. The carboxylic acid metabolite of the drug accumulated in plasma after repeated dosing such that by day 14 of chronic dosing, the mean area under the concentration curve (measured from 0 to 24 h) for this metabolite was 74% greater than that obtained after acute administration of the drug.

Ward *et al.* [125] investigated the disposition of ^{14}C-radiolabeled primaquine in the isolated perfused rat liver preparation, after the administration of 0.5, 1.5, and 5 mg doses of the drug. The pharmacokinetics of primaquine in the experimental model was dependent on dose size. Increasing the dose from 0.5 to 5 mg produced a significant reduction in clearance from 11.6 to 2.9 mL/min. This decrease was accompanied by a disproportionate increase in the value of the area under the curve from 25.4 to 1128.6 μg/mL, elimination half-life from 33.2 to 413 min, and volume of distribution from 547.7 to 1489 mL. Primaquine exhibited dose dependency in its pattern of metabolism. While the carboxylic acid derivative of primaquine was not detected perfusate after the 0.5 mg dose, it was the principal perfusate metabolite after 5 mg dose. Primaquine was subject to extensive biliary excretion at all doses, the total amount of ^{14}C-radioactivity excreted in the bile decreased from 60 to 30% as the dose of primaquine was increased from 0.5 to 5 mg.

Prasad *et al.* [126] developed and used a sensitive and specific spectrophotometric method for the estimation of primaquine to study the plasma kinetics of primaquine in Rhesus monkeys. It was observed that the drug completely disappeared from the plasma in 24 h after a single oral dose. Its concentration in the plasma reached a peak at 2 h of administration. The mean absorption and elimination half-lives were 0.36 ± 0.08 and 3.44 ± 0.37 h, respectively.

Mihaly *et al.* [127] examined the pharmacokinetics of primaquine in healthy volunteers who received single oral doses of 15, 30, and 45 mg of the drug, on separate occasions. Each subject received an intravenous tracer dose of ^{14}C-primaquine (7.5 μCi), simultaneously with 45 mg oral dose. Absorption of primaquine was virtually complete with a mean absorption bioavailability of 0.96. Elimination half-life, oral clearance, and apparent volume of distribution for both primaquine and the carboxylic acid metabolite were unaffected by either dose size or route of administration.

Mihaly *et al.* [128] identified the carboxylic acid derivative of primaquine as a major plasma metabolite. After oral administration of 45 mg of primaquine to healthy volunteers, absorption of the drug was rapid, with peak primaquine levels of 153.3 ng/mL at 3 h, followed by an elimination half-life of 7.1 h, systemic clearance of 21.1 L/h, volume of distribution of 205 L and cumulative urinary excretion of 1.3% of the dose. Primaquine was converted rapidly to the carboxylic acid metabolic, which achieved peak levels of 1427 ng/mL at 7 h.

Ma *et al.* [129] prepared a new pharmaceutical form, primaquine–liposome and determined the toxicity and the therapeutic efficacy of the primaquine–liposome in mice. The LD_{50} of intravenous primaquine–liposome in mice was 2–3 times less than that of free primaquine. Primaquine–liposome concentration in blood was higher

than free primaquine in blood (at the beginning of 2 h). After intravenous administration in mice, primaquine–liposome showed a high concentration in the spleen and liver, and lesser uptake by the lung and heart.

Ward *et al.* [130] studied the pharmacokinetics of (+)- and (−)-primaquine in the isolated perfused rat liver preparation. The perfusate plasma concentrations of primaquine in the isolated, perfused rat liver, declined biexponentially following the addition of either (+)- or (−)-primaquine at doses 0.5–2.5 mg in the perfusate reservoir. There were no differences between pharmacokinetic profiles of the two isomers at the 0.5 mg dose. By contrast, the elimination of (−)-primaquine was greater than (+)-primaquine when either was added in a dose of 2.5 mg; also, the clearance of the (−)-isomer was greater, the half-life was shorter, and the area under the plasma concentration curve was shorter. The volume of distribution was similar for the two isomers. These results are relevant to both the therapeutic efficacy and toxicity of primaquine.

Singhasivanon *et al.* [131] investigated the pharmacokinetics of primaquine in eight healthy subjects (four males and four females). The volunteers received 15 mg base of primaquine daily for 14 days. The results showed that the concentration–time profiles in whole blood and in plasma were similar. The mean values (±SD) of the area under the curve of the last dose were significantly decreased when compared to the values of the first dose both in the whole blood and in plasma.

Yoshimura *et al.* [132] studied the pharmacokinetics of primaquine in calves of 180−300 kg live weight. The drug was injected at 0.29 mg/kg (0.51 mg/kg as primaquine diphosphate) intravenously or subcutaneously and the plasma concentrations of primaquine and its metabolite carboxyprimaquine were determined by high performance liquid chromatography. The extrapolated concentration of primaquine at zero time after the intravenous administration was 0.5 ± 0.48 μg/mL which decreased with an elimination half-life of 0.16 ± 0.07 h. Primaquine was rapidly converted to carboxyprimaquine after either route of administration. The peak concentration of carboxyprimaquine was 0.5 ± 0.08 μg/mL at 1.67 ± 0.15 h after intravenous administration. The corresponding value was 0.47 ± 0.07 μg/mL at 5.05 ± 1.2 h after subcutaneous administration. The elimination half-lives of carboxyprimaquine after intravenous and subcutaneous administration were 15.06 ± 0.99 h and 12.26 ± 3.6 h, respectively.

Kim *et al.* [133] studied the pharmacokinetics of primaquine and carboxyprimaquine in Korean patients with *vivax* malaria. Thirty *vivax* malaria patients were given 15 mg primaquine daily for 14 days after 3 days of chloroquine treatment. Plasma samples were taken at intervals after each daily dose of primaquine for 3 days. Plasma concentrations of primaquine and carboxyprimaquine were measured by high performance liquid chromatography. The primaquine concentrations reached a maximum of 0.28 ± 0.18 μg/mL at 1.5 h after the first dose. The maximum concentration of carboxyprimaquine was 0.32 ± 0.13 μg/mL at 4 h. Higher drug concentrations with repeated dosing were observed for carboxyprimaquine, but not for the parent drug primaquine. The elimination half-life was 3.76 ± 1.8 h and 15.7 ± 12.2 h, for the drug and the metabolite, respectively.

Arica *et al.* [134] reviewed and discussed the pharmacokinetics and bioavailability of primaquine diphosphate.

7. METABOLISM

Clark *et al.* [53] used ^{13}C NMR spectrometry to study the metabolism of primaquine by microorganism. A total of 77 microorganisms were evaluated for their ability to metabolize primaquine. Of these, 23 were fund to convert primaquine to one or more metabolites as studied by thin-layer chromatography analysis. Preparative scale fermentation of primaquine with four different microorganisms resulted in the isolation of two metabolites identified as 8-(4-acetamido-1-methylbutylamino)-6-methoxyquinoline and 8-[3-carboxy-1-methylpropyl amino]-6-methoxyquinoline. The structures of the two metabolites were proposed primarily on a comparison of the ^{13}C NMR spectra of the first metabolite and the methyl ester of the second metabolite with that of primaquine. The structures of both metabolites were confirmed by direct comparison with authentic samples.

Strother *et al.* [135] studied the metabolism of primaquine in adult dogs dosed with tritium-labeled primaquine diphosphate and were observed to excrete approximately 16% of the injected radioactivity in the urine within 8 h. Organic extracts of the urine were fractionated by thin-layer chromatography and the metabolic pattern obtained. Some of primaquine was excreted along with at least five metabolites including: 5-hydroxy-6-methoxy-8-[4-amino-1-methylbutylamino)quinoline and a small amount of 6-hydroxy-8-(4-amino-1-methylbutylamino)quinoline. The first metabolite could form a quinoneimine-type compound, which may induce methemoglobin formation. This metabolite and the other metabolites isolated from urine were active methemoglobin inducers *in vitro*. *In vitro* metabolism of primaquine by mouse liver enzymes also produced compounds capable of methemoglobin formation.

Clark *et al.* [136] studied the excretion, distribution, and metabolism of primaquine in rats. The drug was administered intravenously, intraperitoneally, and orally and blood samples were collected at various time intervals. Primaquine was metabolized by oxidative deamination to give 8-(3-carboxy-1-methylpropylamino)-6-methoxy quinoline. The plasma levels of both primaquine and its metabolites were determined by high performance liquid chromatography.

Baker *et al.* [137] reported that Rhesus monkeys were administered primaquine (6–10.5 mg as the phosphate/kg intravenously) and plasma samples were analyzed by high performance liquid chromatography for the presence of the unchanged drug and the major metabolite, 8-[3-carboxy-1-methylpropylamino)-6-methoxyquinoline. Primaquine had an unusually high affinity for tissue compartments, which produced a rapid initial drop in plasma concentration. Within 15 min, the plasma concentration of the metabolite far exceeded that of primaquine. Thirty-five to eighty-three percent of the primaquine dose was converted to the major metabolite. This metabolite possessed much lower affinity for the tissues compartments than the drug itself.

Baker *et al.* [138] studied the excretion of metabolites in bile following the administration of primaquine in rats. Six metabolites of primaquine were found in the bile of rats. Quantitative high performance liquid chromatography analysis of the metabolites revealed that the sum of the six metabolites excreted in the bile represented quantitative recovery of the dose of primaquine.

Price and Fletcher [139] studied the metabolism and toxicity of primaquine in human and monkeys. Results of a number of studies by the authors on primaquine

metabolism and pharmacokinetics are summarized. Other studies on primaquine metabolism and toxicity in man as well as *in vitro* studies are reviewed.

Baker *et al.* [140] characterized the urinary metabolites of primaquine in rats. Following the synthesis of reference standards of primaquine metabolites, a high performance liquid chromatographic analytical method for carboxyprimaquine, its glycine conjugate, and its glucuronide conjugate in urine samples were developed. After administration of the drug only trace quantities of primaquine and carboxyprimaquine (each $<1\%$ of dose) and no significant quantity of the two conjugates of carboxyprimaquine were excreted in the urine. When carboxyprimaquine was administered to rats, only 0.3% of the dose was excreted in the urine. When carboxyprimaquine glycinate was administered, the compound was found in the 700–1300 μg/mL concentration range in the urine within the first few hours. With the use of ^{14}C-labeled primaquine, six new metabolites were found in the urine.

Hufford *et al.* [57] used proton and ^{13}C NMR spectrometric data to establish the novel sulfur containing microbial metabolite of primaquine. Microbial metabolic studies of primaquine using *S. roseochromogenus* produced an *N*-acetylated metabolite and a methylene linked dimeric product, both of which have been previously reported, and a novel sulfur containing microbial metabolite.

Frischer *et al.* [141] studied the biotransformation of primaquine *in vivo* with human erythroleukemic K562 cells and bone marrow cells. The biotransformation of primaquine was investigated *in vitro* in serum-supplemented liquid cultures of partially synchronized and exponentially growing human erythroleukemic K562 cells and in bone marrow cells. Primaquine was rapidly and predominantly converted *in vitro* into carboxyprimaquine in a quantitative manner and without further modification. In addition to this metabolite, a compound Xc that was not 6-methoxy-8-aminoquinoline, and was not derived from carboxyprimaquine appeared in minor amounts in a delayed fashion. With erythroleukemic K562 cells as well as the bone marrow cells the formation of carboxyprimaquine from primaquine could be totally blocked by large concentrations of the nitrosourea, 1,3-bis(2-chloroethyl) nitrosourea. With bone marrow, increasing blockade of carboxyprimaquine formation by 1,3-bis(2-chloroethyl)nitrosourea led invariably to a progressive and striking accumulation of Xc.

Bangchang *et al.* [142] studied a number of antimalarial drugs for their effect on the metabolism of primaquine by human liver microsomes ($N = 4$) *in vitro*. The only metabolite generated was identified as carboxyprimaquine by cochromatography with the authentic standard.

Ni *et al.* [143] investigated the profile of the major metabolites of primaquine produced by *in vitro* liver microsomal metabolism, with silica gel thin-layer and high performance liquid chromatography analysis. Results indicated that the liver microsomal metabolism could simultaneously produce both 5-hydroxyprimaquine (quinoline ring oxidation product) and carboxyprimaquine (side-chain oxidative deamination product). However, the quantitative comparative study of microsomal metabolism showed that the production of 5-hydroxyprimaquine was far much higher than that of carboxyprimaquine.

Ni *et al.* [144] also investigated the profiles of major metabolites of primaquine produced from liver microsomal and mitochondrial metabolism, *in vitro* by silica gel thin-layer and reversed-phase high performance liquid chromatography. The results

indicated that 5-hydroxyprimaquine and 5-carboxyprimaquine were simultaneously produced by either microsomes or pure mitochondrial preparations. However, the quantitative study showed that microsomes produced approximately 19 times more 5-hydroxyprimaquine and only 1/34 of the carboxyprimaquine produced by mitochondria.

Constantino *et al.* [145] studied the role of monoamine oxidase and cytochrome P450 in the oxidative deamination of primaquine by rat liver fractions. Rat liver fractions including liver homogenate, mitochondria, microsomes, and 100,000 g supernatant fractions were prepared from a pool of rat livers and characterized using benzylamine as a probe for monoamine oxidase activity and *N,N*-dimethylbenzamide as a probe for cytochrome P450 *N*-dealkylation activity. Incubation of all fractions with primaquine yielded carboxyprimaquine as the only metabolite detectable by high performance liquid chromatography. The mitochondrial fraction, which contained monoamine oxidase activity but no cytochrome P450 activity, presented the highest $V_{max}/K(M)$ value for the formation of carboxyprimaquine.

Bergqvist and Churchill [146] reviewed the methods used for the detection and determination of primaquine and other antimalarial drugs and their metabolites in body fluids.

Wernsdorfer and Trigg [147] reviewed the pharmacokinetics, metabolism, toxicity, and activity of primaquine.

8. BINDING TO DNA

Whichard *et al.* [148] studied the binding of primaquine and three other aminoquinoline antimalarial agents to native and denatured calf thymus DNA, by equilibrated dialysis and direct spectrophotometry. The binding of these drugs to DNA is (1) accompanied by a decrease in absorbance of the ligand, (2) decreased by an increase in ionic strength, (3) decreased by addition of magnesium ion to a greater extent than would be expected from ionic strength effects alone, and (4) decreased under some conditions by the presence of four molar urea. In 0.01 M potassium phosphate (pH 6), the total binding of primaquine and the other drugs to various DNA preparations at DNA nucleotide-to-amioquinoline ratios $\geq$6 occurs in the following order: native DNA = denatured DNA > native DNA in 4 M urea > denatured DNA in 4 M urea.

Morris *et al.* [149] studied the binding of primaquine and pentaquine, some of their potential metabolites and chloroquine to DNA, RNA, and various polydeoxyribonucleotides and polyribonucleotides, by equilibrium dialysis and direct spectrophotometry. The extent of binding of the three drugs to native calf thymus DNA, as measured by equilibrium dialysis, does not vary in the range of pH 6–8. A major portion of each 6-hydroxy derivative of the 8-aminoquinolines binds to DNA, although, in the two examples studied, the extent of binding is somewhat less than for the corresponding 6-methoxy parent compound. Removal of the protonated terminal nitrogen of the 8-diamino side chain decreases the binding of the 8-aminoquinolines to very slow level.

9. IMMUNOASSAY

Al-Abdulla *et al.* [150] developed a magnetisable solid-phase fluorimmunoassay method for the analysis of primaquine and carboxyprimaquine. Primaquine coupled to keyhole limpet hemocyanin was used as an immunogen to produce antiprimaquine antibodies in three sheep. The antisera obtained were characterized by the increase in fluorescence polarization found upon binding to fluorescein-labeled primaquine prepared through same route. All sheep showed a good antibody response and one antiserum was coupled to megnetisable solid-phase particles to facilitate the separation of the antibody bound from free labeled antigen and the removal of interfering components which may be present in the sample. The fluoroimmunoassay requires addition of 100 μL of standard or sample (urine or serum) to 100 μL tracer (150 nmol/L) followed by 100 μL of megnetisable solid-phase particles (12.2 g/L). After 1-h incubation followed by the usual washing and eluting procedures, using a magnetic rack, the fluorescence of the supernatant was measured directly in a fluorimeter. Sodium salicylate was incorporated in the tracer solution to block the nonspecific binding of tracer to the protein in serum samples. Cross-reactivity studies showed that the antibodies have high specificity for the 8-amioquinoline nucleus but not to the 8-*N*-aminobutyl side chain. Thus, carboxyprimaquine cross-reacted equally with primaquine and the assay can be used to measure their combined level. After extraction of primaquine from a basified sample with methylene chloride, the assay may be applied for the quantitation of either primaquine (in the organic phase) or its acidic metabolites including carboxyprimaquine (in the aqueous phase) separately. This approach was applied for the determination of total primaquine (primaquine and its metabolites) and extracted primaquine in urine samples following a single oral dose of 45 mg primaquine.

Al-Abdulla *et al.* [151] presented a comparison between the three different activation methods for coupling antibodies to magnetisable cellulose particles. The periodate and 1,1′-carbonyldiimidazole activation methods were compared with the cyanogen bromide procedure for coupling antibodies to magnetisable cellulose/iron oxide solid-phase particles. Fluoroimmunoassay for primaquine and other compounds were employed to assess the binding properties of such coupled solid-phases. The cyanogen bromide and 1,1′-carbonyldiimidazole methods gave similar products in most cases, while the specific binding capacity of periodate coupled particles was between two and five times lower. Nevertheless, comparable standard curves could be obtained with solid-phase coupled by each method. The periodate and 1,1′-carbonyldiimidazole methods are acceptable alternatives, notably for laboratories lacking the facility to handle the toxic cyanogens bromide.

10. PHARMACOLOGY

Olenick [152] presented a review on primaquine. Fernex and Leimer [153] reviewed the pharmacology and clinical properties of primaquine and other antimalarial agents.

Baird *et al.* [154] reported that primaquine base (30 mg/day) had protective efficacy against *Plasmodium falciparum* and *P. vivax* of 85–93%. Among 339

children with an age of less than 8 years and adults taking this regimen for 12–52 weeks, there was no greater risk of adverse symptomatic events among primaquine users than among recipients of placebo in double-blind studies. Among 151 subjects evaluated after 20–52 weeks of daily primaquine therapy, methemoglubinemia was mild (<13%; typically <6%) and transient (duration, <2 weeks). The authors considered primaquine base (0.5 mg/kg/day consumed with food) to be safe, well-tolerated, and effective prophylaxis against malaria for nonpregnant persons and those with normal glucose-6-phosphate dehydrogenase levels. Primaquine's major advantage over most drugs for chemoprophylaxis is that it does not have to be taken before entering or beyond 3 days after leaving a malarious area.

Baird and Hoffman [155], in a review, examined the wide range of clinical applications of primaquine described in the medical literature between 1946 and 2004. The risk of relapse of *P. vivax* malaria without primaquine therapy ranged from 5% to 80% or more, depending largely upon geographical location. Supervision of therapy profoundly impacts the risk of relapse, and almost all reports of malaria resistant to primaquine are associated with lack of such supervision. The authors suspect that there is widespread resistant to the stated course of primaquine therapy, which is 15 mg primaquine base daily for 14 days. Clinical evidence confirms that the course of 15 mg daily for just 5 days, a regimen widely used in areas where malaria is endemic, has no discernible efficacy. The authors recommended a regimen of 0.5 mg/kg primaquine daily for 14 days, on the basis of superior efficacy and good tolerability and safety in nonpregnant persons without glucose-6-phosphate dehydrogenase deficiency.

ACKNOWLEDGEMENT

The author wishes to thank Mr. Tanvir A. Butt, Pharmaceutical Chemistry Department, College of Pharmacy, King Saud University, Riyadh, Saudi Arabia for his secretarial assistance in preparing this profile.

REFERENCES

[1] Budavari (ed.), *The Merck Index*, 12th edn., Merck and Co., NJ, 1996, p. 1330.
[2] A. C. Moffat (ed.), *Clarke's Isolation and Identification of Drugs*, 2nd edn., Pharmaceutical Press, London, 1986, p. 921.
[3] *British Pharmacopoeia*, 16th edn., Vol. 1, Her Majesty Stationary Office Publication Ltd., London, 2000 (CD-Rom).
[4] *United States Pharmacopoeia*, 23rd edn., United States Pharmaceutical Conversion, Inc., Rockville, MD, 2003.
[5] Sean C. Sweetman (ed.), *Martindale, The Complete Drug Reference*, 33rd edn., Pharmaceutical Press, 2002, p. 434.
[6] Swiss Pharmaceutical Society (ed.), *Index Nominum 2000, International Drug Directory*, 17th edn., Medpharm GmbH Scientific Publisher, Stuttgart, 2000, p. 875.
[7] R. C. Elderfield, H. E. Mertel, R. T. Mitch, I. M. Wempen and E. Werble, *J. Am. Chem. Soc.*, 1955, **77**, 4816.
[8] T. H. Chu, C. K. Liu, C. S. Yang, K. T. Lu and C. C. Chang, *Yaoxue Xuebao*, 1956, **4**, 197.
[9] P. Nickel, *Pharmazeutische Zeitung*, 1968, **113**, 1609.

[10] M. I. Walash, M. Rizk, A. A. Abou-Ouf and F. Belal, *Anal. Lett.*, 1983, **16**, 129.
[11] S. J. Ahmad and I. C. Shukla, *Analyst*, 1984, **109**, 1103.
[12] C. X. Yang, Y. G. Li, Z. F. Xiao, H. J. Liu and P. X. Liu, *Yaoxue Xuebao*, 1991, **26**, 531.
[13] C. D. Hufford, J. D. McChesney and J. K. Baker, *J. Heterocyclic Chem.*, 1983, **20**, 273.
[14] R. B. Papovic, K. I. Nikolic and M. D. Bodiroga, *Glasnik Hemijskog Drustva Beograd*, 1980, **45**, 373.
[15] A. S. Amin and Y. M. Issa, *J. Pharm. Biomed. Anal.*, 2003, **31**, 785.
[16] A. A. Abou-Ouf, S. M. Hassan and M. E. S. Metwally, *Analyst*, 1980, **105**, 1113.
[17] R. N. Prasad, S. K. Garg, R. C. Mahajan and N. K. Ganguly, *Indian J. Med. Res.*, 1983, **77**, 388.
[18] S. M. Hassan, M. E. S. Metwally and A. M. Abou-Ouf, *J. Assoc. Off. Anal. Chem.*, 1983, **66**, 1433.
[19] S. T. Sulaiman and D. Amin, *Int. J. Environ. Anal. Chem.*, 1985, **20**, 313.
[20] P. K. Chatterjee, C. L. Jain and P. D. Sethi, *Indian Drugs*, 1986, **23**, 563.
[21] M. Abdel-Salam, A. S. Issa and H. Lymona, *J. Pharm. Belg.*, 1986, **41**, 314.
[22] H. S. G. Vishwavidyalaya, N. Talwar, P. J. Gogoi, S. P. Vyas and N. K. Jain, *Indian Drugs*, 1990, **28**, 156.
[23] Q. Min, P. Chen, C. Li, J. Wang and G. Liu, *Yaowu Fenxi Zazhe*, 1992, **12**, 110.
[24] I. H. Refaat, M. E. El-Kommos, H. H. Farag and N. A. El-Rabat, *Bull. Pharm. Sci. Assiut Univ.*, 1987, **10**, 85.
[25] S. S. Artemchenko, V. V. Petrenko and V. A. Tsilinko, *Patent No*. SU 1113722, USSR, 1984.
[26] N. Talwar, P. J. Gogoi, S. P. Vyas and N. K. Jain, *Indian Drugs*, 1990, **28**, 156.
[27] Z. Gu, H. He, D. Rong, G. Yao, Z. Qin, D. Li, H. Xu and M. Cao, *Yao Wu Fen Hsi Tsa Chih*, 1982, **2**, 9.
[28] J. J. Aaron, S. A. Ndiaye and J. Fidanza, *Analusis*, 1982, **10**, 433.
[29] M. Tsuchiya, E. Torres, J. J. Aaron and J. D. Winefordner, *Anal. Lett.*, 1984, **17**, 1831.
[30] F. A. Ibrahim, F. Belal and A. El-Brashy, *Microchem. J.*, 1989, **39**, 65.
[31] Y. Cheng, N. N. Que, S. L. Li and L. Li, *Yaowu Fenxi Zazhi*, 1993, **13**, 167.
[32] G. Fuhrmann and K. Werrbach, *Z. Tropenmedizin Parasitologie*, 1965, **16**, 397.
[33] Y. P. Rao and G. R. Rao, *Indian Drugs*, 1981, **18**, 152.
[34] A. S. Issa, M. S. Mahrous, M. Abdel-Salam and M. Abdel-Hamid, *Journal de Pharmacie de Belgique*, 1985, **40**, 339.
[35] D. L. A. De Faria and P. S. Santos, *Mol. Biomol. Spectrosc.*, 1991, **47A**, 1653.
[36] S. M. El-Ashry, F. A. Aly and A. M. El-Brashy, *Arch. Pharmac. Res.*, 1994, **17**, 415.
[37] T. John, S. Rani and R. Hiremath, *Indian Drugs*, 1996, **33**, 293.
[38] A. S. Amin and Y. M. Issa, *Mikrochim. Acta*, 2000, **134**, 133.
[39] S. M. Hassan, M. E. S. Metwally and A. M. Abou-Ouf, *Anal. Lett.*, 1982, **15**, 213.
[40] B. S. Sastry, E. V. Rao, M. V. Suryanarayana and C. S. P. Sastry, *Pharmazie*, 1986, **41**, 739.
[41] B. S. Sastry, E. V. Rao, M. K. Tummuru and C. S. P. Sastry, *Indian J. Pharm. Sci.*, 1986, **48**, 190.
[42] B. S. Sastry, E. V. Rao, M. K. Tummuru and C. S. P. Sastry, *Indian Drug*, 1986, **24**, 105.
[43] M. S. Mahrous, M. Abdel-Salam, A. S. Issa and M. Abdel-Hamid, *Talanta*, 1986, **33**, 185.
[44] M. E. El-Kommos and K. M. Emara, *Bull. Pharm. Sci. Assiut Univ.*, 1988, **11**, 18.
[45] G. R. Rao, S. S. N. Murthy and I. R. K. Raju, *Indian Drugs*, 1988, **25**, 475.
[46] G. R. Rao, S. S. N. Murthy and I. R. K. Raju, *Indian Drugs*, 1988, **26**, 86.
[47] M. E. El-Kommos and K. M. Emara, *Alexandria J. Pharm. Sci.*, 1988, **2**, 171.
[48] B. S. Sastry, J. V. Rao, T. N. V. Prasad and C. S. P. Sastry, *Indian Drugs*, 1989, **26**, 194.
[49] F. A. Ibrahim, A. El-Brashy and F. Belal, *Mikrochem. Acta*, 1989, **1**, 321.
[50] B. S. Sastry, E. V. Rao, M. V. Suryanarayana and C. S. P. Sastry, *Indian Drugs*, 1990, **27**, 260.
[51] A. M. El-Brashy, *Anal. Lett.*, 1993, **26**, 2595.
[52] J. K. Baker, J. D. McChesney and L. Jorge, *Bull. World Health Organ.*, 1985, **63**, 887.
[53] A. M. Clark, C. D. Hufford and J. D. McChesney, *Antimicrob. Agents Chemother.*, 1981, **19**, 337.
[54] S. P. Singh, S. S. Parmar and V. I. Stenberg, *J. Heterocyclic Chem.*, 1978, **15**, 9.
[55] J. D. McChesney and S. Sarangan, *Pharm. Res.*, 1984, **4**, 184.
[56] C. D. Hufford and J. K. Baker, *Spectrosc. Lett.*, 1989, **19**, 595.
[57] C. D. Hufford, J. K. Baker, J. D. McChesney and A. M. Clark, *Antimicrob. Agent Chemother.*, 1986, **30**, 234.
[58] J. R. Perussi, V. E. Yushmanov, S. C. Monté, H. Imasato and M. Tabak, *Physiol. Chem. Phys. Med. NMR*, 1995, **27**, 1.

[59] A. Berka, K. Nicolic and K. Velasevic, *Acta Pol. Pharm.*, 1990, **47**, 7.
[60] Y. F. Zhan and J. Z. Mao, *Huaxue Shijie*, 1992, **33**, 165.
[61] Y. Zhan, *Fenxi Huaxue*, 1992, **20**, 493.
[62] B. B. Saad, Z. A. Zahid, S. A. Rahman, M. N. Ahmad and A. H. Husin, *Analyst*, 1992, **117**, 1319.
[63] G. B. Mohamed, *Alexandria J. Pharm. Sci.*, 1989, **3**, 180.
[64] Q. S. Yu, A. Brossi and J. L. Flippen-Anderson, *FEBS Lett.*, 1987, **221**, 325.
[65] S. M. Hassan, M. E. S. Metwally and A. M. Abou-Ouf, *Analyst*, 1982, **107**, 1235.
[66] S. A. Fusari, I. J. Holcomb and R. B. Luers, *J. Chromatogr. Sci.*, 1975, **13**, 589.
[67] H. Zheng and H. Sun, *Yaowu Fenxi Zazhi*, 1983, **3**, 113.
[68] A. K. Dwivedi, M. Khanna, R. Pal and S. Singh, *Indian J. Pharm. Sci.*, 1997, **59**, 321.
[69] A. K. Dwivedi, D. Saxena and S. Singh, *J. Pharm. Biomed. Anal.*, 2003, **33**, 851.
[70] A. H. Stead, R. Gill, T. Wright, J. P. Gibbs and A. C. Moffat, *Analyst*, 1982, **107**, 1106.
[71] R. E. Andrey and A. C. Moffat, *J. Chromatogr.*, 1981, **220**, 195.
[72] T. G. Rajagopalan, B. Anjaneyulu, V. D. Shanbag and R. S. Grewal, *J. Chromatogr.*, 1981, **224**, 265.
[73] J. D. Baty, D. A. Price-Evan, H. M. Gilles and J. Greaves, *Biomed. Mass Spectrom.*, 1978, **5**, 76.
[74] J. Greaves, D. A. Price-Evans, H. M. Gilles and J. D. Baty, *Biomed. Mass Spectrom.*, 1979, **6**, 109.
[75] M. Nitin, M. Rajanikanth, J. Lal, K. P. Madhusudanan and R. C. Gupta, *J. Chromatogr.*, 2003, **793**, 253.
[76] V. K. Dua, S. N. Sinha and V. P. Sharma, *J. Chromatogr. Biomed. Appl.*, 1998, **708**, 316.
[77] V. K. Dua, P. K. Kar, R. Sarin and V. P. Sharma, *J. Chromatogr. Biomed. Appl.*, 1996, **675**, 93.
[78] I. Jane, A. McKinnon and R. J. Flanagan, *J. Chromatogr.*, 1985, **323**, 191.
[79] G. W. Parkhurst, M. V. Nora, R. W. Thomas and P. E. Carson, *J. Pharm. Sci.*, 1984, **73**, 1329.
[80] B. B. Wheals, *J. Chromatogr.*, 1980, **187**, 65.
[81] A. M. Clark, S. L. Evans, C. D. Hufford and J. D. McChesney, *J. Natural Products*, 1982, **45**, 574.
[82] J. K. Baker, J. D. McChesney, C. D. Hufford and A. M. Clark, *J. Chromatogr.*, 1982, **230**, 69.
[83] C. D. Hufford, A. M. Clark, J. D. McChesney and J. K. Baker, *J. Org. Chem.*, 1984, **49**, 2822.
[84] N. Katori, T. Shibazaki and M. Uchiyama, *Iyakuhin Kenkyu*, 1985, **16**, 1407.
[85] Y. Okamoto, R. Aburatani, K. Hanato and K. Hatada, *J. Liq. Chromatogr.*, 1988, **11**, 2147.
[86] A. S. Sidhu, J. M. Kennedy and S. Deeble, *J. Chromatogr.*, 1987, **391**, 233.
[87] G. R. Rao, S. S. N. Murty, I. R. K. Raju and C. M. R. Srivastava, *Indian Drugs*, 1989, **26**, 430.
[88] R. B. Taylor, R. G. Reid, R. H. Behrens and I. Kanfer, *J. Pharm. Biomed. Anal.*, 1992, **10**, 867.
[89] X. Liu and R. Wu, *Zhongguo Yaoke Daxue Xuebao*, 1989, **20**, 240.
[90] T. L. Li, Q. J. Pang, Y. L. He and P. Wang, *Yaoxue Xuebao*, 1995, **30**, 721.
[91] J. Fang, X. Xia and Y. Wu, *Zhongguo Yaowu Huaxue Zazhi*, 2003, **13**, 48.
[92] L. Jawahar, M. Nitin and G. R. Chandra, *J. Pharm. Biomed. Anal.*, 2003, **32**, 141.
[93] R. A. Dean, W. Ochieng, J. Black, S. F. Queener, M. S. Bartlett and N. G. Dumaual, *J. Chromatogr. Biomed Appl.*, 1994, **655**, 89.
[94] S. A. Ward, G. Edwards, M. L. E. Orme and A. M. Breckenridge, *J. Chromatogr.*, 1984, **305**, 239.
[95] M. V. Nora, G. W. Parkhurst, R. W. Thomas and P. E. Carson, *J. Chromatogr.*, 1984, **307**, 451.
[96] S. C. Bhatia, S. N. Revankar, E. D. Bharucha and K. J. Doshi, *Anal. Lett.*, 1985, **18**, 1671.
[97] X. Fang, S. Dong, P. Zhou, R. Wu and D. An, *Nanjing-Yaoxueyuan-Xuebao*, 1985, **16**, 43.
[98] J. K. Baker, A. M. Clark and C. D. Hufford, *J. Liq. Chromatogr.*, 1986, **9**, 493.
[99] V. Das-Gupta, *Anal. Lett.*, 1986, **19**, 1523.
[100] G. R. Rao, S. S. N. Murty, I. R. K. Raju and C. M. R. Srivastava, *Indian Drugs*, 1989, **26**, 430.
[101] S. K. Sanghi, A. Verma and K. K. Verma, *Analyst*, 1990, **115**, 333.
[102] N. Talwar, A. K. Shakya, P. J. Gogoi, S. P. Vyas and N. K. Jain, *Indian Drugs*, 1991, **28**, 437.
[103] Y. S. Endoh, H. Yoshimura, N. Sasaki, Y. Ishihara, H. Sasaki, S. Nakamura, Y. Inoue and M. Nishikawa, *J. Chromatogr. Biomed. Appl.*, 1992, **117**, 123.
[104] J. K. Paliwal, R. C. Gupta and P. K. Grover, *J. Chromatogr. Biomed. Appl.*, 1993, **127**, 155.
[105] T. Li, G. Pang, Y. Jia, P. Wang, T. Ma, J. Meng and S. Zhao, *Hua Hsi I Ko Ta Hsueh Hsueh Pao.*, 1995, **26**, 109.
[106] G. Fan, J. Hu, M. Lin, Z. Zhang and D. An, *Yaowu Fenxi Zazhi*, 1999, **19**, 84.
[107] C. L. Ng, Y. L. Toh, S. F. Y. Li and H. K. Lee, *J. Liq. Chromatogr.*, 1993, **16**, 3653.
[108] R. B. Taylor and R. G. Reid, *J. Pharm. Biomed. Anal.*, 1993, **11**, 1289.
[109] A. M. Stalcup and N. M. Agyei, *Anal. Chem.*, 1994, **66**, 3054.

[110] H. Nishi, S. Izumoto, K. Nakamura, H. Nakai and T. Sato, *Chromatographia*, 1996, **42**, 617.
[111] W. K. Phinney, L. A. Jinadu and L. C. Sander, *J. Chromatogr.*, 1999, **857**, 285.
[112] R. Bortocan and P. S. Bonato, *Electrophoresis*, 2004, **25**, 2848.
[113] S. Kristensen, A. L. Grislingaas, J. V. Greenhill, T. Skjetne, J. Karlsen and H. H. Toennesen, *Int. J. Pharm.*, 1993, **100**, 15.
[114] Y. G. Chyan, M. W. Hsiao, C. M. Catuara and C. T. Lin, *J. Phys. Chem.*, 1994, **98**, 10352.
[115] L. E. Gaudette and G. R. Coatney, *Am. J. Trop. Med. Hygiene*, 1960, **9**, 532.
[116] K. Cheng, C. Yang and M. Wang, *Fushe Yanjiu Yu Fushe Gongyi Xeubao*, 1986, **4**, 34.
[117] S. Kristensen, *Biol. Eff. Light 1993*, *Proceedings of the 3rd Symposium, 1994*, p. 144.
[118] S. Kristensen, K. Nord, A. L. Orsteen and H. H. Tonnesen, *Pharmazie*, 1998, **53**, 98.
[119] D. E. Moore and V. J. Hemmens, *Photochem. Photobiol.*, 1982, **36**, 71.
[120] A. G. Motten, L. J. Martinez, N. Holt, R. H. Sik, K. Reszka, C. F. Chignell, H. H. Tonnesen and J. E. Roberts, *Photochem. Photobiol.*, 1999, **69**, 282.
[121] J. Greaves, D. A. P. Evans, H. M. Gilles, K. A. Fletcher, D. Bunnag and T. Harinasuta, *Br. J. Clin. Pharmacol.*, 1980, **10**, 399.
[122] J. Greaves, D. A. Evans and K. A. Fletcher, *Br. J. Clin. Pharmacol.*, 1980, **10**, 293.
[123] K. A. Fletcher, D. A. P. Evans, H. M. Gilles, J. Greaves, D. Bunnag and T. Harinasuta, *Bull. World Health Org.*, 1981, **59**, 407.
[124] S. A. Ward, G. W. Mihaly, G. Edwards, S. Looareesuwan, R. E. Phillips, P. Chanthavanich, D. A. Warrell, M. L. Orme and A. M. Breckenridge, *Br. J. Clin. Pharmacol.*, 1985, **19**, 751.
[125] S. A. Ward, G. W. Mihaly, D. D. Nicholl, G. Edwards and A. M. Breckenridge, *Drug Metabolism Disposition*, 1985, **13**, 425.
[126] R. N. Prasad, S. K. Garg, R. C. Mahajan and N. K. Ganguly, *Int. J. Clin. Pharmacol., Therapy Toxicol.*, 1985, **23**, 45.
[127] G. W. Mihaly, S. A. Ward, G. Edwards, D. D. Nicholl, M. L. Orme and A. M. Breckenridge, *Br. J. Clin. Pharmacol.*, 1985, **19**, 745.
[128] G. W. Mihaly, S. A. Ward, G. Edwards, M. L. Orme and A. M. Breckenridge, *Br. J. Clin. Pharmacol.*, 1984, **17**, 441.
[129] Y. Ma, Y. Jiang, H. Xu, B. Shao, X. Ye, D. Shen and X. Zhao, *Shanghai Yike Daxue Xuebao*, 1987, **14**, 21.
[130] S. A. Ward, G. W. Mihaly, D. D. Nicholl, A. M. Breckenridge and G. Edwards, *Biochem. Pharmacol.*, 1987, **36**, 2238.
[131] V. Singhasivanon, A. Sabcharoen, P. Attanath, T. Chongsuphajaisiddhi, B. Diquet and P. Turk, *Southeast Asian J. Tropical Med. Public Health*, 1991, **22**, 527.
[132] H. Yoshimura, Y. S. Endoh, Y. Ishihara, S. Nakamura and Y. Inoue, *Vet. Res. Commun.*, 1993, **17**, 129.
[133] Y. R. Kim, H. J. Kuh, M. Y. Kim, Y. S. Kim, W. C. Chung, S. Kim II and M. W. Kang, *Arch. Pharm. Res.*, 2004, **27**, 576.
[134] B. Arica, A. Ozer, H. Yekta and A. Atilla, *FABAD Farmasotik Bilimler Dergisi*, 1992, **17**, 149.
[135] A. Strother, I. M. Fraser, R. Allahyari and B. E. Tilton, *Bull. World Health Org.*, 1981, **59**, 413.
[136] A. M. Clark, J. K. Baker and J. D. McChesney, *J. Pharm. Sci.*, 1984, **73**, 502.
[137] J. K. Baker, J. A. Bedford, A. M. Clark and J. D. McChesney, *Pharm. Res.*, 1984, **2**, 98.
[138] J. K. Baker, J. D. McChesney and L. A. Walker, *Pharm. Res.*, 1985, **5**, 231.
[139] A. H. Price and K. A. Fletcher, *Prog. Clin. Biol. Res.*, 1986, **214**, 261.
[140] J. K. Baker, J. D. McChesney and L. F. Jorge, *Pharm. Res.*, 1986, **3**, 132.
[141] H. Frischer, T. Ahmad, M. V. Nora, P. E. Carson, M. Sivarajan, R. Mellovitz, L. Ptak, G. W. Parkhurst, H. S. Chow and H. Kaiser, *J. Lab. Clin. Med.*, 1987, **109**, 414.
[142] K. N. Bangchang, J. Karbwang and D. J. Back, *Biochem. Pharmacol.*, 1992, **44**, 587.
[143] Y. C. Ni, M. J. Wang, Y. Q. Xu and Hu-Ling, *Chinese J. Parasitol. Parasitic Dis.*, 1992, **10**, 275.
[144] Y. Ni, Y. Xu and M. Wang, *Zhongguo Yaoli Xueboa*, 1992, **13**, 431.
[145] L. Constantino, P. Paixoa, R. Moreira, M. J. Portela, V. E. Do Rosario and J. Iley, *Exp. Toxicol. Pathol.*, 1999, **51**, 299.
[146] Y. Bergqvist and F. C. Churchill, *J. Chromatogr.*, 1988, **434**, 1.
[147] W. H. Wernsdorfer and P. I. Trigg (eds), *Proceedings of a Meeting of the Scientific Working Group on the Chemotherapy of Malaria*, Geneva, Suitz 27–28 February 1984, John Wiley & Sons, Chichester, UK, 1987, p. 164.

[148] L. P. Whichard, C. R. Morris, J. M. Smith and J. D. Holbrook Jr., *Mol. Pharmacol.*, 1968, **4**, 630.
[149] C. R. Morris, L. V. Andrew, L. P. Whichard and D. J. Holbrook Jr., *Mol. Pharmacol.*, 1970, **6**, 240.
[150] I. H. Al-Abdulla, A. M. Sidki, J. Landon and F. J. Rowell, *Southeast Asian J. Trop. Med. Public Health*, 1989, **20**, 361.
[151] I. H. Al-Abdulla, G. W. Mellor, M. S. Childerstone, A. M. Sidki and D. S. Smith, *J. Immunol. Methods*, 1989, **122**, 253.
[152] J. G. Olenick, *Antibiotics*, 1975, **5**, 516.
[153] M. Fernex and R. Leimer, *Medecine et Hygiene*, 1986, **44**, 2113, 2117, 2120.
[154] J. K. Baird, D. J. Fryauff and S. L. Hoffman, *Clin. Infect. Dis.*, 2003, **37**, 1659.
[155] J. K. Baird and S. L. Hoffman, *Clin. Infect. Dis.*, 2004, **39**, 1336.

Valproic Acid and Sodium Valproate: Comprehensive Profile

Ibrahim A. Alsarra,[1] M. Al-Omar,[2] and F. Belal[2]

[1]*Department of Pharmaceutics, College of Pharmacy, King Saud University, P.O. Box 2457, Riyadh 11451, Kingdom of Saudi Arabia*
[2]*Department of Pharmaceutical Chemistry, College of Pharmacy, King Saud University, P.O. Box 2457, Riyadh 11451, Kingdom of Saudi Arabia*

Contents

PROFILES OF DRUG SUBSTANCES, EXCIPIENTS, AND RELATED METHODOLOGY, VOLUME 32
ISSN: 0099-5428

DOI: 10.1016/S0099-5428(05)32008-9

1. GENERAL INFORMATION

1.1. Nomenclature

1.1.1. Systemic chemical names [1,2]

Valproic acid
2-Propylvaleric acid
2-Propylpentanoic acid
di-*n*-Propylacetic acid
Sodium valproate
Sodium 2-propylvalerate
Sodium 2-propylpentanoate
Sodium di-*n*-propylacetic acid
Sodium di-*n*-propylacetate

1.1.2. Nonproprietary names

Valproic acid, Sodium valproate

1.1.3. Proprietary names [2–4]

Epival®, Epicon®, Epilim® (Sanofi Winthorp), Ergenyl® (Sanofi Winthorp), Convulex® (Pharmacia & Uplohn), Dépakine® (Sanofi Winthorp), Depamide®, Depa®, Depakene® (Abbott), Depakin®(Sanofi Winthorp), Depakine® (Sanofi Winthorp), Depakote®, Depamide®, Deproic®, Leptilan® (Novartis), Mylproin® (Desitin), Orfilept® (Leo), Orfril® (Desitin), Orlept® (CP Pharmaceuticals), Valcote®, Vistora®.

1.1.4. Synonyms [3]

Valproic acid
Abbott-44089
Sodium valproate
Abbott-44090

1.2. Formulae

1.2.1. Empirical formula, molecular weight, and CAS number [3,4]

Acid form	$C_8H_{16}O_2$	144.2	99-66-1
Sodium salt	$C_8H_{15}NaO_2$	166.5	1069-66-5

1.2.2. Structural formulae

Valproic acid

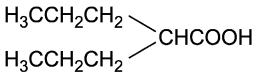

Sodium valproate

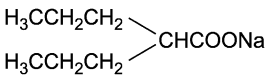

1.3. Elemental analysis

The calculated elemental composition is as follows:

C 66.63% H 11.18% O 22.19%

1.4. Appearance [1,3]

Acid form

Valproic acid is a colorless to pale yellow, slightly viscous, and clear liquid having a characteristic odor.

Salt form

Sodium valproate is a white or almost white, hygroscopic, crystalline, and deliquescent powder.

2. PHYSICAL CHARACTERISTICS

2.1. Properties

Colorless liquid with characteristic odor. Boiling point 219.5 °C. $n_D^{24.5}$ 1.425. d_4° 0.9215. pK_a 4.6. LD_{50} orally in rats 670 mg/kg [2].

2.2. Solution pH

The USP solutions of valproic acid and sodium valproate, which are prepared with the aid of sodium hydroxide, have a pH of 7–8 [3].

2.3. Solubility characteristics

Valproic acid is slightly soluble in water. It is freely soluble in acetone, alcohol, chloroform, ether, benzene, *n*-heptane, methyl alcohol, and 0.1 N sodium hydroxide; slightly soluble in 0.1 N hydrochloric acid [2,3].

Sodium valproate is very soluble in water, slight to freely soluble in alcohol [2,3].

2.4. Optical activity

Valproic acid and sodium valproate have no optical activity.

2.5. X-ray powder diffraction pattern

The X-ray powder diffraction pattern of valproic acid was performed using a Simons XRD–5000 diffractometer. Table 1 shows the values of the scattering angles (degrees 2θ), the interplanar *d*-spacings (Å), and the relative intensities (%) for valproic acid, which were automatically obtained on a digital printer. Figure 1 shows the X-ray powder diffraction pattern of valproic acid, which was carried on a pure sample of the drug.

2.6. Thermal methods of analysis

2.6.1. Melting point

Sodium valproate does not melt, decompose, or physically change in the normal working range of the Thomas–Hoover capillary melting point apparatus [5]. Valproic acid boils at 120–121 °C [2].

Table 1. Crystallographic data from the X-ray powder diffraction pattern of sodium valproate

Scattering angle (degrees 2θ)	d-spacing (Å)	Relative intensity (%)	Scattering angle (degrees 2θ)	d-spacing (Å)	Relative intensity (%)
5.633	15.6762	42.80	6.088	14.5046	4.85
6.691	13.1992	100.00	7.319	12.0678	9.72
11.293	7.8290	9.61	12.178	7.2620	4.25
13.412	6.5962	9.42	15.372	5.7595	14.71
16.907	5.2397	38.40	18.177	4.8765	18.85
18.626	4.7599	13.67	20.164	4.4002	14.92
20.984	4.2299	43.92	21.772	4.0787	42.78
22.519	3.9450	15.40	24.120	3.6867	14.83
24.414	3.6430	33.88	25.112	3.5433	4.54
26.250	3.3921	36.23	28.417	3.1382	11.38
29.473	3.0281	7.53	30.022	2.9740	5.74
30.881	2.8932	12.71	31.626	2.8268	9.03
31.920	2.8013	12.25	32.462	2.7558	4.69
33.565	2.6677	6.05	34.224	2.6168	5.81
34.620	2.5888	3.81	36.396	2.4665	4.54
36.999	2.4277	8.87	37.491	2.3969	5.10
37.797	2.3782	5.61	40.294	2.2364	5.81
41.110	2.1939	3.60	44.367	2.0401	25.37
44.848	2.0193	2.56	45.817	1.9788	3.36
47.086	1.9284	3.84	48.781	1.8653	4.14
50.101	1.8192	4.50	51.052	1.7875	2.32
52.238	1.7497	1.20	53.815	1.7021	2.78
55.227	1.6619	1.84	55.782	1.6466	0.91
64.744	1.4387	1.48	77.926	1.2250	1.63

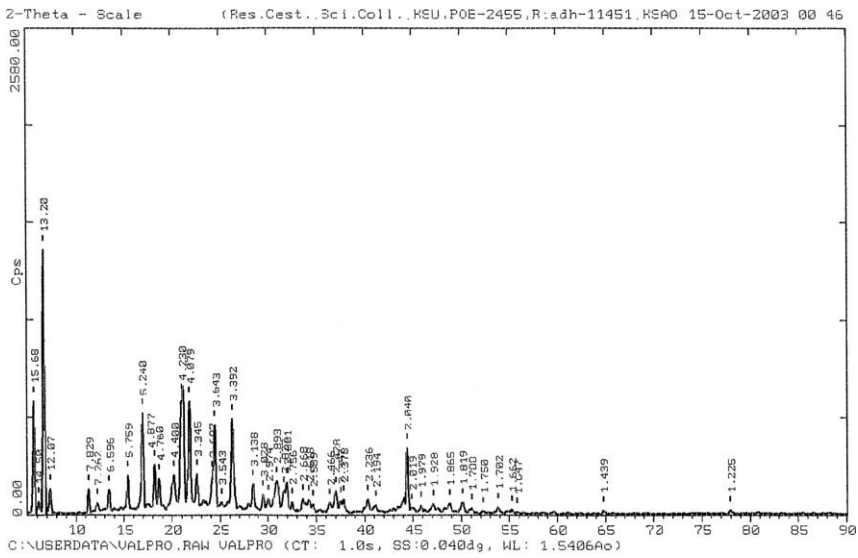

Fig. 1. X-ray powder diffraction pattern of sodium valproate.

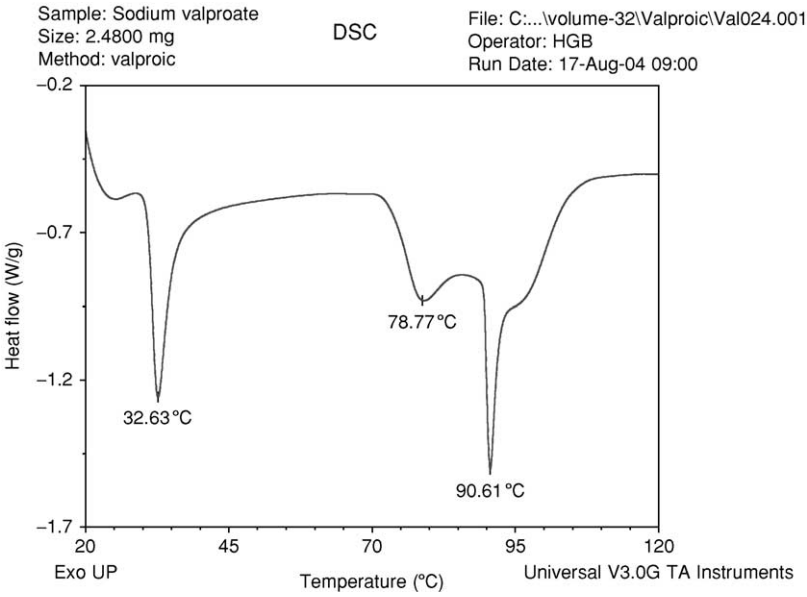

Fig. 2. Differential scanning calorimetry thermogram of sodium valproate.

2.6.2. Differential scanning calorimetry

Measurements of differential scanning calorimetry (DSC) were obtained on a TA Instruments 2910 thermal analysis system (Fig. 2). Samples of approximately 1–2 mg were accurately weighed into an aluminum DSC pan, and covered with an aluminum lid that was crimped in place. The samples were then heated over the range of 20–140 °C, at a heating rate of 10 °C/min. Valproic acid was found to boil at 227 °C.

2.7. Spectroscopy

2.7.1. Ultraviolet spectroscopy

The UV spectrum of valproic acid (0.1% solution) in methanol is shown in Fig. 3, was recorded using a Shimadzu UV–Visible Spectrophotometer 160 PC. The acid form of the drug has one maximum at 212 nm. In contrast, the sodium salt of the compound has no UV maximum between 800 and 205 nm, this in agreement with previous results reported by Chang [5].

λ_{max} (nm)	*A* (1%, 1 cm)	Molar absorptivity
212	732	105.6

2.7.2. Vibrational spectroscopy

The infrared absorption spectrum of sodium valproate and valproic acid were obtained in a KBr disc using a Perkin-Elmer infrared spectrophotometer. The infrared spectra of sodium valproate and valproic acid are shown in Figs. 4A and

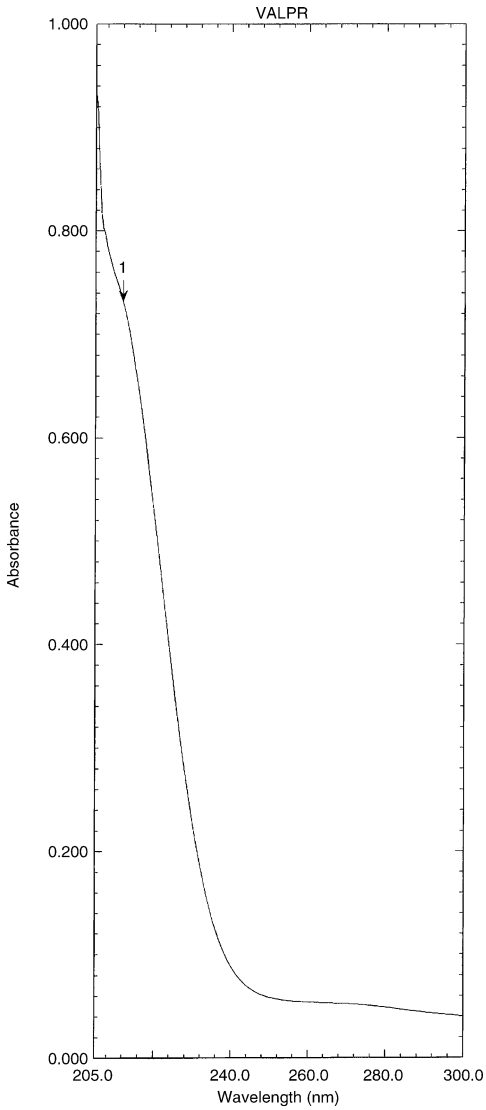

Fig. 3. The ultraviolet absorption spectrum of sodium valproate in water.

B, respectively. The infrared absorption bands assignments for sodium valproate and valproic acids are shown in Table 2(A) and (B), respectively.

2.7.3. Nuclear magnetic resonance spectrometry

2.7.3.1. ^{1}H NMR spectrum

The proton nuclear magnetic resonance (NMR) spectrum of valproic acid was obtained using a Bruker Avance Instrument operating at 300, 400, and 500 MHz. Standard Bruker Software was used to obtain COSY and HETCOR spectra. The

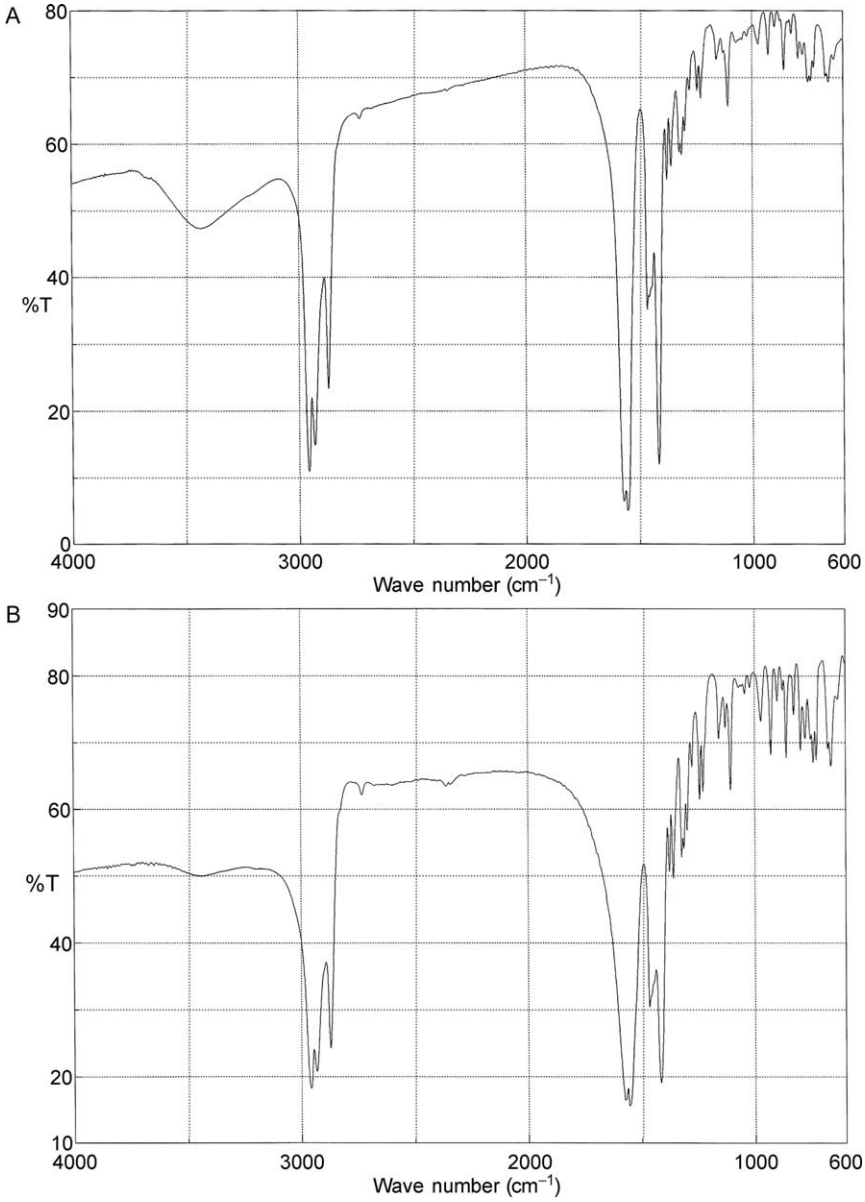

Fig. 4. (A) The infrared absorption spectrum of sodium valproate obtained in a KBr pellet. (B) The infrared absorption spectrum of valproic acid obtained in a KBr pellet.

sample was dissolved in D_2O and tetramethylsilane (TMS) was used as the internal standard. The proton NMR spectrum is shown in Figs. 5 and 6. The COSY ^{1}H-NMR spectra are shown in Figs. 7 and 8 and the gradient HMQC NMR spectrum is shown in Fig. 9. The assignments for the ^{1}H NMR spectral of valproic acid are shown in Table 3.

Table 2.

A. Assignments for the infrared absorption bands of sodium valproate

Frequency (cm^{-1})	Assignments
2960 2930 2870	Aliphatic C–H stretch
1565 1555 1465 1415	Antisymmetrical and symmetrical stretching vibration of COO^- group

B. Assignments for the infrared absorption bands of sodium valproate

Frequency (cm^{-1})	Assignments
3435	O–H stretching vibration of carboxylic acid
2965 2875	Aliphatic C–H stretch
1705	C=O stretch
1080	O–H bending vibration

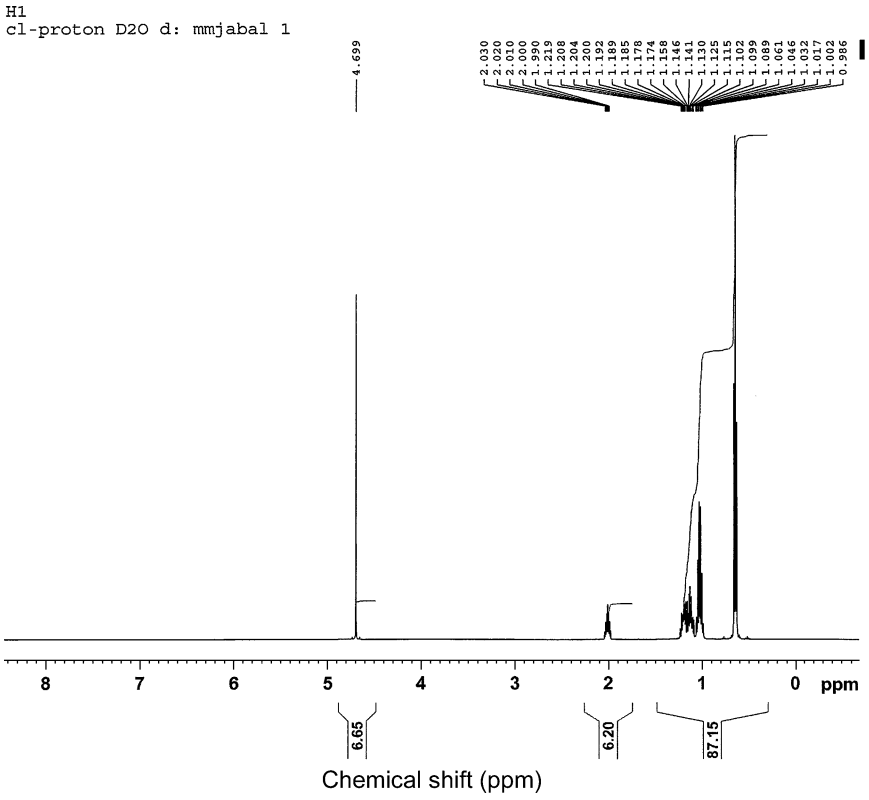

Fig. 5. The ^1H NMR spectrum of sodium valproate in D_2O.

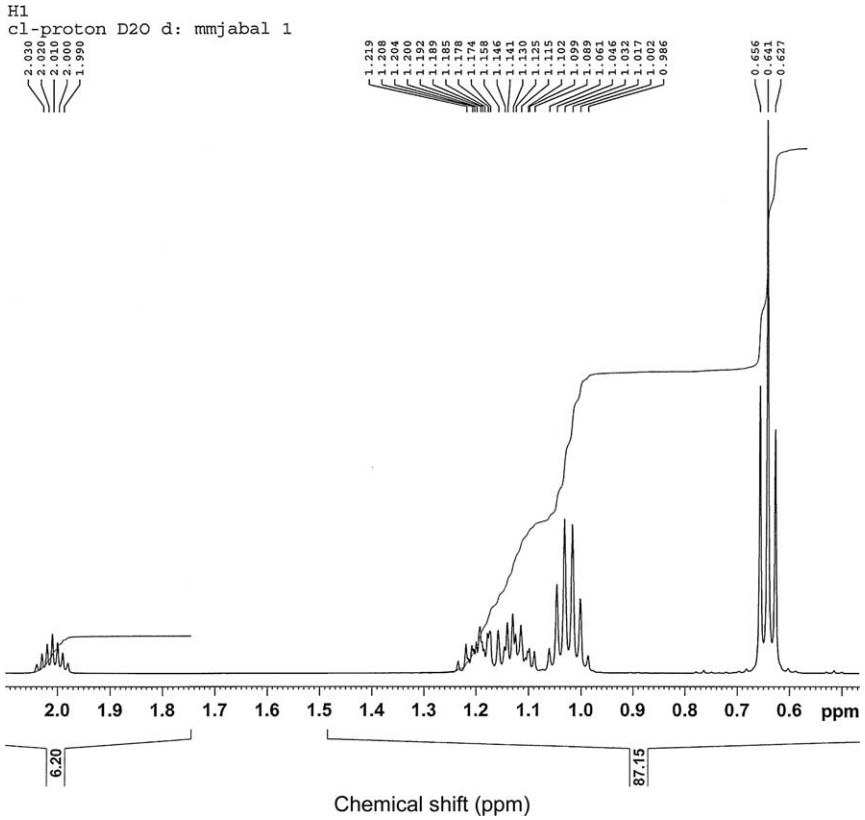

Fig. 6. Expanded ^{1}H NMR spectrum of sodium valproate in D_2O.

2.7.3.2. ^{13}C NMR spectrum

The ^{13}C NMR spectrum of valproic acid was obtained using a Bruker Avance Instrument operating at 75, 100, and 125 MHz. Standard Bruker Software was used to obtain DEPT spectra. The sample was dissolved in D_2O and tetramethylsilane (TMS) was used as the internal standard. The ^{13}C NMR spectrum of valproic acid is shown in Fig. 10. The DEPT NMR spectra are shown in Figs. 11 and 12. The assignments for the various carbons of valproic acid are presented in Table 4.

2.8. Mass spectrometry

The mass spectrum of valproic acid was obtained using a Shimadzu PQ–5000 mass spectrometer. The parent ion was collided with helium gas a carrier gas. Figure 13 shows the detailed mass fragmentation pattern. Table 5 shows the proposed mass fragmentation pattern of valproic acid.

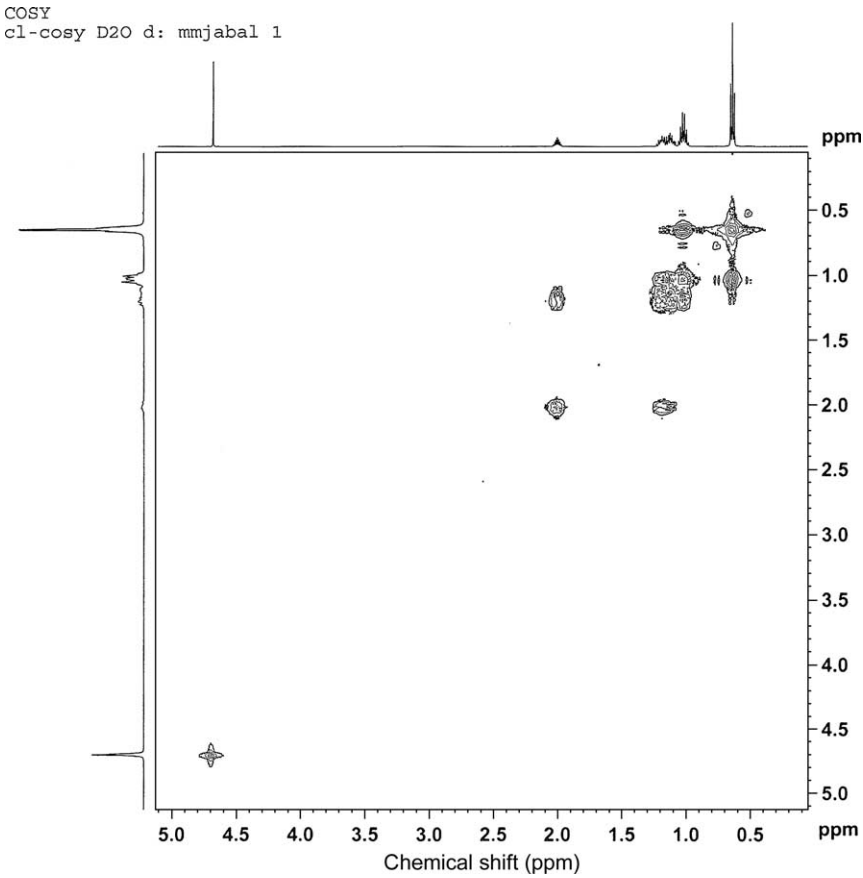

Fig. 7. COSY ^{1}H NMR spectrum of sodium valproate in D_2O.

3. STORAGE AND STABILITY

Valproic acid was found to be stable at room temperature [6]. The refrigeration or freezing of a supernatant, from blood samples containing the drug, for 7 days did not alter the total concentration of valproic acid [6,7]. Valproic acid should be stored in airtight glass, stainless steel, or polyethylene containers [3]. Valproic acid and sodium valproate should be stored in tight containers at a temperature less than 40 °C, preferably between 15 and 30 °C; freezing should be avoided [8]. Tablets and capsule should not be crushed [9].

4. COMPENDIAL METHODS OF ANALYSIS

4.1. Identification methods for the drug substance

4.1.1. Test A

Compare the refractive index of the substance to be examined with the refractive index of the reference standard of valproic acid, which has a known refractive index of 1.422–1.425 [10,11].

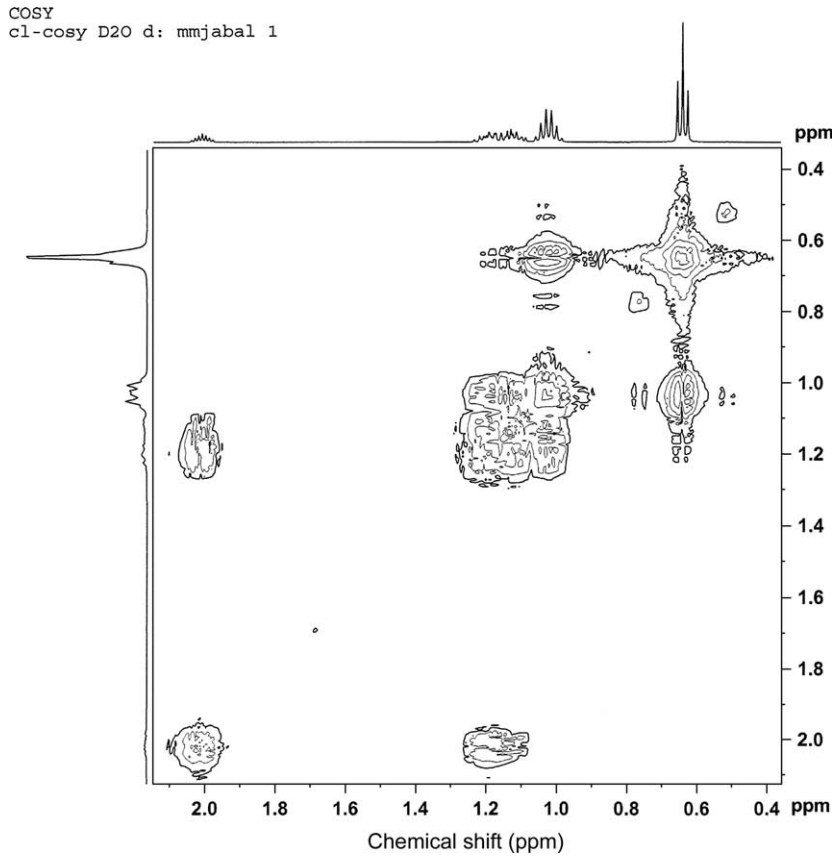

Fig. 8. COSY ^{1}H NMR spectrum of sodium valproate in D_2O.

4.1.2. Test B

Examine the test article by infrared absorption spectrophotometry, and compare with the spectrum obtained with a valproic acid reference standard [10,11].

4.1.3. Test C [10,11]

Examine by thin-layer chromatography (TLC) using a suitable TLC silica gel as the coating substance on the TLC plate. The method requires preparation of the following solutions:

Test solution. Dissolve 50 mg of the substance to be examined in methanol and dilute to 5 mL with the same solvent.

Reference solution. Dissolve 50 mg of valproic acid reference standard in methanol and dilute to 5.0 mL with the same solvent.

Apply separately to the plate 2.0 μL of each solution, and develop over a path of 15 cm using a mixture of equal volumes of ether and methylene chloride. Allow the plate to dry in air and spray with bromocresol green solution. The principal spot in

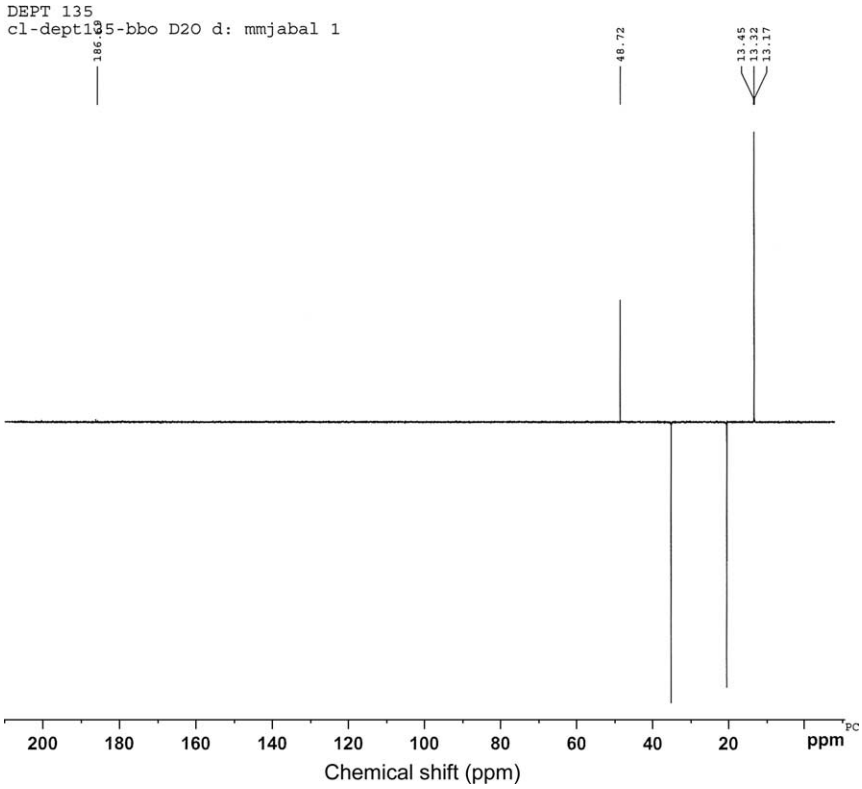

Fig. 9. Gradient HMQC NMR spectrum of sodium valproate in D_2O.

the chromatogram obtained with the test solution is similar in position, color, and size to the principal spot in the chromatogram obtained with the reference solution.

4.1.4. Test D

To 1.0 mL of the test solution, add 3.0 mL of dilute sodium hydroxide solution and 3.0 mL of water and 1.0 mL of a 100 g/L solution of cobalt nitrate. The test is positive if violet precipitate is formed. The precipitate dissolves in methylene chloride [10,11].

4.2. Identification methods for formulated valproic acid

The United States Pharmacopoeia [12] describes two tests for the identification of valproic acid in its formulations (capsules or syrup).

4.2.1. Test A

The retention time ratio of the valproic acid peak to the internal standard peak is obtained from the standard preparation and the assay preparations.

Table 3. Proton nuclear magnetic resonance assignments for spectrum of sodium valproate

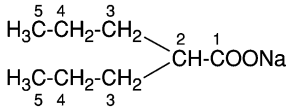

Assignment (proton at carbon #)	Chemical shift, δ, (ppm relative to TMS)	Multiplicity (J = Htz) t: triplet, q: quartet, m: multiplet
2	2.01	tt (5.0, 5.0)
3	1.16	m
4	1.02	tq (7.5, 7.5)
5	0.64	t (7.5)

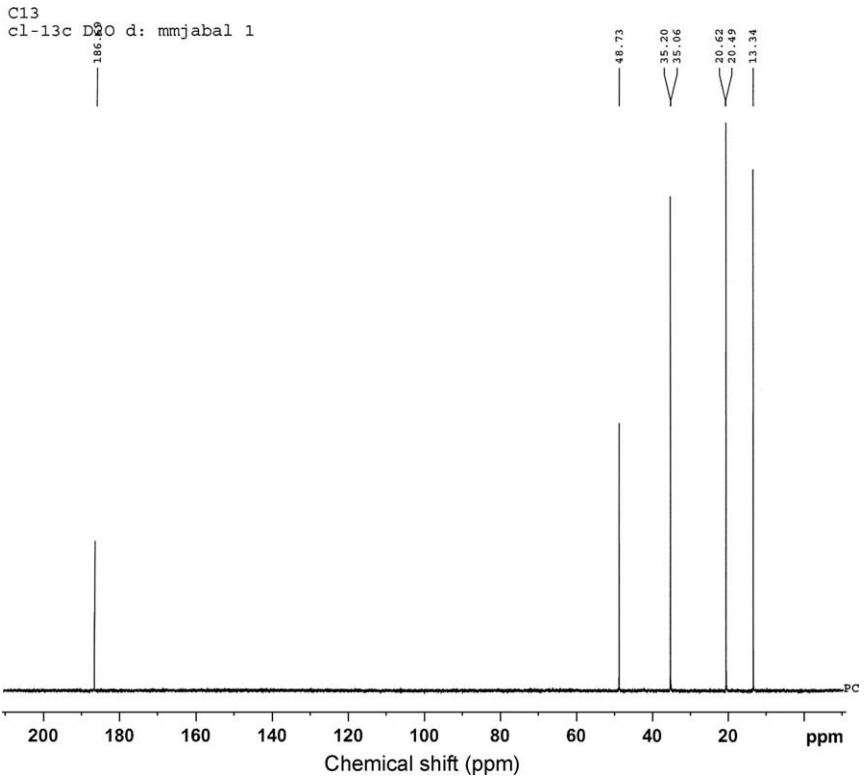

Fig. 10. ^{13}C NMR spectrum of sodium valproate in D_2O.

4.2.2. Test B

Place a portion of capsules contents or place a volume of syrup, equivalent to about 250 mg of valproic acid, in a separator. Add 20 mL of 1.0 M sodium hydroxide shake and allow the layers to separate. Transfer the aqueous layer to a second separator, add 4.0 mL of hydrochloric acid, mix, and extract with 40 mL *n*-heptane. Filter the *n*-heptane layer through glass wool into a beaker, and evaporate the

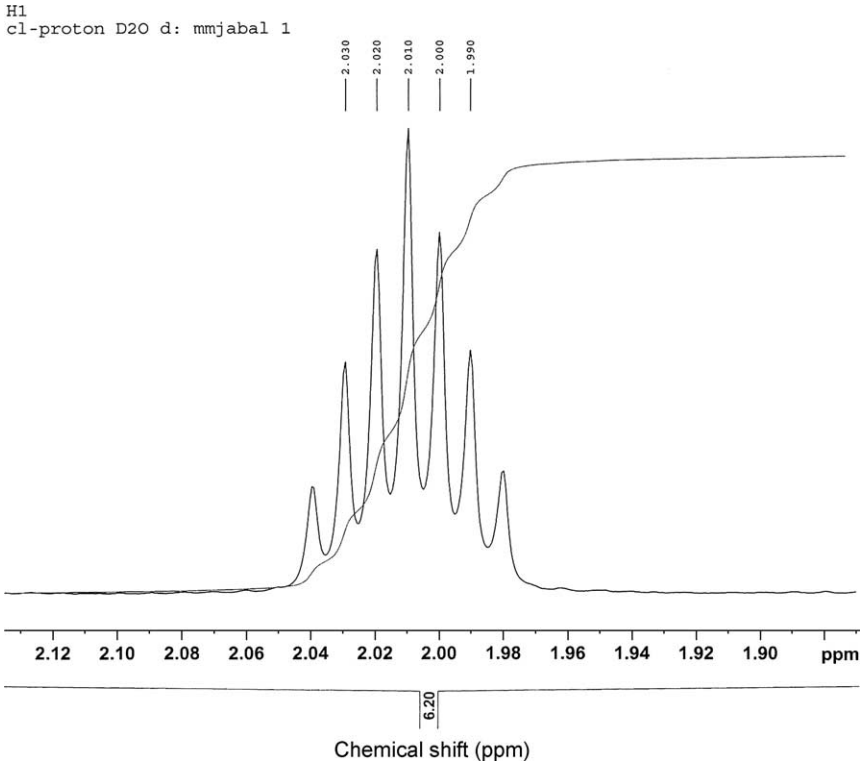

Fig. 11. DEPT 45 ^{1}H NMR spectrum of sodium valproate in D_2O.

solvent completely on a steam bath with the aid of a current air. Transfer two drops of the residue to a test tube containing 0.5 µL each of KI (1 in 5) solution and KIO_3 (1 in 25) and mix, a yellow color is predicted.

4.3. Methods for impurities and related substances

The European Pharmacopoeia [11] contains methods to determine ten impurities in valproic acid and sodium valproate:

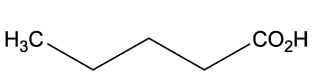

Pentanoic acid (valeric acid)

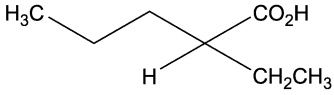

(2RS)-2-Ethylpentanoic acid

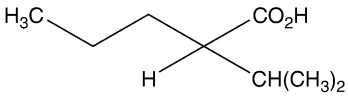

(2RS)-2-(1-Methylethyl) pentanoic acid

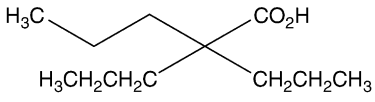

2, 2-Dipropylpentanoic acid

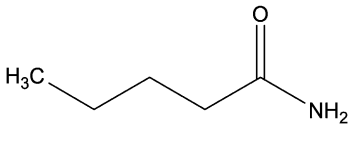

Pentamide (valeramide)

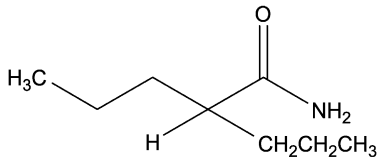

2-Propylpantanamide

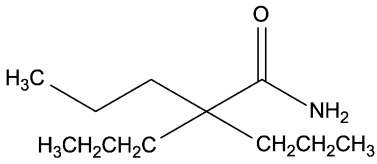

2, 2-Dipropylpantanamide

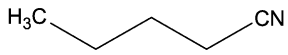

Pentanenitrile (valeronitrile)

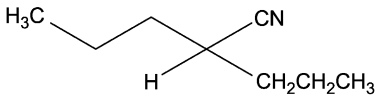

2-Propylpentanenitrile

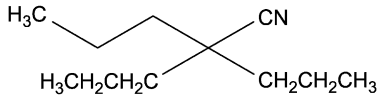

2, 2-Dipropylpentanenitrile

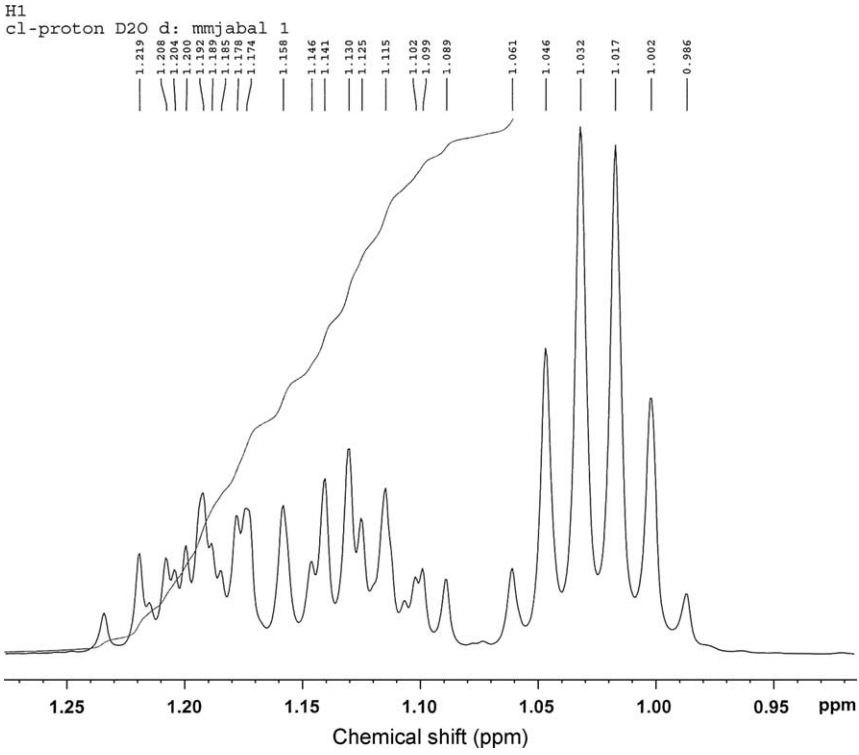

Fig. 12. DEPT 45 ^{1}H NMR spectrum of sodium valproate in D_2O.

Table 4. ^{13}C NMR assignments for sodium valproate

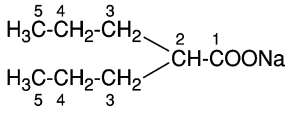

Assignments at carbon number	Chemical shift, δ,(ppm relative to TMS)
1	186.7
2	48.7
3	35.1
4	20.5
5	13.3

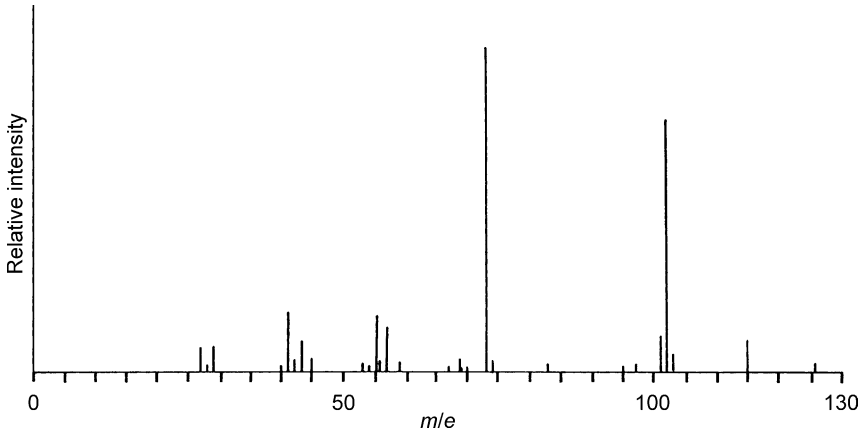

Fig. 13. Mass spectrum of sodium valproate.

Table 5. Assignments for the fragmentation pattern observed in the mass spectrum of sodium valproate

m/z	Fragment
145	$M + H^+$ mass peak (M^+)
126	$C_8H_{14}O$
102	$C_5H_{10}O_2$
73	$C_3H_5O_2$

The related substances are determined by gas chromatography (GC) using butyric acid as the internal standard, and the method requires preparation of the following three solutions.

Internal standard solution. Dissolve 10 mg of butyric acid in heptane and dilute to 200 mL with the same solvent.

Test solution. Dissolve 0.25 g of the substance to be examined in the internal standard solution and dilute to 5.0 mL with the same solvent. Dilute 1.0 mL of the solution to 10 mL with heptane.

Reference solution. Dissolve 20 mg of substance to be examined and 20 mg of 2-(1-medthyethyl)pentanoic acid in heptane and dilute to10 mL with the same solvent. Dilute 1.0 mL of the solution to 10 mL with heptane.

The chromatographic procedure [11] is carried out using a wide-bore fused-silica column 30 m long and 0.53 mm in internal diameter coated with macrogel 20 000 2-nitrotere-phthalate with film thickness of 0.5 μm. In addition, for chromatography, helium should be used as the carrier gas at a flow rate of 8.0 mL/min using a flame ionization detector.

The procedure is to inject 1.0 μL of each solution. The test is not valid unless, in the chromatogram obtained with reference solution, the resolution between the peaks corresponding to 2-(1-methylethyl) pentanoic acid and valproic acid is at least 2.0. In the chromatogram obtained with the test solution: the sum of the areas of the peaks, apart form the principal peak, is not greater than three times the area of the peak due to the internal standard (3.0%); none of the peaks, apart from the principal peak, has an area greater than that of the peak due to the internal standard (0.1%). Disregard any peak with an area less than 0.1 times that of the peak due to the internal standard.

4.4. Official methods of analysis

4.4.1. Raw material

The United States Pharmacopoeia [12] recommends the following assay method for valproic acid. Dissolve about 160 mg of valproic acid, accurately weighed, in 100 mL of acetone. Titrate the solution with tetrabutylammonium hydroxide titrant, taking precautions against the absorption of atmospheric carbon dioxide, determining the endpoint potentiometrically, using a glass electrode and a calomel electrode containing 0.1 M tetrabutylammonium chloride (aqueous). Perform a blank determination, and make any necessary correction. Each milliliter of 0.1 M tetrabutylammonium hydroxide titrant is equivalent to 14.42 mg of $C_8H_{16}O_2$.

The British Pharmacopoeia [10] and the European Pharmacopoeia [11] also recommend a potentiometric method for valproic acid. Dissolve 0.100 g in 25 mL of alcohol. Add 2 mL of water. Titrate with 0.1 M sodium hydroxide determining the endpoint potentiometrically. Each 1 mL of 0.1 M sodium hydroxide is equivalent to 14.42 mg of $C_8H_{16}O_2$.

4.4.2. Dosage forms

4.4.2.1. Capsules

The USP [12] recommends the following GC method.

Internal standard solution. Dissolve a quantity of biphenyl in *n*-heptane to obtain a solution having a concentration of about 5 mg/mL.

Standard solution. Dissolve an accurately weighed quantity of United States Pharmacopoeia valproic acid reference solution in *n*-heptane to obtain a solution having a known concentration of about 2.5 mg/mL. Transfer 5.0 mL to a container equipped with a closure. Add 2.0 mL of internal standard solution, close the container, and mix.

Assay preparation. Transfer not less than 20 Capsules to a blender jar or other container, and add about 150 mL of methylene chloride, and cool in a solid carbon dioxide–acetone mixture until the contents have solidified. If necessary, transfer the mixture of capsules and methylene chloride to a blender jar, and blend with high-speed blender until all the solids are reduced to fine particles. Transfer the mixture to a 500-mL volumetric flask, add *n*-heptane to volume, mix, and allow solids to settle. Transfer an accurately measured volume of this solution, equivalent to 250 mg of valproic acid, to a 100 mL volumetric flask, dilute with *n*-heptane to volume, and mix. Transfer 5.0 mL to a container equipped with a closure. Add 2.0 mL of the internal standard solution, close the container, and mix.

Chromatographic system. The gas chromatograph is equipped with a flamionization detector and a 2 mm × 1.8 m glass column packed with 10% phase G34 on 80- to 100-mesh support S1A. The column temperature is maintained at about 150 °C, and the injection port and the detector block temperatures are maintained at about 250 °C. Dry helium is used as the carrier gas at a flow rate of about 40 mL/min. Chromatograph the Standard preparation, measure the peak responses, and calculate the ratio, R_S, as directed for procedure: the relative retention times are about 0.5 for valproic acid and 1.0 for biphenyl; the resolution, R, between valproic acid and biphenyl is not less than 3.0; the relative standard deviation for replicate injections is not more than 2.0%.

Procedure. Separately inject about 2.0 µL each of the standard preparation and the assay preparation, record the chromatograms, and measure the peak responses, for valproic acid and biphenyl peaks. Calculate the quantity, in mg, of $C_8H_{16}O_2$ in the portion of capsules taken using the following formula:

$$100C\frac{R_U}{R_S}$$

in which C is the concentration, in mg/mL, of United States Pharmacopoeia valproic acid in the standard preparation, and R_U and R_S are the peak response ratios obtained from the assay preparation and standard preparation, respectively.

4.4.2.2. Syrup

The USP [12] recommends the following GC method.

Internal standard solution, standard preparation, and chromatographic system are prepared as directed in the assay under valproic acid capsules.

Assay preparation. Transfer an accurately measured volume of syrup, equivalent to about 250 mg of valproic acid, to a separator. Add 40 mL of water and 2.0 mL of hydrochloric acid not less than 20 capsules to a blender jar or other container, and add about 150 mL of methylene chloride, and cool in a solid

carbon dioxide–acetone mixture until the contents have solidified. If necessary, transfer the mixture of capsules and methylene chloride, mix, and extract gently with 80 mL of *n*-heptane until the aqueous layer is clear (about 3.0 min). Filter n-heptane layer through glass wool, collecting the filtrates in a 100 mL volumetric flask. Rinse the separator and the glass wool with small portions of *n*-heptane, add the risings to the flask, dilute with *n*-heptane to volume, and mix. Transfer 5.0 mL to a container equipped with a closure. Add 2.0 mL of the internal standard solution, close the container, and mix.

Procedure. Separately inject about 2.0 μL each of the standard preparation and the assay preparation, record the chromatograms, and measure the peak responses, for valproic acid and biphenyl peaks. Calculate the quantity, in mg, of $C_8H_{16}O_2$ in each mL of the syrup taken using the following formula:

$$100C\left(\frac{C}{V}\right)\left(\frac{R_U}{R_S}\right)$$

in which C is the concentration, in mg/mL, of USP valproic acid in the standard preparation, V is the volume, in mL, of syrup taken, and R_U and R_S are the peak response ratios obtained from the assay preparation and standard preparation, respectively.

5. REPORTED METHODS OF ANALYSIS

Most of the reported methods of analysis of valproic acid and its sodium salt in biological fluids rely on the use of chromatography, especially gas chromatography, although high performance liquid chromatography (HPLC) is also reported. Other methods, such as flow injection analysis, enzyme-immunoassay, fluorescence-polarization capillary electrophoresis, and potentiometry are sometimes used. The reported methods can be classified as follows.

5.1. Potentiometric method

Sodium valproate has been determined in pharmaceuticals using a valproate selective electrode [13,14]. The electroactive material was a valproate–methyl–tris (tetradecyl)ammonium ion-pair complex in decanol. Silver–silver chloride electrode was used as the reference electrode. The electrode life span was $\geq$1 month. Determination of 90–1500 μg/mL in aqueous solution by direct potentiometry gave an average recovery of 100.0% and a response time of 1 min.

5.2. Flow injection analysis

Three anticonvulsant drugs including valproic acid were determined using different dyes as ion-pair reagents. Gentian violet was used for the spectrophotometric detection at 588 nm and acridine orange for the fluorimetric detection at 470 nm after excitation at 297 nm. Calibration graphs were linear for 5–50 μg/mL 2.5 $\pm$ 0.50 μg/mL for the spectrophotometric and fluorimetric methods, respectively [15].

Valproic acid was determined in serum by flow injection analysis adopting automated fluoroimmunoassay method for the detection [16]. The serum was mixed with the reagents (β-galactosyl ambelliferone-drug conjugate and β-galactosidase-labeled antiserum). The mixture was heated at 30 °C for 16 min and then injected into the carrier reagent. Fluorescence was measured at 450 nm after excitation at 405 nm. The detection limit was 1 μg/L.

5.3. Nuclear magnetic resonance spectroscopy

Nuclear magnetic resonance spectroscopy was investigated as a method to screen for organic substances (and metabolites) in patients with indications of a drug overdose [17]. Urine specimens containing valproic acid were examined by ^{1}H-NMR spectroscopy at 300 MHz and the results compared with GC–MS.

5.4. Immunoassay methods

A competitive fluorescence-polarization immunoassay method was described for the monitoring of 12 drugs including valproic acid [18]. Samples (serum or plasma) were deproteinated. Fluorescence from the fluorescein-labeled analyte used as tracer was excited at 488 nm and polarization of light emitted at 531 nm was measured. The calibration was stable for 4 weeks and the coefficient of variation was below 10%. A single measurement took 8–10 min.

The chiral evaluation of five drugs including valproic acid using dry film multilayer technology was performed using immunoassay [19]. The test modules are coated multilayer film chips encased in plastic and contains all the reagents required. After loading into the analyzer, a rotor transports the modules to the pipetting station when plasma or serum samples are automatically pipetted into the test modules, fluorescence measurements are made after 6 min.

A microenzyme multiplied immunoassay technique was developed for antiepileptics including valproic acid [20]. The assay is performed in a total volume of 75 μL and uses only 3–5 μL of serum. A reagent containing a monoclonal drug antibody, the cofactor NAD and the enzyme substrate was added, followed by the drug and glucose-6-phosphate dehydrogenase. The rate of reduction of NAD to NADH was determined by measuring the absorbance at 340 nm at 3 and 4 min after addition of the conjugate. This rate was proportional to the concentration of the drug for 2–150 μg/mL.

Stamp *et al.* [21] studied the performance of fluorescence polarization immunoassay reagents for some drugs including valproic acid on a Cobas Fara II Analyzer. The method is comparable to the reference method. The calibration graphs are stable for at least 1 month. 6-Amino–2-propylhexanoic acid was used as a direct single reagent for valproic acid in serum [22]. The fluorescence polarization immunoassays were carried out at room temperature. Serum diluted in phosphate buffer of pH 7.5 containing sodium dodecyl sulphate (SDS). Triton X-100 and NH_3 was mixed with fluorescein-labeled valproic acid in buffer-anti valproic acid antiserum and after 10 min, fluorescence polarization was measured.

Five anticonvulsants including valproic acid were determined by the Abbott TD × fluorescence polarization immunoassay automatic analyzer. Recoveries were 94.8–106% and the coefficients of variations were 1.0–9.7% [23]. Fluorescence polarization immunoassay and enzyme immunoassay were compared for the determination of free valproic acid in serum [24]. Good correlation ($R = 0.9992$) was obtained between the two assays. Higgins [25] reported on the determination of valproic acid in serum by enzyme immunoassay with use of EMIT reagents and the Abbot ABA-200 analyzer. Responses were rectilinear up to 150 mg/L.

5.5. Capillary electrophoresis

Valproic acid has been determined in human serum using capillary electrophoresis and indirect laser induced fluorescence detection [26]. The extract is injected at 75 mbar for 0.05 min onto a capillary column (74.4 cm × 50 μm i.d., effective length 56.2 cm). The optimized buffer 2.5 mM borate/phosphate of pH 8.4 with 6 μL fluorescein to generate the background signal. Separation was carried out at 30 kV and indirect fluorescence detection was achieved at 488/529 nm. A linear calibration was found in the range 4.5–144 μg/mL ($0 = 0.9947$) and detection and quantitation limits were 0.9 and 3.0 μg/mL. Polonski *et al.* [27] described a capillary isotachephoresis method for sodium valproate in blood. The sample was injected into a column of an EKI 02 instrument for separation. The instrument incorporated a conductimetric detector. The mobile phase was 0.01 M histidine containing 0.1% methylhydroxycellulose at pH 5.5. The detection limit was 2 μg/mL.

5.6. Chromatographic methods

5.6.1. Thin-layer chromatography

Valproic acid was determined in plasma by treatment with 2,4-dibromoacetophenone or 2-bromoacetonapththalone and with dicyclohexano-18-crown-6 and heated at 70 °C for 40 min. The solution was subjected to TLC on C8F octyl plates or to high performance TLC on RP 8 254 S or Kieselgel 60 F_{254} plates with developing solvents of aq. 63% ethanol, aq. 73% ethanol or $CHCl_3$-cyclohexane (2:1), respectively, with detection at 280 or 254 nm for the naphthoylmethyl or phenacyl derivative, respectively. The limits of detection were 9.7 and 4.9 μg/mL of valproic acid for the TLC RP 8 and HPTLC RP 8 plates, respectively. Recovery was 84–92.74% [28].

5.6.2. Ion chromatography

Valproic acid was determined in tablets and plasma using ion-chromatography [29]. The extract was injected onto a column (6.5 cm × 6 mm) of Dionex ICE separator resin fitted with a guard column of Aminex cation exchange resin and operated with aq. 0.5 mM CO_2 as mobile phase (0.7 mL/min) and conductivity detection. For tablets, the calibration graph was rectilinear for 0.2–25 μg/mL with limit of detection of 50 μg/mL. For plasma, the response was linear for 50–200 μg/mL and limit of detection was 2 μg/mL.

5.6.3. *Micellar electrokinetic capillary chromatography*

Lee et al. [30] described a micellar electrokinetic capillary chromatographic method for the determination of some antiepileptics including valproic acid. They used a fused silica capillary column (72 cm × 50 μm) and SDS as the micellar phase and multiwavelength UV detection. Reaction conditions, such as pH and concentration of running buffer were optimized. Solutes were identified by characterizing the sample peak in terms of retention time and absorption spectra. Recoveries were 93–105%.

5.6.4. *High performance liquid chromatography*

Several HPLC methods have been described for the determination of valproic acid, either per se, in formulation or in biological fluids. These methods have been abridged in Table 6.

5.6.5. *Gas chromatography*

Valproic acid, like short chain fatty acids is volatile and therefore enormous methods have been recommended for its determination in dosage forms and biological fluids. These methods are shown in Table 7.

6. REPORTED METHODS OF ANALYSIS

6.1. Application and associated history

Valproic acid is the common name for 2-propylpentanoic acid (Epival; usually used as its sodium salt), also referred to as *n*-dipropylacetic acid, is a simple branched-chain carboxylic acid with unique anticonvulsant properties. Valproic acid was first synthesized in 1882 by Burton [75], but there was no known clinical use until its anticonvulsant activity was fortuitously discovered by Pierre Eymard in 1962 in the laboratory of G. Carraz, which was published by Meunier *et al.* in 1963 [76].

Valproic acid is an effective agent for control of both absence and primarily generalized tonic-clonic seizures. Valproic acid has recently been licensed for the treatment of diseases other than epilepsy, for example, manic episodes associated with bipolar disorder and migraine. By mouth, valproic acid should be initiated at 600 mg twice daily, preferably after food, increasing by 200 mg/day at 3-day intervals to a maximum. The maximum recommended dose of valproic acid is 60 mg/kg/day [77]. By intravenous injection or infusion same as oral route but the injection should be given over 3–5 min. In addition to acid form, the drug is available in several forms, including the sodium or magnesium salts and a combination of acidic form and its sodium salt (divalproex sodium) or an amide form (valpromide). For clinical used the drug is available in capsule, tablet, enteric-coated tablet, sprinkle-capsule, syrup, intravenous, suppository, and sustained-release formulations.

Several mechanisms have been suggested for the action of valproic acid, including blockade of voltage-dependent Na^+ channel, potentiation of γ-aminobutryric acid

Table 6. Reported HPLC method for valproic acid and sodium valproate

No.	Material	Column	Mobile phase	Flow rate	Detection	Reference
1	Rat liver	Micro Bondapka C_{18} ODS	16.9 mM sodium pyrophosphate (pH 6.9) containing 10–45% acetonitrile	3 mL/min	258 nm	[31]
2	Serum	YMC-Pak ODS-A (25 cm × 4.6 mm) 5 μm	Methanol–20 mM sodium acetate buffer of pH 3.5 (67:33)	1 mL/min	365/440 nm	[32]
3	Pharmaceutical preparations	3 μm Adsorpsphene (10 cm × 4.6 mm i.d.)	Methanol–acetonitrile–0.1 M sodium acetate buffer of pH 6.5 (11:4:5)	1 mL/min	Coulometric	[33]
4	Serum	5 μm Zorbax ODS (25 cm × 4.6 mm i.d.)	Aqueous H_2SO_4 at pH 4.2	0.8 mL/min	210 nm	[34]
5	Serum	5 μM Spherisorb C_{18} (15 cm × 4.6 mm i.d.)	Aqueous 73% methanol	0.9 mL/min	265 nm	[35]
6	Plasma	5 μm Vydac C_{18} (15 cm × 4.6 mm i.d.)	1 μg/mL Rhodamine 800 solution in methanol–H_2O (1:1) of pH 2.4	1 mL/min	674/700 nm	[36]
7	Plasma	5 μM Zorbax ODS (25 cm × 4.6 mm i.d.)	Acetonitrile–water–0.25 mM imidazole	1.2 mL/min	Chemiluminescence	[37]
8	Human plasma and serum	Pecosphere 3 × 3 CR C_{18} (3.3 cm × 4.6 mm i.d.)	Methanol–0.067 M KH_2PO_4 buffer of pH 5 (3:1)	1.5 mL/min	245 nm	[38]
9	Serum	5 μm Hypersil ODS (10 cm × 2.1 mm)	Aqueous 80% ethanol	0.3 mL/min	312/695 nm or 322 nm	[39]
10	Plasma or serum	Pecosphere 3 × 3 C_{18} 3 μm (3 cm × 4.6 mm)	Acetonitrile–0.03 M KH_2PO_4	Gradient elution	195 nm	[40]
11	Capsules	Hypersil RP-8, 5 μm (15 cm × 4.6 mm)	Aqueous 68% acetonitrile	1 mL/min	300/460 nm	[41]

12	Serum	Ultrosphere TM ODS (5 μm) 25 cm × 4.6 mm	Aqueous 80% methanol	1.5 mL/min	254 nm	[42]
13	Mouse brain	Superphase RP-18 (12.5 cm × 6 mm) 4 μm	Methanol–acetonitrile–water	1 mL/min	370/455 nm	[43]
14	Raw material	RP-8 (5 μm) 10 cm × 4.6 mm i.d.	Methanol–phosphate buffer pH 7 (3:7)	1 mL/min	355/460 nm	[44]
15	Human plasma	Microporasil 10 μm (30 cm × 3.9 mm)	Hexane–chloroform (47:3)	1.3 mL/min	254 nm	[45]
16	Blood, serum and brain	Chromospher ODS (20 cm × 3 mm) 5 μm	Acetonitrile–2.5 M formic acid (3:1)	0.4 mL/min	325/398 nm	[46]
17	Plasma	Lichroprep RP-8 5 to 20 μm	Methanol–water (4:1)	Gradient elution	330/395 nm	[47]
18	Serum	Shimpack CLC-ODS, 5 μm (15 cm × 6 mm)	Methanol–acetonitrile–H_2O (23:11:6)	1 mL/min	303/376 nm	[48]
19	Human plasma	Zorbax ODS (pH 5 μm (15 cm × 4.6 mm)	0.01 M NaH_2PO_4 (pH 1.3)–acetonitrile (63:37)	2.5 mL/min	210 nm	[49]
20	Plasma	LiChrosorb RP-18 (25 cm × 4 mm) 5 μm	Methanol–tetrahydrofuran–0.05 M phosphate buffer pH 5.9 (44:1:55)	1.1 mL/min	201 nm	[50]
21	Serum	Sil C_{18}, 5 μm	Aqueous acetonitrile	1 mL/min	245 nm	[51]
22	Dosage forms	Microsorb-MV C_{18} (25 cm × 4.6 mm i.d.) 5 μm	Acetonitrile–methanol–water (5:2:3)	2 mL/min	245 nm	[52]
23	Human plasma	RPC_{18} (25 cm × 4.6 mm) 5 μm	Acetonitrile–0.05 M phosphate buffer pH 3 (45:55)	4.2 mL/min	380 nm	[53]
24	Human plasma	RPC_{18} (25 cm × 4.6 mm) 5 μm	Acetonitrile–phosphate buffer pH 3 (45:55)	1.2 mL/min	380 nm	[54]

Table 7. Reported gas chromatographic methods for valproic acid

No.	Material	Column	Carrier gas	Detection	Parameter	Reference
1	Tears or plasma	DB5-MS capillary (30 m × 0.25 mm i.d.; 0.25 μm film)	H_2 (1.5 mL/min)	Electron capture negative CIMS	1–15 μg/mL and 1–20 μg/L in plasma and tears, LOD 20 μg/mL	[55]
2	Human plasma	Chromosorb W HP column packed with 1.5% OV 210 (2 m × 2 mm i.d.)	N_2 (43 mL/min)	FID	10–150 μg/mL, LOD 0.5 μg/mL	[56]
3	Blood, bile	0.5 μm column (15 m × 0.53 mm i.d.) coated with polyethyleneglycol operated at 14°C	H_2 (20 mL/min)	FID		[57]
4	Serum	0.5 μm Column (15 m × 0.53 mm i.d.) nitrophthalic acid bonded phase capillary	He, H_2, and air (20, 20, and 300 mL/min)	FID	Recovery 84–101%	[58]
5	Rat plasma	0.25 μm Column (15 m × 0.25 mm i.d.) coated with stabilwax-DA	H_2	FID	Range 0.1–1.0 μg/mL, LOD 0.1 μg/mL	[59]
6	Plasma of brain homogenate	0.35 μm column (30 m × 0.32 mm i.d.) coated with stabilwax	H_2 (45 cm/s)	ECD	1 pg to 100 ng	[60]
7	Brain tissue and serum	Fused silica column (30 × 0.75 mm i.d.) coated with DB 1701 (0.25 μm)	H_2 (1 mL/min)	EIMS	LOD 0.5 μg/mL	[61]
8	Plasma	Carbowax column (15 m × 0.53 mm i.d.) 1 μm operated at 190 °C	N_2 (8 μL/min)	FID	1–200 μg/mL, RSD 1.32–1.5%	[62]
9	Human plasma	GC column (30 m × 0.2 mm i.d.) coated with Nucol (0.25 μm)	Not given	FID	2–20μg/mL, limit of detection 1μg/mL, RSD 1.35%	[63]
10	Serum	Fused-silica capillary (25 m) coated with SB-11	H_2 (4 mL/min)	CIMS	25–5000 μg/mL, LOD 10 ng/mL, RSD 1.1–1.3%	[64]

11	Serum and urine of sheep	GC column (30 m × 0.25 mm i.d.) coated with DB-1701 (0.25 μm)		MS	0.01–4 μg/mL, LOD 3 ng/mL, RSD <10%	[65]
12	Serum	GC column (25 m × 0.2 mm i.d.) coated with HPI (0.33 μm)	H_2 (7.5 kPa)	SIM	LOD was in the low ng/mL, metabolite 100 ng/mL	[66]
13	Tablet	U-tube glass column (2 m × 3 mm i.d.) of Chromosorb AW-DMCS (80–100 mesh coated with 10% PEG-20 M plus 2% H_2PO_4	N_2 (50 mL/min)	FID	Range 2–4 μg/mL	[67]
14	Serum	GC column (25 m × 0.31 mm) coated with HP-5 (0.25 μm)	H_2	FID	LOD 51 pg, recovery >84%	[68]
15	Plasma	GC column (1.2 m × 4 mm)	N_2 (0.55 kg/cm^2)	FID	Range 5–150 mg/L, LOD 2 mg/L	[69]
16	Serum and urine	GC column (30 m × 0.53 mm) coated with DB 1701 (1 μm)	H_2 (20 mL/min)	EIMS	Range 1–120 μg/mL, coefficient of variation 8%, recovery 90%	[70]
17	Serum	GC column (30 m × 0.25 mm) coated with SPB 20	H_2	MS	Range 3.5–35 μg/mL	[71]
18	Serum	Fused silica column (25 m × 0.2 mm) coated with 5% phenylmethylsilicone germ phase HP-5 (0.33 μm)	N_2	FID	Range 0.01–0.1 μg/mL	[72]
19	Urine, saliva, serum	Bonded-phase column (25 m × 0.32 mm) of OV-1701 (0.25 μm)	H_2	Negative ion Cl–MS	The method determined and identified valproic acid and 15 of its metabolites	[73]
20	Serum	Steel column (1 m × 4 mm) of 3% of OV 17 on Gas-Chrom Q (80–100 mesh)	N_2 (50 mL/min)	FID	Range 2–12 μg/mL, recovery 97%, coefficient of variation 0.5%	[74]

(GABA) mechanisms, and blockade of glutamatergic mechanisms. Because epilepsy is a disease with multiple etiologies, these combinations of mechanisms explain the clinical efficacy of this drug in this disease [78].

6.2. Absorption and bioavailability

Valproic acid is rapidly absorbed after oral administration is provided using conventional formulations. It is found in serum, brain, cerebrospinal fluid (CSF), urine, saliva, breast milk, placenta, and fetal tissue in considerable levels. While on the contrary, it is almost completely bioavailable in human plasma. Hence valproic acid has a high degree of ionization at pH 7.4, it is much less lipid soluble than other anticonvulsant [79]. Twenty percent of the plasma drug is concentrated in the brain and CSF [80]. Placental transfer studies indicate that parent compound and some metabolites are present in cord blood in higher concentrations than in maternal blood [81]. The levels of the drug in fetal circulation and placental tissues were found to be 28 ± 4 and $7 \pm 3\%$ [82, 83]. Usually the levels of drugs in cord blood are equal or lower than that of maternal blood. Drug concentration in the breast milk was found to be only 3% of maternal plasma concentration [84]. Valproic acid is strongly bound to serum albumin (>92%) [85].

6.3. Metabolism

Valproic acid is predominantly cleared by biotransformation to give over 50 known metabolites that exert anticonvulsant activity [80]. Although valproic acid is a simple fatty acid, its metabolism is complex with a variety of overlapping phases I and II pathways. It undergoes metabolism by a variety of oxidation and conjugation processes, which result in formation of unsaturated and oxygenated fatty acid metabolites. Of the metabolites of valproic acid, the unsaturated compounds 4-en-valproic acid and trans-isomer of 2-en-valproic acid were 60–100% as potent as the parent drug. Other metabolites are less lipid-soluble than the parent compound; therefore, the brain concentrations of the metabolite are too low to produce any significant anticonvulsant activity [86]. However, they involve in the side effect and toxicity of valproic acid including neurotoxic and hepatic side effects [87,88]. In human, valproic acid is metabolized mainly by cytochrome P450 isoenzymes [89].

The following scheme summarizes the metabolic profile of valproic acid [84].

6.4. Excretion

The main rout of excretion of the drug and its metabolites is the kidney with a half-life of 9–18 h in human. In contrast to human, animal models have a lower elimination half-life ranging from 0.6–9 h [78]. The elimination half-life of valproic acid and some metabolites was found to be much longer in the neonates (40–50 h) than adult subjects (9–18 h) [78,81]. One study reported no difference between the elimination half-life between elderly and young subjects (15.4 and 13.0 h, respectively) while other found an increase in for older patients (14.9 versus 7.2 h for young patients) [78,90]. Insignificant amounts of valproic acid are found in breast milk, approximately 3% of maternal drug levels [84].

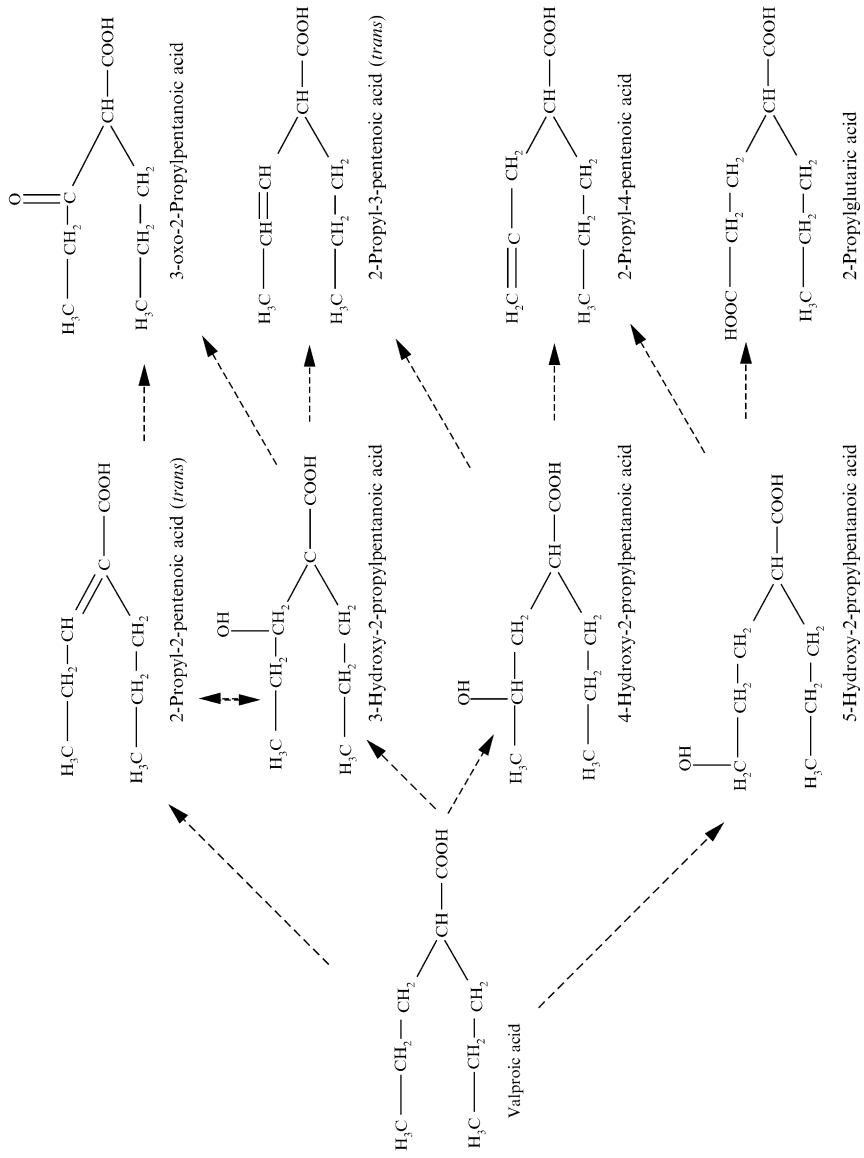
Valproic acid
2-Propyl-2-pentenoic acid (trans)
3-Hydroxy-2-propylpentanoic acid
3-oxo-2-Propylpentanoic acid
2-Propyl-3-pentenoic acid (trans)
4-Hydroxy-2-propylpentanoic acid
2-Propyl-4-pentenoic acid
5-Hydroxy-2-propylpentanoic acid
2-Propylglutaric acid

6.5. Distribution and protein binding

The drug is highly bound to albumin (approximately 90%) [91]. Protein binding is concentration dependent and decreases at high valproate concentration [91]. Free fraction plasma protein concentration increases from approximately 10% at 40 μg/mL to 18.5% at 130 μg/mL [91]. Protein binding decreased markedly in elderly [92], in patients with renal failure [92], and in liver diseases [93].

REFERENCES

[1] A. R. Gennaro (ed.), *Remington's: Pharmaceutical Sciences*, 18th edn., Mack Publishing Co., Pennsylvania, USA, 1990, p. 1079.
[2] S. Budavari (ed.), *The Merck Index*, 12th edn., Merck and Co., NJ, USA, 1996, p. 1961.
[3] S. C. Sweetman (ed.), *Martindale, The Complete Drug Reference*, 33rd edn., The Pharmaceutical Press, Chicago, USA, 2002, p. 366.
[4] Swiss Pharmaceutical Society (ed.), *Index Nominum 2000: International Drug Directory*, 17th edn., Medpharm Scientific Publishers, 2000, p. 1087.
[5] Z. L. Chang, *Anal. Prof. Drug Subs.*, 1979, **8**, 529.
[6] C. G. Tarasidis, W. R. Garnett, B. J. Kline, *et al.*, *Ther. Drug Monit.*, 1986, **8**, 373.
[7] M. W. Veerman, R. C. Hatton and M. E. Knight, *Clin. Pharmacy*, 1991, **10**, 282.
[8] G. K. McEvoy (ed.), *Drug Information*, 95th edn., American Society of Health-System Pharmacists, VA, USA, 1995, p. 1259.
[9] *Drugdex Drug Evaluations, Micromedex®, Healthcare Series*, Vol. **116**, Expires 6/2003.
[10] *British Pharmacopoeia*, Vol. I, 16th edn., HMSO Publication, Ltd., London 2000, CD.
[11] *European Pharmacopoeia*, 3rd edn., Supplement 13, Council of Europe, Strasbourg, 2001, p. 1578.
[12] *United States Pharmacopoeia*, 23rd edn., United States Pharmacopoeial Convention, Inc., Rockville, MD, USA, 2000, pp. 1619–1620.
[13] *The International Pharmacopoeia*, 3rd edn., World Health Organization, Geneva, 1994, p. 210.
[14] H. Suzuki, K. Akimot and H. Nakagawa, *Chem. Pharm. Bull.*, 1991, **39**, 133.
[15] J. T. Stewart, J. R. Lang and I. L. Hanigber, *J. Liq. Chromatogr.*, 1988, **11**, 3353.
[16] P. Allain, A. Turcant and A. Premel-Cabic, *Clin. Chem.*, 1989, **35**, 469.
[17] E. M. Komorski, R. A. Komoroski, J. L. Valentine, J. M. Pearce and G. L. Kearns, *J. Anal. Toxicol.*, 2002, **24**, 180.
[18] W. Ehrenthol, U. Schoenefeld, H. Gaul, H. Hente and A. Heubner, *Lab. Med.*, 1992, **15**, 453.
[19] M. A. Jandreski, J. C. Shah, J. Garbincius and E. W. Bermes, *J. Clin. Lab. Anal.*, 1991, **5**, 415.
[20] T. V. Tittle and B. A. Schaumann, *Ther. Drug Monit.*, 1992, **14**, 159.
[21] R. J. Stamp, G. P. Mould, C. Muller and A. Burlina, *Ther. Drug Monit.*, 1991, **13**, 518.
[22] A. M. Sidki, K. Staleg, H. Boyes, J. London and A. H. Williams, *J. Clin. Chem. Clin. Biochem.*, 1988, **26**, 69.
[23] S. T. Wang and F. Peter, *Clin. Chem.*, 1985, **31**, 493.
[24] D. Haidukewych, *Clin. Chem.*, 1985, **31**, 156.
[25] T. N. Higgins, *Clin. Biochem.*, 1983, **16**, 222.
[26] L. J. Jin, T. L. Wang and S. F. Y. L. Li, *Electrophoresis*, 1999, **20**, 1856.
[27] J. Polonski, T. Berzinkaiwoa, E. Gazzalowa and J. Volmut, *Zh. Anal. Khim.*, 1993, **48**, 569.
[28] P. Corti, A. Cenni, G. Corbini, E. Deassi, C. Murratzu and A. M. Caricchia, *J. Pharm. Biomed. Anal.*, 1990, **8**, 431.
[29] H. Itoh, Y. Shinbori and N. Tanura, *Bull. Chem. Soc. Jpn.*, 1986, **59**, 997.
[30] K. J. Lee, G. S. Heo, N. J. Kim and D. C. Moon, *J. Chromatogr.*, 1992, **608**, 243.
[31] M. F. B. Silva, J. P. N. Ruiter, L. Ljlst, P. Alers, H. J. ten-Brink, C. Jacobs, M. Duran, I. Tavares-de-Almeida and R. J. A. Wanders, *Anal. Biochem.*, 2001, **290**, 60.
[32] S. Hara, M. Kamura, K. Inoue, M. Fukuzawa, N. Dno and T. Kuroda, *Biol. Pharm. Bull.*, 1999, **22**, 975.

[33] E. Bonsquet, V. Cavrini, R. Gatti and A. Spadaro, *J. Liq. Chromatogr. Relat. Technol.*, 1998, **21**, 2837.
[34] H. Xiao and S. N. Zhang, *Sepu*, 1998, **16**, 365.
[35] R. X. Hao, C. P. Yan and Y. X. Liu, *Yaowu Fenxi Zazhi*, 1997, **17**, 172.
[36] S. V. Rahavendram and H. T. Kames, *Anal. Chem.*, 1996, **68**, 3763.
[37] B. W. Sandmann and M. L. Grayeski, *J. Chromatogr. B.*, 1994, **633**, 123.
[38] M. Monari, G. Sanchez, I. Cudiz, S. Mera and P. Castaneda, *G. Ital. Chim. Clin.*, 1992, **17**, 353.
[39] H. Liu, L. J. Forman, J. Montoya, C. Eggers, C. Barham and M. Delgado, *J. Chromatogr. Biomed. Appl.*, 1992, **114**, 163.
[40] C. Lucarelli, P. Villa, E. Lombaradi, P. Prandini and A. Brega, *Chromatographia*, 1992, **33**, 37.
[41] R. Gatti, V. Cavrini and P. Roveri, *Chromatographia*, 1992, **33**, 13.
[42] W. Liao, K. Zhu and X. Lu, *Yaowu Fenxi Zazhi*, 1999, **10**, 347.
[43] K. Matsuyama, C. Miyazki, T. Yamashita and M. Ichikawa, *Bunseki Kagaku*, 1989, **38**, T174.
[44] M. Kim and J. T. Stewart, *J. Liq. Chromatogr.*, 1990, **13**, 213.
[45] B. Gentile-de-Illiano and A. Quintana-de-Gainzarain, *J. High Resolut. Chromatogr. Commun.*, 1989, **12**, 540.
[46] J. H. Wolf, L. Veemma-Van-de-Duia and J. Korf, *J. Chromatogr. B*, 1989, **79**, 496.
[47] F. A. L. Van der-Horst, G. G. Eikelboom and J. J. M. Holthuis, *J. Chromatogr.*, 1988, **456**, 199.
[48] M. Nakajima, A. Sato and K. Shimada, *Anal. Sci.*, 1988, **4**, 385.
[49] L. J. Lovett, G. A. Nggard, G. R. Erdmann, C. Z. Burley and S. K. W. Khalil, *J. Liq. Chromatogr.*, 1987, **10**, 687.
[50] K. Kushida and T. Ishizki, *J. Chromatogr. B*, 1985, **39**, 131.
[51] M. Nakamura, K. Kendo, R. Nishioka and S. Mawai, *J. Chromatogr. B*, 1984, **35**, 450.
[52] S. V. Rahavendran and H. T. Kames, *Anal. Chem.*, 1996, **68**, 3763.
[53] P. Kishore, V. R. Kumar, V. Satyanarayana and D. R. Krishua, *Pharmazie*, 2003, **58**, 378.
[54] P. Kishore, V. R. Kumar, V. Satyanarayana and D. R. Krishua, *Pharmazie*, 2003, **56**, 378.
[55] M. Nakajima, S. Yamato, K. Shimada, S. Sato, S. Kitagawa, A. Honda, J. Miyamato, J. Shoda, M. Okya and H. Miyazaki, *Ther. Drug Monit.*, 2000, **22**, 716.
[56] A. Kebriaeizadeh, M. Valaie and A. Zarghi, *Pharm. Pharmacol. Comm.*, 1998, **4**, 525.
[57] A. Poklis, J. L. Poklis, D. Trautman, C. Treece, R. Backer and C. M. Harvey, *J. Anal. Toxicol.*, 1998, **22**, 537.
[58] A. S. Wohler and A. Poklis, *J. Anal. Toxicol.*, 1997, **21**, 306.
[59] A. Carlin and J. Sommons, *J. Chromatogr.*, 1997, **694**, 115.
[60] R. L. Dills and D. D. Shen, *J. Chromatogr.*, 1997, **690**, 139.
[61] J. Darius, *J. Chromatogr.*, 1996, **682**, 67.
[62] H. Y. Ju and M. C. Shih, *Ther. Drug Monit.*, 1996, **18**, 107.
[63] M. Krogh, K. Johansen, F. Tonnesen and K. E. Rasmussen, *J. Chromatogr.*, 1995, **673**, 299.
[64] F. Susanto and H. Reinauer, *Chromatographia*, 1995, **41**, 407.
[65] D. C. Yu, J. D. Gordon, J. J. Zheng, S. K. Panesur, K. W. Riggs, D. W. Rurak and F. S. Abbott, *J. Chromatogr. B*, 1995, **666**, 269.
[66] J. Darius and F. P. Mayer, *J. Chromatogr. B*, 1994, **656**, 343.
[67] R. Zhang, X. Wang and W. Wei, *Yaowu-Fenxi-Zazhi.*, 1993, **13**, 338.
[68] J. Volmut, M. Melnik and E. Matisova, *J. High Resolut. Chromatogr.*, 1993, **16**, 27.
[69] M. Pokrajac, B. Miljkovic, D. Spiridonovic and V. M. Varagic, *Pharm. Acta Helgv.*, 1992, **67**, 237.
[70] E. Fisher, W. Wittfolt and H. Nau, *Biomed. Chromatogr.*, 1992, **6**, 24.
[71] E. Gaetani, C. F. Laureri and M. Vitto, *J. Pharm. Biomed. Anal.*, 1992, **10**, 143.
[72] J. Volmut, E. Matisova and Thi-Ha Pharm, *J. Chromatogr. B*, 1990, **92**, 428.
[73] K. Kassahun, R. Burton and F. S. Abbott, *Biomed. Environ. Mass Spectrom.*, 1989, **18**, 918.
[74] J. Al-Zehouri and W. Schmollack, *Pharm. Chem. Pharm. Bull Mazie*, 1989, **44**, 493.
[75] B. S. Burton, *Am. Chem. J.*, 1882, **3**, 385.
[76] H. Meunier, G. Carraz and Y. Meunier, *Therapie.*, 1963, **18**, 435.
[77] M. A. Koda-Kimble, and L. Y. Young (eds.) *Applied Therapeutics, The Clinical Use Of Drugs*, 7th edn., Vancouver, Washington, DC, 2001.
[78] W. Löscher, *Prog. Neurobiol.*, 1999, **58**, 31.
[79] W. Löscher and H. H. Frey, *Epilepsia*, 1984, **25**, 346.

[80] R. H. Levy, R. H. Matson and B. S. Meldrum (eds.), *Antiepileptic Drugs*, 4th edn., Raven Press, New York, 1995, pp. 605–619.
[81] H. Nau, W. Wittfoht, D. Rating, *et al*. (eds.), *Epilepsy, Pregnancy and the Child*, Raven Press, New York, 1981, pp. 131–139.
[82] M. M. Barzago, A. Bortolotti and F. F. Stellari, *J. Pharmacol. Exp. Ther.*, 1996, **277**, 79.
[83] D. W. Fowler, M. J. Eadie and R. G. Dickinson, *J. Pharmacol. Exp. Ther.*, 1989, **249**, 318.
[84] H. Nau and W. Wittfoht, *J. Chromatog.*, 1981, **226**, 69.
[85] N. Fukuoka, T. Tsukamoto, J. Kimura, *et al*., *Jpn. J. Hosp. Pharm.*, 1998, **24**, 652.
[86] W. Löscher, *Arch. Int. Pharmacodyn. Ther.*, 1981, **249**, 158.
[87] R. H. Lavey, and J. K. Penny (eds.), *Idiosyncratic Reactions to Valproate: Clinical Risk Patterns and Mechanism of Toxicity*, Raven Press, New York, 1991, pp. 19–24.
[88] T. Baillie, *Pharm. Weekbl. Sci.*, 1992, **14**, 122.
[89] M. R. Anari, R. W. Burton, S. Gopaul, *et al*., *J. Chromatog. B*, 2000, **742**, 217.
[90] J. L. Stephen, *Drug Aging*, 2003, **20**, 141.
[91] J. Hardman, A. Gilman and A. G. Limbird (eds.) *Goodman and Gilman's The Pharmacological Basis of Therapeutics*, 9th edn., McGraw-Hill, New York, NY, 1996.
[92] U. Klotz, T. Rapp and W. A. Muller, *Eur. J. Clin. Pharmacol.*, 1978, **13**, 55–60.
[93] O. Lapierre, *Can. J. Psychiatry*, 1999, **44**, 188.

Validation of Chromatographic Methods of Analysis

Mochammad Yuwono and Gunawan Indrayanto

Assessment Service Unit, Faculty of Pharmacy, Airlangga University, Surabaya 60283, Indonesia

Contents

1. INTRODUCTION

According to USP 28 [1], validation of an analytical method is the process by which it is established, through the conduct of laboratory studies, that the performance characteristics of the method meet the requirements for the intended analytical applications. Therefore, validation is an important step in determining the reliability and reproducibility of the method because it is able to confirm that the intended method is suitable to be conducted on a particular system.

The necessity for validation in analytical laboratories is derived from regulations such as the current Good Manufacturing Practices (cGMP), Good Laboratory Practices (GLP), and the Good Clinical Practices (GCP). Other regulatory requirements are found in quality and accreditation standards such as the International Standards Organization (ISO) 9000 series, ISO 17025, the European Norm (EN 45001), United States Pharmacopoeia (USP), Food and Drug Administration (FDA) and Environmental Protection Agency (EPA) [2, 3]. The reliability of analytical data is critically dependent on three factors, namely the reliability of the instruments, the validity of the methods, and the proper training of the analysts [4].

As stated by IUPAC [5], a validation method can be differentiated into categories of '*fully validated*' and '*single-laboratory method*' validation. A fully validated

PROFILES OF DRUG SUBSTANCES, EXCIPIENTS, AND RELATED METHODOLOGY, VOLUME 32
ISSN: 0099-5428

DOI: 10.1016/S0099-5428(05)32009-0

method is one where the characteristics of that method were evaluated by multiple laboratories through a collaborative trial. The use of a single-laboratory method is appropriate when ensuring the viability of the method before a formal inter-laboratory study is conduct, ensuring that an '*off-the-shelf*' validated method is used correctly, and when a formal collaborative trial is not practical or not feasible.

Analytical procedures are classified as being compendial or non-compendial in character. Compendial methods are considered to be valid, but their suitability should be verified under actual conditions of use. To do so, one verifies several analytical performance parameters, such as the selectivity/specificity of the method, the stability of the sample solutions, and evaluations of intermediate precision.

For non-compendial procedures, the performance parameters that should be determined in validation studies include specificity/selectivity, linearity, accuracy, precision (repeatability and intermediate precision), detection limit (DL), quantitation limit (QL), range, ruggedness, and robustness [6]. Other method validation information, such as the stability of analytical sample preparations, degradation/stress studies, legible reproductions of representative instrumental output, identification and characterization of possible impurities, should be included [7]. The parameters that are required to be validated depend on the type of analyses, so therefore different test methods require different validation schemes.

The most common types of analyses are the identification test, the quantitative determination of active ingredients or major component, and the determination of impurities. The *identification test* provides data on the identity of the compound or compounds present in a sample. A negative result signifies that the concentration of the compound(s) in sample is below the DL of the analyte(s). The *quantitative method for the major component* provides data of the exact quantity of the major component (or active ingredients) in the sample, and a reported concentration of the major component must be higher than the QL. In a *Determination of impurities* test, one obtains data regarding the impurity profile of a sample, and can be divided into a limit test or quantitative reporting of impurities (see Table 1, which has been modified from Refs. [1] and [8]).

Besides the general validation parameters mentioned above, the software and hardware of all chromatography instrumentation (HPLC, GC, and TLC) should also be validated first. The validation of the instrument (a procedure known as instrument qualification) is divided into design qualification (DQ), installation qualification (IQ), operation qualification (OQ), and performance qualification (PQ) [2, 3]. The chromatography system should also be evaluated as to whether the equipment can provide data having acceptable quality, or in other words, that performance of a System Suitable Test (SST) yielded acceptable data. The relative standard deviation (RSD) associated with the repeatability of the retention time (Rt) should be less than or equal to 1% (for $n = 5$), the tailing factor (T) should be less than or equal to 2, the resolution (Rs) should be greater than 2, the number of theoretical plates (N) should be greater than 2000, and the capacity factor should be greater than 2.0 [8]. For a TLC method, the retention factor (Rf) should be 0.1–0.3 $\leq$ Rf $\leq$ 0.8–0.9, the tailing factor should be $0.9 \leq T \leq 1.1$ and the resolution should be greater than or equal to 1.0 [9, 10].

Table 1. Data elements required for analytical method validation [1, 8]

Type of analytical procedure	Assay		Impurity testing				Performance characteristics		Identification	
			Quantitative		Limit tests					
Parameter	USP	ICH	USP	ICH	USP	ICH	USP	ICH	USP	ICH
Accuracy	Yes	Yes	Yes	Yes	*	No	*	N/A	No	No
Precision	Yes	N/A	Yes	N/A	No	N/A	Yes	N/A	No	N/A
Repeatability	N/A	Yes	N/A	Yes	N/A	No	N/A	N/A	N/A	No
Interim precision	N/A	Yes	N/A	Yes	N/A	No	N/A	N/A	N/A	No
Specificity	Yes	Yes	Yes	Yes	Yes	Yes	*	N/A	Yes	Yes
DL	No	No	No	No	Yes	No	*	N/A	No	No
QL	No	No	Yes	Yes	No	No	*	N/A	No	No
Linearity	Yes	Yes	Yes	Yes	No	No	*	N/A	No	No
Range	Yes	Yes	Yes	Yes	*	No	*	N/A	No	No

* May be required, depending on the nature of the specific test.
N/A: not available.

A very important prevalidation method requirement concerns the stability of the standards and samples, which obviously must exhibit sufficient stability for the time frames of the analyses. The acceptable criterion is that both standard(s) and sample(s) solutions should be stable within 2% for 24 h. The aged mobile phase should also give the same values of Rs, T, and N when compared to fresh mobile phase, and in addition, the results of analyses are within $\pm 2\%$ [8].

Before performing a validation method for a certain application, the scope of the method and its validation criteria should be defined first. The parameters to be investigated include compounds, matrices, types of formation, qualitative or quantitative method, detection or quantitation limit, linear range, precision and accuracy, types of equipment that will be used, and the location of the system. These steps of the validation method are illustrated in Fig. 1, which has been modified from Ref. [11].

2. SELECTIVITY AND SPECIFICITY

In the common vernacular, the terms specificity and selectivity are often interchangeably used. More properly, a method is said to be 'specific' if it provides a response for only a single analyte, while the term 'selective' means that the method provides responses for a number of chemical entities that may be distinguished from each other. Selectivity also implies the ability to separate the analyte from degradation products, metabolites, and coadministrated drugs [12]. USP 28 [1] defines 'specificity' as the ability to assess the analyte unequivocally in the presence of other components such as impurities, degradation products, and the matrix. IUPAC and AOAC have preferred the use of the term 'selectivity' than 'specificity' for methods that are completely selective, while USP, ICH, and FDA used the term 'specificity'. Due to the very number of limited methods that respond to only one analyte, the term 'selectivity' is usually more suitable, and this usage will be used in this work.

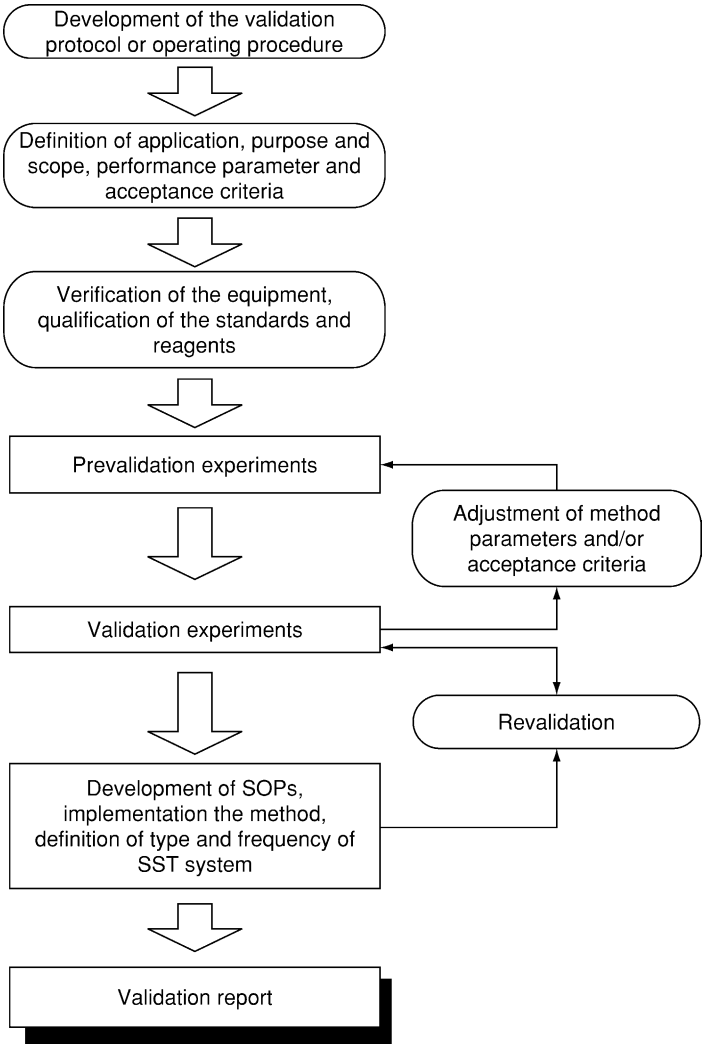

Fig. 1. Steps taken during the validation of an analysis method.

In chromatography techniques, selectivity can be proved by the existence of good separation between the analyte and the other components (such as the matrix, impurities, degradation product(s), and metabolites). A consequence of this requirement is that the resolution of the analyte from the other components should be more than 1.5–2.0. In order to detect the possibility of coelution of other substance(s), the purity of the analyte peak should also be determined. For instance, the UV–Vis spectrum of the analyte peak/spot can be used to determine '*the purity*' of the analyte peak/spot, in this case the *correlation coefficient* '*r*' (this term is used by the software of DAD System Manager Hitachi, and CATS from Camag). With the same meaning and mathematical equation, other terms are used, such as *Match*

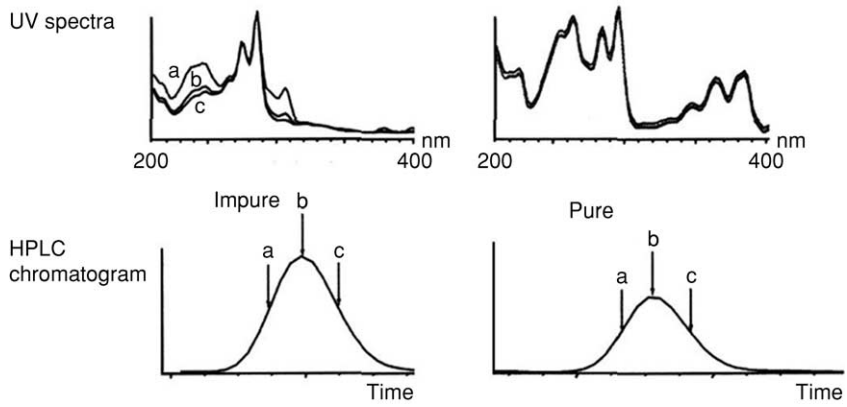

Fig. 2. Schematic of peak purity determination by using the upslope, top, and downslope methods.

Factor 'MF' (Agilent ChemStation), or *Similarity Index* 'SI' (Shimadzu Class-VP, Chromatography Data System or Shimadzu/LCsolution).

A representative example of this process is shown in Fig. 2. The spectra of the analyte peaks can be measured at the upslope, the top, and at the downslope, or the whole spectrum of the chromatography peak can be compared. In the latter case, the term '*total peak purity*' is used, and a '*purity curve*' of the peak can also be recorded. These operations can be performed by a HPLC system equipped with a DAD detector [13], or for TLC a densitometer that can measure the UV–Vis spectrum of the analyte spot should be used. If the value of the purity is 0.000–0.8900, it is not pure, and a purity of 0.9000–0.9500 means that the peak is contaminated (Shimadzu Class-VP, Chromatography Data System).

For determining peak identity, the whole spectral data of the standard and the analyte should be compared, and the value of r or MF or SI can be calculated using the software of the HPLC/densitometer equipment as described above.

If the laboratory does not have a diode-array detector, the purity of the HPLC peak can also be demonstrated by calculating of the tailing factor at different wavelengths. The HPLC peak can be assumed to be pure, if the tailing factors of the peaks calculated at various wavelengths (at least five being used) are identical. The ratio of signals acquired at two different wavelengths can also be used for proving the purity of the HPLC peak (see Fig. 3). Ebel [14] proposed using the peak width at half-height method and symmetry factor for determining the purity of the HPLC peak. Although the spectral data of the analyte peak and a standard peak might be identical, for some reasons the analyte peak may still be impure. This can happen when the impurity has very similar spectrum to the analyte, is present at much lower concentration, or is characterized by the same peak profile as the analyte [13].

The most discriminating technique for proving the identity and purity of analyte peak of a chromatogram, especially for analyzing biological samples and natural products, is by using online LC–UV/MS or GC–MS/FTIR methods [15]. Alternatively, one could use a combination of TLC and MS, where direct determination on the TLC plates is made by matrix-assisted laser desorption ionization mass spectrometry (MALDI MS) [16].

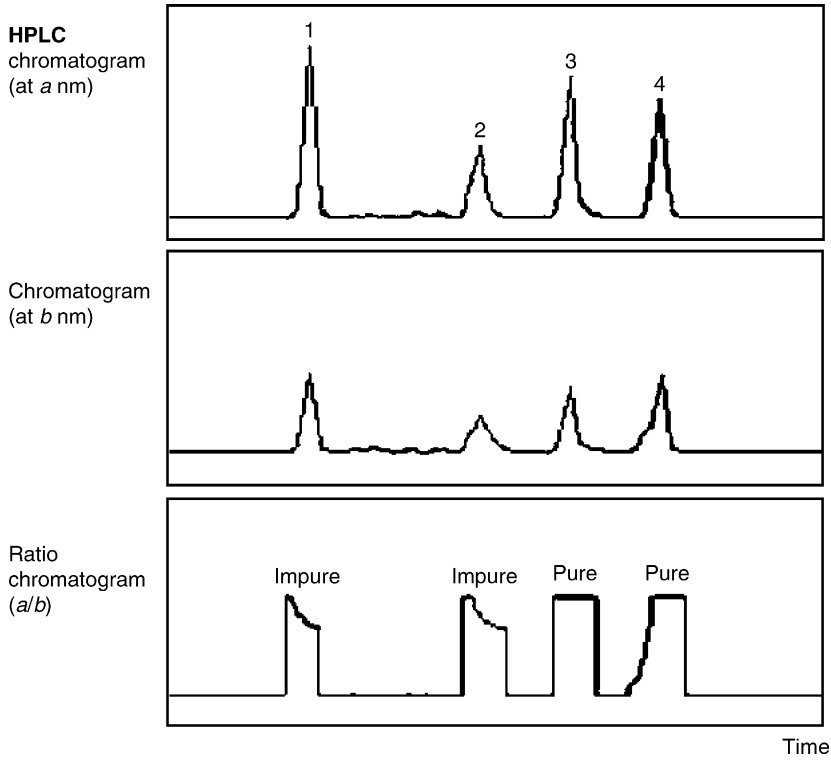

Fig. 3. Schematic of peak purity determination by using the ratio-plot method.

For developing a method of analysis in a Quality Control laboratory, the selectivity can be easily proved by injecting or spotting the standard, blank sample, possible impurities, or degradation product(s) in the chromatography system. In the proposed system, the analyte peak/spot should not be interfered with by other peaks, which can be proved by calculating the resolution. The purity and identity of the analyte peak can be proved by comparing to the standard. Orr *et al.* [17] recommended using a LC–MS system to evaluate the selectivity of the method for impurity testing.

If no references for the degradation products or impurities are available in the laboratory, the sample should be exposed to stress conditions such as heat (50–80 °C), ultraviolet light (2000 lux), acid and base (0.1–1 M HCl and NaOH), and oxidant (3% H_2O_2). After incubation in the allotted time, the purity and identity of the analyte peak/spot should be proved by using DAD or MS detection (for LC), MS (for GC), or *in situ* UV–Vis measurement using a densitometry or TLC-MALDI MS (for TLC).

In a bioanalytical method, analyses of blank samples (plasma, urine, or other matrix) should be obtained from at least six sources. Each blank sample should be tested for the possible interference of endogenous substances, metabolites, or degradation products. The response of the peaks interfering at the retention time of the analyte should be less than 20% of the response of a lower quantitation limit standard, and should be less than 5% of the response of the internal standard that was used [18, 19]. For dissolution studies, the dissolution media or excipients should not give a peak or spot that has an identical Rt or Rf value with the analyte [20].

Due to the possible change in retention time and peak profile that may take place during day-to-day operation, it is necessary to measure peak characteristics every day to verify the status of the method validation. A blank sample should be evaluated for an analysis run, where the resolution is determined. For asymmetric peaks, the Gaussian equation cannot be used, so the modified equation, using an exponentially modified Gaussian (EMG) method has been proposed [21].

3. LINEARITY

The linearity of a method is defined as its ability to provide measurement results that are directly proportional to the concentration of the analyte, or are directly proportional after some type of mathematical transformation. Linearity is usually documented as the ordinary least squares (OLS) curve, or simply as the linear regression curve, of the measured instrumental responses (either peak area or height) as a function of increasing analyte concentration [22, 23]. The use of peak areas is preferred as compared to the use of peak heights for making the calibration curve [24].

The linearity of the detector can be obtained by diluting the analyte stock solution and measuring the associated responses, while the linearity of the analytical method can be determined by making a series of concentrations of the analyte from independent sample preparations (weighing and spiking) [15]. It is also essential that the basic calibration linear curve be obtained by using independent samples, and not by using samples that have been prepared by dilution and injected into HPLC/GC, or spotted on one TLC plate.

The linearity range to be tested depends on the purpose of the test method, and is usually ±20% of the target concentration. Alternatively, a range can be validated from the QL to 150% of the target concentration. For impurity methods, the range would be +20% of the target concentration down to its lower limit of quantitation (QL), and for uniformity assays the range would be ±30% of the target concentration. For degradation studies, the range should be 0–2% of the expected concentration. For dissolution studies, the range should be 20% below to 20% above the specified range. At least five concentrations over the whole working range should be prepared for this aspect of the linearity study [3, 15, 25–27].

In the bioanalytical studies, the basic calibration should be prepared in the same biological matrix as in the samples of the intended study, which can be achieved by spiking the matrix with known concentration of the analyte. In this case, a blank sample, a zero sample (blank and internal standard), six to eight nonzero samples covering the expected range (including the anticipated QL) should be evaluated as part of the linearity study [27].

For the basic evaluation of a linear calibration line, several parameters can be used, such as the relative process standard deviation value (V_{xo}), the Mandel-test, the X_p value [28], the plot of response factor against concentration, the residual plot, or the analysis of variance (ANOVA). The lowest concentration that has been used for the calibration curve should not be less than the value of X_p (see Fig. 4). V_{xo} (in units of %) and X_p values of the linear regression line $Y = a + bX$ can be calculated using the following equations [28]:

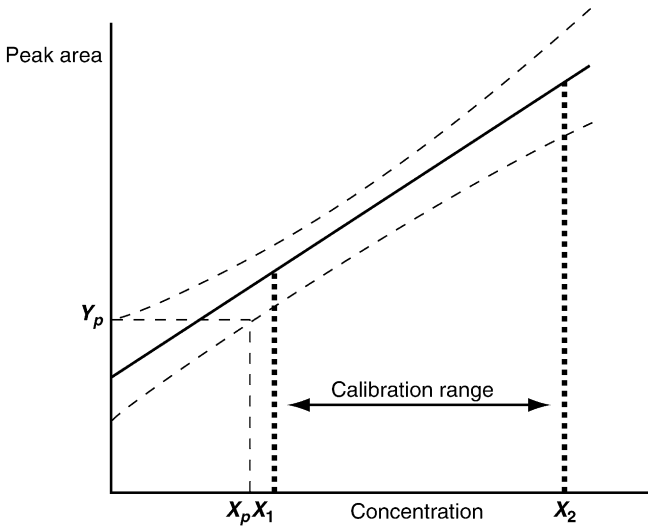

Fig. 4. Securing the lower limit of the calibration curve. The calibration range is from X_1 (lower limit concentration) to X_2 (upper limit concentration). The calculated value of X_p ($p = 0.05$) must be $< X_1$. For calculation of X_p and Y_p, see text. (Modified from Ref. [28].)

$$V_{xo} = \frac{S_{xo}}{\overline{X}} \cdot 100\ \%$$

where

$$S_{xo} = \frac{Sy}{b};\ Sy = \sqrt{\frac{\sum \left(Y_i - \hat{Y}_i\right)^2}{N-2}} \quad \text{with} \quad \hat{Y}_i = a + bX_i$$

$$X_p = 2S_{xo}\, t_{\text{table}} \sqrt{\frac{1}{N} + 1 + \frac{\left(Y_p - \overline{Y}\right)^2}{b^2\, \text{Qxx}}}$$

$$Y_p = a + Sy \cdot t_{\text{table}} \sqrt{\frac{1}{N} + 1 + \frac{\overline{X}^2}{\text{Qxx}}} \quad \text{Qxx} = \sum Xi^2 - \frac{1}{N}\left(\sum X_i\right)^2$$

(t_{table} = Student-t-factor; $f = N - 2$; $p = 0.05$)

For an acceptable accuracy test, the value of V_{xo} should be not more than 5%, and the intercept should not be significantly different from zero ($p > 0.05$). Kromidas [29] suggested that the maximum value of the intercept is about 2–5% of the target concentration and the maximum RSD of the response factor is 2.5%, while the maximum y-intercept of the impurity is $\leq$25% to its specification limit [30]. As a matter principle, calibration data should be free of outlier values, which can be proved by using a 'F-' or 't-test' [28].

Sole use of the correlation coefficient (r) alone is not recommended as a means to demonstrate linearity. The correlation coefficient describes the relation between two random parameters, and shows no relevance for the analytical calibration [31]. The correlation coefficient does not indicate the linearity or lack thereof, unless r exceeds 0.999 [8, 32, 33]. If the value of r is less than 0.999, other parameters such as V_{xo}, X_p value, ANOVA linear testing, etc., should be calculated. Ebel [34] described using the transformation of r (i.e., 'r_u') for expressing the degree of linearity, where the acceptance value of $(1 - r_u^2)$ should be less than 0.05. Camag (Muttents) described the 'sdv' parameter (i.e., the relative standard deviation of the calibration curve) for expressing the linearity of a calibration curve for TLC/HPTLC in its CATS software, and can be calculated as follows:

$$\text{sdv} = 100 \times \frac{\sqrt{\text{var}\, Y_i}}{\overline{Y_i}}$$

According to our experience, the acceptance criterion is not more than 5.0.

The variance homogeneity (homoscedasticity) over the whole range of the basic calibration line should also be proved using the F-, Bartlett-, or Hartley-tests [28, 34]. When heteroscedasticity is confirmed, and the calibration range cannot be reduced, a weighting factor should be used, such as $1/C$ or $1/C^2$, where C = concentration [19]. Other weighting factors may be used, and a discussion on the weighted least squares was presented in detail by Baumann and coworkers [35, 36].

If the concentration range of the calibration curve is very broad, one may observe the existence of deviations from the linear model. In such instances, other models such as polynomial regression, logarithm, or others can be used. For example, if the calculated value of V_{xo} by the linear model exceeds V_{xo} of the second-degree model, or the test value PW in the Mandel-test exceeds F table, the second-degree model calibration should be used for the entire experiment. If working with the CATS software, the smallest value of sdv should be selected to determine the most suitable regression model that will be used for the calibration.

For analyses using TLC/HPTLC method, the calibration curve should be performed on each plate (containing unknown samples and standards).

4. ACCURACY

The accuracy of an analytical method is given by the extent by which the value obtained deviates from the true value. One estimation of the accuracy of a method entails analyzing a sample with known concentration and then comparing the results between the measured and the true value. The second approach is to compare test results obtained from the new method to the results obtained from an existing method known to be accurate. Other approaches are based on determinations of the per cent recovery of known analyte spiked into blank matrices or products (i.e., the standard addition method). For samples spiked into blank matrices, it is recommended to prepare the sample at five different concentration levels, ranging over 80–120%, or 75–125%, of the target concentration. These preparations used for accuracy studies usually called 'synthetic mixtures' or 'laboratory-made preparations'.

Table 2. Acceptance criteria of accuracy and precision studies for different analyte concentrations

Analyte concentration (%)	Unit	Mean recovery (%)	Precision (RSD, %)
100	100%	98–102	1.3
≥10	10%	98–102	2.7
≥1	1%	97–103	2.8
≥0.1	0.1%	95–105	3.7
0.01	100 ppm	90–107	5.3
0.001	10 ppm	80–110	7.3
0.0001	1 ppm	80–110	11
0.00001	100 ppb	80–110	15
0.000001	10 ppb	60–115	21
0.0000001	1 ppb	40–120	30

The table has been modified from information contained in Ref. [11].

On the other hand, for the standard addition method, the spiking concentrations are in the range of 50–150% of the label-claimed value, and are made by spiking of known analyte concentrations in matrices such as serum, plasma, etc.

The accuracy of a method should be assessed using a minimum of nine determinations conducted over a minimum range of three concentration levels (80%, 100%, and 120% of the target concentration) [37]. Experience from our laboratory has showed that by using at least five levels of concentrations in duplicate (i.e., 80%, 90%, 100%, 110%, and 120% of the target concentration), a better result can be achieved. For dissolution studies, the accuracy of the required profile should be tested at 40%, 75%, and 110% of the theoretical release) [20].

The acceptance criterion for recovery data is 98–102% or 95–105% for drug preparations. In biological samples, the recovery should be ±10%, and the range of the investigated concentrations is ±20% of the target concentrations. For trace level analysis, the acceptance criteria are 70–120% (for below 1 ppm), 80–120% (for above 100 ppb), and 60–100% (for below 100 ppb) [2]. For impurities, the acceptance criteria are ±20% (for impurity levels ≤0.5%) and ±10% (for impurity levels ≥0.5%) [30]. The AOAC (cited in Ref. [11]) described the recovery acceptance criteria at different concentrations, as detailed in Table 2. A statistically valid test, such as a *t*-test, the Doerffel-test, or the Wilcoxon-test, can be used to prove whether there is no significant difference between the result of accuracy study with the 'true value' [29].

To prove whether or not systematic errors have occurred, a linear regression of recovery curve of X_f (concentration of the analyte measured by the propose method) against X_c (nominal concentration of the analyte) should be constructed. The equation for the recovery curve is

$$X_f = a_f + b_f X_c$$

The confidence range of the intercept (Cr a_f) and slope (Cr b_f) from the recovery curves are calculated for $p = 0.05$, as described in Fig. 5. These confidence ranges

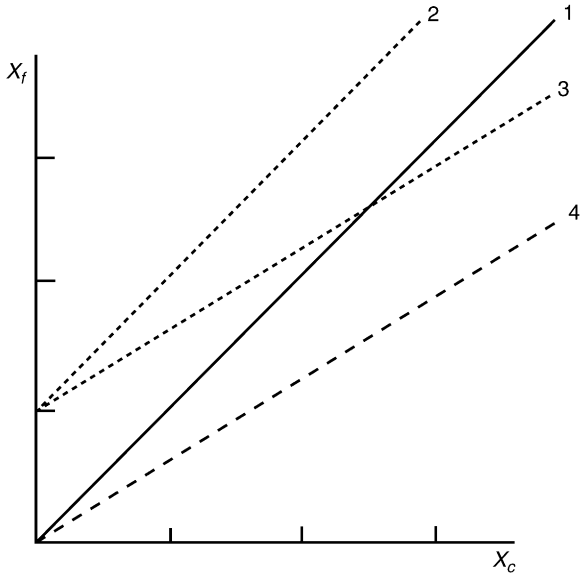

Fig. 5. Recovery curve of X_f against X_c: (1) no systematic errors were occurred; in this case an ideal recovery curve was observed ($a_f = 0$; $b_f = 1$); (2) constant systematic errors were observed; (3) constant and proportional systematic errors were observed; and (4) proportional systematic errors were observed. (Modified from Refs. [28] and [29].)

of intercept and slope should be not significantly different from zero and one, respectively, and can be calculated using the following equations [28].

$$\text{Cr } a_f = a_f \pm t_{\text{table}} S_{yf} \sqrt{\frac{1}{N} + \frac{\overline{X} c^2}{\text{Qxx}}};\ \text{Cr } b_f = b_f \pm \frac{t_{\text{table}} S_{yf}}{\sqrt{\text{Qxx}}}$$

$$S_{yf} = \sqrt{\frac{\sum \left[X_{if} - \left(a_f + b_f - X_i\right)\right]^2}{N - 2}}$$

$$(t_{\text{table}} = \text{Student-}t\text{-factor};\ f = N - 2;\ p = 0.05)$$

5. PRECISION

The determination of precision can divided into three categories, namely repeatability, intermediate precision, and reproducibility. *Repeatability*, or intraassay within-day precision, is determined when the analysis is performed in one laboratory by one analyst, using one definite piece of equipment, and is performed within one working day. *Intermediate precision* is obtained when the analysis is performed within a single laboratory by different analysts over a number days or weeks, using different equipment, reagents, and columns. *Reproducibility* represents the

precision obtained from results measured in different laboratories with the aim of verifying the method as to whether it can yield same results in different facilities.

For the determination of repeatability, at least six independent analyses of three concentration levels should be performed (typically 80%, 100%, and 120% of the target concentration). For performing an intermediate precision study, the minimum number of samples to be analyzed should be at least six determinations at three different concentrations made at three different times, for a total of 54 samples.

The acceptance criterion for the RSD value for a precision study of the assay of a finished product and of its content uniformity is $\leq$2% (repeatability; $n \geq 6$) or $\leq$3% (intermediate precision; $n \geq 6$). For measurement of the dissolution rate, the acceptance criterion for the RSD value is $\leq$3% (repeatability; $n \geq 6$) [30]. For a bioanalytical study, the RSD should not be $\geq$15%, and at the QL $\geq$ 20% for $n \geq 5$ determinations [27].

Ermer and coworkers [15, 38], recommended that the acceptance criteria for the standard deviation of the determinations should be lower than 1/6 of the specification range (upper specification limit, USL minus lower specification limit, LSL), or calculated using the following equation:

$$\mathrm{SD}_{\max} = \frac{|(\mathrm{BL} - \mathrm{SL})|\sqrt{n}}{t}$$

For the t-table test $n - 1$, and $p = 0.05$; BL is basic limit, obtained from the theoretical content and manufacturing variability with respect to the critical 'half' of the specification range. SL is the overall specification limit with respect to the critical 'half' of the specification range.

Kromidas [29] described other acceptance criteria of the precision studies, within the scope of the following equation:

$$\mathrm{RSD}(\%) < \frac{(\mathrm{USL} - \mathrm{LSL})\sqrt{n}}{4 \times (1.96) \times \mathrm{Mean}} \times 100$$

The AOAC (cited in Ref. [11]) described the precision acceptance criteria at different concentrations within or between days, the details of which are provided in Table 2. Other parameters that should be tested in the precision study are the David-, Dixon- or Grubbs-, and Neumann-tests. The David-test is performed when determining whether the precision data are normally distributed. Outlier testing of the data is performed by the Dixon-test (if $n <$ 6–8) or by the Grubbs-test (if $n >$ 6–8), while trend testing of the data is performed by Neumann-test. Detailed methods have been described in the book written by Kromidas [29].

6. DETECTION LIMIT AND QUANTITATION LIMIT

The DL is defined as the lowest concentration of an analyte that can be detected under the analytical conditions to be used. The presence of analytes can be seen at the DL; however, their concentrations cannot be quantitatively measured. The QL

is the lowest concentration that can be determined with acceptable accuracy and precision under the analytical conditions. Generally, the QL can be estimated as three times that of the DL [39].

The DL and QL for chromatographic analytical methods can be defined in terms of the signal-to-noise ratio, with values of 2:1–3:1 defining the DL and a value of 10:1 defining the QL. Alternatively, in terms of the ratio of the standard deviation of the blank response, the residual standard deviation of the calibration line, or the standard deviation of intercept (s) and slope (S) can be used [40, 42], where:

$$\mathrm{DL} = 3.3\ s/S$$

$$\mathrm{QL} = 10\ s/S$$

According to Carr and Wahlich [39], DL and QL can be calculated using the equation:

$$C = kS_{\mathrm{b}}/S$$

where S is the slope of response versus concentrations, k is a constant (having values of $k = 3$ for DL, and $k = 10$ for QL). The value of S_b is calculated using $S_b = N/5$, where N is largest peak-to-peak fluctuation in the corresponding blank chromatogram in the region of 20 times the width of the analyte peak.

By constructing a linear regression analysis at relatively low concentrations of analyte, and calculating the X_p value, DL can be determined as $\mathrm{DL} = X_p$ [28]. The authors recommend using 5–10 samples at relatively low concentrations of analyte for determining of X_p by diluting until no response is detected. In this case, the requirements of the linearity parameters (V_{xo}, r, X_p value, etc.) of the regression line should be fulfilled before DL can be estimated using the value of X_p.

QL can be also determined as the lowest concentration of the analyte in which duplicate injections have RSD values less than or equal to 2%. For clinical applications, QL should be at least 10% of the minimum effective concentration [2], and it should always be within the linear working range [3].

7. ROBUSTNESS/RUGGEDNESS

The robustness of an analytical method can be defined as a measure of the capability of the method to remain unaffected by small, but deliberate, variations in method parameters. The parameter therefore provides an indication of the method reliability during normal usage. The ruggedness of a method is the degree of reproducibility of test results obtained by the analysis of the same samples under a variety of conditions, such as different laboratories, different analysts, different instruments, different lot of reagents, different days, etc.

Some important parameters for testing the robustness of TLC methods include the stability of analyte in the solution being analyzed and on the plate before and

after development; the influence of temperature and humidity; the method of application, scanning, and evaluation, the spot shape and size, eluent composition, and pH, the batch/supplier of the TLC plate, the sample volume, the geometry of the chamber, and the drying conditions of the plate [21, 30, 40].

Parameters that should be tested in HPLC method development are flow rate, column temperature, batch and supplier of the column, injection volume, mobile phase composition and buffer pH, and detection wavelength [2]. For GC/GLC methods, one should investigate the effects of column temperature, mobile phase flow rate, and column lots or suppliers [38]. For capillary electrophoresis, changes in temperature, buffer pH, ionic strength, buffer concentrations, detector wavelength, rinse times, and capillaries lots and supplier should be studied [35, 36]. Typical variation such as extraction time, and stability of the analytical solution should be also evaluated [37].

Ruggedness can be determined by an interlaboratory study with a sufficient ($n \geq 8$) participating laboratories following one and the same procedure as performed by different analysts, and using operational and environmental conditions that may differ but are still within the specified parameters of the assay [1, 41]. Detailed guidance for robustness and ruggedness testing is available [42, 43].

8. RANGE

According to USP 28 [1], the range of an analytical method can be defined as the interval between upper and lower levels (in the Pharmaceutical Industry usually a range from 80 to 120% of the target concentrations tested) of the analyte that have been demonstrated to be determined with a acceptable level of precision, accuracy, and linearity. Routine analyses should be conducted in this permitted range. For pharmacokinetic measurements, a wide range should be tested, where the maximum value exceeds the highest expected body fluid concentration, and the minimum value is the QL.

9. STABILITY IN MATRICES

For bioanalytical studies, the stability of analyte(s) in appropriate biological matrices should be evaluated, since it is important to verify that no degradation takes place between the time of sample collection and their analysis. Analyte instability can arise from various factors, such as interaction with container surfaces, reaction with air, thermal decomposition, evaporation of volatiles, or photolysis. To minimize degradation, some treatment of the sample can be made, such as lowering the temperature or freezing the samples, protecting from light, adding some stabilizing agent, adjusting the pH, making a chemical derivatization, or adding enzyme inhibitors. Certain analytes (such as captopril or aspirin) undergo immediate degradation in biological matrices. Reconstituted samples should remain stable in the solvents at the working-temperature until injected. Analyte stability should be evaluated after three freeze and thaw cycles [18, 19, 27, 44].

10. VALIDATION OF ANALYSIS METHODS DURING DRUG DEVELOPMENT

Before new pharmaceutical drug can be marketed, a lengthy three-stage process is involved, commonly referred to as Phase I, Phase II, and Phase III. As would be expected, the analytical method validation development also consists of three phases [15, 28, 45, 46]. Phase I consists of preparation of calibration functions for testing the linearity, variance homogeneity, and evaluations of the lower limit of the calibration range. Selectivity is demonstrated using stressed samples, and testing for the influence of matrix on the accuracy is performed. A system precision is performed with six injections.

The validation process begun in Phase I is extended during Phase II. In this phase, selectivity is investigated using various batches of drugs, available impurities, excipients, and samples from stability studies. Accuracy should be determined using at least three levels of concentration, and the intermediate precision and the quantitation limit should be tested. For quality assurance evaluation of the analysis results, control charts can be used, such as the Shewart-charts, the R-charts, or the Cusum-charts. In this phase, the analytical method is refined for routine use.

In Phase III, the final dosage formulation has been established and the pivotal clinical trials are being conducted. Degradation products have been identified, so the method selectivity should be reevaluated to ensure that all degradants can be detected and quantitated. The analytical methods are completely validated, and appropriate for routine quality assurance and control purposes. The type and frequency of system suitable testing (SST) should be determined, and an excellent publication on SST for chromatography systems is available [47].

If the new operating range was used outside of the existing operating range (changes in column temperature, sample matrix, column or instrument type, etc.), the method should be revalidated [11]. When all of this work is complete, during the marketing phase, an interlaboratory testing is recommended for standardization of the method [28].

In addition, for reporting a routine analytical result, the result should include its *confidence interval* 'CI' [28], or with same meaning term, *uncertainty* '*U*' [29] or *standard certainty* 'STC' [48]. The result should be reported as:

$$\text{Result} \pm \frac{t \times \text{SD}}{\sqrt{N}} \ (\text{CI or } U \text{ or STC})$$

In his book, Kromidas [29] described, the value of "t" can be replaced with "k" (constant), for $p = 0.05$ that $k = 2$, or for $p = 0.01$ that $k = 3$. Kaiser [48] recommended using $N = 4$, so in this case the STC is about three times of the SD (for $p = 0.01$, and $F = N - 1$). In this case, if SD is about 1%, the reported result is (result ± 3)%.

11. CONCLUSION

Analytical method validation, which must be performed by every regulated laboratory, deals with the testing of significant method characteristics to ensure that under

routine use, the analytical method will be accurate, precise, specific, reproducible, and rugged over the whole specified range for which an analyte(s) will be determined. The validation of chromatographic methods should be performed before the first routine use of the procedure, and validation of methods of analysis is crucial in all phases of drug development.

ACKNOWLEDGEMENTS

The authors thank Mr Fajar Zulkarnain Lubis, Mr Deddy Triono (Faculty of Pharmacy, Arlangga University, Surabaya), and Ms Bertha Oktarina (Bernofarm, Sidoarjo), for their kind technical assistance.

REFERENCES

[1] *The United States Pharmacopoeia 28*, United States Pharmacopoeial Convention, Rockville, MD, 2004, pp. 2748–2751.
[2] I. N. Papadoyannis and V. F. Samanidou, Validation of HPLC, *Encyclopedia of Chromatography, online*, Marcel-Dekker, Inc., 2003, http://www.dekker.com.
[3] M. Wells and M. Dantus, Validation of chromatographic method, in *Ewing's Analytical Instrumentation HandBook* (ed. J. Cazes), 3rd edn., Marcel-Dekker, 2005, pp. 1015–1033.
[4] C. Incledon and H. Lam, Development and validation of automated methods, in *Analytical Method Validation and Instrument Performance Verification* (eds. C. C. Chan, H. Lam, Y. C. Lee and X.-U. Zhang), Wiley-Interscience, Hoboken, NJ, 2004, pp. 67–84.
[5] M. Thompson, S. L. R. Ellison and R. Wood, IUPAC Technical Report, *Pure Appl. Chem.*, 2002, **74**, 835–855.
[6] R. Brown, M. Caphart, P. Faustino, R. Frankkewich, J. Gibbs, E. Leutzinger, G. Lunn, L. Ng, R. Rajagopalan, R. Chiu, Y. Scheinin, *LC-GC*, January 2001, **19**, 75–79.
[7] CDER, *Guidance for Industry*, http://www.fda.gov/cder/gidance/2396dtf.htm (1/2/2004).
[8] G. A. Shabir, *J. Chromatogr. A*, 2003, **987**, 57–66.
[9] B. Renger, H. Jehle, M. Fischer and W. Funk, *J. Planar Chromatogr.*, 1995, **8**, 269–277.
[10] H.-P. Frey and K. Zieloff, *Qualitative und quantitative Duennschichtchromatographie*, VCH, Weinheim, 1993, pp. 324–325.
[11] L. Huber, Validation of Analytical Methods: Review and Strategy, http://www.labcompliance.com (6/8/2004).
[12] F. Bressole, M. Bromet-Petit and M. Audran, *J. Chromatogr. B*, 1996, **686**, 3–10.
[13] I. N. Papadoyannis and H. G. Gika, Peak purity determination with a diode array detector, *Encyclopedia of Chromatography,* online, Marcel-Dekker, Inc., 2003, http://www.dekker.com.
[14] S. Ebel, *Fresenius J. Anal. Chem.*, 1992, **342**, 769–778.
[15] J. Ermer and J. S. Landy, Validation of analytical procedures, *Encyclopedia of Pharmaceutical Technology*, Marcel-Dekker, Inc., 2002, pp. 1–22.
[16] A. Crecelius, M. R. Clench and D. S. Richard, *Curr. Trends Mass Spectrom.*, 2004, **19**, 28–34.
[17] J. D. Orr, I. S. Krull and M. E. Swatrz, *LC-GC*, December 2003, www.chromatograhyonline.com.
[18] F. Garofolo, Bioanalytical method validation, in *Analytical Method Validation and Instrument Performance Verification* (eds. C. C. Chan, H. Lam, Y. C. Lee and X.-U. Zhang), Wiley-Interscience, Hoboken, NJ, 2004, pp. 105–138.
[19] C. Hartmann, J. Smeyers-Verbeke, D. L. Massart and R. D. McDowall, *J. Pharm. Biomed. Anal.*, 1998, **17**, 193–218.
[20] C. C. Chan, N. Pearson, A. Rabelo-Cameiro and Y. C. Lee Dissolution method validation, in *Analytical Method Validation and Instrument Performance Verification* (eds. C. C. Chan, H. Lam, Y. C. Lee and X-U Zhang), Wiley-Interscience, Hoboken, NJ, 2004, pp. 51–66.

[21] S. L. Karolak, M. Tod, P. Bonnardel, M. Czok and P. Cardot, *J Pharm. Biomed. Anal.*, 1995, **13**, 959–970.
[22] K. Baumann and H. Waetzig, *Process Quality Control and Quality*, 1997, **10**, 59–73.
[23] E. Hahn-Deinstrop, *Applied Thin-Layer Chromatography*, Wiley-VCH Verlag GmbH, Weinheim, 2000, pp. 201–205.
[24] H. Waetzig, *J. Chromatogr. A*, 1995, **700**, 1–7.
[25] *Reviewer Guidance, Validation Method of Chromatographic Method*, Center for Drug Evaluation and Research, CEDER, 1994.
[26] C. C. Chan, Potency method validation, in *Analytical Method Validation and Instrument Performance Verification* (eds. C. C. Chan, H. Lam, Y. C. Lee and X.-U. Zhang), Wiley-Interscience, Hoboken, NJ, 2004, pp. 11–26.
[27] Guidance for Industry, Bioanalytical method validation, US Department of Health Services, Food and Drug Administration, Center for Drug Evaluation and Research, Center for Veterinary Medicine.
[28] W. Funk, V. Dammann and G. Donnevert, *Qualitätssicherung in der Analytischen Chemie*, VCH Verlagsgesellschaft GmbH, Weinheim, 1992, pp. 10–44, 161–200.
[29] S. Kromidas, *Validerung in der Analytik*, Wiley-VCH, Weinheim, 1999, pp. 52–106, 147–171.
[30] K. Ferenczi-Fodor, Z. Vegh, A. Nagy-Turak, B. Renger and M. Zeller, *J. AOAC Int.*, 2001, **84**, 1265–1276.
[31] K. Danzer, Significance of statistical quality assurance, in *Accreditation and Quality Assurance in Analytical Chemistry* (ed. H. Guenzler), Springer, Berlin, 1996, p. 128.
[32] Analytical Method Committee, Uses (proper and improper) of correlation coefficient, *Analyst*, 1988, **113**, 1469–1471.
[33] J. Van Loco, M. Elskens, C. Croux and H. Beernaert, *Accred. Qual. Assur.*, 2002, **7**, 281–285.
[34] S. Ebel, *Wuerzburger Skripten zur Analytik, Teil 4.*, Bayerische Julius-Maximilians Universitaet, Wuerzburg, 1992.
[35] K. Baumann and H. Waetzig, *J. Chromatogr. A*, 1995, **700**, 9–29.
[36] K. Bauman, *Process Control Qual.*, 1997, **10**, 75–112.
[37] Guidance for Industry, *Q2B Validation of Analytical Procedures: Methodology*, US Department of Health Services, Food and Drug Administration, Center for Drug Evaluation and Research, Center for Veterinary Medicine.
[38] J. Ermer, *J. Pharm. Biomed. Anal.*, 2001, **24**, 755–767.
[39] G. P. Carr and J. C. Wahlich, *J. Pharm. Biomed. Anal.*, 1990, **8**, 613–618.
[40] G. Indrayanto and M. Yuwono, Validation of TLC Analyses, in *Encyclopedia of Chromatography,* online (ed. J. Cazes). Marcel-Dekker Inc., 2003, http://www.dekker.com.
[41] W. Wegscheider, Validation of analytical method, in *Accreditation and Quality Assurance in Analytical Chemistry* (ed. H. Guenzler), Springer, Berlin, 1996, pp. 135–157.
[42] Y. Vander Heyden, F. Questier and D. L. Massart, *J. Pharm. Biomed. Anal.*, 1998, **17**, 153–168.
[43] Y. Vander Heyden, A. Nijhuis, J. Smeyers-Verbeke, B. G. M. Vandeginste and D. L. Massart, *J. Pharm. Biomed. Anal.*, 2001, **24**, 723–753.
[44] D. Dadgar, P. E. Burnet, M. G. Choc, K. Gallicano and J. W. Hooper, *J. Pharm. Biomed. Anal.*, 1995, **13**, 89–97.
[45] C. C. Chan and E. Jensen, Overview of pharmaceutical product development and its associated quality system, in *Analytical Method Validation and Instrument Performance Verification* (eds. C. C. Chan, H. Lam, Y. C. Lee and X.-U. Zhang), Wiley-Interscience, Hoboken, NJ, 2004, pp. 1–10.
[46] Chow and Shein-Chung, *Drug Inform. J.*, 1997, **31**, 1195–1201.
[47] J. C. Wahlich and G. P. Carr, *J. Pharm. Biomed. Anal.*, 1995, **8**, 619–623.
[48] R. E. Kaiser, *J. Planar. Chromatogr. Modern TLC*, 2005, **18**, 51–56.

Polymorphism and Solvatomorphism 2004

Harry G. Brittain

Center for Pharmaceutical Physics, 10 Charles Road, Milford, New Jersey 08848

Contents

1. INTRODUCTION

Over the past two decades, the pharmaceutical community has become acutely aware that many substances of interest can be obtained in more than one crystal form, and that the properties of these solids may often be quite different. *Polymorphism* is the term used to denote crystal systems where a substance can exist in different crystal packing arrangements, but all of which are characterized by exactly the same elemental composition. Other crystal variations are known where a given substance exists in different crystal packing arrangements, but each of which exhibits a different elemental composition. Since this latter phenomenon usually involves the inclusion of one or more solvent molecules in the crystal, the term *solvatomorphism* has been coined to replace the inconsistent nomenclature used over the years. These and related phenomena have been the focus of several recent monographs [1–3].

The pharmaceutical industry has taken great interest of late in the study of polymorphism and solvatomorphism in its materials, since a strong interest in the phenomena has developed now that regulatory authorities understand that the nature of the structure adopted by a given compound upon crystallization can exert a profound effect on its solid-state properties. For a given material, the heat capacity, conductivity, volume, density, viscosity, surface tension, diffusivity, crystal

PROFILES OF DRUG SUBSTANCES, EXCIPIENTS,
AND RELATED METHODOLOGY, VOLUME 32
ISSN: 0099-5428

DOI: 10.1016/S0099-5428(05)32010-7

hardness, crystal shape and color, refractive index, electrolytic conductivity, melting or sublimation properties, latent heat of fusion, heat of solution, solubility, dissolution rate, enthalpy of transitions, phase diagrams, stability, hygroscopicity, and rates of reactions, were all affected by the nature of the crystal structure.

As might be expected, the literature associated with studies of polymorphism and solvatomorphism has grown in proportion to the interest in the field. As a result, an annual review of the area has been initiated, and will be continued in succeeding volumes in the *Profiles* series. The citations in this article are drawn primarily from the major pharmaceutical and crystallographic journals, and therefore are not represented to be comprehensive. However, they should represent the bulk of work that was conducted with pharmaceutical interest in mind.

2. REVIEW ARTICLES

Herbstein [4] has written an intriguing review that begins with formal definitions, and which sets forth a number of key concepts in terms of their phase diagrams and underlying thermodynamics. He goes on to discuss the subjects of phase transformation, concluding that more studies need to be conducted on monotropic systems. In his concluding thoughts, Herbstein emphasizes that experimental studies rest on the twin foundations of structure and thermodynamics, and that while the science of structure determination has become exceedingly advanced, insufficient attention is being paid to the accompanying thermodynamic measurements.

Fabian and Kalman [5] retrieved 50 structures from the Cambridge Structural Database, including the polymorphs of 22 compounds, in order to evaluate the frequency of isostructurality among polymorphs. It was found that one-, two-, or three-dimensional isostructurality was exhibited by approximately one-half of the compounds studied. Three-dimensional isostructurality was connected to the gradual ordering of crystal structures, while one- and two-dimensional isostructurality could be related to specific packing interactions. Interestingly, conformational polymorphs were not found to exhibit isostructurality.

3. THERMODYNAMIC AND THEORETICAL ISSUES

As indicated above, evaluation of the thermodynamics of a polymorphic or solvatomorphic system provides valuable insight into the nature of the system, but is all too often overlooked in many studies. However, Sacchetti [6] used aqueous/organic slurries of the anhydrate and hydrate forms of GW2016 to determine the relative stability of crystal forms interrelated by solution-mediated transformation. It was reported that the use of slurries enabled experiments to be completed in a day that enabled an understanding of the relative stability of the forms as a function of relative humidity.

The solubility of (*S*)–3,5-dichloro-2-hydroxy-[[2-[[[3-hydroxy-5[1,4,5,6-tetrahydro-5-hydroxypyrimidin-2-yl-amino]phenyl]carbonyl]amino]acetyl]amino]-benzenepropanoic acid and its monohydrate was measured at several temperatures in different aqueous acetonitrile solvent systems [7]. The data were fitted to a frame-

work consisting of Van't Hoff and enthalpy–entropy compensation analyses, with the two solvatomorphs exhibiting linear temperature dependence over a wide temperature range (26–65°C). The solubility increased due to entropy effects in the acetonitrile-rich region, while enthalpy effects determined the degree of solubilization in water-rich regions. Quantification of this phenomenon was demonstrated by plotting ΔH against ΔG, and noting the nonlinearity and discontinuity between the regions.

Grant and coworkers [8] studied the dehydration kinetics of piroxicam monohydrate using both model-free and model-fitting approaches in an effort to understand the effects of lattice energy and crystal structure. The dehydration kinetics was found to differ when determined under isothermal and nonisothermal conditions. Ultimately, the dehydration behavior of piroxicam monohydrate was determined by details of the crystal structure, which was characterized by an absence of channels and a complicated hydrogen-bonding network, and *ab initio* calculations proved useful in understanding the structural ramifications of the dehydration process.

The importance of temperature-controlled scanning calorimetry for measurements of heat capacity and of scanning transitiometry for simultaneous caloric and pVT analysis has been demonstrated for polymorphic systems [9]. This approach was used to study an enantiotropic system characterized by multiphase (and hindered) transitions, the role of heat capacity as a means to understand homogeneous nucleation, and the creation of (p, T) phase diagrams. The methodology was shown to possess distinct advantages over the more commonly used combination of characterization techniques.

An experimental study of barbituric acid found one new polymorph where molecules in the asymmetric unit adopted two different conformations [10]. The conformational aspect was investigated through the use of *ab initio* calculations, which permitted the deduction that the new form found would have a lower lattice energy than would the known form. It was also found that many hypothetical structures characterized by a variety of hydrogen-bonding structures were possible, and so the combined theoretical and experimental studies indicated that a search for additional polymorphs might yield new crystal structures.

Two new polymorphs of (2E)-2-cyano-3-[4-(diethylamino)phenyl]-prop-2-enethioamide and an acetone solvate were crystallized, and the structures compared to the known nonsolvated form [11]. One of the new forms was found to be considerably more stable than the others, and subsequently the other two new forms became 'vanishing polymorphs' that could only be produced under strictly controlled conditions. The structures of all three polymorphs could be found using polymorph predictor, if the initial molecular structure was obtained from the X-ray data, the molecule held to be rigid during the energy minimization, and both VDW and Coulomb interactions taken into account.

A derived crystal packing model proved to be useful in resolving the crystal structure of a metastable polymorph of racemic modafinil, where details of the solved crystal structure of one polymorph was used as a basis for developing the structure of the other [12]. It was found that the calculated XRPD pattern matched well with the experimental data, indicating the correctness of the analysis. The powder diffraction of two polymorphs of chlorothalonil were solved to obtain

the respective crystal structures using Monte Carlo simulations and Rietveld refinement [13].

The modeling of phase transformations continues to be the subject of investigational work. A simulation model was developed for the solvent-mediated transformation of the metastable α-form of (*L*)-glutamic acid to the stable β-form using the concept of population balance [14]. Using dissolution, nucleation, and growth parameters fitted from experimental data, it proved possible to understand and predict the observed crystallization behavior. In another study, a four-parameter logistic equation was used to describe phase transformations at high temperatures, with the predictions of the model being found to conform with actual experimental results [15].

4. PREPARATIVE METHODS FOR POLYMORPHS AND SOLVATOMORPHS

Crystallization remains the primary means of controlling the polymorphic or solvatomorphic state of a compound, and various groups have examined the influences of processing parameters on the identity and quality of the isolated form. Seeding was used to reduce the size of the metastable zone of eflucimibe, and thereby control the identity of the desired polymorphic identity of the product through a reduction in concomitant crystallization [16]. Process improvements have been developed that were found to improve the filterability and enhance the bulk density of ranitidine Form-1 [17], while the variation of process parameters used in an oscillatory baffled crystallizer enabled better selection to be made between the metastable α- and β-forms of (*L*)-glutamic acid [18].

In one detailed study, variations in process parameters were used to control the polymorphic crystallization of amino acids and a thiazole derivative [19]. Little effect of processing parameters during cooling crystallization was found on the nature of (*L*)-glutamic or (*L*)-histidine. While seeding experiments did not greatly influence the quality of (*L*)-glutamic products, the effects of seed crystals were found to be substantial for (*L*)-histidine. These differences were attributed to conformational differences between the molecules comprising the embryo nucleation crystals.

The use of *in situ* observation technology has been shown to be very useful as means to identify the polymorphic forms being crystallized. Raman spectroscopy has found such use during a solution-mediated transformation of the α-forms to the β-forms of (*L*)-glutamic acid [20], while in-process X-ray powder diffraction has been used for identification purposes during batch crystallization reactions [21]. The metastable α-form of glycine has been produced through the inclusion of a seeding step in the crystallization [22], and process control of this crystallization has been achieved using *in situ* infrared spectroscopy (attenuated total reflectance observation mode) and particle monitoring (Lasentec probe) [23].

Crystallization conditions can often be manipulated to favor the nucleation of alternate crystal forms. A metastable polymorph of metformin hydrochloride has been isolated using capillary crystallization techniques, and subsequently studied using thermal microscopy [24]. Calculations based on classical nucleation theory indicated that a metastable form could be obtained using high degrees of

supersaturation before nucleation was allowed to take place. After nucleation took place, the dynamics of slow evaporation and capillary crystallization proved to be conducive toward continued growth of the metastable phase. Two new polymorphs of acridine were prepared using terephthalic and *cis,trans*-muconic acid as epitaxial crystallization template, as these were shown to be able to influence the nucleation phenomena [25].

A piperidene-based intermediate was found to crystallize as either an anhydrate or a hydrate, but the impurity profile of the crystallized solids differed substantially [26]. Considerations of molecular packing led to the deduction that there was more void volume in the anhydrate crystal structure than in that of the hydrate form, thereby facilitating more clathration in the anhydrate than in the hydrate phase. This phenomenon was led to a decision to crystallize the hydrate form, since lower levels of the undesired impurity could be occluded and greater compound purity could be achieved in the crystallization step.

5. STRUCTURAL CHARACTERIZATION AND PROPERTIES OF POLYMORPHS AND SOLVATOMORPHS

Given that scientists are usually most interested in learning about the particular defining properties of a system capable of existing in more than one crystal form, it is not surprising that the largest number of published works during 2004 entailed either the structural investigation of a polymorphic or solvatomorphic system, or some type of correlation between empirically observed properties and the structural characteristics of the system.

5.1. Polymorphic systems

The two structurally similar polymorphs of (*R,S*)-ethambutol dihydrochloride have been shown to bear an enantiotropic relationship, and can reversibly interconvert in a single crystal transformation mode [27]. It was reported that despite the identity in space group type and similarity in unit cell constants, the two forms could be distinguished on the basis of their X-ray powder diffraction and solid-state nuclear magnetic resonance properties. Interestingly, while the (*S,S*)-diastereomer of ethambutol dihydrochloride can be obtained in four polymorphic forms, the (*R,S*)-diastereomer was only obtained in two different polymorphs.

The existence of two polymorphs was reported for a NO-releasing derivative of acetyl-salicylic acid [28]. Selection crystallization of one form or the other was achieved from a number of solvent systems (14 solvents and 3 preparative methods), but several systems were identified that yielded mixtures of the two forms. The single-crystal structure of Form I was reported, but the habit of the Form II crystals precluded their characterization. The transition point of the two forms was calculated from intrinsic dissolution data to be higher than the melting points of both polymorphs and thus the two forms bear a monotropic relationship.

Thermal methods of analysis were used to study the polymorphism associated with pindolol [29]. The overlapping melting endotherms of the different forms were separated by peak fitting analysis and grouping of materials by the temperature of

their peak maxima, and in this manner three forms were formed by crystallization from molten substance. Only two forms had been found in the pindolol sample prior to its fusion.

The polymorphism in the piroxicam system has been the subject of conflict, with disagreements existing regarding the number and nomenclature of its polymorphs, as well as descriptions of the hydrogen-bonding patterns. The system was re-investigated in detail, and it was shown that the two authentic crystal forms differed in their lattice energies rather than in their conformational energies [30]. Interestingly, different types of amorphous material were obtained by the cryogenic grinding of the two forms, leading to differences in recrystallization behavior between amorphous piroxicam prepared from Forms I and II.

An enantiotropically related pair of polymorphs was obtained for *p*-aminobenzoic acid, with the system being characterized by a transition temperature of 25°C [31]. The α-form was obtained as fibrous needles, while the *β*-form was obtained in the form of prisms. The solubilities of the two forms are almost the same, indicating the existence of comparable values for ΔG, which in turn explained the slow transformation of the α-form into the *β*-form. Nucleation of the α-form was found to be favored, which is reasonable considering that the structural motif of the α-form consists of carboxylic acid dimmers that would be expected to be stable association species in solution.

Olanzapine appears to exist in at least five polymorphic forms, and the structure of Form II has been reported [32]. Two molecules form centrosymmetric dimmers stabilized by a series of C—H····π interactions, and the dimmers are connected by a system of intermolecular N—H····N, C—H····N, and C—H····S hydrogen bonds. The structure of a monoclinic polymorph of isoxsuprine hydrochloride has been reported [33]. The molecular conformation existing in the new monoclinic polymorph was found to be very similar to that existing in the known triclinic polymorph.

The isolation of crystalline products having mixed polymorphic compositions (often referred to as concomitant polymorphism) remains a topic of interest, even though the phase rule predicts that a system at equilibrium consisting two components (solvent + solute) and three phases (solution + Form I + Form II) is univariant. Hence, for crystallizations performed at a fixed pressure (typically atmospheric) the system becomes nonvariant and genuine equilibrium can exist at only one temperature. Therefore, concomitant products must be obtained under nonequilibrium conditions. Flexibility in molecular conformation was attributed to the concomitant polymorphs of a spirobicyclic dione [34] and of 3-acetylcoumarin [35].

The structures of two polymorphs of pleconaril, enantiotropically related with a transition temperature of 35.7°C, have been reported [36]. Form I was described as consisting of a network of dimers, while Form III was described as a three-dimensional network of monomers. The two forms contradicted the density rule, and the solid–solid transition could occur only through a destructive–reconstructive mechanism. A quantitative differential scanning calorimetry method was also described that enabled the quantitative determination of Form I in bulk Form III to be made at levels as low as 0.1%.

The effect of structural variation on crystal structure was studied for 12 phenyl-substituted derivatives of 6-amino-2-phenylsulfonylimino-1,2-dihydropyridine [37]. The title compound contains both hydrogen bond donor and acceptor sites, and the

different derivatives were found to differ in their use of the hydrogen bonding functionalities. Methyl and chloro substitution in the *ortho* position, or fluoro substitution in the *para* position, led to a catemer motif that was related to the kinetic form of the title molecule. *Meta* substation by methyl and larger substituents in the *para* position were found to block this structural option.

Even though 2,4,6-trimethoxy-1,3,5-triazine adopts a planar conformation in its three polymorphs, the various crystal forms were found to exhibit different molecular packing modes [38]. It was found that tautomerization of 4-mercaptopyridine existing in absolute ethanol at different temperatures led to the crystallization of two polymorphs [39]. In one form the molecules were arranged in a helical conformation through N—H···S hydrogen bonds, while the other has the molecules arranged in a N—H···S bonded zigzag chain.

Different forms of antiparallel stacking of hydrogen-bonded antidromic rings have been demonstrated in various 2-hydroxycycloalkane carboxylic acid compounds [40]. In two forms of one of the compounds, polymorphs having virtually the same unit cell were described, but where the structural variation originated from different modes of stacking alternating layers. Although some of the crystal forms were isostructural, they were not isomorphous.

In the orthorhombic and monoclinic polymorphs of 1,3,5-triphenylperhydro-1,3,5-triazine-2,4,6-trione, the molecules were reported to be lined by a single C—H···π(arene) hydrogen bond forming molecular chains in one form and molecular sheets in the other [41]. It was found that 2,3,5,6-tetrakis(naphthalene-2-ylsulfanylmethyl) pyrazine could be crystallized in two polymorphic forms of low symmetry that differed in the relative orientations of the naphthalene rings and adjacent substituents [42]. The existence of differing types of hydrogen-bonded sheets was observed in the orthorhombic and monoclinic polymorphs of 2-(4-nitro-phenylaminocarbonyl) benzoic acid [43].

N,N′-bis(2-phyidylmethyl)pyrazine-2,3-dicarboxamide was crystallized in two orthorhombic forms, which differ from each other in the conformational arrangements of the compound [44]. A new polymorph of 2-bromo-5-hydroxybenzaldehyde has been reported where a pair of hydrogen bonds linked molecules related by a center of inversion [45]. One of the intermediates important in the synthesis of an antituberculosis drug, methyl *p*-aminobenzoate, was found to crystallize in a new monoclinic polymorph where molecules were arranged in head-to-tail linear ribbon arrays [46].

5-Methylsulfanyl-1*H*-tetrazole was found to crystallize in a monoclinic form, and could be sublimed into an orthorhombic form, with the structures differing in the relative polarity of the molecular layers in the two forms [47]. *p*-Iodoacetophenone was found to crystallize in two polymorphs that both contained C—H···π points of contact, but where the contacts were shorter in one form than in the other [48]. A second monoclinic modification of the mixed salt benzimidazolium 3-carboxyphenoxyacetate 3-carboxyphenoxyacetic acid was reported, where the acid hydrogen atom and the two monoanions comprised a carboxylate monoanion/neutral molecule in which the acid proton was disordered between the two anionic units [49].

A second monoclinic polymorph of anilinium picrate has been found, showing a three-dimensional hydrogen-bonded polymer with strong primary interactions between the proximal phenolate and adjacent nitro groups and separate anilinium

hydrogen-bonding donors in two cyclic associations [50]. A high-temperature form of 5-*t*-butylpyrazole has been reported that contains N—H····N hydrogen-bonded tetramers [51]. The structure of the seventh polymorph of cabergoline has been reported, crystallizing in the same space group as the more stable Form I but containing a different number of independent molecules in the unit cell and an altered pattern of hydrogen-bonding [52].

The structure of a second polymorph of 4,5-diphenyl-1H-imidazole has been discussed, with the new form exhibiting significantly different phenyl/imidazole dihedral angles and mode of crystal packing relative to the known form [53]. A new triclinic polymorph of 1,4-dibenzoyl-butane was found, differing from the monoclinic form in the torsional angles of the central chain [54]. Two polymorphs of diphenyl-(4-pyridyl)methyl methacrylate have been found, where the molecules in the two forms contain weak C—H····π and C—H····O/N contacts that lead to the existence of different conformations [55].

5.2. Solvatomorphic systems

Fluconazole was shown to be crystallizable in the form of a monohydrate and as a 1/4 ethyl acetate solvate, as well as a new nonsolvated form [56]. In the hydrate phase the water molecules were established as isolated sites, while the ethyl acetate molecules occupied constricted channels in its phase. In all of the structures, the fluconazole molecule adopted a common overall conformation, but one that was capable of some degree of flexibility. Hydrogen-bonding effects were deduced to be dominant in determining the structure of the different solvatomorphs.

The crystal structures of the 2:1 solvates formed by phenylbutazone with benzene, cyclohexane, 1,4-dioxane, tetrahydrofuran, and tetrachloromethane were found to be isostructural, while the structure of the chloroform solvate differed [57]. In all of the solvatomorphs, the solvent molecules were found to be located in channels along the (0 1 0) direction, and their inclusion served to increase the length of the unit cell along the *a*-axis. The solvent inclusion was also found to alter the β-angle.

The effect of relative humidity and temperature on the physical and structural properties of the 1:1 isopropanol solvatomorph of warfarin has been studied [58]. Below the critical relative humidity of 60–68% the solid is not hygroscopic, but becomes deliquescent at higher values of relative humidity without exchange of water for isopropanol. Storage of the solvate-morph at elevated temperatures causes formation of an amorphous solid owing to loss of isopropanol, which may proceed through an intermediate crystalline phase.

3,5-bis(Biphenyl)-4-hydroxybenzoic acid was obtained as the pyridine solvatomorph, and as two polymorphic dimethyl sulfoxide solvates [59]. In all three structures, a layered structure was formed through a combination of strong O—H····N hydrogen bonds and supporting intermolecular C—H····O, C—H····π, and π····π interactions. Discrete solvent molecules were identified in one of the dimethyl sulfoxide solvates, while hydrogen bonding with phenolic —OH groups was noted in the pyridine solvate.

1,3,5-tris(4-Cyanobenzoyl)benzene has been found to form isostructural solvatomorphs with ethyl acetate, 3-pentanone, nitromethane, dimethyl sulfoxide, acetone,

and methyl chloroacetate [60]. In the structures, the triaroylbenzene host molecule self-assembled in a two-dimensional lamellar pattern by means of C—H····O and C—H····N hydrogen bonds. The solvent molecules were located in channels between the molecular layers. A bifurcated C—H····O hydrogen bond between host donors and guest acceptors was identified in the solvatomorphs, and it was determined that C—H····N/O hydrogen bonding significantly influenced the supramolecular isomerism in the system.

The physical properties of the anhydrate form and two polymorphic monohydrates of niclosamide have been reported [61]. The anhydrate form exhibited the highest solubility in water and the fastest intrinsic dissolution rate, while the two monohydrates exhibited significantly lower aqueous solubilities. In a subsequent study, the 1:1 solvates of niclosamide with methanol, diethyl ether, dimethyl sulfoxide, *N,N′*-dimethyl formamide, and tetrahydrofuran, and the 2:1 solvate with tetraethylene glycol, were studied [62]. The relative stability of the different solvatomorphs was established using desolvation activation energies, solution calorimetry, and aqueous solubilities. It was found that although the nonaqueous solvates exhibited higher solubilities and dissolution rates, they were unstable in aqueous media and rapidly transformed to one of the monohydrates.

6-Methoxypurine was found to crystallize as a hemihydrate from *N,N′*-dimethyl formamide, and as a trihydrate from water [63]. Thermal treatment of the trihydrate could be used to obtain the hemihydrate. Zafirlukast was obtained in the form of monohydrate, methanol, and ethanol solvatomorphs, with the drug substance adopting a similar conformation in all three structures [64]. In the isostructural methanol and ethanol solvates, the solvent molecules are hydrogen-bonded to two zafirlukast molecules, while in the monohydrate, the water molecules are hydrogen-bonded to three zafirlukast molecules. The structures of the acetone and isopropanol solvatomorphs of brucine have been reported, where the solvent controlled the self-assembly of brucine on the basis of common donor–acceptor properties [65].

The structure of the 1:1 methanol solvate of olanzapine has been reported, where pairs of olanzapine molecules form a centrosymmetric dimer by means of C—H····π interactions [66]. The solvent molecule was linked to the drug substance through O—H····N, N—H····O, and C—H····O interactions. In a new polymorph of the 1:1 dioxane solvatomorph of (+)-pinoresinol, the structure was stabilized by O—H····O hydrogen bonds between the compound and the solvent [67]. Two new polymorphs of 2-cyano-3-[4-(*N*,*N*-diethylamino)-phenyl]prop-2-enethioamide and its acetonitrile solvatomorph have been characterized [68]. Although crystallization of the title compound was conducted out of a number of solvents, only the acetonitrile solvatomorph could be formed.

6. INTERCONVERSION OF POLYMORPHS AND SOLVATOMORPHS

The existence of more than one crystal phase for a given material, and the fact that only one form can be the most stable, naturally leads to studies of the interconversion between the various phases. Most often, such phase transformations are either by thermally initiated or solution mediated.

6.1. Thermally initiated phase transformations

Of the four known polymorphs of (*S,S*)-ethambutol dihydrochloride, two have been found to transform in an enantiotropic phase transformation on heating [69]. The phase transition takes place as a rapidly moving front that passes through single crystals of the compound, leaving a new crystal of the transformed substance. Using a hot stage microscope, it was shown that crystallization from the melt (124 ± 5°C) produced a thin film of Form III that transformed to Form IV upon cooling. Forms I and II could be reversibly interconverted about a temperature of 72°C.

In situ FT–Raman spectroscopy has been used to study the kinetics associated with the solid-state transformation of carbamazepine Form III to Form I [70]. The rate of transformation was followed by measuring the relative intensities of peaks associated with two C—H bending modes, and the data fitted to various solid-state kinetic models. Arrhenius plots from the kinetic models yielded a range of 344–368 kJ/mol for the activation energy of the transition. It was suggested that FT–Raman spectroscopy would be highly useful as an in-process monitor of phase composition during a manufacturing procedure.

The phase transformation relationships for the solvatomorphs of naproxen sodium have been reported [71]. The dihydrate phase is obtained upon crystallization from water, and a monohydrate phase could be prepared by the dehydration of the dihydrate phase in a desiccator (RH = 0%) for two days. The anhydrate phase could be obtained from either the monohydrate or dihydrate by drying the substance in an oven at 120°C for two hours. Thermal analysis data was used to demonstrate the existence of two types of water in the dihydrate phase, and that each could be removed at a characteristic temperature.

The hydration equilibria and phase transformations associated with a cytotoxic drug, BBR3576, have been studied [72]. The initially hydrated form could be made to undergo a phase transition where it lost approximately half of its water content, but the hemidesolvated product could be easily rehydrated to regenerate the starting material. If however, the original sample was completely dehydrated, the substance first formed a metastable anhydrate phase that underwent an irreversible exothermic transition to a new anhydrate crystal form. The hydration of this latter anhydrate form yielded a new hydrate phase whose structure was different from that of the initial material.

Raman spectroscopy has been used to study the intramolecular and low-frequency vibrations of the polymorphs of pentacene as a function of temperature [73]. By describing the vibrational contribution to the Gibbs energy using quasi-harmonic lattice dynamics methods, it was possible to compute the temperature dependences of the crystal structures and phonon frequencies. Solid-state ^{13}C nuclear magnetic resonance was used to study an order-to-disorder phase transition of oleic acid, since it was found that there was a significant difference between the two hydrocarbon chains straddling the *cis*-olefin group [74]. The structure of the low temperature form of 3-dimethylammonio-1-phenyl-propan-1-one chloride monohydrate was been reported [75].

The structural phase transitions and nature of the Br…N and Br…Br interactions in 1-phenyl-2-methyl-4-nitro-5-bromoimidazole have been studied [76]. The compound was found to undergo a reversible order–disorder transition over a wide

temperature range that was associated with the doubling of the length of the *c*-axis in the unit cell and a change in the space group itself. A second phase transition was identified to take place at much lower temperatures that resulted in a change from monoclinic to triclinic crystal symmetry, and crystal twinning.

A single-to-single crystal phase transition was found to take place at 333 K in a new polymorph of *ortho*-ethoxy-*trans*-cinnamic acid [77]. In this study, the structures of the title compound obtained at two temperatures above the transition point were determined in addition to the structures of the stabilized forms existing at lower temperatures. It was found that the phase transition involved a cooperative conformational transformation coupled with a shift in layers of the constituent molecules.

6.2. Solution mediated phase transformations

It has been found that both the anhydrous Form III and dihydrate phases of carbamazepine exhibit fluorescence in the solid state [78]. The fluorescence intensity associated with the dihydrate phase was determined to be significantly more intense than that associated with the anhydrate phase, and this difference was exploited to develop a method for study of the kinetics of the aqueous solution-mediated phase transformation between these forms. Studies were conducted at temperatures over the range of 18–40 °C, and it was found that the phase transformation was adequately characterized by first-order reaction kinetics. The temperature dependence in the calculated rate constants was used to calculate activation energy of 11.2 kCal/mol (47.4 cal/g) for the anhydrate-to-dihydrate phase conversion.

The formation of niclosamide hydrates, and the effect of relative humidity on the solvatomorphs obtained from acetone and ethyl acetate has been studied [79]. The acetone and ethyl acetate solvatomorphs could be desolvated, and exposure to elevated humidity resulted in the formation of two hydrate structures. Each hydrate could be dehydrated into a different anhydrate phase, but only the hydrate formed from the acetone desolvate could be rehydrated to form a hydrate phase. Dynamic vapor sorption has been used to develop a method for determining the onset relative humidity of a glass transition and associated crystallization process [80].

Glancing angle X-ray powder diffraction has been used as a method for profiling phase transformations as a function of tablet depth [81]. The methodology was then used to study the crystallization of indomethacin during the dissolution of tablets containing partially amorphous drug substance, and to profile the transformation of theophylline anhydrate into its hydrate phase during dissolution of its tablets. Samples in which a greater amorphous content had been generated by the secondary processing were found to undergo more rapid phase transformations than did the corresponding unprocessed drug. A detailed discussion of the significance of the technique, as well as its inherent limitations, has also been provided.

A rate enhancement effect due to secondary nucleation has been identified in the solution-mediated transformation of the α-phase of (L)-glutamic acid to its β-phase [82]. In this study, the kinetics of the polymorphic transition were studied using optical microscopy combined with Fourier transform infrared, Raman, and ultraviolet absorption spectroscopies. The crystallization process of *n*-hexatriacontane was investigated using micro-IR methodology, where it was confirmed that single

crystals of one polymorphic form exhibited a polytypic transformation during solution growth [83]. At the start of the crystallization process, single crystals appeared as the single-layered polytype, but these subsequently became over-grown by the double-layered polytype.

Polymorphism and solvatomorphism are not, of course, limited to small molecules, and such phenomena can be observed in protein crystals as well. Two polymorphic forms of aprotinin have been identified, and the solubility of these studied in a variety of aqueous media [84]. The needle polymorph was found to exhibit increased solubility with increased temperature (i.e., an endothermic heat of solution), while the solubility of the bipyramid form decreased by with increasing temperature (i.e., an exothermic heat of solution). The solubility curves crossed at 25°C for a pH of 4.75, and hence one could obtain the desired crystal form through a judicious selection of crystallization temperature.

7. EFFECTS ASSOCIATED WITH SECONDARY PROCESSING OF CRYSTAL FORMS

One factor that must be considered during the secondary processing of a drug substance into one of its dosage forms is that pharmaceutical manufacturing processes can alter the physical characteristics of the drug entity [85]. A transformed drug substance in a dosage form could exhibit an altered solubility or dissolution rate that might produce an undesirable profile, and this effect would be particularly pronounced when developing a metastable form of the drug substance.

The effects of pharmaceutical unit processes, such as size reduction, granulation, consolidation, and compression on celecoxib and its solvatomorphs have been studied [86]. The non-solvated drug substance was found to be stable under various processing conditions, retaining its crystalline nature without formation of any amorphous material during processing. Milling the *N*,*N*′-dimethylacetamide solvatomorph generated crystal defects, while milling the *N*,*N*′-dimethylformamide solvatomorph yielded partial transformation to the non-solvated phase. The solvates were found to desolvate when these were wet granulated, and compressional force also served to desolvate the solvatomorphs.

Changes in crystal form during the formulation of the three polymorphs of chloramphenicol palmitate with sugar spheres were followed as a function of mixing speeds and time [87]. It was found that crystal Form A exhibited a lower degree of affinity for the beads than did Form B or Form C, and hence formed less homogeneous mixtures during the blending process. It was concluded that the requirements of a mixing process validated on the formulation of one particular crystal form might not be directly translatable to the formulation of one of the other crystal forms, and such effects would have to be evaluated when changes in the polymorphic state of the drug substance were being considered.

The phase composition of glycine crystal forms during the drying step of a wet granulation process has been studied, and a model developed for the phase conversion reactions [88]. X-ray powder diffraction was used for qualitative analysis, and near-infrared spectroscopy for quantitative analysis. It was shown that when glycine was wet granulated with microcrystalline cellulose, the more rapidly the granulation

was dried the more pronounced became the kinetic trapping of the metastable α-polymorph. It was concluded that the magnitude of the drying rate determined the overall phase composition, as more conversion was noted in fluid bed-dried products than in tray-dried products.

Since it was known that theophylline monohydrate can be thermally dehydrated to form either the stable Form I or the metastable Form I*, the effect of different drying methods on the phase composition was studied [89]. Using either a multi-chamber microscale fluid bed dryer or the hot stage of a variable-temperature XRPD diffractometer, Form I* was produced when the drying was conducted at 40–50°C. Drying at 60°C in the VT-XRPD unit yielded only Form I, while mixtures of products were produced in the microscale fluid bed dryer even at temperatures as high as 90°C.

The chemical and physical stability of aqueous and nonaqueous suspensions of a number of solvatomorphs of niclosamide has been evaluated in an effort to develop pharmaceutically acceptable suspension formulations [90]. Studied in this work was the anhydrate, two polymorphic monohydrates, the 1:1 *N,N′*-dimethylformamide solvatomorph, the 1:1 dimethyl sulfoxide solvatomorph, the 1:1 methanol solvatomorph, and the 2:1 tetraethylene glycol hemisolvate. All of the solvatomorphs were found to convert initially to one of the polymorphic monohydrates, and over time converted to the more stable monohydrate phase. The various solvatomorphs could be readily desolvated into isomorphic desolvates, but these were unstable and became re-hydrated or re-solvated upon exposure to the appropriate solvent.

The effect of physical aging on the crystallization state and water vapor sorption behavior of amorphous non-solvated trehalose was studied [91]. It was found that annealing the amorphous substance at temperatures below the glass transition temperature caused nucleation in the sample that served to decrease the onset temperature of crystallization upon subsequent heating. Physical aging caused a decrease in the rate and extent of water vapor adsorption at low relative humidities, but water sorption could serve to remove the effects of physical aging due to a volume expansion that took place in conjunction with the adsorption process.

Secondary processing does not always lead to phase transformations, as was shown during studies of the polymorphs of ranitidine hydrochloride [92]. No solid–solid transformation could be detected during either the grinding or compression of metastable Form I, stable Form II, or of a 1:1 mixture of these forms. The dissolution rates of both forms were found to be equivalent, and the solution-mediated transformation of Form I to Form II was observed to be slow.

8. TOPOCHEMICAL REACTIONS

When the course taken by a given solid-state reaction is determined by geometrical details of the crystal lattice, the reaction type falls under the general category of topochemistry. In a topochemical reaction, the reaction takes place in the solid state with a minimum amount of molecular motion. For example, bimolecular reactions are expected to take place between nearest neighbors, which then suggests that the product of the reaction would be a function of the geometric relation in the crystal structure of the reactant molecules.

The structural changes that accompanied the [2 + 2] photodimerization of the metastable α′-polymorph of *ortho*-ethoxy-*trans*-cinnamic acid have been studied [93]. In this study, the photochemical reaction was carried out at 293 K, and observed *in situ* by single-crystal X-ray diffraction. In the structure of the title compound, the three molecules in the asymmetric unit are arranged to form two potential reaction sites, but only one of these was found to be photoreactive. Since only two out of three molecules in the asymmetric unit take place in the photodimerization reaction, the crystal of the final product contains an ordered arrangement of the photodimer and the unreacted monomer.

A new photoactive monoclinic polymorph of 6-(2′,4′-dinitrobenzyl)-2,2′-bipyridine was obtained from an acetone/methanol solution, and the structure compared to the previously known photoactive orthorhombic and photoinactive monoclinic forms [94]. Correlation of these structures with those of related nitrobenzylpyridines was used to understand the relationships existing between structure and photochromism. The comparison of the reaction cavities around the reactive pyridyl-benzyl-nitro fragment indicated that photochromic activity required rotational freedom of the *ortho*-nitro group in the crystal and its accessibility from the proton-donor and proton-acceptor sites.

The photostability of two polymorphs of nicardipine hydrochloride have been studied using a number of techniques [95]. After irradiation, the drug substance decomposes to a pyridine derivative, and the photodegradation of the β-form exceeded that of the α-form. It was also found that the color of the two different forms differed with the polymorphic state, but that grinding the two forms lessened the difference in their photochemistries. A correlation between the heat of fusion (measured by differential scanning calorimetry) and the photodegradation rate constant was observed.

9. UNITED STATES POLYMORPH AND SOLVATOMORPH PATENTS ISSUED DURING 2005

The listing of patents published by the United States Patent Office was searched for polymorph and solvatomorph patents using the keywords polymorph(s), polymorphic, solvate(s), hydrate(s), crystal form(s), and crystal modification, and the following patents issued during 2005 were returned using these keywords.

US patent 6,677,373, "Polymorphic B form of 3-(cyclopropylmethoxy)-4-[4-(methylsulfonyl)phenyl]-5,5-dimethyl-5H-furan-2-one" [96]. This invention concerns Form B of the title compound, crystallizing in the hexagonal R-3 space group, and which was characterized by its unit cell parameters. For this form, $a = 18.183$ Å, $b = 18.183$ Å, $c = 26.950$ Å, $\alpha = \beta = 90°$, and $\gamma = 120°$. The unit-cell volume was found to be 7716.5 Å^3, and there were 18 molecules per unit cell.

US patent 6,677,453, "Production of polymorphic forms I and II of finasteride by complexation with group I or II metal salts" [97]. Finasteride Form I of was prepared by first forming a substantially insoluble complex of the compound and a Group I or Group II metal salt (such as lithium bromide), and then dissociating the complex by dissolving away the salt component with water to obtain substantially pure crystalline finasteride Form I.

US patent 6,683,085, ''Salt form and polymorphs'' [98]. This invention encompasses 4-amino-6,7-dimethoxy-2-(5-methanesulfonamido-1,2,3,4-tetrahydroisoquinol-2-yl)-5-(2-pyridyl)quinazoline mesylate, together with processes for its preparation and its compositions. The invention also relates to the substantially pure anhydrous crystalline polymorphic forms of the free base. The compounds are particularly useful in the treatment of benign prostatic hyperplasia.

US patent 6,689,800, ''β_3-adrenergic receptor agonist crystal forms, processes for the production thereof, and uses thereof'' [99]. This invention provides the tosylate salt of (R)-2-(2-(4-oxazol-4-yl-phenoxy)-ethylamino)-1-pyridin-3-yl-ethanol, the monohydrate of such salt, processes useful in the preparation of such salt and such monohydrate, pharmaceutical compositions comprising such salt, or such monohydrate, methods of treating β_3-adrenergic receptor-mediated diseases, conditions, and disorders in a mammal using such salt, such monohydrate, or such pharmaceutical compositions; and methods of increasing the content of lean meat in edible animals using such salt, monohydrate, or pharmaceutical compositions.

US patent 6,689,802, ''Polymorphs of an epothilone analog'' [100]. This invention describes two crystalline polymorphs, as well as mixtures of these, of an epothilone analog. Also provided are methods of forming the novel polymorphs, therapeutic methods utilizing them, and pharmaceutical dosage forms containing them.

US patent 6,696,458, ''Compositions and formulations of 9-nitrocamptothecin polymorphs and methods of use thereof'' [101]. Amorphous forms of 9-nitrocamptothecin are obtained by grinding or pulverizing different polymorphic forms of 9-nitrocamptothecin, and the polymorphic forms are characterized by having an X-ray powder diffraction pattern with discernable diffraction lines at different scattering angles for Cu Kα radiation.

US patent 6,696,601, ''Hydrate forms of alendronate sodium, processes for manufacture thereof, and pharmaceutical compositions thereof'' [102]. New hydrate forms of alendronate sodium, having a water content of about 1–12%, and processes for their manufacture, are disclosed. New crystalline forms of alendronate sodium, and processes for manufacturing these, are also disclosed. These new forms of alendronate sodium are suitable for incorporation into pharmaceutical compositions for combating bone resorption in bone diseases.

US patent 6,703,410, ''Crystal forms of 3-(2,4-dichlorobenzyl)-2-methyl-*N*-(pentylsulfonyl)-3h-benzimidazole-5-carboxamide'' [103]. 3-(2,4-Dichlorobenzyl)-2-methyl-*N*-(pentylsulfonyl)-3H-benzimidazole-5-carboxamide, a compound having hypoglycemic activity or PDE5 inhibitory effect, has three forms of crystal forms that are distinguishable by their X-ray powder diffraction values. The most crystallographically stable crystal form is useful as a drug substance for medicines. Another crystal form can be purified efficiently by crystallization, since it forms larger crystals and can be very easily isolated by filtration. Thus, this crystal form is use ful for purifying 3-(2,4-dichlorobenzyl)-2-methyl-*N*-(pentylsulfonyl)-3H-benzimidazole-5-carboxamide.

US patent 6,713,481, ''Crystalline antifungal polymorph'' [104]. This patent discloses the crystalline polymorph Form I of (−)-4-[4-[4-[4-[[(2R-*cis*)-5-(2,4-difluorophenyl)tetrahydro-5-(1H-1,2,4-triazol-1-ylmethyl)furan-3-yl]methoxy]phenyl]-1-piperazinyl]phenyl-2,4-dihydro-2-[(S)–1-ethyl–2(S)-hydroxylpropyl]-3H–1,2,4-triazol-3-one,

pharmaceutical compositions containing such a polymorph, and methods of using such a polymorph to treat fungal infections in mammals.

US patent 6,720,453, "Formoterol tartrate polymorph" [105]. A method of preparation of a highly pure salt of R,R-formoterol L-tartrate is disclosed. The process provides the most thermodynamically stable polymorph by recrystallization of a novel polymorph.

US patent 6,723,728, "Polymorphic and other crystalline forms *cis*-FTC" [106]. The present invention relates to polymorphic and other crystalline forms of (−)- and (±)-*cis*-(4-amino-5-fluoro-1-(2-(hydroxymethyl)-1,3-oxathiolan-5-yl)-2(1H)-pyrimidinone, or FTC) [106]. Solid phases of (−)-*cis*-FTC that were designated as amorphous (−)-FTC, and Forms II and III were found to be distinguishable from Form I by X-ray powder diffraction, thermal analysis properties, and their methods of manufacture. A hydrated crystalline form of (±)-*cis*-FTC and a dehydrated form of the hydrate, were also disclosed, and can similarly be distinguished from other forms of FTC by X-ray powder diffraction, thermal properties, and their methods of manufacture. These FTC forms can be used in the manufacture of other forms of FTC, or as active ingredients in pharmaceutical compositions. Particularly preferred uses of these forms are in the treatment of HIV or hepatitis B.

US patent 6,730,678 "Benzoylguanidine salt and hydrates thereof" [107]. 4-[4-(2-Pyrrolylcarbonyl)-1-piperazinyl]-3-trifluoromethylbenzoylguanidine hydrochloride and its hydrates, processes for preparing this benzoylguanidine salt and its hydrates, pharmaceutical compositions containing this benzoylguanidine salt and its hydrates, and its use in treating diseases, particularly those in which inhibition of the cellular Na^+/H^+ exchange is of therapeutic benefit.

US patent 6,734,308, "Crystal forms of 6-[(4-chloro-phenyl)-hydroxy-(3-methyl-3H-imidazol-4-yl)-methyl]-4-(3-ethynyl-phenyl)-1-methyl-1H-quinolin-2-one, 2,3,-dihydroxy-butanedioate salts and method of production" [108]. The invention relates to crystal forms of 6-[(4-chloro-phenyl)-hydroxy-(3-methyl-3H-imidazol-4-yl)-methyl]-4-(3-ethynyl-phenyl)-1-methyl-1H-quinolin-2-one, 2,3-dihydroxy butanedioate salts, and to pharmaceutical compositions containing the above compound, methods of treating hyperproliferative diseases, such as cancers, in mammals, especially humans by administering the above compound, and to methods of preparing the crystal forms of the above compound and related compounds.

US patent 6,740,669, "Crystal modification of 1-(2,6-difluorobenzyl)-1H-1,2,3-triazole-4-carboxamide and its use as antiepileptic" [109]. The invention relates to the novel modification A or A′ of the compound 1-(2,6-difluorobenzyl)-1H-1,2,3-triazole-4-carboxamide, and its use and pharmaceutical preparations comprising this crystal modification.

US patent 6,740,753, "Olanzapine crystal modification" [110]. This invention concerns a novel crystal form of olanzapine, processes for its preparation, and its pharmaceutical use.

US patent 6,753,426, "Polymorph and process for preparing same" [111]. In this patent are disclosed are processes, a new polymorph, and intermediate compounds for preparing various aryl- and heteroaryl-substituted urea compounds. The product compounds are useful in pharmaceutical compositions for treating diseases

or pathological conditions involving inflammation such as chronic inflammatory diseases.

US patent 6,756,381, "Compositions and formulations of 9-nitrocamptothecin polymorphs and methods of use thereof" [112]. This invention discloses a polymorphic form of 9-nitrocamptothecin, the polymorph being characterized as having an infrared spectrum with an absorption centered between 3625 and 3675 cm^{-1} and containing more than a trace of water.

US patent 6,759,521, "Polarization switching to control crystal form" [113]. This patent describes a method to select and prepare polymorphs of materials by switching the polarization state of light and employing non-photochemical laser-induced nucleation.

US patent 6,767,913, "Crystal Forms III, IV, V, and novel amorphous form of clopidogrel hydrogen sulfate, processes for their preparation, processes for the preparation of Form I, compositions containing the new forms and methods of administering the new forms" [114]. This invention provides new crystalline Forms III, IV, and V of clopidogrel hydrogen sulfate and the amorphous form of clopidogrel hydrogen sulfate. Also disclosed are their pharmaceutical compositions and method of treatments with such compositions. The invention also includes novel processes for preparation of clopidogrel hydrogen sulfate Forms I, III, IV, V, and the amorphous form. The invention further provides a novel process where the amorphous form is converted to Form I by contacting Form I with ether.

US patent 6,767,921, "Polymorphic forms of fasidotril, their methods of preparation and pharmaceutical compositions comprising them" [115]. The subject of this invention are polymorphic Forms I, II, III, IV of benzyl (S,S)-2-(2-acetylsulphanylmethyl-3-benzo[1,3]dioxol-5-ylpropionyl-amino)propionate (i.e., fasidotril), their methods of preparation, and novel pharmaceutical compositions containing them.

US patent 6,784,176, "Solvates of pymetrozine" [116]. This invention discloses compounds having the general formula (pymetrozine)$(L)_R(H_2O)_S$, where R and S, can independently take on any value between 0.00 and 12.00, with the proviso that R and S cannot simultaneously equal zero. L can be methanol, ethanol, propanol, isopropanol, butanol, isobutanol, *t*-butanol, cyclohexanol, tetrahydrofurfuryl alcohol, ethylene glycol, glycerol, methyl acetate, ethyl acetate, ethyl lactate, butyrolactone, ethylene carbonate, propylene carbonate, acetonitrile, dimethyl sulfoxide, dimethylformamide, dimethylacetamide, *N*-methyl-2-pyrrolidone, *N*-octyl-2-pyrrolidone, *N*-decyl-2-pyrrolidone, acetone, butanone, methyl isobutyl ketone, methylpropyl ketone, acetophenone, cyclohexanone, methylene chloride, trichloromethane, trichloroethane, tetrahydrofuran, diethylether, 1,2-dimethoxyethane, dioxane, methyl-*tert*-butylether, ethanolamine, pyridine, chlorobenzene, toluene, xylene or tetramethylurea. The invention covers the free form or the salt form and their tautomers, a method for the preparation and usage of these compounds, their salts, and tautomers.

US patent 6,806,280, "Polymorph of 5-[4-[2-(*n*-methyl-*n*(2-pyridyl)amino)ethoxy] benzyl]-thiazolidine-2,4-dione, maleic acid salt" [117]. This invention discloses a polymorphic form of 5-[4-[2-(*N*-methyl-*N*-(2-pyridyl)amino)ethoxy]benzyl]-thiazolidine-2,4-dione, maleic acid salt. The polymorphic form is characterized by (i) an infrared spectrum containing peaks at 1763, 912, 856, and 709 cm^{-1} and/or

(ii) a Raman spectrum containing peaks at 1762, 1284, 912, and 888 cm^{-1}. In addition the crystal form has (iii) a solid-state ^{13}C nuclear magnetic resonance spectrum containing peaks at 111.0, 113.6, 119.8, 129.1, 130.9, 131.8, 134.7, 146.5, 152.7, 157.5, 169.5, 171.0, and 178.7 ppm, and/or (v) an X-ray powder diffraction pattern which gives calculated lattice spacings at 5.87, 5.30, 4.69, 4.09, 3.88, 3.61, 3.53, and 3.46 Å. Also disclosed is a process for preparing the crystal form, a pharmaceutical composition containing the polymorph, and the use of the compound in medicine.

US patent 6,821,990, "Ethanol solvate of (−)-*cis*-2-(2-chlorophenyl)-5,7-dihydroxy-8 [4R-(3S-hydroxy-1-M ethyl) piperidinyl]-4H-1-benzopyran-4-one" [118]. Disclosed in this invention is an ethanol solvate of (−)-*cis*-2-(2-chlorophenyl)-5,7-dihydroxy-8[4R-(3S-hydroxy-1-methyl)piperid inyl]-4H-1-benzopyran-4-one hydrochloride (identified as Form II), a method of making Form II, and a composition comprising Form II.

US patent 6,833,379, "Crystal modification of torasemide" [119]. This invention relates to the characterization of a new crystal modification III of torasemide, to a process for its preparation by the use of controlled acidifying of alkaline solutions of torasemide with inorganic or organic acids with or without addition of a crystal seed, to its use as a raw material for the preparation of the crystal modification I of torasemide and of pharmaceutically acceptable salts of torasemide, as well as to pharmaceutical forms containing this new torasemide crystal modification.

REFERENCES

[1] H. G. Brittain, *Polymorphism in Pharmaceutical Solids*, Marcel-Dekker, New York, 1999.
[2] S. R. Byrn, R. R. Pfeiffer and J. G. Stowell, *Solid State Chemistry of Drugs*, 2nd edn., SSCI Inc., West Lafayette, IN, 1999.
[3] J. Bernstein, *Polymorphism in Molecular Crystals*, Clarendon Press, Oxford, 2002.
[4] F. H. Herbstein, *Cryst. Growth Design*, 2004, **4**, 1419–1429.
[5] L. Fabian and A. Kalman, *Acta Cryst.*, 2004, **B60**, 547–558.
[6] M. Sacchetti, *Int. J. Pharm.*, 2004, **273**, 195–202.
[7] F. L. Nordstrom, A. Rasmuson and A. Y. Sheikh, *J. Pharm. Sci.*, 2004, **93**, 995–1004.
[8] A. R. Sheth, D. Zhou, F. X. Muller and D. J. W. Grant, *J. Pharm. Sci.*, 2004, **93**, 3013–3026.
[9] G. Defossemont, S. L. Randzio and B. Legendre, *Cryst. Growth Design*, 2004, **4**, 1169–1174.
[10] T. C. Lewis, D. A. Tocher and S. L. Price, *Cryst. Growth Design*, 2004, **4**, 979–987.
[11] T. V. Timofeeva, T. Kinnibrugh, O. Y. Borbulevych, B. B. Averkiev, V. N. Nesterov, A. Sloan and M. Y. Antipin, *Cryst. Growth Design*, 2004, **4**, 1265–1276.
[12] M. Pauchet, G. Gervais, L. Courvoisier and G. Coquerel, *Cryst. Growth Design*, 2004, **4**, 1143–1151.
[13] X. Hu, Z. Yuan and G. Lu, *Powder Diffract.*, 2004, **19**, 325–328.
[14] T. Ono, H. J. M. Kramer, J. H. ter Horst and P. J. Jansens, *Cryst. Growth Design*, 2004, **4**, 1161–1167.
[15] A. Menon and S. Bhandarkar, *Int. J. Pharm.*, 2004, **286**, 125–129.
[16] S. Teychene, J. M. Autret and B. Biscans, *Cryst. Growth Design*, 2004, **4**, 971–977.
[17] M. Mirmehrabi, S. Rohani, K. S. K. Murthy and B. Radatus, *J. Pharm. Sci.*, 2004, **93**, 1692–1700.
[18] X.-W. Ni, A. Valentine, A. Liao, S. B. C. Sermage, G. B. Thomson and K. J. Roberts, *Cryst. Growth Design*, 2004, **4**, 1129–1135.
[19] M. Kitamura, *Cryst. Growth Design*, 2004, **4**, 1153–1159.
[20] T. Ono, J. H. ter Horst and P. J. Jansens, *Cryst. Growth Design*, 2004, **4**, 465–469.
[21] R. B. Hammond, X. Lai and K. J. Roberts, *Cryst. Growth Design*, 2004, **4**, 943–948.

[22] N. Doki, M. Yokota, K. Kido, S. Sasaki and N. Kubota, *Cryst. Growth Design*, 2004, **4**, 103–107.
[23] N. Doki, H. Seki, K. Takano, H. Asatani, M. Yokota and N. Kubota, *Cryst. Growth Design*, 2004, **4**, 949–953.
[24] S. L. Childs, L. J. Chyall, J. T. Dunlap, D. A. Coates, B. C. Stahly and G. P. Stahly, *Cryst. Growth Design*, 2004, **4**, 441–449.
[25] X. Mei and C. Wolf, *Cryst. Growth Design*, 2004, **4**, 1099–1103.
[26] S. N. Black, M. W. Cuthbert, R. J. Roberts and B. Stensland, *Cryst. Growth Design*, 2004, **4**, 539–544.
[27] J. M. Rubin-Preminger, J. Bernstein, R. K. Harris, I. R. Evans and P. Y. Ghi, *J. Pharm. Sci.*, 2004, **93**, 2810–2819.
[28] A. Foppoli, M. E. Sangalli, A. Maroni, A. Gazzaniga, M. R. Caira and F. Giordano, *J. Pharm. Sci.*, 2004, **93**, 521–531.
[29] S. S. C. Nunes, M. E. Eusebio, M. L. P. Leitao and J. S. Redinha, *Int. J. Pharm.*, 2004, **285**, 13–21.
[30] A. R. Sheth, S. Bates, F. X. Muller and D. J. W. Grant, *Cryst. Growth Design*, 2004, **4**, 1091–1098.
[31] S. Gracin and A. C. Rasmuson, *Cryst. Growth Design*, 2004, **4**, 1013–1023.
[32] I. Wawrzycka-Gorczyca, A. E. Koziol, M. Glice and J. Cybulski, *Acta Cryst.*, 2004, **E60**, o66–o68.
[33] H. S. Yathirajan, B. Nagaraj, R. S. Narasegowda, P. Nagaraja and M. Bolte, *Acta Cryst.*, 2004, **E60**, o2228–o2229.
[34] V. S. S. Kumar, K. C. Sheela, V. Nair and N. P. Rath, *Cryst. Growth Design*, 2004, **4**, 1245–1247.
[35] P. Munshi, K. N. Venugopala, B. S. Jayashree and T. N. G. Row, *Cryst. Growth Design*, 2004, **4**, 1105–1107.
[36] S. Coste, J.-M. Schneider, M.-N. Petit and G. Coquerel, *Cryst. Growth Design*, 2004, **4**, 1237–1244.
[37] M. T. Kirchner, L. S. Reddy, G. R. Desiraju, R. K. R. Jetti and R. Boese, *Cryst. Growth Design*, 2004, **4**, 701–709.
[38] N. Fridman, M. Kapon, Y. Sheynin and M. Kafory, *Acta Cryst.*, 2004, **B60**, 97–102.
[39] S. Muthu and J. J. Vittal, *Cryst. Growth Design*, 2004, **4**, 1181–1184.
[40] A. Kalman, L. Fabian, G. Argay, G. Bernath and Z. C. Gyarmati, *Acta Cryst.*, 2004, **B60**, 755–762.
[41] M. B. Mariyatra, K. Panchanatheswaran, J. N. Low and C. Glidewell, *Acta Cryst.*, 2004, **C60**, o682–o685.
[42] J. Pacifico and H. Stoeckli-Evans, *Acta Cryst.*, 2004, **C60**, o152–o155.
[43] C. Glidewell, J. N. Low, J. M. S. Skakle and J. L. Wardell, *Acta Cryst.*, 2004, **C60**, o120–o155.
[44] D. S. Cati and H. Stoeckli-Evans, *Acta Cryst.*, 2004, **E60**, o210–o212.
[45] M. R. Silva, J. A. Paixao, A. M. Beja, A. J. F. N. Sobral and A. M. R. Gonsalves, *Acta Cryst.*, 2004, **E60**, o84–o85.
[46] A. C. Doriguetto, C. H. T. de Paula Silva, D. R. Rando, E. I. Ferreira and J. Ellena, *Acta Cryst.*, 2004, **C60**, o69–o71.
[47] N. Fridman, M. Kapon and M. Kaftory, *Acta Cryst.*, 2004, **C60**, o47–o49.
[48] D. Britton and W. W. Brennessel, *Acta Cryst.*, 2004, **C60**, o552–o556.
[49] S. Gao, L.-H. Huo, C.-S. Gu, H. Zhao and S. W. Ng, *Acta Cryst.*, 2004, **E60**, o1914–o1916.
[50] G. Smith, U. D. Wermuth and P. C. Healy, *Acta Cryst.*, 2004, **E60**, o1800–o1803.
[51] F. Zhang, M. Wagner and J. W. Bats, *Acta Cryst.*, 2004, **E60**, o1804–o1806.
[52] R. Bednar, L. Cvak, J. Cejka, B. Kratochvil, I. Cisarova and A. Jegorov, *Acta Cryst.*, 2004, **E60**, o1167–o1169.
[53] R. T. Stibrany, H. J. Schugar and J. T. Potenza, *Acta Cryst.*, 2004, **E60**, o1182–o1184.
[54] Q. C. Ton and M. Bolte, *Acta Cryst.*, 2004, **E60**, o1019–o1020.
[55] G. G. du Sart, G. O. R. Alberda van Ekenstein, A. Meetsma and G. Ten Brinke, *Acta Cryst.*, 2004, **C60**, o824–o826.
[56] M. R. Caira, K. A. Alkhamis and R. M. Obaidat, *J. Pharm. Sci.*, 2004, **93**, 601–611.
[57] T. Hosokawa, S. Datta, A. R. Sheth, N. R. Brooks, V. G. Young and D. J. W. Grant, *Cryst. Growth Design*, 2004, **4**, 1195–1201.
[58] A. R. Sheth, W. W. Brennessel, V. G. Young, F. X. Muller and D. J. W. Grant, *J. Pharm. Sci.*, 2004, **93**, 2669–2680.
[59] A. Jayaraman, V. Balasubramaniam and S. Valiyavettil, *Cryst. Growth Design*, 2004, **4**, 1403–1409.
[60] V. S. S. Kumar, F. C. Pigge and N. P. Rath, *Cryst. Growth Design*, 2004, **4**, 1217–1222.
[61] E. C. van Tonder, T. S. P. Maleka, W. Liebenberg, M. Song, D. E. Wurster and M. M. de Villiers, *Int. J. Pharm.*, 2004, **269**, 417–432.

[62] E. C. van Tonder, M. D. Mahlatji, S. F. Malan, W. Liebenberg, M. R. Caira, M. Song and M. M. de Villiers, *AAPS Pharm. and Sci. Tech.*, 2004, **5**, (1), article 12.
[63] N. Fridman, M. Kapon and M. Kaftory, *Acta Cryst.*, 2004, **C60**, o44–o46.
[64] D. Goldring, M. Botoshansky, R. L. Khalfin, B. Pertsikov, G. Nisevitch, V. Ponomarev, I. Zaltxman, A. Gutman and M. Kaftory, *Acta Cryst.*, 2004, **C60**, o843–o846.
[65] A. Biatonska and Z. Ciunik, *Acta Cryst.*, 2004, **C60**, o853–o855.
[66] I. Wawrzycka-Gorczyca, L. Mazur and A. E. Koziol, *Acta Cryst.*, 2004, **E60**, o69–o71.
[67] R. Stomberg, V. Langer and K. Lundquist, *Acta Cryst.*, 2004, **E60**, o81–o83.
[68] V. N. Nesterov and V. V. Nesterov, *Acta Cryst.*, 2004, **C60**, o781–o785.
[69] J. M. Rubin-Preminger, J. Bernstein, R. K. Harris, I. R. Evans and P. Y. Ghi, *Cryst. Growth Design*, 2004, **4**, 431–439.
[70] L. E. O'Brien, P. Timmins, A. C. Williams and P. York, *J. Pharm. Biomed. Anal.*, 2004, **36**, 335–340.
[71] Y.-S. Kim and R. W. Rousseau, *Cryst. Growth Design*, 2004, **4**, 1211–1216.
[72] A. Marini, V. Berbenni, G. Bruni, P. Cofrancesco, C. Margheritis, A. Orlandi and M. Villa, *J. Pharm. Sci.*, 2004, **93**, 2222–2231.
[73] R. G. Della Valle, E. Venuti, L. Farina, A. Brillante, M. Massino and A. Girlando, *J. Phys. Chem. B*, 2004, **108**, 1822–1826.
[74] C. Akita, T. Kawaguchi, F. Kaneko, H. Yamamoto and M. Suzuki, *J. Phys. Chem. B*, 2004, **108**, 4862–4868.
[75] C. Ton and M. Bolte, *Acta Cryst.*, 2004, **E60**, o616–o617.
[76] M. Kubicki, *Acta Cryst.*, 2004, **B60**, 333–342.
[77] M. A. Fernandes, D. C. Levendis and F. R. L. Schoening, *Acta Cryst.*, 2004, **B60**, 300–314.
[78] H. G. Brittain, *J. Pharm. Sci.*, 2004, **93**, 375–383.
[79] R. V. Manek and W. M. Kolling, *AAPS Pharm. Sci. Tech.*, 2004, **5**, (1), article 14.
[80] D. J. Burnett, F. Thielmann and J. Booth, *Int. J. Pharm.*, 2004, **287**, 123–133.
[81] S. Debnath, P. Predecki and R. Suryanarayanan, *Pharm. Res.*, 2004, **21**, 149–159.
[82] E. S. Ferrari and R. J. Davey, *Cryst. Growth Design*, 2004, **4**, 1061–1068.
[83] H. Kubota, F. Kaneko, T. Kawaguchi and M. Kawasaki, *Cryst. Growth Design*, 2004, **4**, 369–375.
[84] S. Vessler, N. Ferte, M.-S. Costes, M. Czjzek and J.-P. Astier, *Cryst. Growth Design*, 2004, **4**, 1137–1141.
[85] H. G. Brittain, *J. Pharm. Sci.*, 2002, **91**, 1573–1580.
[86] G. Chawla and A. K. Bansal, *Pharm. Dev. Tech.*, 2004, **9**, 419–433.
[87] M. Song and M. M. de Villiers, *Pharm. Dev. Tech.*, 2004, **9**, 387–433.
[88] T. D. Davis, G. E. Peck, J. G. Stowell, K. R. Morris and S. R. Byrn, *Pharm. Res.*, 2004, **21**, 860–866.
[89] S. Airaksinen, M. Karjalainen, E. Rasanen, J. Rananen and J. Yliruusi, *Int. J. Pharm.*, 2004, **276**, 129–141.
[90] M. M. de Villiers, M. D. Mahlatji, E. C. van Tonder, S. F. Malan, A. P. Lotter and W. Liebenberg, *Drug Dev. Ind. Pharm.*, 2004, **30**, 581–592.
[91] R. Surana, A. Pyne and R. Suryanarayanan, *Pharm. Res.*, 2004, **21**, 867–874.
[92] M. Mirmehrabi, S. Rohani, K. S. K. Murthy and B. Radatus, *Int. J. Pharm.*, 2004, **282**, 73–85.
[93] M. A. Fernandes and D. C. Levendis, *Acta Cryst.*, 2004, **B60**, 315–324.
[94] P. Naumov and Y. Ohaski, *Acta Cryst.*, 2004, **B60**, 343–349.
[95] R. Teraoka, M. Otsuka and Y. Matsuda, *Int. J. Pharm.*, 2004, **286**, 1–8.
[96] B. Calais, E. Chassagneux and J.-M. Bonard, US patent 6,677,373, issued January 13, 2004.
[97] S. Clarke, US patent 6,677,453, issued January 13, 2004.
[98] P. A. Basford and P. B. Hodgson, US patent 6,683,085, issued January 27, 2004.
[99] J. F. Krzyaniak and J. A. Lafontaine, US patent 6,689,800, issued February 10, 2004.
[100] J. D. DiMarco, J. Z. Gougoutas, I. M. Vitez, M. Davidovich, M. A. Galella, T. M. Malloy, Z. Guo and Denis Favreau, US patent 6,689,802, issued February 10, 2004.
[101] S. Redkar and A. Gore, US patent 6,696,458, issued February 24, 2004.
[102] N. Finkelstein, R. Lidor-Hadas and J. Aronhime, US patent 6,696,601, issued February 24, 2004.
[103] Y. Murai, N. Yamasaki, T. Imoto, M. Nishikawa and K. Dohtsu, US patent 6,703,410, issued March 9, 2004.
[104] D. R. Andrews, W. Leong and A. Sudhakar, US patent 6,713,481, issued March 30, 2004.

[105] G. J. Tanoury, C. H. Senanayake and D. W. Kessler, US patent 6,720,453, issued April 13, 2004.
[106] Y. Hu, D. Law and K. R. Phares, US patent 6,723,728, issued April 20, 2004.
[107] C. Eickmeier, P. Sieger, W. Rall, V. Koerner and R. Herter, US patent 6,730,678, issued May 4, 2004.
[108] J. P. Lyssikatos, D. L. Tickner, L. S. Newton, Z. J. Li and C. N. Meltz, US patent 6,734,308, issued May 11, 2004.
[109] R. Portmann, U. C. Hofmeier, A. Burkhard, W. Scherrer and M. Szelagiewicz, US patent 6,740,669, issued May 25, 2004.
[110] J. Davies and J. E. Gano, US patent 6,740,753, issued May 25, 2004.
[111] L.-H. Zhang and L. Zhu, US patent 6,753,426, issued June 22, 2004.
[112] S. Redkar and A. Gore, US patent 6,756,381, issued June 29, 2004.
[113] A. S. Myerson and B. A. Garetz, US patent 6,759,521, issued July 6, 2004.
[114] R. Lifshitz, E. Kovalevski-Ishai, S. Wizel, S. A. Maydan and R. Lidor-Hadas, US patent 6,767,913, issued July 27, 2004.
[115] M. Capet, G. Coquerel, D. Danvy, J.-M. Lecomte, M.-N. Petit and J.-C. Schwartz, US patent 6,767,921, issued July 27, 2004.
[116] S. Gutmann, US patent 6,784,176, issued August 31, 2004.
[117] P. D. J. Blackler, C. M. Browne, T. G. Coakley, R. G. Giles and G. Morrissey, US patent 6,806,280, issued October 19, 2004.
[118] K. M. Kesseler, US patent 6,821,990, issued November 23, 2004.
[119] F. Darko, M. Dumic, A. Danilovski, B. Klepic, I. Fistric, M. Oresic and J. H. Mikulcic, US patent 6,833,379, issued December 21, 2004.

Cumulative Index

Bold numerals refer to volume numbers.